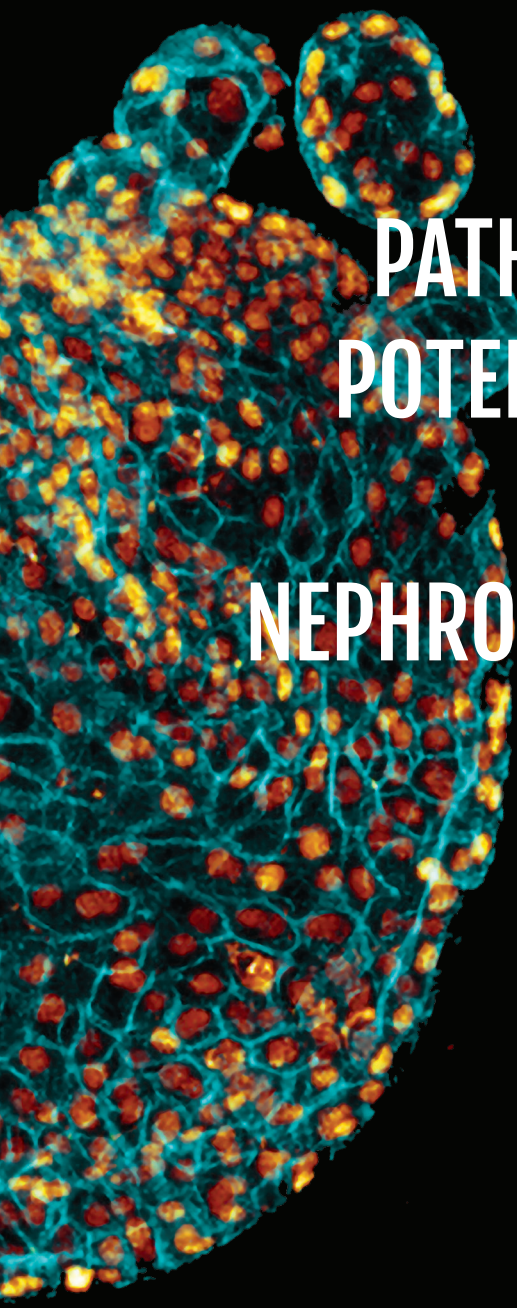

INVESTIGATING THE PATHOPHYSIOLOGY AND POTENTIAL THERAPEUTIC APPROACHES FOR NEPHROPATHIC CYSTINOSIS

Amer Jamalpoor

Investigating the pathophysiology and potential therapeutic approaches for nephropathic cystinosis

Amer Jamalpoor

Layout and cover design: Vera van Ommeren, persoonlijkproefschrift.nl
Printed by: Gildeprint, Enschede, The Netherlands
ISBN: 978-94-6419-099-1

Financial support by the Utrecht Institute for Pharmaceutical Sciences and the Cystinosis Ireland for the printing of this thesis is gratefully acknowledged.

The research presented in this thesis was performed at the Division of Pharmacology, Utrecht Institute for Pharmaceutical Sciences, Faculty of Science, Utrecht University.

This research project was financially supported by the Dutch Kidney Foundation (grant nr.150KG19), the Stofwisselkracht (Druggable Targets In Lysosomal V-ATPase Dysfunction), and the Cystinosis Ireland Seedcorn.

Investigating the pathophysiology and potential therapeutic approaches for nephropathic cystinosis

Onderzoek naar de pathofysiologie van nefropathische cystinose en ontwikkeling van een nieuwe farmacologische behandeling van de ziekte
(met een samenvatting in het Nederlands)

Proefschrift

ter verkrijging van de graad van doctor aan de Universiteit Utrecht op gezag van de rector magnificus, prof. dr. H.R.B.M. Kummeling, ingevolge het besluit van het college voor promoties in het openbaar te verdedigen op
maandag 15 februari 2021 des middags te 2.30 uur

door

Amer Jamalpoor

geboren op 15 januari 1988
te Dubai, Verenigde Arabische Emiraten

PROMOTOR:
Prof. dr. R. Masereeuw

COPROMOTOR:
Dr. M. J. Janssen

“Only those who attempt the absurd can achieve the impossible.”
Albert Einstein

To my family

TABLE OF CONTENT

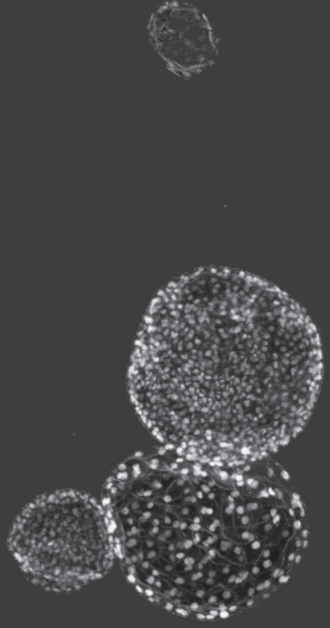

1

General introduction and thesis outline

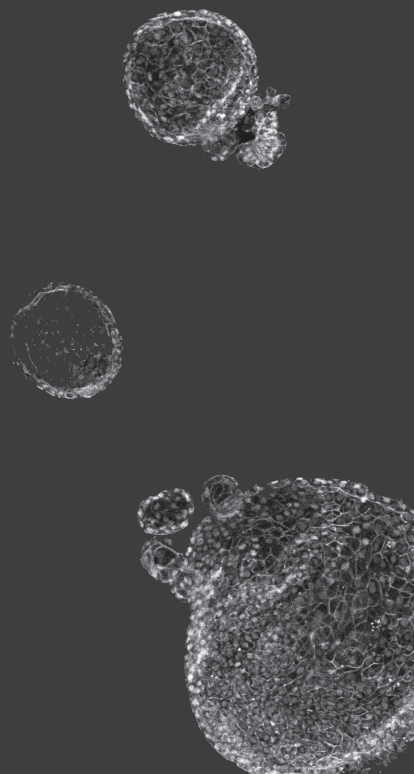

INTRODUCTION

Cystinosis was first described in 1903 by the Swiss biochemist and physiologist, Emil Abderhalden as a hereditary cystine accumulation disease [1]. Abderhalden found cystine crystals in multiple organs of a 21-month-old patient at post mortem examination [1], who was initially examined by Professor Eduard Kaufmann. Furthermore, in 1924 the Dutch pathologist George Lignac was first to provide a clear systematic description of the disease, and the first to associate rickets, growth retardation and renal damage as major symptoms linked to cystinosis. This is why cystinosis was originally termed as Abderhalden-Kaufmann-Lignac syndrome. The swiss pediatrician, Guido Fanconi also significantly contributed to the understanding of the cystinosis pathophysiology by explaining the urinary substance losing features of the disease. Cystinosis was also described in the literature as the Lignac-Fanconi syndrome for a period of time [2].
Cystinosis is an autosomal recessive disorder belonging to the family of lysosomal storage diseases. It is caused by mutations in the *CTNS* gene, which encodes for the lysosomal cystine transporter cystinosin, transporting cystine from the lysosome into the cytoplasm [2]. Mutations in this gene result in accumulation of the amino acid cystine in the lysosomes throughout the body, revealing systemic organ damage [3]. Cystinosis is the leading cause of renal Fanconi syndrome in young patients, accounting for approximately 20% of the cases of hereditary tubular disorders [4]. Patients with cystinosis develop symptoms of renal Fanconi syndrome and typically progress to end stage renal disease (ESRD) within the first 12 years of life.

ETIOLOGY AND GENETICS

Cystinosis is a rare, but severe monogenic autosomal recessive disorder caused by mutations in *CTNS* (17p13.2), encoding the lysosomal H^+/cystine symporter cystinosin, resulting in lysosomal cystine accumulation throughout the body [5]. Since the mapping and cloning of the *CTNS* gene, over 140 pathogenic mutations have been reported so far in the literature [6-8]. The most commonly detected pathogenic mutation within North European and North American is the 57-kb deletion mutation. In this mutation, the first 9 exons and a part of the 10th exon of *CTNS*, the entire sedoheptulose kinase gene (*SHPK*; also known as *CARKL*), and part of the adjacent transient receptor potential vanilloid 1 gene (*TRPV1*) are deleted [9-11]. However, the effects of the deletion of *CARKL* and *TRPV1* genes in patients with 57-kb deletion mutation is yet not fully understood [12]. Of note, this founder mutation is almost completely absent in any studies from the Middle East or Africa [13-17]. The c.681G>A mutation in the exon 9 of the *CTNS* gene, however, is the most prevalent and possibly a founder mutation in countries of the Middle East [8, 18]. Moreover, approximately 15% of cystinotic patients worldwide carry a non-sense mutation. The most common non-sense mutations is W138X, which results in a premature termination codon in the 7th exon of the *CTNS* gene [19].

It is worth mentioning that the severity of cystinosis disease correlates with specific *CTNS* mutations [20]. Severe or truncating mutation usually lead to the infantile form of the disease, while other mild mutations are associated with juvenile and ocular forms of cystinosis [21]. Figure 1 demonstrates a summary of the *CTNS* gene mutations identified and reported in the literature and indexed in the Human Gene Mutation Database (HGMD®).

CLINICAL PRESENTATION

There are three clinical forms of cystinosis; infantile (nephropathic) cystinosis, Juvenile (late-onset) cystinosis and adult (ocular) cystinosis. Nephropathic cystinosis (OMIM 219800) is the most common (95% of all patients) and the most severe form of cystinosis. The first clinical sign of nephropathic cystinosis develops during infancy (age of ~6 months) in the form of renal Fanconi syndrome, accounting for almost 20% of the cases of hereditary tubular disorders [3]. Without specific treatment, patients develop progressive renal damage leading to ESRD by the age of 10. Patients with juvenile cystinosis (OMIM 219900), however, are usually diagnosed during their late childhood or adolescence. They present with the same clinical manifestation as those of nephropathic cystinosis, but with a much slower disease progression. The adult, non-nephropathic ocular form of cystinosis has no systemic involvement and is characterized only by photophobia due to cystine crystal deposition in the cornea. In the next sections, a detailed overview of the cystinosis clinical manifestations and complications is given [22, 23] (Figure. 2).

1. RENAL MANIFESTATIONS

Failure of proximal tubule cells due to the early loss of expression of apical proximal tubular cell receptors megalin/cubilin, the phosphate transporter NaPi-IIa, and the SGLT-2 glucose transporter, provides an explanation why renal complications are the major symptoms of cystinosis [24]. By the age of 6 to 12 months, proximal tubular dysfunction develops into full blown renal Fanconi syndrome, characterized by excessive urinary loss of amino acids, potassium, bicarbonate, sodium, magnesium, calcium, carnitine, phosphate, glucose and low molecular weight proteins. Moreover, patients with nephropathic cystinosis also present hypokalemia, metabolic acidosis, hypophosphatemia, hypocalcemia, low carnitine levels and less frequently hyponatremia. Infants present with polyuria, polydipsia, failure to thrive, severe dehydration, constipation, vomiting, and electrolyte imbalance [25].

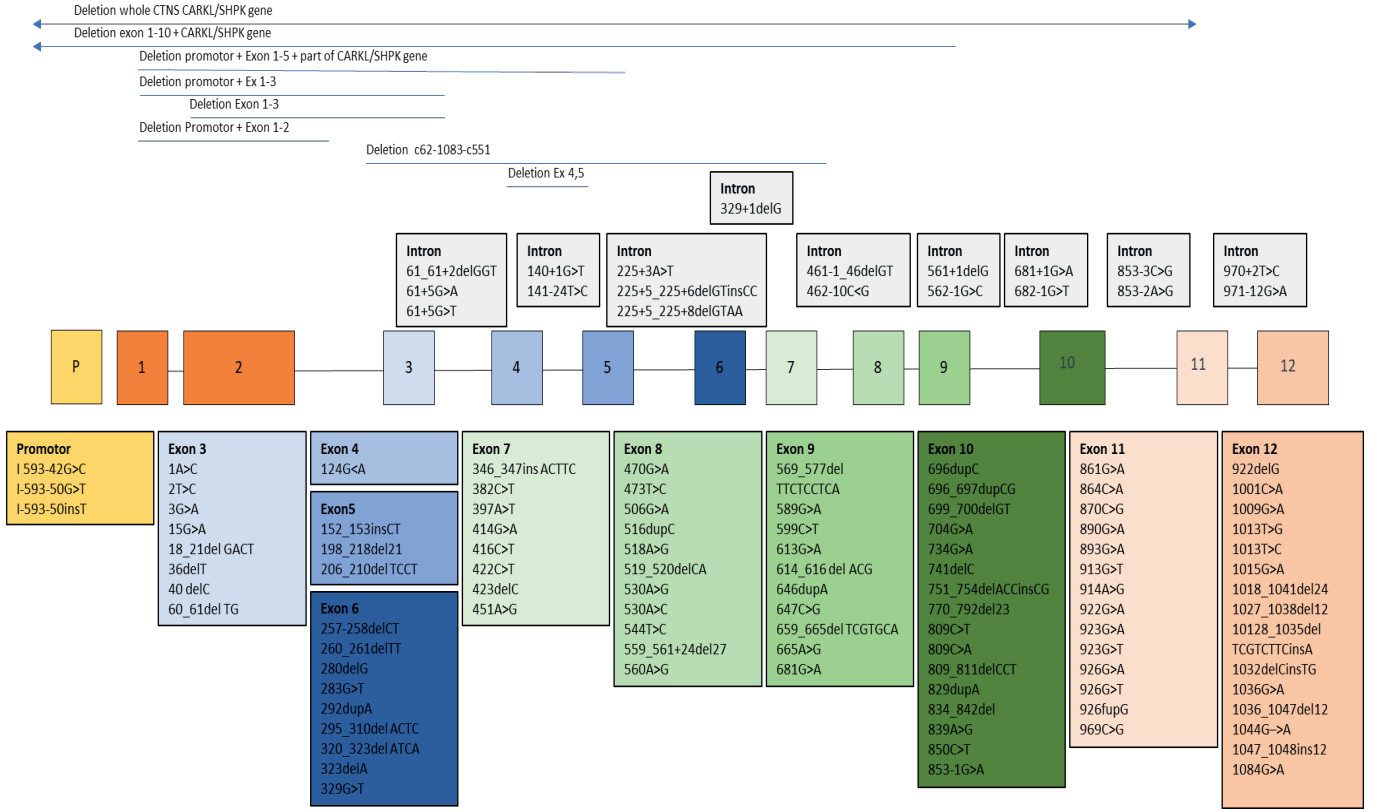

FIGURE 1. Schematic representation of the reported mutations in the CTNS gene. Adapted from Elmonem et al. [127] and updated from the Human Gene Mutation Database (HGMD®).

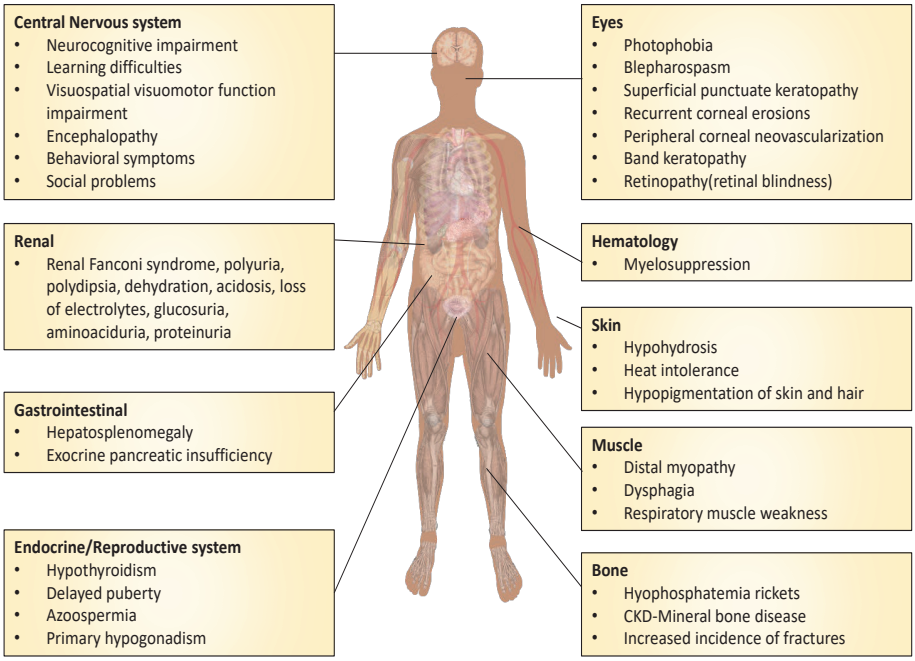

FIGURE 2. Cystinosis clinical manifestations and complications.

2. EXTRARENAL MANIFESTATIONS

Growth retardation and rickets

Growth retardation is a common symptom in young children with nephropathic cystinosis [26-30]. Coexisting renal and gastrointestinal complications, endocrine alterations, and poor nutrition all contribute to the delayed growth in cystinotic children. In addition, phosphaturia as well as decreased renal vitamin D conversion due to impaired activity of alpha-1 hydroxylase in kidney proximal tubules often leads to severe hypophosphatemia and vitamin D-resistant rickets [31, 32]. Although early initiation and adequate adherence to cysteamine therapy significantly reduces growth retardation, cystinotic children who underwent a renal transplantation are considerably shorter than matched non-cystinotic children with renal transplants [33].

Eye symptoms

Corneal cystine accumulation with crystal formations was first reported in literature by Burki, in 1941 [34]. Photophobia is the most common ocular symptom, and it is thought to be associated with the accumulation of cystine in the cornea, however, the exact pathological mechanism is yet to be explored. The needle-shaped cystine crystals can be observed from the age of 12-18 months through a slit lamp examination that progressively accumulate with age, leading to ocular symptoms including blepharospasm,

keratopathies, and recurrent corneal erosions. Peripheral corneal neovascularization and band keratopathy are also reported to be more prominent in older cystinotic patients [35-37]. Cystine crystal deposition in other tissues of eye including conjunctiva, lens and the retina may lead to retinopathy or vision loss if untreated [38-41].

Endocrine symptoms

Hypothyroidism is the most common endocrine complication in cystinotic patients, manifesting in 50% to 70% of the patients in the second decade of life. If left untreated, hypothyroidism results in growth retardation, that could be managed by hormone replacement therapy. Exocrine and endocrine pancreatic insufficiency is common in 5% of cystinotic patients that may progress to type 1 diabetes mellitus by age 20 or 30 [42-44]. Male cystinosis patients are usually infertile and develop hypergonadotropic hypogonadism and azoospermia despite an early initiation of cysteamine treatment [27, 45, 46]. Female patients, on the other hand, have pubertal retardation but are usually fertile [47]. Moreover, splenomegaly and hepatomegaly have also been reported in cystinotic patients, as a result of lysosomal cystine accumulation and Kupffer's cells enlargement.

Neurocognitive symptoms

Patients with cystinosis are shown to have normal intelligence quotient (IQ) levels [48-51]. However, central nervous system involvement have shown to be present in young children and becomes more frequent with advancing age, suggesting an early influence of *CTNS* loss-of-function on neural development rather than a long-term effect of cystine accumulation [52]. The neurological impairment is evident as cystinotic patients perform poorly in short-term visual memory, visuomotor and visuospatial skills [53]. Accordingly, Bava *et al.* reported visual processing deficits in children with cystinosis, associating it with early microstructural changes in the white matter integrity in the inferior and superior parietal lobules of the patients [54]. These visual processing deficits combined with poorly maintained planning, attention, and motor processing lead to an overall poor academic achievement in school-aged patients [48], and are often linked to social and behavioral problems [33, 49]. Other neuropathological complications include, but are not limited to, cerebral atrophy [45, 55-57], non-absorptive hydrocephalus[58], intracranial hypertension [59], demyelination of white matter [33], and encephalopathy [60].

Distal and respiratory muscle weakness

Gahl *et al.* was first to describe myopathy in cystinosis in 1988 [61]. The prevalence of myopathy in patients with nephropathic cystinosis varies between 24 to 60% [62, 63]. However, due to limited data reporting distal myopathy in cystinosis, its etiology is far from understood [61, 64, 65]. Accumulation of cystine in muscle fibers is shown to result in formation of phagocytic vacuoles, rather than crystals [63]. While some other symptoms such as sleep apnea and swallowing difficulties negatively affect the quality of

life of patients, other serious complications, such as respiratory failure and respiratory muscle weakness, may lead to patients' death [62, 66].

Hematological symptoms

Only few cases have reported the involvement of the symptomatic bone marrow in cystinotic patients, though this is very uncommon [67]. Accumulation of cystine crystal in the bone marrow tissue could lead to pancytopenia and myelosuppression [68, 69].

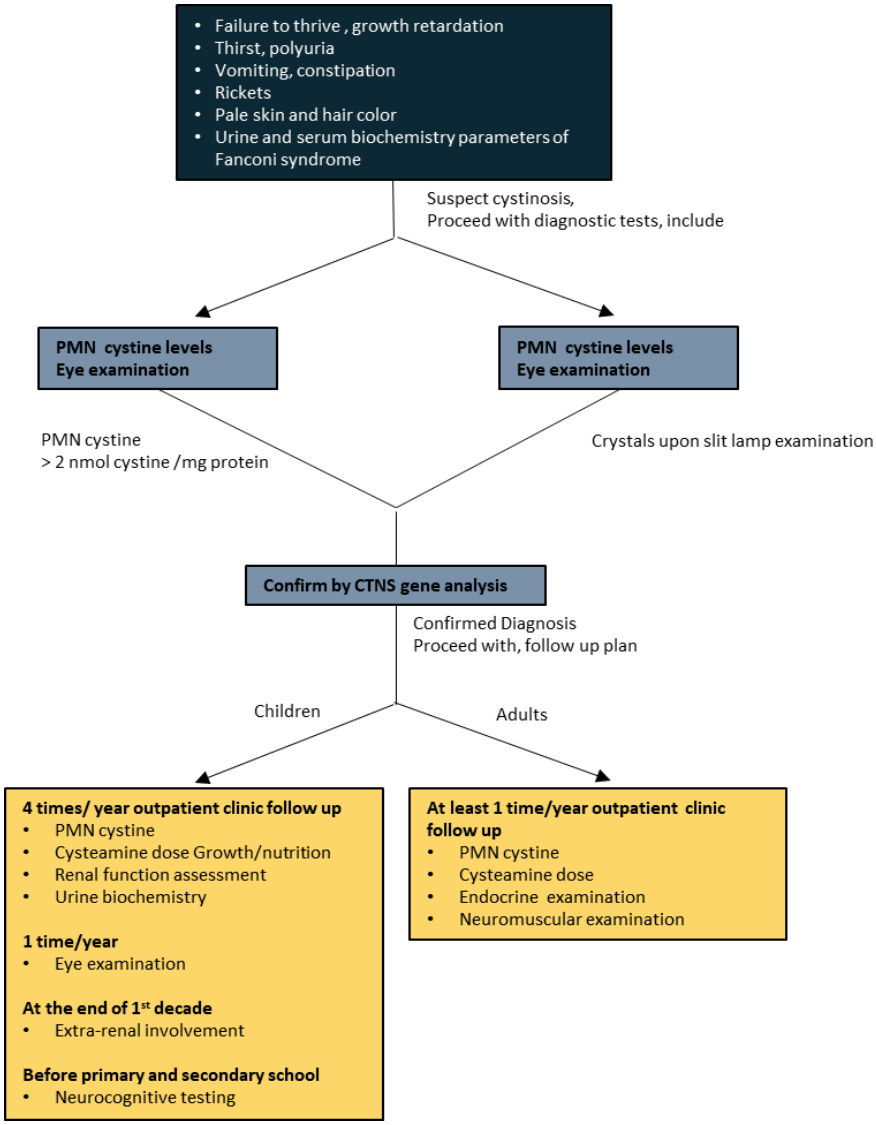

FIGURE 3. Outline for cystinosis diagnosis, and follow-up of patients with cystinosis. Adapted from Wilmer et al. [24]. PMN: polymorphonuclear cells.

DIAGNOSIS AND TESTING

Early diagnosis of cystinosis is of high importance for the clinical outcome of the patients. There are three clinically used modalities for diagnosing cystinosis. Elevated cystine content in white blood cells is the gold standard technique for diagnosis of cystinosis. Detection of the characteristic corneal cystine crystals by slit lamp examination is yet another diagnostic modality. Although relatively cheap and reliable, it requires an experienced ophthalmologist to identify and grade corneal cystine crystals properly. More importantly, corneal cystine crystals are pathognomonic, and can be absent until the second year of life, which could delay the start of the therapy in patients [24]. The last clinically used confirmatory option is genetic testing of the *CTNS* gene. It is a well-established process revealing 95% of disease-causing mutations. Figure 3 shows the outline for cystinosis diagnosis, and follow-up of patients with cystinosis.

CURRENT TREATMENT

The mainstay for cystinosis treatment is life-long therapy with cysteamine, a cystine depleting agent [70]. In lysosomes, cysteamine reacts with cystine, leading to the formation of cysteine and cysteine-cysteamine molecules which are exported out of the lysosome via the cysteine transporter and the PQLC2 transporter, respectively [70, 71]. Immediate-release cysteamine bitartrate (IR-CYS) (Cystagon®, Mylan Pharma, Morgantown, WV, USA and Orphan Europe, Paris, France) is the most commonly used cysteamine preparation.

Cysteamine slows down the progression of renal deterioration, delays the progression to ESRD by 6 to 10 years and the need for renal transplantation during childhood [72]. Early initiation and adequate adherence to cysteamine therapy has also been shown to postpone or prevent the development of some extra-renal complications. It reduces myopathy and the need for thyroid hormone replacement therapy, delays pancreatic and pulmonary dysfunction, and improves the growth retardation [48, 72-74]. Despite the fact that adequate cysteamine therapy can prevent or delay the complications of cystinosis, it is not curative [75]. The established proximal tubular dysfunction associated with cystinosis, hypogonadism or corneal cystine accumulation are not resolved by cysteamine therapy [75, 76]. This can be explained by the fact that cysteamine mainly acts by lowering lysosomal cystine levels but does not replace cystinosin. Moreover, emerging evidence highlights a multifaceted impact of cystinosin loss-of-function; including increased apoptosis, oxidative stress, and impaired energy metabolism and autophagy that further add to the complexity of cystinosis pathophysiology (see details in chapter 2. Molecular mechanisms underlying nephropathic cystinosis).

MODELS TO STUDY CYSTINOSIS PATHOGENESIS

Although the dysfunction in cystinosin and the subsequent intra-lysosomal accumulation of cystine have long been identified as the basic mechanism underlying cystinosis disease, the complex network of subsequent pathological processes contributing to the disease pathology remains largely unknown. To better understand different pathological mechanisms contributing to cystinosis, several *in vitro* and *in vivo* models of cystinosis have been developed (Table. 1).

In vitro models

Our current understanding of the pathogenesis of cystinosis is largely based on *in vitro* cell models. The pioneering studies which established intra-lysosomal accumulation of cystine as the hallmark of cystinosis were mainly performed on human cystinotic leukocytes [77], fibroblasts [78], or other lymph node cells [79]. Moreover, due to their relative availability, cystinotic skin fibroblasts are commonly used to study cystinosis pathology. Cystinotic fibroblasts have been shown to accumulate cystine, have decreased ATP content [80], increased apoptosis [81, 82] and altered glutathione metabolism [83-85]. However, these cell types typically lack the renal phenotype and cannot be used to evaluate the transcellular transport under various stimuli [86]. To overcome these issues, many researchers use cultured cells loaded with cystine dimethyl ester (CDME) as *an in vitro* cystinosis model [87-92]. Foreman *et al.* preincubated isolated rat renal tubule cells with CDME, which resulted in a significant elevation in cystine levels, similar to that observed in cystinotic patients [88, 89, 93]. Comparable results were observed in isolated rabbit renal proximal tubules loaded with CDME, in addition to inhibition of active transport of glucose and bicarbonate [87, 90]. However, a direct toxic effect on mitochondrial ATP, an increase in superoxide radicals and a dose dependent reduction in viability has been demonstrated upon CDME loading in fibroblasts [89, 93, 94]. Although oxidative stress has been shown to be a part of the cellular changes in cystinotic cells, these effects need to be confirmed as a part of the cystinosis pathology and not as inherent toxic effects of CDME loading [93, 94].

To overcome these drawbacks, researchers have attempted to culture cells directly from the kidneys of cystinotic patients. Pellet *et al.* initiated a primary cell line from fresh autopsy material of two pediatric cystinotic patients. However, in addition to its limited availability, these cells could only be grown in culture for 3-7 passages [95]. Biopsies from cystinotic patients can also be utilized, but are very limited in availability [96, 97]. Alternatively, renal epithelial cell cultures can be established from the cells exfoliated in human urine [98-100]. Racusen *et al.* established a proximal tubule cell culture from the urine of cystinotic patients. These cells displayed epithelial morphology and characteristics, and contained 100 times higher cystine levels than healthy controls [101, 102], which is comparable to the differences observed in cystinotic kidney tissue (60-350 folds) [86, 103]. In addition, the cells responded to cysteamine treatment and cystine could be depleted. However, it was still a primary culture with a limited number of sub-culturing possible.

TABLE 1. *In vitro* and *in vivo* models of cystinosis.

Model	Cell type	Source	Advantages	Disadvantages	Reference
In vitro	**Human Blood cells**	Cystinotic patients	· Easy to withdraw · Shows cystine accumulation	· No renal phenotype	[77]
	Human Skin Fibroblasts	Cystinotic patients	· Easy to generate · Shows cystine accumulation	· No renal phenotype	[78]
	Human PTEC	Cystinotic patients	· Renal phenotype · Shows cystine accumulation	· Difficult to obtain due limited availability · Difficult to maintain in culture, only 3-7 passages	[95]
		Cystinotic patients	· Renal phenotype · Shows cystine accumulation	· Difficult to obtain due limited availability	[96, 97]
		Cystinotic patients	· Renal phenotype · Can be used to study tubular function · Shows cystine accumulation	· Limited proliferation · Should obtain control cells in parallel	[101, 102]
			· Renal phenotype · Can be used to study tubular function · Shows cystine accumulation	· Relatively low cystine accumulation · Controls are non-isogenic	[104]
			· Renal phenotype · Can be used to study tubular function · Shows cystine accumulation	· High cystine accumulation · Controls are non-isogenic · Immortalized	[101, 105]
		siRNA knockdown	· Shows cystine accumulation · Isogenic	· High level of clustering of endosomal vesicles interfere with many assays	[106]
		CRISPR knockout	· Renal phenotype · Shows cystine accumulation · Isogenic	· Reduced endocytosis is lacking	[107]
	Human Podocytes	Cystinotic patients	· Possibility to study podocyte pathology in cystinosis	· Patient-related variability	[108]

TABLE 1. Continued.

Model	Cell type	Source	Advantages	Disadvantages	Reference
		siRNA knockdown urinary podocytes	· Reduced variability		
	Isolated rabbit PTEC	siRNA knockdown	· Renal phenotype · Reduced variability		[109, 110]
		CDME loading	· Can be used to study perfusion	· Inherent toxic effects of CDME might interfere with analysis	[87, 91]
	Mouse skin Fibroblasts	Cystinotic mouse	· Shows cystine accumulation	· No renal phenotype	[111, 112]
In vitro	**Human kidney organoids**	iPSC from cystinotic patients	· Renal phenotype · Cystinotic phenotype	· Glutathione levels are unchanged · mTORC1 pathway is unaffected	[113]
		CRISPR knockout	· Renal phenotype · Cystinotic phenotype · Reduced variability	· Glutathione levels are unchanged · mTORC1 pathway is unaffected	
	Human kidney Tubuloids	Cystinotic patients	· Renal phenotype · Cystine accumulation	· Not fully characterized	[107]
	FVB/N mice		· Possibility to study multiple organs	· No renal phenotype · Incomplete tubulopathy	[114]
	C57BL/6 mice		· Possibility to study multiple organs · Shows renal phenotype	· No proximal tubular dysfunction	[115]
In vivo	**Zebrafish**	Morpholino knockdown	· Possibility of high throughput · Shows cystine accumulation, impaired autophagy and enhanced apoptosis	· Difficult to correlate with mammals · Difference in hemodynamics, physiology and organs (lack of lungs and mammary glands)	[116]
	Zebrafish	TALENs knockdown	· Possibility of high throughput · Shows cystine accumulation, impaired autophagy and enhanced apoptosis · Reduced variability	· Difficult to correlate with mammals · Difference in hemodynamics, physiology and organs (lack of lungs and mammary glands)	[117]

In an attempt to maintain proliferation, exfoliated renal cells have been transfected with HPV 16 E6/E7 or SV40T/hTERT [101, 104-106]. In HPV 16 E6/E7 immortalized cystinotic cells, the levels of cystine are only 10 folds higher than those in control cells [104, 105]. On the other hand, conditionally immortalized proximal tubular epithelial cells (ciPTEC) from cystinotic patients displayed an average of 37-fold higher levels of cystine as compared to ciPTEC from healthy individuals, which is closer to the differences observed in corresponding kidney tissues [105]. Additionally, ciPTEC have been shown of good utility to study the role of GSH metabolism in cystinosis pathology by comparing healthy and cystinotic cells [105, 118]. Nevertheless, healthy and cystinotic ciPTEC are provided by different donors and are non-isogenic. Therefore, the detected differences might be inherent to the individual differences between donors and not (completely) attributed to cystinosis pathology. In this thesis, we describe the generation of isogenic cystinotic ciPTEC using CRISPR/Cas9 technology to overcome this problem [107]. The model we developed exhibited robust cystinotic phenotypes of increased cystine accumulation and disrupted lysosomal-autophagy dynamics. Moreover, we have also established kidney tubuloids from urine samples of pediatric cystinotic patients demonstrating robust cystinosis phenotype [107]. Hollywood *et al.* also generated and characterized the first human induced pluripotent stem cell and kidney organoid models of cystinosis [113]. Organoids are of particular interest as they are three dimensional (3D) renal tubule epithelial cultures that offer physiological heterogeneity and recapitulate the *in vivo* situation. They are grown in 3D, allowing neighboring cells to interact in a more physiological way than in conventional 2D culture models. More importantly, they are not genetically modified or reprogrammed and can accurately mimic patients genotype and phenotype, allowing to develop personalized medicines [119].

In vivo models

Since cystinosis is a multisystem disorder, animal models have been utilized to study the pathological effects of cystine accumulation in the affected organs. Foreman *et al.* first reported modeling the cystinotic phenotype through lysosomal loading of CDME in adult rats [88]. A four-day twice daily regimen of 400 µmol parenteral CDME resulted in increased urinary volume, excretion of phosphate, glucose and amino acids, all symptoms of renal Fanconi syndrome [88]. Interestingly, HPLC analysis revealed elevated levels of intracellular cysteine, but not cystine, after 4 days of CDME administration. This questioned the role of cystine accumulation in the development of renal Fanconi syndrome in this model [86]. However, in a follow up study, an increase in intracellular cystine levels was observed in kidney homogenates of CDME treated rats, when analyzed using a cystine binding protein technique [120]. In addition, induction of oxidative stress was observed in young rats injected with CDME [89]. However, as previously mentioned, cystine-depleting therapy does not ameliorate cystinosis symptoms, indicating that cystine accumulation is not the only factor contributing to pathology, therefore, modeling cystinosis by merely loading the lysosomes with CDME ignores other contributing

factors and does not fully capture the spectrum of the disease pathology in cystinosis patients.

Cherqui *et al.* developed the first *CTNS*$^{-/-}$ mice knockout model by replacing the last four exons of *CTNS* by an IRES-βgal-neo cassette, using homologous recombination [121]. This mouse model has been shown to have cystine accumulation in all tissues tested (liver, kidney, muscle and brain) as well as ocular and skeletal muscles manifestations similar to those in cystinosis patients. Intriguingly, no proximal tubular dysfunction was observed in *CTNS*$^{-/-}$ mice up to 18 months, despite a high level of cystine accumulation [121]. However, congenic C57BL/6 *CTNS*$^{-/-}$ mouse models bred for 10 generations developed incomplete tubulopathy markedly different from that observed in cystinosis patients. In addition, this tubular dysfunction was not observed in congenic FVB/N *CTNS*$^{-/-}$ mice [115]. These results highlight the influence of genetic background on mouse renal phenotype and suggest the presence of modifier genes that rescue the disease phenotype in FVB/N *CTNS*$^{-/-}$ model [115, 122].

Recently, Elmonem *et al*. utilized anti-sense morpholino technology to develop a mutant zebrafish model with a homozygous nonsense mutation in the eighth exon of *CTNS*[116]. The mutant larvae showed cystine accumulation, enhanced apoptosis, delayed development and increased embryonic mortality. Moreover, reduced megalin expression, signs of glomerular and tubular dysfunction were observed, similar to the early disease manifestations in the human disease [116, 123]. This model holds promise for high throughput screening of new treatments for cystinosis *in vivo* [116, 124]. More recently, Festa *el al*. established a new cystinotic zebrafish model with a premature stop codon within the third exon of the *CTNS* gene, using transcription activator-like effector nucleases technique. Interestingly, although cystine accumulation and impaired lysosome-autophagy pathways were observed, the developing cystinotic zebrafish larvae displayed normal morphology with no developmental defects or proximal tubular dysfunction [117]. Although the zebrafish *CTNS* knockout model holds promise for high throughput screening of new treatments for cystinosis *in vivo* [116, 124], it is difficult to translate a therapeutic approach from zebrafish to mammals, due to different hemodynamics, physiology and the lack of some organs in zebrafish (such as lungs and mammary glands) [125, 126].

SCOPE AND OUTLINE OF THIS THESIS

Over the last decades, our understanding of cystinosis pathology has greatly extended beyond cystine accumulation. Recent studies based on *in vitro* and *in vivo* cystinosis models demonstrated that the loss of cystinosin is associated with disrupted autophagy dynamics, accumulation of distorted mitochondria and increased oxidative stress, leading to abnormal proliferation and dysfunction of kidney cells. Regardless of the observed cellular defects associated with the disease, the mechanism linking cystinosin loss and epithelial dysfunction remains largely unknown.

The aim of this thesis was to investigate and identify new pathologies and potential therapeutic approaches for nephropathic cystinosis. Following this introductory note, **chapter 2** reviews the novel insights on the molecular mechanisms driving nephropathic cystinosis as well as the link between cystinosin loss and the cellular defects. This information can be used to expand the knowledge on developing new treatment options for cystinosis. **In chapter 3,** a fast and reliable method to measure cystine in both healthy and cystinotic ciPTEC using liquid chromatography-tandem mass spectrometry is described. The method can be applied in screening potential drugs to reverse cystinotic symptoms, as well as in clinical studies as a diagnostic and biochemical follow-up tool. Further exploiting the pathophysiology of nephropathic cystinosis, in **Chapter 4** we combine the use of experimentally advanced *in vitro* and *in vivo* models, *viz.* human isogenic CRISPR-mediated *CTNS*$^{-/-}$ ciPTEC, primary adult stem cell-derived cystinotic tubuloids from pediatric patients, and cystinotic zebrafish with omics technologies (metabolomics and proteomics) to expand our knowledge on the complexity of the disease and prioritize drug targets in cystinosis. The study identifies novel pathways affected in cystinosis that cannot be restored by treatment with cysteamine. Further, it identifies alpha-ketoglutarate as an important metabolite linking cystinosin loss, autophagy, cell death, and proximal tubular impairment in cystinosis. The study also demonstrates the beneficial effect of the dual target therapy, combining cysteamine and an autophagy modulator, bicalutamide, as potential novel treatment for patients with cystinosis.

Continuing the emphasis on identifying cystinosis non-transport functions, **chapter 5** describes the interaction of the B1 subunit of the vacuolar H^+-ATPase (*ATP6V1B1*) with cystinosin in proximal tubules. Mutations in *ATP6V1B1* generally lead to distal renal tubular acidosis and hearing loss of variable degree. This study indicates that ATP6V1B1 is expressed not only along the human distal but also the proximal segments of the nephron, and identifies this enzyme as a central player in proximal tubule cells regulating cystine transport and autophagy. Finally, **Chapter 6** discusses gene repair as a new treatment option for cystinosis. A unique CRISPR/Cas9-based strategy, termed homology-independent targeted insertion (HITI) is used to repair and restore the *CTNS* gene function in cystinotic ciPTEC containing the large 57kb deletion. Restoring the *CTNS* gene function in kidney cells could provide a long-lasting cure for patients with cystinosis and prevent kidney function decline in the future. **Chapter 7** offers an up to date perspective on the findings described in this thesis, providing a comprehensive discussion as well as an overview on the current developments and trends in the field of cystinosis. To conclude, **chapter 8** presents a summary of the work in hand.

REFERENCES

1. Abderhalden, E., *Familiäre Cystindiathese,* in *Hoppe-Seyler´s Zeitschrift für physiologische Chemie*. 1903. p. 557.
2. Elmonem, M.A., et al., *Cystinosis: a review.* Orphanet Journal of Rare Diseases, 2016. **11**(1): p. 47.
3. Cherqui, S. and P.J. Courtoy, *The renal Fanconi syndrome in cystinosis: pathogenic insights and therapeutic perspectives*. Nature reviews. Nephrology, 2017. **13**(2): p. 115-131.
4. Cherqui, S. and P.J. Courtoy, *The renal Fanconi syndrome in cystinosis: pathogenic insights and therapeutic perspectives.* Nat Rev Nephrol, 2017. **13**(2): p. 115-131.
5. Rocca, C.J. and S. Cherqui, *Potential use of stem cells as a therapy for cystinosis.* Pediatr Nephrol, 2018.
6. Pape, L., et al., *Cystinose.* Der Nephrologe, 2017. **12**(3): p. 223-229.
7. Baumner, S. and L.T. Weber, *Nephropathic Cystinosis: Symptoms, Treatment, and Perspectives of a Systemic Disease.* Front Pediatr, 2018. **6**: p. 58.
8. Jaradat, S., et al., *Molecular analysis of the CTNS gene in Jordanian families with nephropathic cystinosis.* Nefrología (English Edition), 2015. **35**(6): p. 547-553.
9. Gahl, W.A., J.Z. Balog, and R. Kleta, *Nephropathic cystinosis in adults: natural history and effects of oral cysteamine therapy.* Ann Intern Med, 2007. **147**(4): p. 242-50.
10. Touchman, J.W., et al., *The Genomic Region Encompassing the Nephropathic Cystinosis Gene (CTNS): Complete Sequencing of a 200-kb Segment and Discovery of a Novel Gene within the Common Cystinosis-Causing Deletion.* Genome Research, 2000. **10**(2): p. 165-173.
11. Anikster, Y., et al., *Identification and detection of the common 65-kb deletion breakpoint in the nephropathic cystinosis gene (CTNS).* Mol Genet Metab, 1999. **66**(2): p. 111-6.
12. Freed, K.A., et al., *The 57 kb deletion in cystinosis patients extends into TRPV1 causing dysregulation of transcription in peripheral blood mononuclear cells.* J Med Genet, 2011. **48**(8): p. 563-6.
13. Soliman, N.A., et al., *Mutational Spectrum of the CTNS Gene in Egyptian Patients with Nephropathic Cystinosis.* JIMD Rep, 2014. **14**: p. 87-97.
14. Topaloglu, R., et al., *Genetic basis of cystinosis in Turkish patients: a single-center experience.* Pediatr Nephrol, 2012. **27**(1): p. 115-21.
15. Aldahmesh, M.A., et al., *Characterization of CTNS mutations in Arab patients with cystinosis.* Ophthalmic Genet, 2009. **30**(4): p. 185-9.
16. Shahkarami, S., et al., *The first molecular genetics analysis of individuals suffering from nephropatic cystinosis in the Southwestern Iran.* Nefrologia, 2013. **33**(3): p. 308-15.
17. Sadeghipour, F., et al., *Mutation analysis of the CTNS gene in Iranian patients with infantile nephropathic cystinosis: identification of two novel mutations.* Human Genome Variation, 2017. **4**: p. 17038.
18. Shotelersuk, V., et al., *CTNS mutations in an American-based population of cystinosis patients.* Am J Hum Genet, 1998. **63**(5): p. 1352-62.
19. Brasell, E.J., et al., *The aminoglycoside geneticin permits translational readthrough of the CTNS W138X nonsense mutation in fibroblasts from patients with nephropathic cystinosis.* Pediatr Nephrol, 2018.

20. Attard, M., et al., *Severity of phenotype in cystinosis varies with mutations in the CTNS gene: predicted effect on the model of cystinosin.* Human Molecular Genetics, 1999. **8**(13): p. 2507-2514.
21. Zykovich, A., et al., *CTNS mutations in publicly-available human cystinosis cell lines.* Molecular Genetics and Metabolism Reports, 2015. **5**: p. 63-66.
22. Servais, A., et al., *Late-Onset Nephropathic Cystinosis: Clinical Presentation, Outcome, and Genotyping.* Clinical Journal of the American Society of Nephrology : CJASN, 2008. **3**(1): p. 27-35.
23. Ariceta, G., et al., *A coordinated transition model for patients with cystinosis: from pediatric to adult care.* Nefrología (English Edition), 2016. **36**(6): p. 616-630.
24. Wilmer, M.J., et al., *Cystinosis: practical tools for diagnosis and treatment.* Pediatric nephrology (Berlin, Germany), 2011. **26**(2): p. 205-215.
25. Wilmer, M.J.E., F.; Levtchenko, E. N., *The pathogenesis of cystinosis: mechanisms beyond cystine accumulation.* Am J Physiol Renal Physiol, 2010. **299**(5): p. F905-16.
26. Van Stralen, K.J., et al., *Improvement in the renal prognosis in nephropathic cystinosis.* Clin J Am Soc Nephrol, 2011. **6**(10): p. 2485-91.
27. Winkler, L., et al., *Growth and pubertal development in nephropathic cystinosis.* Eur J Pediatr, 1993. **152**(3): p. 244-9.
28. Broyer, M., M.J. Tete, and M.C. Gubler, *Late symptoms in infantile cystinosis.* Pediatr Nephrol, 1987. **1**(3): p. 519-24.
29. Besouw, M.L., E., *Growth retardation in children with cystinosis.* Minerva Pediatr, 2010. **62**(3): p. 307-14.
30. Hertel, N.T., et al., *GROWTH RETARDATION AND URINARY LOSS OF GROWTH HORMONE IN CYSTINOSIS.* Pediatric Research, 1993. **33**: p. S39.
31. Elmonem, M.A., et al., *Cystinosis: a review.* Orphanet Journal of Rare Diseases, 2016. **11**: p. 47.
32. Bacchetta, J., et al., *Skeletal implications and management of cystinosis: three case reports and literature review.* BoneKEy Rep, 2016. **5**.
33. Ariceta, G., et al., *Cystinosis in adult and adolescent patients: Recommendations for the comprehensive care of cystinosis.* Nefrología (English Edition), 2015. **35**(3): p. 304-321.
34. Bürki, E., *Ueber die Cystinkrankheit im Kleinkindesalter unter besonderer Berücksichtigung des Augenbefundes.* Ophthalmologica, 1941. **101**(5): p. 257-272.
35. Tsilou, E.T., et al., *Age-related prevalence of anterior segment complications in patients with infantile nephropathic cystinosis.* Cornea, 2002. **21**(2): p. 173-6.
36. Gahl, W.A.K., E. M.; Iwata, F.; Lindblad, A.; Kaiser-Kupfer, M. I., *Corneal crystals in nephropathic cystinosis: natural history and treatment with cysteamine eyedrops.* Mol Genet Metab, 2000. **71**(1-2): p. 100-20.
37. Kaiser-Kupfer, M.I., et al., *Long-term ocular manifestations in nephropathic cystinosis.* Arch Ophthalmol, 1986. **104**(5): p. 706-11.
38. Richler, M., et al., *Ocular manifestations of nephropathic cystinosis. The French-Canadian experience in a genetically homogeneous population.* Arch Ophthalmol, 1991. **109**(3): p. 359-62.
39. Dufier, J.L., et al., *Ocular changes in long-term evolution of infantile cystinosis.* Ophthalmic Paediatr Genet, 1987. **8**(2): p. 131-7.
40. Liang, H., et al., *A New Viscous Cysteamine Eye Drops Treatment for Ophthalmic Cystinosis: An Open-Label Randomized Comparative Phase III Pivotal Study.* Invest Ophthalmol Vis Sci, 2017. **58**(4): p. 2275-2283.
41. Yamamoto, G.K., et al., *Long-term ocular changes in cystinosis: observations in renal transplant recipients.* J Pediatr Ophthalmol Strabismus, 1979. **16**(1): p. 21-5.

42. Robert, J.J., et al., *Diabetes mellitus in patients with infantile cystinosis after renal transplantation.* Pediatr Nephrol, 1999. **13**(6): p. 524-9.
43. Bäumner, S. and L.T. Weber, *Nephropathic Cystinosis: Symptoms, Treatment, and Perspectives of a Systemic Disease.* Frontiers in Pediatrics, 2018. **6**: p. 58.
44. Bernadette, M., et al., *Cystine accumulation attenuates insulin release from the pancreatic ß-cell due to elevated oxidative stress and decreased ATP levels.* The Journal of Physiology, 2015. **593**(23): p. 5167-5182.
45. Nichols, S.L., et al., *Cortical atrophy and cognitive performance in infantile nephropathic cystinosis.* Pediatr Neurol, 1990. **6**(6): p. 379-81.
46. Besouw, M.T., et al., *Fertility status in male cystinosis patients treated with cysteamine.* Fertil Steril, 2010. **93**(6): p. 1880-3.
47. Reiss, R.E., et al., *Successful pregnancy despite placental cystine crystals in a woman with nephropathic cystinosis.* N Engl J Med, 1988. **319**(4): p. 223-6.
48. Besouw, M. and E. Levtchenko, *Growth retardation in children with cystinosis.* Minerva Pediatr, 2010. **62**(3): p. 307-14.
49. Delgado, G., et al., *Behavioral profiles of children with infantile nephropathic cystinosis.* Developmental Medicine & Child Neurology, 2005. **47**(6): p. 403-407.
50. Trauner, D.A., et al., *Neurologic and cognitive deficits in children with cystinosis.* J Pediatr, 1988. **112**(6): p. 912-4.
51. Aly, R., et al., *Neurocognitive functions and behavioral profiles in children with nephropathic cystinosis.* Saudi J Kidney Dis Transpl, 2014. **25**(6): p. 1224-31.
52. Trauner, D.A.S., A. M.; Williams, J.; Babchuck, L., *Specific cognitive deficits in young children with cystinosis: evidence for an early effect of the cystinosin gene on neural function.* J Pediatr, 2007. **151**(2): p. 192-6.
53. Ballantyne, A.O. and D.A. Trauner, *Neurobehavioral consequences of a genetic metabolic disorder: visual processing deficits in infantile nephropathic cystinosis.* Neuropsychiatry Neuropsychol Behav Neurol, 2000. **13**(4): p. 254-63.
54. Bava, S., et al., *Developmental changes in cerebral white matter microstructure in a disorder of lysosomal storage.* Cortex, 2010. **46**(2): p. 206-16.
55. Cochat, P., et al., *Cerebral atrophy and nephropathic cystinosis.* Archives of Disease in Childhood, 1986. **61**(4): p. 401-403.
56. Ehrich, J.H., et al., *Evidence for cerebral involvement in nephropathic cystinosis.* Neuropadiatrie, 1979. **10**(2): p. 128-37.
57. Fink, J.K., et al., *Neurologic complications in long-standing nephropathic cystinosis.* Arch Neurol, 1989. **46**(5): p. 543-8.
58. Ross, D.L., et al., *Nonabsorptive hydrocephalus associated with nephropathic cystinosis.* Neurology, 1982. **32**(12): p. 1330-4.
59. Dogulu, C.F., et al., *Idiopathic intracranial hypertension in cystinosis.* J Pediatr, 2004. **145**(5): p. 673-8.
60. Broyer, M., et al., *Clinical polymorphism of cystinosis encephalopathy. Results of treatment with cysteamine.* J Inherit Metab Dis, 1996. **19**(1): p. 65-75.
61. Gahl, W.A., et al., *Myopathy and cystine storage in muscles in a patient with nephropathic cystinosis.* N Engl J Med, 1988. **319**(22): p. 1461-4.
62. Cheung, W.W., et al., *Muscle wasting and adipose tissue browning in infantile nephropathic cystinosis.* Journal of Cachexia, Sarcopenia and Muscle, 2016. **7**(2): p. 152-164.
63. Cabrera-Serrano, M., et al., *Cystinosis distal myopathy, novel clinical, pathological and genetic features.* Neuromuscul Disord, 2017. **27**(9): p. 873-878.
64. Charnas, L.R., et al., *Distal vacuolar myopathy in nephropathic cystinosis.* Ann Neurol, 1994. **35**(2): p. 181-8.

65. Kastrup, O., et al., *Myopathy in two siblings with nephropathic cystinosis.* Eur J Neurol, 1998. **5**(6): p. 609-612.
66. Sonies, B.C., et al., *Swallowing Dysfunction in 101 Patients with Nephropathic Cystinosis: Benefit of Long-Term Cysteamine Therapy.* Medicine, 2005. **84**(3): p. 137-146.
67. Gebrail, F., et al., *Crystalline histiocytosis in hereditary cysinosis.* Arch Pathol Lab Med, 2002. **126**(9): p. 1135.
68. Lyou, Y.Z., X.; Nangia, C. S., *Pancytopenia in a patient with cystinosis secondary to myelosuppression from cystine crystal deposition: a case report.* J Med Case Rep, 2015. **9**: p. 205.
69. Quinn, J.P., D. Royston, and P.T. Murphy, *Bone marrow findings in hereditary cystinosis with renal failure.* Am J Hematol, 2004. **76**(1): p. 79.
70. Ariceta, G., V. Giordano, and F. Santos, *Effects of long-term cysteamine treatment in patients with cystinosis.* Pediatr Nephrol, 2017.
71. Jezegou, A., et al., *Heptahelical protein PQLC2 is a lysosomal cationic amino acid exporter underlying the action of cysteamine in cystinosis therapy.* Proc Natl Acad Sci U S A, 2012. **109**(50): p. E3434-43.
72. Brodin-Sartorius, A., et al., *Cysteamine therapy delays the progression of nephropathic cystinosis in late adolescents and adults.* Kidney Int, 2012. **81**(2): p. 179-89.
73. Vaisbich, M.H. and V.H. Koch, *Report of a Brazilian multicenter study on nephropathic cystinosis.* Nephron Clin Pract, 2010. **114**(1): p. c12-8.
74. Greco, M., et al., *Long-term outcome of nephropathic cystinosis: a 20-year single-center experience.* Pediatr Nephrol, 2010. **25**(12): p. 2459-67.
75. Cherqui, S., *Cysteamine therapy: a treatment for cystinosis, not a cure.* Kidney International, 2012. **81**(2): p. 127-129.
76. Viltz, L. and D.A. Trauner, *Effect of age at treatment on cognitive performance in patients with cystinosis.* J Pediatr, 2013. **163**(2): p. 489-92.
77. Schneider, J.A., K. Bradley, and J.E. Seegmiller, *Increased cystine in leukocytes from individuals homozygous and heterozygous for cystinosis.* Science, 1967. **157**(3794): p. 1321-2.
78. Schneider, J.A., et al., *Increased free-cystine content of fibroblasts cultured from patients with cystinosis.* Biochem Biophys Res Commun, 1967. **29**(4): p. 527-31.
79. Patrick, A.D. and B.D. Lake, *Cystinosis: electron microscopic evidence of lysosomal storage of cystine in lymph node.* J Clin Pathol, 1968. **21**(5): p. 571-5.
80. Levtchenko, E.N., et al., *Decreased Intracellular ATP Content and Intact Mitochondrial Energy Generating Capacity in Human Cystinotic Fibroblasts.* Pediatric Research, 2006. **59**: p. 287.
81. Park, M.A., et al., *Increased apoptosis in cystinotic fibroblasts and renal proximal tubule epithelial cells results from cysteinylation of protein kinase Cdelta.* J Am Soc Nephrol, 2006. **17**(11): p. 3167-75.
82. Park, M., A. Helip-Wooley, and J. Thoene, *Lysosomal cystine storage augments apoptosis in cultured human fibroblasts and renal tubular epithelial cells.* J Am Soc Nephrol, 2002. **13**(12): p. 2878-87.
83. Levtchenko, E., et al., *Altered status of glutathione and its metabolites in cystinotic cells.* Nephrol Dial Transplant, 2005. **20**(9): p. 1828-32.
84. Chol, M., et al., *Glutathione precursors replenish decreased glutathione pool in cystinotic cell lines.* Biochem Biophys Res Commun, 2004. **324**(1): p. 231-5.
85. Mannucci, L., et al., *Impaired activity of the gamma-glutamyl cycle in nephropathic cystinosis fibroblasts.* Pediatr Res, 2006. **59**(2): p. 332-5.

86. Wilmer, M.J., F. Emma, and E.N. Levtchenko, *The pathogenesis of cystinosis: mechanisms beyond cystine accumulation.* American Journal of Physiology-Renal Physiology, 2010. **299**(5): p. F905-F916.
87. Salmon, R.F. and M. Baum, *Intracellular cystine loading inhibits transport in the rabbit proximal convoluted tubule.* J Clin Invest, 1990. **85**(2): p. 340-4.
88. Foreman, J.W., et al., *Effect of cystine dimethylester on renal solute handling and isolated renal tubule transport in the rat: a new model of the Fanconi syndrome.* Metabolism, 1987. **36**(12): p. 1185-91.
89. Rech, V.C., et al., *Promotion of oxidative stress in kidney of rats loaded with cystine dimethyl ester.* Pediatr Nephrol, 2007. **22**(8): p. 1121-8.
90. Coor, C., et al., *Role of adenosine triphosphate (ATP) and NaK ATPase in the inhibition of proximal tubule transport with intracellular cystine loading.* J Clin Invest, 1991. **87**(3): p. 955-61.
91. Sakarcan, A., R. Aricheta, and M. Baum, *Intracellular cystine loading causes proximal tubule respiratory dysfunction: effect of glycine.* Pediatr Res, 1992. **32**(6): p. 710-3.
92. Cetinkaya, I., et al., *Inhibition of Na(+)-dependent transporters in cystine-loaded human renal cells: electrophysiological studies on the Fanconi syndrome of cystinosis.* J Am Soc Nephrol, 2002. **13**(8): p. 2085-93.
93. Wilmer, M.J., et al., *Cystine dimethylester model of cystinosis: still reliable?* Pediatr Res, 2007. **62**(2): p. 151-5.
94. Wilmer, M.J., L.P. van den Heuvel, and E.N. Levtchenko, *The Use of CDME in Cystinosis Research.* Neurochemical Research, 2008. **33**(11): p. 2373-2374.
95. Pellett, O.L., et al., *Renal cell culture using autopsy material from children with cystinosis.* In Vitro, 1984. **20**(1): p. 53-8.
96. Haq, M.R., et al., *Immunolocalization of cystinosin, the protein defective in cystinosis.* J Am Soc Nephrol, 2002. **13**(8): p. 2046-51.
97. Sansanwal, P., N. Kambham, and M.M. Sarwal, *Caspase-4 may play a role in loss of proximal tubules and renal injury in nephropathic cystinosis.* Pediatr Nephrol, 2010. **25**(1): p. 105-9.
98. Detrisac, C.J., et al., *In vitro culture of cells exfoliated in the urine by patients with diabetes mellitus.* J Clin Invest, 1983. **71**(1): p. 170-3.
99. Hintz, D.S., et al., *Tissue culture of epithelial cells from urine. I. Serum-free growth of cells from newborn infants.* Pediatr Pathol, 1984. **2**(2): p. 153-63.
100. Sutherland, G.R. and A.D. Bain, *Culture of cells from the urine of newborn children.* Nature, 1972. **239**(5369): p. 231.
101. Racusen, L.C., et al., *Renal proximal tubular epithelium from patients with nephropathic cystinosis: immortalized cell lines as in vitro model systems.* Kidney Int, 1995. **48**(2): p. 536-43.
102. Racusen, L.C., et al., *Culture of renal tubular cells from the urine of patients with nephropathic cystinosis.* J Am Soc Nephrol, 1991. **1**(8): p. 1028-33.
103. Gahl WA, Thoene JG, and S. JA, *Cystinosis: a disorder of lysosomal membrane transport.*, in *The Metabolic and Molecular Bases of Inherited Disease*, Scriver CR, et al., Editors. 2001. p. 5085–6108.
104. Wilmer, M.J., et al., *Elevated oxidized glutathione in cystinotic proximal tubular epithelial cells.* Biochem Biophys Res Commun, 2005. **337**(2): p. 610-4.
105. Wilmer, M.J., et al., *Cysteamine restores glutathione redox status in cultured cystinotic proximal tubular epithelial cells.* Biochim Biophys Acta, 2011. **1812**(6): p. 643-51.

106. Ivanova, E.A., et al., *Endo-lysosomal dysfunction in human proximal tubular epithelial cells deficient for lysosomal cystine transporter cystinosin.* PloS one, 2015. **10**(3): p. e0120998-e0120998.
107. Jamalpoor, A., et al., *Cysteamine-bicalutamide combination treatment restores alpha-ketoglutarate and corrects proximal tubule phenotype in cystinosis.* bioRxiv, 2020: p. 2020.02.10.941799.
108. Ivanova, E.A., et al., *Cystinosin deficiency causes podocyte damage and loss associated with increased cell motility.* Kidney Int, 2016. **89**(5): p. 1037-1048.
109. Taub, M. and F. Cutuli, *Activation of AMP kinase plays a role in the increased apoptosis in the renal proximal tubule in cystinosis.* Biochem Biophys Res Commun, 2012. **426**(4): p. 516-21.
110. Taub, M.L., J.E. Springate, and F. Cutuli, *Reduced phosphate transport in the renal proximal tubule cells in cystinosis is due to decreased expression of transporters rather than an energy defect.* Biochem Biophys Res Commun, 2011. **407**(2): p. 355-9.
111. Harrison, F., et al., *Hematopoietic stem cell gene therapy for the multisystemic lysosomal storage disorder cystinosis.* Mol Ther, 2013. **21**(2): p. 433-44.
112. Naphade, S., et al., *Brief reports: Lysosomal cross-correction by hematopoietic stem cell-derived macrophages via tunneling nanotubes.* Stem cells (Dayton, Ohio), 2015. **33**(1): p. 301-309.
113. Hollywood, J.A., et al., *Use of Human Induced Pluripotent Stem Cells and Kidney Organoids To Develop a Cysteamine/mTOR Inhibition Combination Therapy for Cystinosis.* J Am Soc Nephrol, 2020.
114. Cherqui, S.S., C.: Hamard, G.: Kalatzis, V.: Sich, M.: Pequignot, M. O.: Gogat, K.: Abitbol, M.: Broyer, M.: Gubler, M. C.: Antignac, C., *Intralysosomal cystine accumulation in mice lacking cystinosin, the protein defective in cystinosis.* Mol Cell Biol, 2002. **22**(21): p. 7622-32.
115. Nevo, N., et al., *Renal phenotype of the cystinosis mouse model is dependent upon genetic background.* Nephrol Dial Transplant, 2010. **25**(4): p. 1059-66.
116. Elmonem, M.A., et al., *Cystinosis (ctns) zebrafish mutant shows pronephric glomerular and tubular dysfunction.* Sci Rep, 2017. **7**: p. 42583.
117. Festa, B.P., et al., *Impaired autophagy bridges lysosomal storage disease and epithelial dysfunction in the kidney.* Nat Commun, 2018. **9**(1): p. 161.
118. Bellomo, F., et al., *Impact of atypical mitochondrial cyclic-AMP level in nephropathic cystinosis.* Cell Mol Life Sci, 2018. **75**(18): p. 3411-3422.
119. Schutgens, F., et al., *Tubuloids derived from human adult kidney and urine for personalized disease modeling.* Nat Biotechnol, 2019. **37**(3): p. 303-313.
120. Ben-Nun, A., et al., *Cystine loading induces Fanconi's syndrome in rats: in vivo and vesicle studies.* Am J Physiol, 1993. **265**(6 Pt 2): p. F839-44.
121. Cherqui, S., et al., *Intralysosomal cystine accumulation in mice lacking cystinosin, the protein defective in cystinosis.* Mol Cell Biol, 2002. **22**(21): p. 7622-32.
122. Kleta, R. and A. Medlar, *Cystinosis and Mickey Mouse.* Nephrology Dialysis Transplantation, 2009. **25**(4): p. 1032-1033.
123. Elmonem, M.A., et al., *Genetic Renal Diseases: The Emerging Role of Zebrafish Models.* Cells, 2018. **7**(9).
124. Outtandy, P., et al., *Zebrafish as a model for kidney function and disease.* Pediatric Nephrology, 2018.
125. Vliegenthart, A.D., et al., *Zebrafish as model organisms for studying drug-induced liver injury.* Br J Clin Pharmacol, 2014. **78**(6): p. 1217-27.
126. Santoriello, C. and L.I. Zon, *Hooked! Modeling human disease in zebrafish.* J Clin Invest, 2012. **122**(7): p. 2337-43.
127. Elmonem, M.A., et al., *Cystinosis: a review.* Orphanet J Rare Dis, 2016. **11**: p. 47.

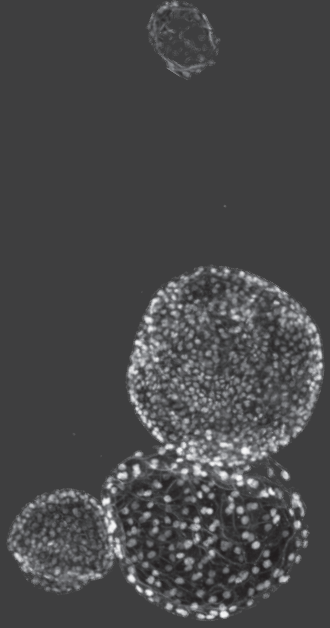

Molecular mechanisms underlying nephropathic cystinosis

2

Amer Jamalpoor[1¥], Amr Othman[1¥], Elena N. Levtchenko[2], Rosalinde Masereeuw[1], Manoe J. Janssen[1]

¥ These authors contributed equally to this work

[1]Division of Pharmacology, Utrecht Institute for Pharmaceutical Sciences, Faculty of Science, Utrecht University, 3584 CG Utrecht, The Netherlands. [2]Department of Pediatric Nephrology & Growth and Regeneration, University Hospitals Leuven & KU Leuven, Leuven, Belgium.

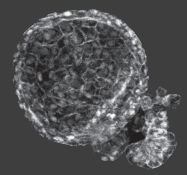

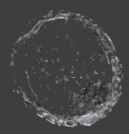

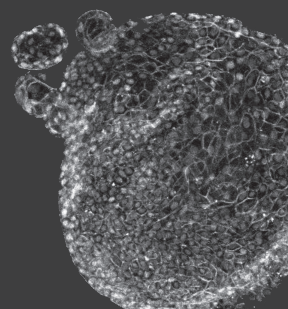

Submitted

ABSTRACT

Nephropathic cystinosis is a severe monogenetic systemic disorder that presents itself early in life and leads to progressive organ damage, particularly the kidneys. It is caused by mutations in the *CTNS* gene, encoding the lysosomal transporter cystinosin, resulting in intralysosomal accumulation of cystine throughout the body. Over the last decades, our understanding of cystinosis pathology has greatly extended beyond cystine accumulation. Recent studies based on *in vitro* and *in vivo* cystinosis models demonstrated that the loss of cystinosin is associated with disrupted autophagy dynamics, accumulation of distorted mitochondria and increased oxidative stress, leading to abnormal proliferation and dysfunction of kidney cells. Regardless of the observed cellular defects associated with the disease, the mechanism linking cystinosin loss and epithelial dysfunction remains largely unknown. In this review, we describe in detail the novel insights on the molecular mechanisms driving nephropathic cystinosis as well as the link between cystinosin loss and the cellular defects. Further, recent studies on genetic rescue of the disease, *in vitro* and *in vivo* are discussed. This information should aid in developing new therapeutic strategies for cystinosis.

Keywords:
Cystinosis, *CTNS* gene, lysosomal storage disorder, renal Fanconi syndrome, therapeutic management

INTRODUCTION

Key points

• Nephropathic cystinosis is a severe monogenetic systemic disorder caused by mutations in the lysosomal cystine/proton co-transporter, cystinosin; cystinosis is the leading cause of inherited renal Fanconi syndrome.

• Cysteamine treatment efficiently depletes lysosomal cystine and improves the clinical outcomes, however, it does not reverse established renal Fanconi syndrome, suggesting multiple roles for cystinosin, beyond the export of cystine.

• Mechanistic studies suggest a multifaceted impact of cystinosin loss-of-function in cystinosis pathology, involving increased oxidative stress, apoptosis, and impaired autophagy and energy metabolism.

• Several small molecules and biologics correcting non-transport functions of cystinosin are emerging and have shown to be effective either alone or in combination with cysteamine in in vitro and in vivo models of cystinosis.

• Hematopoietic stem cell (HSC) transplantation and translational readthrough drugs pose promising new treatment options for cystinosis, and the first clinical trial testing these therapies are currently ongoing.

Nephropathic cystinosis is a rare monogenic autosomal recessive disease belonging to the family of lysosomal storage disorders (LSDs). It is caused by mutations in the *CTNS* gene, which encodes for cystinosin, a proton/cystine co-transporter widely expressed on the lysosomal membrane. Defective cystinosin is unable to export cystine out of the lysosome into the cytoplasm. As a result, cystine gradually accumulates and forms crystals within the lumen of lysosomes. Given that cystinosin is widely expressed throughout the body, cystinosis is a systemic disease in which multiple organs are affected, however, the kidneys are the most functionally affected organ [1]. Cystinosis is the leading cause of inherited renal Fanconi syndrome (RFS) in young children, accounting for almost 20% of the cases of hereditary tubular disorders [2]. Patients with nephropathic cystinosis develop symptoms of RFS and typically progress to end stage renal disease (ESRD) within the first 12 years of life.

EPIDEMIOLOGY AND GENETICS

Cystinosis has a general incidence rate of 0.5-1/100.000 live births [3, 4]. Higher local incidence rates of cystinosis have been reported in Brittany (Northwestern, France) [4] and Saguenay (Québec, Canada) [5], due to the prevalence of specific *CTNS* mutations in these populations [2]. Since cystinosis is a monogenic autosomal recessive disease, patients normally have bi-allelic mutations in the *CTNS* gene (chromosome 17 p13.2) resulting in loss of functional cystinosin (also known as PQLC4) [1]. As a recessive disease, cystinosis incidence may be correlated with consanguinity. However, accurate epidemiologic data from countries with high levels of consanguinity (such as North Africa and the Middle East) are still lacking [6]. In addition, in other countries, underdiagnosis and improper reporting likely contribute to the low reported incidence of cystinosis [7].

Since the cloning and mapping of *CTNS*, more than 140 mutations have been described in literature [8]. The most prevalent mutation leading to loss of *CTNS* within northern Europe involves a 57-kb deletion of the first 9 exons, a part of the 10th exon and an entire gene upstream of *CTNS,* namely the sedoheptulose kinase gene (*SHPK*, also known as CARKL) [9]. Deletion of the promotor region and first ten exons completely abolishes gene function in these patients. More recently, this 57-kb deletion was found to extend to the adjacent transient receptor potential vanilloid 1 gene (*TRPV1*), leading to dysregulation of its transcription. However, the exact roles of *SHPK* and *TRPV1* in cystinosis pathology in patients with 57-kb deletion is still unclear [9]. Although the 57-kb deletion is the most common pathogenic *CTNS* mutation in Europe, this mutation has not been observed in any studies from the Middle East or Africa [10-14]. On the other hand, the c.681G>A splicing mutation, which involves the last base pair of exon 9 in *CTNS*, is the most prevalent mutation in countries of the Middle East and is a possible founder mutation [15]. In addition, around 15% of cystinosis patients worldwide carry a nonsense mutation [16]. The most common of these nonsense mutations is W138X that causes a premature termination codon in the 7th exon of *CTNS* [17]. It is worth mentioning that the severity of cystinosis disease correlates with specific *CTNS* mutations [18]. Severe truncations or large deletions often lead to infantile cystinosis, while other mutations allowing residual function of the protein are associated with milder forms and/or late onset of the disease [19].

CLINICAL PRESENTATION

There are three recognized clinical phenotypes of cystinosis; infantile nephropathic cystinosis, late-onset (juvenile) nephropathic cystinosis and ocular (adult) cystinosis. Infantile cystinosis (OMIM 219800) is the most common form with the most severe phenotype (95% of cystinosis patients). Although cystine accumulation starts *in utero*, patients with infantile cystinosis usually are asymptomatic at birth and have normal

development during the first 3-6 months of life [20]. However, these patients develop the manifestations of RFS and typically progress to ESRD within the first 12 years of their life when left untreated. On the other hand, patients with juvenile cystinosis (OMIM 219900) present with milder manifestations and with late onset as well as a lower rate of progression [21]. These patients are usually diagnosed in their childhood or during adolescence, but can also present as proteinuric CKD, and may maintain renal function until the age of 30-40 [22]. The renal involvement in the non-infantile patient is largely heterogenous, even within the same family [21]. Adult ocular cystinosis has no systemic involvement and manifests as isolated symptoms of photophobia resulting from cystine crystal deposition in the cornea.

In line with the systemic expression of cystinosin, there are many extra-renal manifestations of nephropathic cystinosis that affect the eyes, thyroid, pancreas, gonads, muscles, bones and central nervous system. Recently there has been special attention to the bone involvement in cystinosis. The effects on bone are severe and affect patients at different disease stages, with more than 10-fold increased risk of short stature, bone deformities and requirement of skeletal surgery compared with other CKD patients [23, 24]. While in infancy and early childhood poor nutrition, extensive urinary losses of calcium and phosphate and vitamin D deficiency cause poor growth rickets [25], along with CKD progression cystinosis patients develop a distinct form of CKD-MBD disorder characterized by ongoing phosphate losses and relatively low FGF-23 and PTH for CKD stages [26]. Furthermore, cystinosin deficiency was also found to directly affect bone cells (osteoblasts and osteoclasts) in mice, resulting in a bone loss independent from renal failure [27]. However, as the clinical manifestations of cystinosis are not the focus of this review, we would like to refer the reader to other excellent reviews for more detailed information on this topic [6, 21, 22, 28-31].

CURRENT TREATMENT

Up until now, there is no curative treatment for cystinosis and the available one aims at preventing and/or delaying renal and extra-renal manifestations and increasing the patients' life expectancy. The mainstay of cystinosis treatment is life-long treatment with cysteamine, a drug that effectively lowers cystine levels [32]. Cysteamine binds to lysosomal cystine and converts it into cysteine-cysteamine disulfide and cysteamine, which are exported out of the lysosome via the lysine/arginine (PQLC2) transporter and cysteine transporter, respectively [32, 33]. Early initiation and adequate adherence to cysteamine therapy is associated with increased life expectancy and fewer long-term complications in comparison to the patients who had no, delayed or inadequate treatment [34-36]. Cysteamine slows down the progression of renal deterioration, delays the onset of ESRD as well as the need for renal transplantation and significantly improves growth retardation, neuromuscular and endocrine manifestations associated with cystinosis [29, 34, 37, 38]. After renal replacement therapy the donor kidney is not

affected by the underying disease of the patietns and cystinosis patients demonstrate excellent kidney graft survival [39-42].
While each year of good compliance with cysteamine is estimated to prolong kidney function survival with one year, some complications, such as the visuomotor impairment, and established proximal tubular dysfunction are not improved by initiation of cysteamine [38, 43-45]. This can be attributed to the fact that cysteamine mainly acts by reducing lysosomal levels of cystine and as an antioxidant, but does not replace cystinosin. Moreover, emerging evidence highlights multiple cellular processes affected by the lack of cystinosin; including autophagy, apoptosis, and energy metabolism that further add to the complexity of cystinosis pathophysiology.

CYSTINOSIN IN HEALTH AND DISEASE

Cystinosin domains and isoforms

CTNS is located on the short arm of chromosome 17 and consists of 12 exons, of which the first two are non-coding. *CTNS* gene encodes for two main cystinosin isoforms that have different targeting motives, namely canonical cystinosin and cystinosin-LKG (Figure 1). The canonical cystinosin encodes a 367 amino-acid long protein comprising seven putative transmembrane α-helix domains, a luminal glycosylated N-terminal region, and a short cytosolic C-terminal GY-DQ-L motif. GY-DQ-L motif is responsible for the direct trafficking of cystinosin to late endosomes and lysosomes [46, 47], through the interaction with adaptor protein complex-3 (AP-3) [48]. Another targeting motif, YFPQA is located in the fifth inter-transmembrane loop of cystinosin and reinforces the association of cystinosin with the lysosomes [46, 49]. On the other hand, cystinosin-LKG is produced by alternative splicing, and is less abundant than the canonical cystinosin (around 5-20% of transcripts). The expression of cystinosin-LKG is highly variable among different tissues, and can account for up to 50% of all *CTNS* transcripts in certain tissues (such as in the testicles) [50]. Moreover, cystinosin-LKG is longer than the canonical cystinosin (400 amino-acids) and it has a plasma membrane targeting C-terminal SSLKG motif instead of GY-DQ-L motif, and thus has a different subcellular distribution. In addition to the lysosome, cystinosin-LKG also resides in the plasma membrane and the Golgi apparatus, where it mediates proton coupled cystine transport [47, 50]. Unlike the canonical cystinosin isoform, cystinosin-LKG can be also trafficked to the lysosome indirectly, by both clathrin-dependent and -independent endocytic retrieval from the plasma membrane [47]. A recent study showed that cystinosin-LKG has similar cystine lowering capacity as the canonical cystinosin [51]. However, it is still unclear if cystinosin-LKG can substitute the canonical cystinosin isoform [51]. Another unique feature of the cystinosin protein is the presence of conserved proline glutamine dipeptides known as PQ-motifs. The exact function of these PQ-motifs is still unclear, however, they may be essential for the cystine/proton symporter function of cystinosin, where cystine

transport is coupled to the reversible protonation of an aspartate residue in the second PQ-loop motif [52].

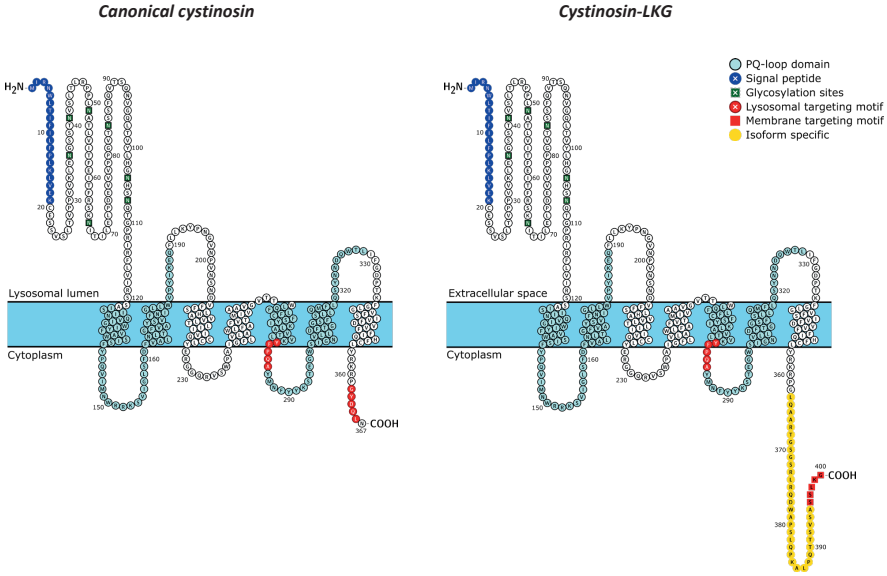

FIGURE 1. Schematic representation of the two cystinosin isoforms. Cystinosin has two protein coding isoforms, the canonical isoform (left), and cystinosin-LKG (right). The latter is produced by alternative splicing of exon 12. Both isoforms have the lysosomal targeting motif YFPQA, however, instead of the additional lysosomal targeting motif GYQDL in the canonical isoform, cystinosin-LKG comprises a plasma membrane targeting peptide (SSLKG). This results in a different cellular distribution of the two isoforms, where the canonical isoform is confined to the lysosome, while cystinosin-LKG is also present at the plasma membrane as well as Golgi apparatus. Information presented is based on Uniprot CTNS_HUMAN (O60931-1 and O60931-2). More splice variants have been predicted, but for these molecular and functional data is not available. PROTTER, an open source tool, was used to visualize the two isoforms of cystinosin [177].

Disruption of cystinosin results in the progressive accumulation of cystine in lysosomes, which exists in a soluble form until a certain threshold (approx. 5 mM), beyond which cystine crystals start to form and accumulate [2, 53]. Although the intra-lysosomal cystine accumulation and crystal formation is the hallmark of cystinosis, the exact role of this accumulation in the pathogenesis of cystinosis remains unclear [54, 55]. Crystals are not present in the lysosomes of *in vitro* cultured cystinotic cells, indicating that the process of cystine crystallization is slow [2]. In addition, cystine crystals are absent or rarely found in renal proximal tubule cells of children with cystinosis, instead these crystals are predominantly deposited in interstitial macrophages[56]. This suggests that cystine crystals are not the main factor contributing to the initiation of RFS. The rate limiting step of cystine transport is the number of cystinosin transporters in the lysosomal membrane. Most studies suggest that the level of residual cystine transport capacity is predictive of the severity of disease phenotype [8, 18, 57]. Nevertheless, other studies showed that

the mere presence of cystinosin, even with undetectable cystine transport capacity, presents with a milder phenotype than the 57-kb deletion, pointing to a more complex cellular function of cystinosin rather than a pure cystine-transporting protein [57]. In the next sections, we discuss recent insights into the molecular mechanisms driving nephropathic cystinosis, as shown in detail in Figure 2.

Energy metabolism

Multiple reports showed reduced levels of intracellular adenosine triphosphate (ATP) in cystinotic cells. Using a *CTNS* knockdown rabbit model, Taub *et al.* revealed an impaired apical sodium/phosphate (Na/Pi) reabsorption and reduced ATP, without affecting sodium–potassium adenosine triphosphatase pump (Na/K-ATPase). Since the apically transported Pi is directly used to form ATP, reduced Pi uptake in cystinosis may explain the observed reduction in intracellular ATP [58]. Decreased ATP levels but intact respiratory chain complex I to V activity, Na/K-ATPase activity, and overall energy secreting capacity was observed in fibroblasts from cystinotic patients [59, 60] and in cystinotic conditionally immortalized proximal tubular epithelial cells (ciPTECs) [61]. Conversely, Sansanwal *et al.* described fewer mitochondria, abnormal mitochondrial function, abnormal mitochondrial morphology and a decrease in ATP in cystinotic fibroblast and proximal tubular cells (PTCs) [62]. In addition, Bellomo *et al.* found significantly lower cAMP levels, complex I and IV activity and mitochondrial potential in cystinotic ciPTECs with a 57-kb deletion in *CTNS* as well as in ciPTECs with heterozygous loss of function [63]. Treatment with either non-hydrolysable cAMP analog, 8-Br-cAMP or cysteamine rescued the mitochondrial abnormalities. More recently, deregulation of several proteins involved in mitochondrial fusion and fission was observed in Ctns-/- ciPTECs. Additionally, a decrease in mitochondrial cristae number and an increase of cristae lumen and cristae junction width were observed. Some of these aberrations were not corrected by cysteamine, rendering cystinotic cells more susceptible to apoptosis[64]. Regardless of the conflicting literature on these mitochondrial abnormalities, the reduced intracellular ATP levels is consistently reported in cystinotic cells.

Adenosine monophosphate-activated protein kinase (AMPK) is a major regulator of energy homeostasis and highly sensitive to intracellular energy stores. Upon its activation, mainly by an increase in the ratio of either AMP or ADP to ATP, the enzyme induces a metabolic switch for multiple cellular pathways in an attempt to restore energy homeostasis by upregulating catabolic processes that produce ATP (such as glycolysis, fatty acid oxidation and autophagy) and reducing energy consuming anabolic processes (such as gluconeogenesis, lipogenesis and protein synthesis). Taub *et al.* reported reduced levels of ATP and activation of AMPK in a cystinosis knock-down model of rabbit proximal tubule cells. This activation of AMPK is associated with increased sensitivity of cystinotic cells to cisplatin, indicating that AMPK might play a role in regulating apoptosis in cystinosis [65].

Oxidative stress

Recently, the role of oxidative stress and altered glutathione (GSH) metabolism in cystinosis have gained much attention [66, 67]. This started when Rizzo *et al.* found elevated levels of pyroglutamic acid (5-oxoproline) in the urine of cystinotic patients. Pyroglutamate is an intermediate metabolite in ATP-dependent gamma glutamyl cycle, which is responsible for GSH synthesis [68]. GSH is a major cellular antioxidant that plays a crucial role in scavenging oxidants and protecting the cells against oxidative stress. Structurally, GSH is a tripeptide of glutamate, cysteine and glycine and is synthesized in a process involving two enzymatic reactions, each requiring one ATP molecule [69, 70]. As cystine is a source for cysteine in the cytoplasm, dysfunctional cystinosin and reduced cytoplasmic cystine have been proposed to cause reduced levels of GSH [2, 71]. Indeed, cystinotic fibroblasts showed significantly reduced levels of GSH and increased oxidative stress, and cysteamine or exogenous cysteine administration corrected the oxidative stress in cystinotic fibroblasts [72]. In addition, cystinotic fibroblasts exposed to hydrogen peroxide were unable to upregulate GSH in response to this oxidative stress environment [67]. However, in another study, cell lines established from urinary shed PTCs of cystinotic patients exhibited elevated levels of oxidative stress, observed as an increase in oxidized GSH, while the total GSH remained unchanged [73]. Furthermore, several studies have found that cystinotic cells demonstrate similar or higher levels of cysteine, indicating that it is most likely not cysteine depletion causing GSH alterations in cystinosis [61, 74-76]. Since the gamma glutamyl cycle is ATP-dependent, reduced ATP may also contribute to the observed impairment of GSH synthesis in cystinosis [77]. In accordance, ATP depletion led to a reduction in GSH levels and this reduction was more severe in cystinotic fibroblasts compared to normal cells [67]. Taken together, all these studies suggest that cystinotic cells are more vulnerable to oxidative stress as a result of impaired GSH synthesis and compromised gamma glutamyl cycle, possibly due to altered mitochondrial function and depleted ATP levels.

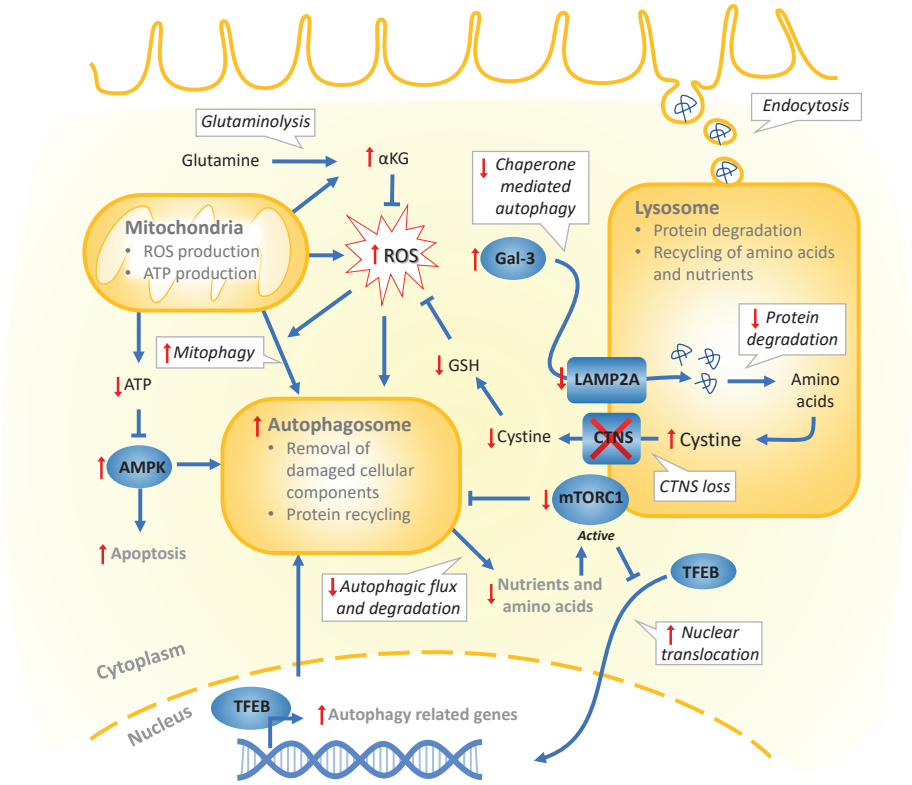

FIGURE 2. Molecular mechanisms underlying nephropathic cystinosis. Dysfunctional cystinosin leads to the accumulation of cystine within the lumen of the lysosome. As a result, it has been hypothesized that cytosolic cystine levels are reduced, leading to diminished GSH levels. Reduced levels of GSH result in inability of the cell to scavenge ROS, which puts the cells under oxidative stress, particularly the mitochondria, the site where most cellular ROS is produced. This results in an increased mitophagy, which may contribute to the increased apoptosis rates in cystinotic cells. Increased oxidative stress resulting from abnormal mitophagy can lead to epithelial dysfunction and dedifferentiation by promoting abnormal cell proliferation and repressing apical endocytic receptors. Increased oxidative stress was also shown to elevate the levels of αKG in cystinotic proximal tubule cells and patients, inducing autophagy and apoptosis. Another factor contributing to lowered GSH synthesis could be the diminished cellular ATP stores observed in cystinosis. As a result of low intracellular ATP, AMPK is activated, and subsequent inhibition of mTORC1, a downstream target of AMPK. mTORC1 inhibition results in increased TFEB nuclear translocation which activates autophagy. Although there is evidence demonstrating abnormal induction of autophagy, impairment of lysosome proteolysis due to defective lysosomal enzyme activation, postulate the lack of autophagy completion in cystinosis. Cystinosin loss-of-function together with disrupted chaperone mediated autophagy was also shown to result in galectin-3 overexpression in cystinotic mice kidneys, enhancing macrophage infiltration and CKD progression. AMPK: 5' adenosine monophosphate-activated protein kinase, ATP: adenosine triphosphate, GSH: glutathione, Gal-3: Galectin-3, LAMP2A: lysosome-associated membrane protein 2A, mTORC1: mammalian target of rapamycin complex 1, ROS: reactive oxygen species, TFEB: transcription factor EB.

This is consistent with data from other disease models in which mitochondrial dysfunction significantly affected GSH biosynthesis [78]. Being a major site of ROS production, mitochondria are more susceptible to damage [62] and together with the observed defective gamma glutamyl cycle and increased susceptibility of cystinotic cells to oxidative stress, this may explain the increase in mitophagy. Festa *et al.* demonstrated that, oxidative stress resulting from abnormal mitophagy stimulates Gα12/Src-mediated phosphorylation of tight junction protein Zonula occludin-1 (ZO-1), and its subsequent misrouting to the endolysosome leading to disrupted tight junction integrity [79]. As a result, ZO-1-associated Y-box factor ZONAB is released, and further leads to epithelial dysfunction and dedifferentiation by promoting abnormal cell proliferation and repressing apical endocytic receptors such as megalin [80]. Accordingly, Courtoy *et al.* reported progressive loss of megalin and cubulin expression in kidney samples from cystinotic patients [56]. They suggested that loss of PT endocytic function and cell differentiation in *Ctns*$^{-/-}$ mice temporally precedes apoptosis and development of the swan-neck deformity [56]. Similarly, several studies showed that the disruption in tight junction proteins triggers a cascade of events resulting in abnormal cell proliferation, reduced differentiation and repression of apical endocytic receptors, causing epithelial dysfunction in cystinosis [81-83]. Mito_TEMPO, a mitochondrial targeted antioxidant, restored the integrity, differentiation and transport function in cystinotic proximal tubular cells as well as in *Ctns*$^{-/-}$ mice [79]. On the other hand, Janssens *et al.* recently showed that blocking the uptake of disulfide-rich plasma proteins, through inhibiting megalin-mediated endocytosis, efficiently prevents accumulation of cystine and delays progression of kidney disease in *Ctns*$^{-/-}$ mice [84].

Apoptosis

Several studies reported an increased rate of apoptosis in cystinotic proximal tubules and cystinotic fibroblasts, as well as in cystinotic mutant zebrafish larvae [85, 86]. The rates of apoptosis also increased in response to pro-apoptotic stimuli such as UV light and tumor necrosis factor-α in cystinotic fibroblasts and renal proximal tubule epithelial cells [87]. In the kidneys of patients with cystinosis this increased rate of apoptosis is particularly evident as swan neck lesions, whereby apoptotic cell death and shedding of PTC leads to tubular atrophy[88, 89]. Cysteamine was able to reduce apoptosis in cystinotic cells and zebrafish larvae, which may be linked to its effects on the redox status in cystinosis (see section on oxidative stress) [62, 90]. Administration of mitochondrial targeted antioxidants such as Mitoquinone was shown to delay swan neck lesions in *Ctns*$^{-/-}$ mice, further signifying a link between apoptosis and oxidative stress [89].

The beneficial effect of cysteamine on apoptosis could also be a link to its capacity to reduce cystine load in the lysosomes [87]. Cystine levels in the cells have been linked to increased activation of pro-apoptotic proteins such as protein kinase C- delta type (PKC-δ). During early apoptosis, the lysosomes are permeabilized and it is suggested that the excess lysosomal cystine released during this phase leads to increased activation of pro-apoptotic proteins such as protein kinase C- delta type (PKC-δ) PKC-δ, by cysteinylation

and contributes to the observed increased apoptosis in cystinotic cells [87, 91]. However, a recent report using kidney organoids could not find a reduction in apoptosis after cysteamine treatment, but instead found a beneficial effect of the mTOR inhibitor everolimus, linking apoptosis to the increase in mTOR activation and autophagy [92]. The cellular processes contributing to apoptosis are likely dependent on the cell type studied, therefore the reported differences in the cellular processes contributing to apoptosis can be attributed to differences in study models and may also change depending on the cystine levels accumulating in the cells [85].

Autophagy

Autophagy is a highly conserved biological mechanism by which dysfunctional organelles and endogenous long-lived cytoplasmic proteins are catabolized via the lysosomal pathway. By degrading and recycling damaged organelles and proteins, autophagy provides new building blocks required for renewal of cellular components, and thereby is a crucial process for intaining homeostasis [93]. Considerable evidence reported abnormal autophagy activation in *in vitro* and *in vivo* models of cystinosis [94-98]. Defective cystinosin induces a major alteration in lysosomal autophagy dynamics, coupled to the impaired activity of mTOR signaling, and delayed lysosomal cargo degradation [80, 99].

The two mTORC1 and mTORC2 complexes are ubiquitously expressed in the kidneys, and play a central role in renal homeostasis, metabolism and proliferation as well as in renal diseases [100-102]. mTORC1 is a nutrient sensor that can be activated by amino acids and nutrients [103]. The pentameric Ragulator complex, and a group of small GTPases known as Ras-related GTP-binding proteins (Rag) GTPases are fundamental for mTORC1 activation as they coordinate recruiting mTORC1 to the lysosomal membrane. The lysosomal vacuolar ATPase (v-ATPase) proton pump is also necessary for amino acid activation of mTORC1, by interacting with the Rag-Ragulator complex [104]. In the presence of amino acids, these regulatory complexes activate mTORC1, triggering protein synthesis and inhibiting autophagy. On the other hand, amino acid starvation inactivates mTORC1, thereby activating autophagy to supply new building blocks, nutrients and energy [94]. Recently, the v-ATPAse, Rag-GTPase, and the Ragulator complex have been demonstrated to interact with cystinosin, suggesting that the absence of cystinosin itself may affect mTOR recruitment and activitation [95]. Ivanova *et al.* observed that the lack of functional cystinosin in human PTCs was associated with decreased retention of mTOR on the lysosomal membrane, and therefore defective mTOR signaling [96]. Similarly, a decreased mTOR activity was observed in PTCs derived from *Ctns*$^{-/-}$ mice, which was not rescued by cysteamine therapy[95]. Transcription factor EB (TFEB) is yet another major transcription factor regulating lysosomal biogenesis and autophagy [105, 106]. mTOR physically interacts with TFEB and is responsible for TFEB cellular distribution. Lysosomal-dissipated mTOR fails to phosphorylate TFEB, leading to TFEB nuclear translocation and therefore induction of lysosomal and autophagic genes expression [107]. In line with the defective mTOR activity and aberrant autophagy activation in cystinosis, increased TFEB

nuclear translocation has been found in cystinotic cells [106]. Rega *et al.* showed that the lack of cystinosin per se, and not cystine accumulation, reduced TFEB expression and induced TFEB nuclear translocation [106]. Overexpression of TFEB or its chemical activation using the phytoestrogen genistein reduced lysosomal cystine levels within 24 hours in PTC derived from cystinotic patient urine [106]. In addition to increased lysosomal cystine exocytosis, TFEB activation facilitated autophagic clearance of abnormal aggregates, an effect not observed with cysteamine treatment[106]. In line with previous studies, Jamalpoor *et al*. demonstrated a reduced mTOR activity with increase autophagy activation in CRISPR-generated and patient-derived cystinotic ciPTECs [75]. Using omics technologies, they also identified elevated levels of alpha-ketoglutarate (αKG) and decreased expression of the mitochondrial enzyme alpha-ketoglutarate dehydrogenase (AKGDH) as a unifying mechanism bridging cystinosin loss to autophagy activation in cystinosis. αKG is of particular interest due to its role in regulating ROS, apoptosis and autophagy [75, 108]. Generally, glutamine catabolism "glutaminolysis" yields αKG and activates mTORC1, thereby regulating autophagy. In cancer cells, Villar *et al.* showed that unbalanced activation of glutaminolysis during amino acid starvation leads to mTORC1 mediated apoptosis [109], highlighting a complex regulatory network involving apoptosis, autophagy and glutamate metabolism [97, 98]. Furthermore, studies on neurons have shown that the attenuated activity of AKGDH may cause prominent alterations in intracellular autophagic/apoptotic signaling [110, 111]. Long term reduction of AKGDH activity was associated with increased oxidative stress, activation of caspase 3 and consequent apoptotic/necrotic cell death [111, 112]. The increased levels of αKG was also evident in plasma of cystinotic patients, irrespective to their age, sex and type of mutations, further signifying the role of αKG in cystinosis pathology [110].

While the abovementioned reports show an abnormal induction of autophagy in cystinosis, the accumulation of the autophagy substrate SQSTM1 and the decreased lysosomal cargo processing postulate the lack of autophagy completion in cystinosis. This is in agreement with the recent studies demonstrating an impairment of autophagy flux in many LSDs, including cystinosis [92, 113, 114]. Jamalpoor *et al*. provided evidence that *CTNS* loss affects lysosomal function by hampering the delivery of newly synthesized lysosomal enzymes from Golgi to lysosomes and/or by inhibiting the maturation of these enzymes within (endo) lysosomal compartments. The latter hypothesis was further confirmed by Festa *et al*. where they have shown the impairment of lysosome proteolysis is a result of defective lysosomal enzymes activation in *in vitro and in vivo* model of cystinosis [79]. mTOR inhibition has been found to resolve the impaired autophagic flux observed in cystinotic cells. Utilizing recently developed iPSCs and organoids model for cystinosis, Hollywood *et al.* showed that an mTOR pathway inhibitor (everolimus) reduced the large lysosomes and activated autophagy, and in combination with cysteamine normalizing the cystine load [92]. Accordingly, Jounaidi *et al.* proposed that cystine export by cystinosin triggers a metabolic pathway that suppresses mTOR signaling and maintains autophagy during starvation. The starvation sensitivity phenotype of cystinosin knock out

models is rescued by reducing mTORC1 activity as well as the dietary supplementation of cysteine and the tricarboxylic acid (TCA) cycle components [115].
Contrary to macro-autophagy, where the autophagosome non-selectively sequesters bulk cytoplasmic organelles and components, the process of chaperone-mediate autophagy (CMA) is a highly selective process through which single proteins are tagged by a specific pentapeptide recognition motif to be degraded. These tagged proteins then bind a cytoplasmic chaperone complex, which delivers them to lysosomal receptors to be translocated into the lysosome allowing their degradation [116]. To date, lysosome-associated membrane protein 2A (LAMP2A) is the only known lysosomal receptor for CMA function. Interestingly, a recent study reported that that neonatal cystinotic mice fibroblasts demonstrate abnormal CMA with decreased LAMP2A expression, while maintaining normal macroautophagic flux as well as normal mTOR activity [117]. The decreased LAMP2A expression was corrected by cystinosin expression but not by cysteamine treatment [117]. It is worth noting that CMA is upregulated during oxidative stress to facilitate the efficient removal of irreversibly modified molecules [118]. Indeed, Zhang *et al.* demonstrated that CMA activators improve cystinotic cell survival which are under oxidative stress [119]. In addition, LAMP2A trafficking and distribution were found to be tightly regulated by cystinosin, Rab-11 and Rab-interacting lysosomal protein (a downstream effector of Rab7), which found downregulated and defective in cystinotic cells [119]. Interestingly, upregulation of Rab27a-dependent lysosomal trafficking resulted in reduced cystine accumulation as well as endoplasmic reticulum stress [120]. Taken together, impaired lysosomal autophagy dynamics as a result of cystinosin-loss-of-functions are emerging mechanisms contributing to cystinosis pathology.

Inflammation

Inflammation is generally associated with tissue infection or tissue injury. In chronic diseases, damaged tissues activate the immune system, resulting in inflammatory responses and, ultimately, tissue degeneration [121]. Cytokines are key modulators of inflammation and are able to activate the inflammation process [122]. In patients with chronic kidney disease (CKD), elevated plasma concentration of cytokines was associated with progression to ESRD [123].
Inflammasomes are a group of cellular protein complexes that recognize a diverse set of inflammation-inducing factors and closely control the maturation and production of the proinflammatory cytokines [124, 125]. The NLRP3 inflammasome is the most characterized inflammasome, and it is activated by diverse stimuli, including endogenous crystals, mitochondrial dysfunction, and the production of ROS, lysosomal destabilization, and potassium efflux have been shown to trigger its activation [126, 127]. Prencipe *et al.*, showed that accumulation of cystine in human peripheral blood mononuclear cells and *Ctns*$^{-/-}$ mice can indeed activate inflammasomes and, eventually, trigger inflammation and tissue fibrosis [54]. On the other hand, Elmonem *et al.* have recently identified the increased plasma chitotriosidase activity, an enzyme produced by activated macrophages, as a sign of non-inflammasome related inflammation in nephropathic

cystinosis [128]. Furthermore, Lobry *et al.* demonstrated a new role for cystinosin in inflammation through its interaction with the lectin and b-galactoside–binding protein family 21, galectin-3 (Gal-3) [129]. They provide evidence that, cystinosin loss-of-function results in Gal-3 overexpression in cystinotic kidneys, enhancing macrophage infiltration and CKD progression. Accordingly, Gal-3 was found to be markedly upregulated in acute tubular injury [130] and in progressive renal fibrosis [131], linking Gal-3 to macrophages activation and the promotion of renal injury in cystinosis. Gal-3 was also shown to be involved in quality control of endolysosomal organelles and kidney function [132, 133]. Jia *et al.* showed that, Gal-3 coordinates lysosomal repair and removal by activating autophagy and lysosomal biogenesis during cellular damage [132]. Hence, identification of the specific stimuli that trigger inflammatory responses can facilitate the discovery of potential drug targets in cystinosis.

NEW EMERGING THERAPIES

New formulations of cysteamine

Cystagon®, an immediate release formulation of cysteamine and the first available treatment for cystinosis, was approved by the FDA in 1994. Although Cystagon® effectively lowers cystine levels, it is associated with significant gastrointestinal symptoms (due to gastrin release and acid hypersecretion, alleviated by concomitant proton pump inhibitors [134, 135]), unpleasant sulfuric body and breath odor [136]. These side effects together with a strict dosing schedule (every 6 hours) substantially influence patients' adherence to treatment and can contribute to compromised clinical outcomes [136]. In 2013, Procysbi®, a delayed release formulation of cysteamine bitartrate, was approved by the FDA that bypasses the stomach and has a sustained absorption in the small intestine, resulting in reduced gastrointestinal side effects[135, 137]. In addition to being as equally effective as Cystagon [138], Procysbi® requires only a twice-daily dosing, and thereby significantly improves the patient's quality of life by relieving the burdens of interrupted sleep for night time dosing [137, 139].

However, Procysbi® still releases cysteamine in the gastrointestinal tract, hence is prone to first pass metabolism, and causes gastric disturbances [138]. In addition, the cysteamine metabolites dimethyl sulfide and methanethiol result in halitosis and poor sweat odors, affecting patient's compliance. Prodrugs of cysteamine are being investigated *in vitro* to increase metabolic stability, achieve a sustained cysteamine concentration and guarantee on-target release of cysteamine thereby reducing poor breath and sweat odors [140]. Esterified g-glutamyl-cysteamine prodrugs maintained the concentration of cysteamine at above baseline levels for at least 24 hours, indicating the potential for less frequent administration [141]. In addition, folate, glutaric acid, succinic acid and pegylate derivates of cysteamine, the disulfide derivative of cysteamine were shown to deplete the cysteine levels in cultured cystinotic fibroblast with higher

efficiency than cysteamine, and with no significant toxicity [142-144]. The potential use of these analogs as pro-drugs needs further investigation *in vitro* as well as *in vivo*.
Because the corneal tissue is non-vascularized, oral cysteamine has no effect on the ocular manifestations, and topical treatment is typically required. Although cysteamine hydrochloride eye drops (Cystaran®) effectively reduce corneal crystal, high frequency of administration (6-12 times per day) results in patient's suboptimal therapy adherence [145, 146]. In addition, formulations of cysteamine eye drops are easily oxidized, even at +4°C, rendering the formulation less effective, and adding the patient's lack of adherence [147]. Recently, a more viscous formulation (Cystadrops®) was shown to be more stable, while having a less frequent dosing regimen than the standard formulation [148, 149]. However, Cystadrops can only be kept for one week after first use. New hydrogel-based formulations of cysteamine were shown to increase the drug's ocular retention, promoting corneal absorption and reducing ocular irritation [150]. Additionally, the ocular Cys-NW (cysteamine nanowafer) also holds promise as a novel formulation offering a single daily dose with long shelf life stability (up to 4 months) compared to standard cysteamine eye drops [151].

Small molecules and biologics

Although cystine depleting therapy greatly improved the clinical outcomes of cystinosis, it is not a curative treatment, and it only delays the progression of complications but does not prevent them [2]. Growing evidence suggests multiple roles for cystinosin, beyond the export of cystine, which are not corrected by cysteamine treatment. A summary of potential treatments for cystinosis is represented in table 1.
Abnormal macroautophagic flux, reduced levels of TFEB, downregulation of mTOR, abnormal energy metabolism and impaired chaperone-mediated autophagy have all been reported in cystinosis and represent new avenues for potential treatments [2]. For example, small molecule CMA activators correct LAMP2A localization and are associated with enhanced cell survival in cystinotic mice embryo fibroblasts, suggesting their potential use in combination with cysteamine in cystinosis [117, 119]. AMPK inhibitors also pose as potential drug candidates to counteract the elevated levels of apoptosis observed in cystinotic cells [65]. Still, the effect of these emerging therapies should be interpreted cautiously given the multiple effects of the treatment on each of the abovementioned molecular pathways. For example, genistein favorably lowers cystine levels and activates TFEB [106], but it may further exacerbate the activation of AMPK and the inhibition of mTOR signaling already existing in cystinotic cells [95]. Bicalutamide, a non-steroidal anti-androgenic agent, was also shown to increase endogenous TFEB activity, restore endocytic cargo processing and αKG levels, and in combination with cysteamine, reversed the proteome and metabolic phenotype and efficiently normalized cystine levels in cystinotic PTCs. The combination therapy was also found beneficial in both patient-derived kidney tubuloids and cystinotic zebrafish, proposing the therapeutic potential of this combination therapy in treating patients with cystinosis [75]. Furthermore, luteolin, a natural flavonoid, was found to rescue the increased sensitivity to oxidative stress

TABLE 1. A summary of new emerging therapies in nephropathic cystinosis.

DNA level – Mutation or deletion in *CTNS*		
	• Direct gene therapy • Stem cell gene therapy (CTNS-RD-04)	Restores all functions of *CTNS* in the transduced cell
RNA level – Nonsense mediated decay		
	• ELX-02 • Geneticin	Restore production of functional cystinosin in case of premature stop codon
Protein level - Affected pathways due to cystinosin loss		
• Cystine transport from lysosomes	• Cysteamine	Lowers lysosomal cystine accumulation
• Reduced ATP production and increased oxidative stress	• Cysteamine • N-acetyl cysteine • 8-Bromo-cyclic AMP • Mitoquinone • Mito_TEMPO • Luteolin	Increase glutathione production, reduce ROS, and restore mitochondrial function
• Increased apoptosis	• Cysteamine • AMPK inhibitor • Everolimus • Luteolin	Reduce apoptosis
• Dysregulation of mTORC1 and autophagy	• Genistein • Everolimus • Biclutamide • CMA activators • Luteolin	Reduce lysosome size, activate autophagy, and improve lysosomal degradation

AMPK: Adenosine monophosphate-activated protein kinase, CMA: chaperone-mediated autophagy.

and the impaired lysosomal dynamics in both human and murine cystinotic PTCs [152]. Luteolin also improved reabsorption of endocytic cargoes in both human and murine cystinotic PTCs and in cystinotic zebrafish.

Additionally, improved clinical outcomes have been associated with cysteine and antioxidant supplementation, whereby a recent patient cohort showed that N-acetyl cysteine reduced oxidative stress and significantly improved renal functions with no detectable side effects. However, this evidence is limited and needs to be confirmed in larger studies [153]. Furthermore, mitochondrial targeted antioxidant such as Mitoquinone was shown to delay the initiation of swan neck lesion in C57BL/6 *Ctns*$^{-/-}$ mice [89]. Mito_TEMPO, yet another mitochondrial targeted antioxidant, restored the integrity, differentiation and transport function *in vitro* cultured cystinotic proximal

tubular cells as well as in *Ctns*$^{-/-}$ mice[79]. These results should be, however, carefully interpreted, in lights of the potential toxicities, as recently highlighted by Gottwald *et al.*, whereby mitoquinone was shown to result in mitochondrial swelling and depolarization in opossum kidney PTCs [154]. Additional tolerability tests as well as the evaluating the possibility of combination therapy with cysteamine should be considered.

Recently, Translational Read-Through-Inducing Drugs (TRIDs) have emerged as a new therapeutic approach for genetic diseases [155]. These compounds are able to bind to the mammalian ribosome and inhibit translation termination at the premature stop codon, by promoting insertion of near-cognate aminoacyl-transfer RNAs, thereby restoring the full-length mRNA and protein[155]. Since faulty mRNA with premature stop codons are unstable and liable for nonsense-mediated mRNA decay (NMD), this eventually results in an overall little or no mRNA available for TRIDs to perform their read through capabilities. Therefore, NMD inhibition has been suggested as an adjunctive therapy to TRIDs to improve the treatment efficiency [156]. Thus, it represents a plausible approach to use TRIDs to overcome the non-sense mutations in a considerable subpopulation of cystinosis patients[156]. While TRIDS originally aim at translational readthrough, some TRIDs have shown to be dually acting, also inhibiting NMD decay, warranting their use without a combination NMD inhibitors [17, 157, 158]. Indeed, Brasell *et al.* showed that geneticin, an aminoglycoside-based TRID, maintains normal *CTNS* mRNA levels, restores full-length functional cystinosin, and reduces cystine accumulation in patient fibroblasts with the W138X mutation [17], suggesting that NMD was fully inhibited by the drug. These results seem promising, especially in lights of the recent approval of Ataluren (Translarna®), another TRID for treating a subset of Duchenne muscular dystrophy patients[159]. More recently, an aminoglycoside-based TRID, ELX-02 (developed by Eloxx pharmaceuticals, Israel), was demonstrated to reduce renal cystine accumulation in a novel CtnsY226X nonsense mutant mouse, without overt renal toxicity [160]. Based on these *in vivo* results, Eloxx pharmaceuticals launched a phase 2 clinical trial for ELX-02 (NCT04069260, Table 2) in patients with cystinosis with nonsense mutation in at least one allele. Table 2 contains a summary of the clinical trial registry for current and emerging treatments for cystinosis.

TABLE 2. A summary of the clinical trial registry of current treatments in cystinosis.

NCT ID	Intervention	Age group	Phase	Status	Study aim	PR
Systemic cysteamine formulations						
01432561	Cystagon®	Adult, Older Adult	NA	Completed	Food effect on bioavailability of the drug	Yes [175]
02012114	Cystagon® Procysbi®	Child, Adult, Older Adult	NA	Unknown status	Compliance to cysteamine and neurological complications	No
00872729	Cystagon® Procysbi®	Child, Adult, Older Adult	Phase 1	Completed	Safety, tolerability, pharmacokinetics, pharmacodynamics	Yes
01000961	Cystagon® Procysbi®	Child, Adult, Older Adult	Phase 3	Completed	Pharmacokinetics, pharmacodynamics	Yes [138]
01733316	Cystagon® Procysbi®	Child, Adult, Older Adult	Phase 3	Completed	Safety and superior effectiveness	Yes
01197378	Procysbi®	Child, Adult, Older Adult	Phase 3	Completed	Long-term safety follow-up	Yes [137]
01744782	Procysbi®	Child	Phase 3	Completed	Safety, effectiveness in cysteamine treatment naive cystinosis patients	Yes
04246060	Procysbi®	Child, Adult, Older Adult	NA	Not yet recruiting	Observational study to assess the quality of life	No
Topical cysteamine formulations (eye drops)						
00001736	Cysteamine	Child, Adult, Older Adult	Phase 1	Completed	Safety, efficacy by corneal crystals score	No
00001213	Cysteamine	Child, Adult, Older Adult	Phase 2	Completed	Safety, efficacy by corneal crystals score	Yes
00010426	Cystaran®	Child, Adult	NA	Completed	Safety, efficacy by corneal crystals score	No
02766855	Cysteamine	Child, Adult	NA	Completed	Efficacy: improvement of photophobia, corneal cystine crystals and visual acuity	No

TABLE 2. Continued.

NCT ID	Intervention	Age group	Phase	Status	Study aim	PR
04125927	Cystadrops®	Child	Phase 3	Not yet recruiting	Safety, efficacy: corneal cystine crystal score and best corrected visual acuity	No
N-acetyl cysteine						
01614431	N-acetyl cysteine	Child, Adult	Phase 4	Completed	Verify the interference of N-acetyl cysteine in the progression of CKD in cystinosis patients	No
Translational read-through drugs						
04069260	ELX-02	Child, Adult, Older Adult	Phase 2	Recruiting	Safety, pharmacokinetics, and efficacy	No
Stem cell gene therapy						
03897361	CTNS-RD-04	Adult, Older Adult	Phase 1, Phase 2	Recruiting	Safety, tolerability, and efficacy	No

NCT ID: National Institute of Health (NIH) Clinical Trial identifier, NA: Not applicable.
PR: Published results. Age (in years): Child (birth-17), adult (18-64), and older adult (65+). Data is extracted from the clinical trial registry database of the NIH, United states [176].

Genetic rescue

Since cystinosis is a multisystemic disease caused by a defective *CTNS* gene, gene transfer with a functional *CTNS* gene has the potential to reverse the cystinotic phenotype. Hematopoietic stem and progenitor cell (HSPCs) transplantation is mainly applied to treat hematological disorders such as immunodeficiency diseases, blood or bone marrow malignancies. However, due to the ability of HSPCs to home to damaged tissues and exert favorable paracrine effects on the neighboring cells, HSPCs transplantation can be used for multisystemic non-hematological disorders [1]. To investigate whether stem cell transplantation can sustain functional cystinosin expression and rescue the disease phenotype, Syres *et al.* performed syngeneic bone marrow cell (BMC), hematopoietic stem cell (HSC), and mesenchymal stem cell (MSC) transplantation from wild-type donors in C57BL/6 *Ctns*$^{-/-}$ mice [161]. A large quantity of wild-type BMC was detected in all tested organs in *Ctns*$^{-/-}$ mice, ranging from 5% to 19% positivity all cells, and were mostly phagocytic in nature. In the kidneys, most of these cells were interstitial with no observed trans-differentiation into renal cells [162]. Overall, these effects reflected as a reduction in organ specific cystine levels by 57% to 94% in BMC-treated mice. Renal dysfunction and corneal cystine deposition in *Ctns*$^{-/-}$ mice was also prevented. Similar results were observed for HSC treated mice. On the other hand, MSCs did not integrate efficiently

in any of the organs tested, and only minor initial improvements were observed in MSC treated mice, followed by an increase in cystine accumulation. This initial improvement could be attributed to the protective paracrine effects of MSCs by secretion of several growth factors rather than cellular trans-differentiation and integration [161, 163-166]. Of note, all the mice were 2-4 months of age at the time of transplantation and were sacrificed after 4 months for analysis. In a follow up study, the long-term effects of BMC-transplantation in *Ctns*$^{-/-}$ mice at 7-15 months post-transplantation were evaluated. The effectiveness of BMC transplantation on kidney dysfunction was found to be dependent on the level of engraftment of BMCs expressing a functional *CTNS*, and not on the age upon transplantation. Treated mice with more than 50% donor derived engraftment had significantly improved kidney function [167]. These BMCs differentiated into lymphoid, dendritic, fibroblastic or myofibroblastic cells, and within the kidney, were localized mostly in the interstitium. The authors showed by confocal imaging that most of these bone marrow derived dendritic cells are of the inflammatory type, suggesting a role in kidney repair, by inhibiting the inflammatory response.

Iglesias *et al.* argued that the observed improvements due to stem cell transplantation could not be attributed to integration and differentiation of the transplanted cells, as the number of engrafted cells did not exceed 15% in most tissues. Instead, they used an *in vitro* co-culture model of cystinotic fibroblasts and amniotic mesenchymal stem cells or bone marrow-derived mesenchymal stem cells to show another mechanism that could explain the improvements observed upon stem cells co-culture or transplantation [168]. MSCs were found to shed stem cell micro-vesicles containing *CTNS* mRNA as well as wild-type functional cystinosin. Using fluorescent tagging, this functional cystinosin was tracked and found to be shuttled to the lysosomal compartment of cystinotic fibroblast[168]. This hypothesis was confirmed in an *in vivo* mice study by Harrison *et al.*, who used a self-inactivating-lentiviral vector (SIN-LV) to modify HSPCs to express a functional *CTNS* [169]. The functional GFP-labeled cystinosin was found to transfer from *CTNS*-expressing to *CTNS*-deficient cells [169]. To elaborate on the mechanism by which cystinosin was transferred, Naphade *et al.* performed a series of *in vivo* and *in vitro* experiments, and concluded that direct cell-cell contact is the main pathway for cross-correction of *CTNS* expression[170]. HSCs could differentiate into tissue resident macrophages that extend tunneling nanotubes, which mediate cross-correction by transferring cystinosin-bearing lysosomes to the *CTNS* deficient cells [170]. This mechanism was confirmed by Rocca *et al.*, who also demonstrated that a single systemic transplantation of wild-type HSPCs prevented ocular pathology in the *Ctns*$^{-/-}$ mice, with effects up to one year post-transplantation [146]. The transfer of proteins through tunneling nanotubes was further confirmed in a recent study by Gabriel *et al.*, in a knock-out mouse model of Dent's disease, another LSD. Gabriel and his colleagues observed no rescue of the phenotype upon inhibition of tunneling nanotubes formation by actin depolymerization or when cells were physically separated by Transwell inserts [171]. Another potential benefit of genetic rescue by HSC transplantation was observed by Gaide Chevronnay *et al.*, who found the engrafted HSCs normalized thyroid function in *Ctns*$^{-/-}$ mice [172]. These results

highlight the potential multisystemic benefits of HSC transplantation, improving renal, ocular and endocrine manifestations of cystinosis [1].
Another study by Hippert *et al.* evaluated a direct *in vivo* gene therapy strategy using an adenoviral-based vector to transduce liver cells in cystinotic C57BL/6 *Ctns*$^{-/-}$ mice [173]. The advantage of using an *in-vivo* approach is that in principle various organs and tissues can be directly targeted and their function restored. If, for instance, the HSC approach does not bring enough functional cystinosin to the kidney cells to restore proximal tubule function a direct gene therapy approach may be able to resolve this. However, as becomes clear in this study the *in-vivo* gene therapy also comes with its own limitations that will have to be addressed, including transduction efficiency, tissue specificity of the viral vector, immune response against the vector or destruction of transduced cells. What they also found was that the cystine levels and crystals seen in the liver were largely attributed by specific macrophages (kupffer cells) residing in the tissue. This further supports a role of the hematopoietic compartment in cleaning up cystine crystals and reducing cystine load in various organs.
Given the promising preclinical results of hematopoietic stem cell transplantation (HSCT) in cystinosis, Elmonem *et al.* recently endeavored to clinically validate these results by allogeneic HSC transplantation that was recently performed on a 16-year-old cystinosis patient with infantile cystinosis who was not able to tolerate cysteamine [174]. These allogenic HSCs were collected from a fully HLA matched unrelated donor using mobilized peripheral blood stem cells. Prior to the transplantation, the patient received a regimen of chemical myoablation comprising treosulfan, fludarabine, thiotepa and anti-thymocyte globulin. After transplantation, the patient showed reduced tissue cystine-crystal and signs of clinical improvement of renal and ocular of cystinosis. Additionally, biopsy analysis showed successful transfer of WT cystinosin protein and RNA to epithelial tissues of multiple organs. Nevertheless, the patient developed early signs of tacrolimus (an immunosuppressive agent) toxicity and, following the second HSC donation, suffered from severe graft-versus-host-disease (GVHD). As a result of these complications, the patient developed a severe systemic infection with MDR pseudomonas that ultimately led to death. Despite the potential of HSCT in treating cystinosis, the study also underscores the associated risks and mortality of allogenic HSCT that must be considered carefully and weighed against the treatment benefits. An alternative strategy is therefore to genetically modify patient-derived HSC *ex vivo* followed by autologous HSCT, with potentially less risk of GVHD. To test the feasibility, efficacy and safety of this approach, a phase 1/2 clinical trial (NCT03897361, Table 2) led by Cherqui *et al.* was launched in 2019, under the product name CTNS-RD-04 or AVR-RD-04. Selected patients will undergo hematopoietic stem cell mobilization and collection, after which a portion of these HSCs will be ex vivo gene-modified with a lentiviral vector, pCCL-CTNS, to express CTNS gene. The subjects will undergo marrow ablation with busulfan prior to infusion of CTNS-RD-04. In October 2019, AVROBIO, Inc (Cambridge, USA) announced that the first patient has been dosed, with the primary endpoints being tolerability measured by the absence of severe adverse events, including the incidence of replication competent

lentivirus, genotoxicity, insertional mutagenesis or monoclonal expansion. As secondary outcomes, the efficacy of CTNS-RD-04 will be assessed by measuring cystine levels in the blood, cystine crystals in the intestinal mucosa, skin, and eye as well as improvement in clinical disease outcomes. These effects and others will be assessed for 24 months after the initial transplantation. These results are highly awaited and may pave the way for future treatment options of cystinosis beyond cysteamine.

CONCLUSIONS

Although, the advances in medicine formulations have already significantly improved the patient's quality of life, no curative therapy is yet available for cystinosis. Over the last decades, our understanding of cystinosis pathology has greatly extended beyond cystine accumulation, to include increased oxidative stress, apoptosis, inflammation, and abnormal autophagy. In the last year a lot of progress has been made in identifying new compounds that are aimed at tackling features of the disease for which the current therapy cysteamine is not sufficient (Table 1). The hope is that one or more of these compounds will provide a safe and cost effective therapy for patients with cystinosis around the world and help them live a longer and healthier life.

In addition to this, the translational read-through-inducing drugs and gene therapy that are currently in clinical trials for cystinosis are aimed at restoring full length cystinosin expression, targeting the disease at its core. If these therapies prove successful they may be able to provide a cure for many aspects of the disease that are currently not met, significantly improving the health and quality of the people living with cystinosis. It should be noted, however, that only a small subset of cystinosis patients with a specific mutation will be able to benefit from the translational read-through-inducing drugs. Also the gene therapy, although in theory suitable for all patients, will most likely only reach a small group of cystinosis patients due to availability and costs. Finally, effective treatment will require early detection and intervention. This is a challenge everywhere and is only expected to fundamentally change once detection of cystinosis can be included in the new born screening programs.

Acknowledgments

This work was financially supported by a grant from the Dutch Kidney Foundation (grant nr.150KG19).

REFERENCES

1. Rocca, C.J. and S. Cherqui, *Potential use of stem cells as a therapy for cystinosis.* Pediatr Nephrol, 2018.
2. Cherqui, S. and P.J. Courtoy, *The renal Fanconi syndrome in cystinosis: pathogenic insights and therapeutic perspectives.* Nature reviews. Nephrology, 2017. **13**(2): p. 115-131.
3. Levy, M. and J. Feingold, *Estimating prevalence in single-gene kidney diseases progressing to renal failure.* Kidney Int, 2000. **58**(3): p. 925-43.
4. Bois, E., et al., *Infantile cystinosis in France: genetics, incidence, geographic distribution.* J Med Genet, 1976. **13**(6): p. 434-8.
5. De Braekeleer, M., *Hereditary disorders in Saguenay-Lac-St-Jean (Quebec, Canada).* Hum Hered, 1991. **41**(3): p. 141-6.
6. Elmonem, M.A., et al., *Cystinosis: a review.* Orphanet J Rare Dis, 2016. **11**(1): p. 47.
7. Elmonem, M.A., et al., *Lysosomal Storage Disorders in Egyptian Children.* Indian J Pediatr, 2016. **83**(8): p. 805-13.
8. David, D., et al., *Molecular Basis of Cystinosis: Geographic Distribution, Functional Consequences of Mutations in the CTNS Gene, and Potential for Repair.* Nephron, 2019. **141**(2): p. 133-146.
9. Freed, K.A., et al., *The 57 kb deletion in cystinosis patients extends into TRPV1 causing dysregulation of transcription in peripheral blood mononuclear cells.* J Med Genet, 2011. **48**(8): p. 563-6.
10. Soliman, N.A., et al., *Mutational Spectrum of the CTNS Gene in Egyptian Patients with Nephropathic Cystinosis.* JIMD Rep, 2014. **14**: p. 87-97.
11. Topaloglu, R., et al., *Genetic basis of cystinosis in Turkish patients: a single-center experience.* Pediatr Nephrol, 2012. **27**(1): p. 115-21.
12. Aldahmesh, M.A., et al., *Characterization of CTNS mutations in Arab patients with cystinosis.* Ophthalmic Genet, 2009. **30**(4): p. 185-9.
13. Shahkarami, S., et al., *The first molecular genetics analysis of individuals suffering from nephropatic cystinosis in the Southwestern Iran.* Nefrologia, 2013. **33**(3): p. 308-15.
14. Sadeghipour, F., et al., *Mutation analysis of the CTNS gene in Iranian patients with infantile nephropathic cystinosis: identification of two novel mutations.* Human Genome Variation, 2017. **4**: p. 17038.
15. Jaradat, S., et al., *Molecular analysis of the CTNS gene in Jordanian families with nephropathic cystinosis.* Nefrologia, 2015. **35**(6): p. 547-53.
16. Shotelersuk, V., et al., *CTNS mutations in an American-based population of cystinosis patients.* Am J Hum Genet, 1998. **63**(5): p. 1352-62.
17. Brasell, E.J., et al., *The aminoglycoside geneticin permits translational readthrough of the CTNS W138X nonsense mutation in fibroblasts from patients with nephropathic cystinosis.* Pediatr Nephrol, 2018.
18. Attard, M., et al., *Severity of phenotype in cystinosis varies with mutations in the CTNS gene: predicted effect on the model of cystinosin.* Hum Mol Genet, 1999. **8**(13): p. 2507-14.
19. Zykovich, A., et al., *CTNS mutations in publicly-available human cystinosis cell lines.* Molecular Genetics and Metabolism Reports, 2015. **5**: p. 63-66.
20. Wilmer, M.J., et al., *Cystinosis: practical tools for diagnosis and treatment.* Pediatric nephrology (Berlin, Germany), 2011. **26**(2): p. 205-215.

21. Baumner, S. and L.T. Weber, *Nephropathic Cystinosis: Symptoms, Treatment, and Perspectives of a Systemic Disease.* Front Pediatr, 2018. **6**: p. 58.
22. Servais, A., et al., *Late-Onset Nephropathic Cystinosis: Clinical Presentation, Outcome, and Genotyping.* Clinical Journal of the American Society of Nephrology : CJASN, 2008. **3**(1): p. 27-35.
23. Ewert, A., et al., *Bone and Mineral Metabolism in Children with Nephropathic Cystinosis Compared with other CKD Entities.* J Clin Endocrinol Metab, 2020. **105**(8).
24. Florenzano, P., et al., *Skeletal Consequences of Nephropathic Cystinosis.* J Bone Miner Res, 2018. **33**(10): p. 1870-1880.
25. Hohenfellner, K., et al., *Management of bone disease in cystinosis: Statement from an international conference.* J Inherit Metab Dis, 2019. **42**(5): p. 1019-1029.
26. Florenzano, P., et al., *Nephropathic Cystinosis: A Distinct Form of CKD-Mineral and Bone Disorder that Provides Novel Insights into the Regulation of FGF23.* J Am Soc Nephrol, 2020.
27. Battafarano, G., et al., *Intrinsic Bone Defects in Cystinotic Mice.* Am J Pathol, 2019. **189**(5): p. 1053-1064.
28. Ariceta, G., et al., *A coordinated transition model for patients with cystinosis: from pediatrics to adult care.* Nefrologia, 2016. **36**(6): p. 616-630.
29. Servais, A., et al., *Central nervous system complications in adult cystinosis patients.* J Inherit Metab Dis, 2020. **43**(2): p. 348-356.
30. Kasimer, R.N. and C.B. Langman, *Adult complications of nephropathic cystinosis: a systematic review.* Pediatr Nephrol, 2020.
31. Machuca-Gayet, I., et al., *Bone Disease in Nephropathic Cystinosis: Beyond Renal Osteodystrophy.* Int J Mol Sci, 2020. **21**(9).
32. Ariceta, G., V. Giordano, and F. Santos, *Effects of long-term cysteamine treatment in patients with cystinosis.* Pediatr Nephrol, 2017.
33. Jezegou, A., et al., *Heptahelical protein PQLC2 is a lysosomal cationic amino acid exporter underlying the action of cysteamine in cystinosis therapy.* Proc Natl Acad Sci U S A, 2012. **109**(50): p. E3434-43.
34. Brodin-Sartorius, A., et al., *Cysteamine therapy delays the progression of nephropathic cystinosis in late adolescents and adults.* Kidney Int, 2012. **81**(2): p. 179-89.
35. Vaisbich, M.H. and V.H. Koch, *Report of a Brazilian multicenter study on nephropathic cystinosis.* Nephron Clin Pract, 2010. **114**(1): p. c12-8.
36. Greco, M., et al., *Long-term outcome of nephropathic cystinosis: a 20-year single-center experience.* Pediatr Nephrol, 2010. **25**(12): p. 2459-67.
37. Besouw, M. and E. Levtchenko, *Growth retardation in children with cystinosis.* Minerva Pediatr, 2010. **62**(3): p. 307-14.
38. Nesterova, G. and W. Gahl, *Nephropathic cystinosis: late complications of a multisystemic disease.* Pediatr Nephrol, 2008. **23**(6): p. 863-78.
39. Cohen, C., et al., *Excellent long-term outcome of renal transplantation in cystinosis patients.* Orphanet J Rare Dis, 2015. **10**: p. 90.
40. Kizilbash, S.J., et al., *Trends in kidney transplant outcomes in children and young adults with cystinosis.* Pediatr Transplant, 2019. **23**(8): p. e13572.
41. Spear, G.S., et al., *Renal allografts in cystinosis and mesangial demography.* Clin Nephrol, 1989. **32**(6): p. 256-61.
42. Van Stralen, K.J., et al., *Improvement in the renal prognosis in nephropathic cystinosis.* Clin J Am Soc Nephrol, 2011. **6**(10): p. 2485-91.
43. Nesterova, G., et al., *Cystinosis: renal glomerular and renal tubular function in relation to compliance with cystine-depleting therapy.* Pediatr Nephrol, 2015. **30**(6): p. 945-51.

44. Cherqui, S., *Cysteamine therapy: a treatment for cystinosis, not a cure.* Kidney Int, 2012. **81**(2): p. 127-9.
45. Viltz, L. and D.A. Trauner, *Effect of age at treatment on cognitive performance in patients with cystinosis.* J Pediatr, 2013. **163**(2): p. 489-92.
46. Cherqui, S., et al., *The targeting of cystinosin to the lysosomal membrane requires a tyrosine-based signal and a novel sorting motif.* J Biol Chem, 2001. **276**(16): p. 13314-21.
47. Bellomo, F., et al., *Carboxyl-Terminal SSLKG Motif of the Human Cystinosin-LKG Plays an Important Role in Plasma Membrane Sorting.* PLoS One, 2016. **11**(5): p. e0154805.
48. Llinares, E., A.O. Barry, and B. Andre, *The AP-3 adaptor complex mediates sorting of yeast and mammalian PQ-loop-family basic amino acid transporters to the vacuolar/lysosomal membrane.* Sci Rep, 2015. **5**: p. 16665.
49. Andrzejewska, Z., et al., *Lysosomal Targeting of Cystinosin Requires AP-3*. Traffic, 2015. **16**(7): p. 712-26.
50. Taranta, A., et al., *Distribution of cystinosin-LKG in human tissues.* Histochem Cell Biol, 2012. **138**(2): p. 351-63.
51. Taranta, A., et al., *Cystinosin-LKG rescues cystine accumulation and decreases apoptosis rate in cystinotic proximal tubular epithelial cells.* Pediatric Research, 2016. **81**: p. 113.
52. Ruivo, R., et al., *Mechanism of proton/substrate coupling in the heptahelical lysosomal transporter cystinosin.* Proc Natl Acad Sci U S A, 2012. **109**(5): p. E210-7.
53. Oude Elferink, R.P., et al., *The intralysosomal pH in cultured human skin fibroblasts in relation to cystine accumulation in patients with cystinosis.* Biochem Biophys Res Commun, 1983. **116**(1): p. 154-61.
54. Prencipe, G., et al., *Inflammasome activation by cystine crystals: implications for the pathogenesis of cystinosis.* J Am Soc Nephrol, 2014. **25**(6): p. 1163-9.
55. Shams, F., et al., *Treatment of corneal cystine crystal accumulation in patients with cystinosis.* Clinical Ophthalmology (Auckland, N.Z.), 2014. **8**: p. 2077-2084.
56. Gaide Chevronnay, H.P., et al., *Time course of pathogenic and adaptation mechanisms in cystinotic mouse kidneys.* J Am Soc Nephrol, 2014. **25**(6): p. 1256-69.
57. Kalatzis, V., et al., *Molecular pathogenesis of cystinosis: effect of CTNS mutations on the transport activity and subcellular localization of cystinosin.* Hum Mol Genet, 2004. **13**(13): p. 1361-71.
58. Taub, M.L., J.E. Springate, and F. Cutuli, *Reduced phosphate transport in the renal proximal tubule cells in cystinosis is due to decreased expression of transporters rather than an energy defect.* Biochem Biophys Res Commun, 2011. **407**(2): p. 355-9.
59. Wilmer, M.J., et al., *Mitochondrial complex V expression and activity in cystinotic fibroblasts.* Pediatr Res, 2008. **64**(5): p. 495-7.
60. Levtchenko, E.N., et al., *Decreased intracellular ATP content and intact mitochondrial energy generating capacity in human cystinotic fibroblasts.* Pediatr Res, 2006. **59**(2): p. 287-92.
61. Wilmer, M.J., et al., *Cysteamine restores glutathione redox status in cultured cystinotic proximal tubular epithelial cells.* Biochim Biophys Acta, 2011. **1812**(6): p. 643-51.
62. Sansanwal, P., et al., *Mitochondrial autophagy promotes cellular injury in nephropathic cystinosis.* J Am Soc Nephrol, 2010. **21**(2): p. 272-83.
63. Bellomo, F., et al., *Impact of atypical mitochondrial cyclic-AMP level in nephropathic cystinosis.* Cell Mol Life Sci, 2018. **75**(18): p. 3411-3422.

64. De Rasmo, D., et al., *Mitochondrial Dynamics of Proximal Tubular Epithelial Cells in Nephropathic Cystinosis.* Int J Mol Sci, 2019. **21**(1).
65. Taub, M. and F. Cutuli, *Activation of AMP kinase plays a role in the increased apoptosis in the renal proximal tubule in cystinosis.* Biochem Biophys Res Commun, 2012. **426**(4): p. 516-21.
66. Sumayao, R., Jr., P. Newsholme, and T. McMorrow, *The Role of Cystinosin in the Intermediary Thiol Metabolism and Redox Homeostasis in Kidney Proximal Tubular Cells.* Antioxidants (Basel), 2018. **7**(12).
67. Mannucci, L., et al., *Impaired activity of the gamma-glutamyl cycle in nephropathic cystinosis fibroblasts.* Pediatr Res, 2006. **59**(2): p. 332-5.
68. Rizzo, C., et al., *Pyroglutamic aciduria and nephropathic cystinosis.* J Inherit Metab Dis, 1999. **22**(3): p. 224-6.
69. Lu, S.C., *Glutathione Synthesis.* Biochimica et biophysica acta, 2013. **1830**(5): p. 3143-3153.
70. Ribas, V., C. García-Ruiz, and J.C. Fernández-Checa, *Glutathione and mitochondria.* Frontiers in Pharmacology, 2014. **5**: p. 151.
71. Kumar, A. and A.K. Bachhawat, *A futile cycle, formed between two ATP-dependant gamma-glutamyl cycle enzymes, gamma-glutamyl cysteine synthetase and 5-oxoprolinase: the cause of cellular ATP depletion in nephrotic cystinosis?* J Biosci, 2010. **35**(1): p. 21-5.
72. Chol, M., et al., *Glutathione precursors replenish decreased glutathione pool in cystinotic cell lines.* Biochem Biophys Res Commun, 2004. **324**(1): p. 231-5.
73. Wilmer, M.J., et al., *Elevated oxidized glutathione in cystinotic proximal tubular epithelial cells.* Biochem Biophys Res Commun, 2005. **337**(2): p. 610-4.
74. Bellomo, F., et al., *Modulation of CTNS gene expression by intracellular thiols.* Free Radic Biol Med, 2010. **48**(7): p. 865-72.
75. Jamalpoor, A., et al., *Cysteamine-bicalutamide combination treatment restores alpha-ketoglutarate and corrects proximal tubule phenotype in cystinosis.* bioRxiv, 2020: p. 2020.02.10.941799.
76. Levtchenko, E., et al., *Altered status of glutathione and its metabolites in cystinotic cells.* Nephrol Dial Transplant, 2005. **20**(9): p. 1828-32.
77. Laube, G.F., et al., *Glutathione depletion and increased apoptosis rate in human cystinotic proximal tubular cells.* Pediatr Nephrol, 2006. **21**(4): p. 503-9.
78. Vali, S., et al., *Integrating glutathione metabolism and mitochondrial dysfunction with implications for Parkinson's disease: a dynamic model.* Neuroscience, 2007. **149**(4): p. 917-30.
79. Festa, B.P., et al., *Impaired autophagy bridges lysosomal storage disease and epithelial dysfunction in the kidney.* Nat Commun, 2018. **9**(1): p. 161.
80. Raggi, C., et al., *Dedifferentiation and aberrations of the endolysosomal compartment characterize the early stage of nephropathic cystinosis.* Human Molecular Genetics, 2013. **23**(9): p. 2266-2278.
81. Luciani, A., et al., *Defective autophagy degradation and abnormal tight junction-associated signaling drive epithelial dysfunction in cystinosis.* Autophagy, 2018. **14**(7): p. 1157-1159.
82. Lima, W.R., et al., *ZONAB promotes proliferation and represses differentiation of proximal tubule epithelial cells.* J Am Soc Nephrol, 2010. **21**(3): p. 478-88.
83. Raggi, C., et al., *Dedifferentiation and aberrations of the endolysosomal compartment characterize the early stage of nephropathic cystinosis.* Hum Mol Genet, 2014. **23**(9): p. 2266-78.

84. Janssens, V., et al., *Protection of Cystinotic Mice by Kidney-Specific Megalin Ablation Supports an Endocytosis-Based Mechanism for Nephropathic Cystinosis Progression.* J Am Soc Nephrol, 2019. **30**(11): p. 2177-2190.
85. Park, M., A. Helip-Wooley, and J. Thoene, *Lysosomal cystine storage augments apoptosis in cultured human fibroblasts and renal tubular epithelial cells.* J Am Soc Nephrol, 2002. **13**(12): p. 2878-87.
86. Elmonem, M.A., et al., *Cystinosis (ctns) zebrafish mutant shows pronephric glomerular and tubular dysfunction.* Scientific Reports, 2017. **7**(1): p. 42583.
87. Park, M.A., et al., *Increased apoptosis in cystinotic fibroblasts and renal proximal tubule epithelial cells results from cysteinylation of protein kinase Cdelta.* J Am Soc Nephrol, 2006. **17**(11): p. 3167-75.
88. Sansanwal, P., N. Kambham, and M.M. Sarwal, *Caspase-4 may play a role in loss of proximal tubules and renal injury in nephropathic cystinosis.* Pediatr Nephrol, 2010. **25**(1): p. 105-9.
89. Galarreta, C.I., et al., *The swan-neck lesion: proximal tubular adaptation to oxidative stress in nephropathic cystinosis.* Am J Physiol Renal Physiol, 2015. **308**(10): p. F1155-66.
90. Park, M.A. and J.G. Thoene, *Potential role of apoptosis in development of the cystinotic phenotype.* Pediatr Nephrol, 2005. **20**(4): p. 441-6.
91. Thoene, J.G., *A review of the role of enhanced apoptosis in the pathophysiology of cystinosis.* Mol Genet Metab, 2007. **92**(4): p. 292-8.
92. Hollywood, J.A., et al., *Use of Human Induced Pluripotent Stem Cells and Kidney Organoids To Develop a Cysteamine/mTOR Inhibition Combination Therapy for Cystinosis.* J Am Soc Nephrol, 2020.
93. Rabinowitz, J.D. and E. White, *Autophagy and metabolism.* Science, 2010. **330**(6009): p. 1344-8.
94. Bar-Peled, L., et al., *Ragulator is a GEF for the rag GTPases that signal amino acid levels to mTORC1.* Cell, 2012. **150**(6): p. 1196-208.
95. Andrzejewska, Z., et al., *Cystinosin is a Component of the Vacuolar H+-ATPase-Ragulator-Rag Complex Controlling Mammalian Target of Rapamycin Complex 1 Signaling.* J Am Soc Nephrol, 2016. **27**(6): p. 1678-88.
96. Ivanova, E.A., et al., *Altered mTOR signalling in nephropathic cystinosis.* J Inherit Metab Dis, 2016. **39**(3): p. 457-464.
97. Tennant, D.A. and E. Gottlieb, *HIF prolyl hydroxylase-3 mediates alpha-ketoglutarate-induced apoptosis and tumor suppression.* Journal of Molecular Medicine, 2010. **88**(8): p. 839-849.
98. Tang, Z., et al., *Atg2A/B deficiency switches cytoprotective autophagy to non-canonical caspase-8 activation and apoptosis.* Cell Death Differ, 2017. **24**(12): p. 2127-2138.
99. Ivanova, E.A., et al., *Endo-lysosomal dysfunction in human proximal tubular epithelial cells deficient for lysosomal cystine transporter cystinosin.* PLoS One, 2015. **10**(3): p. e0120998.
100. Ma, S.K., et al., *Activation of the Renal PI3K/Akt/mTOR Signaling Pathway in a DOCA-Salt Model of Hypertension.* Chonnam medical journal, 2012. **48**(3): p. 150-154.
101. Jiang, L., et al., *Rheb/mTORC1 signaling promotes kidney fibroblast activation and fibrosis.* Journal of the American Society of Nephrology : JASN, 2013. **24**(7): p. 1114-1126.
102. Huber, T.B., G. Walz, and E.W. Kuehn, *mTOR and rapamycin in the kidney: signaling and therapeutic implications beyond immunosuppression.* Kidney Int, 2011. **79**(5): p. 502-11.
103. Jung, C.H., et al., *mTOR regulation of autophagy.* FEBS letters, 2010. **584**(7): p. 1287-1295.

104. Maxson, M.E. and S. Grinstein, *The vacuolar-type H(+)-ATPase at a glance - more than a proton pump.* J Cell Sci, 2014. **127**(Pt 23): p. 4987-93.
105. Sardiello, M., et al., *A gene network regulating lysosomal biogenesis and function.* Science, 2009. **325**(5939): p. 473-7.
106. Rega, L.R., et al., *Activation of the transcription factor EB rescues lysosomal abnormalities in cystinotic kidney cells.* Kidney Int, 2016. **89**(4): p. 862-73.
107. Yao, Z. and D.J. Klionsky, *The symphony of autophagy and calcium signaling.* Autophagy, 2015. **11**(7): p. 973-974.
108. Marino, G., et al., *Dimethyl alpha-ketoglutarate inhibits maladaptive autophagy in pressure overload-induced cardiomyopathy.* Autophagy, 2014. **10**(5): p. 930-2.
109. Villar, V.H., et al., *mTORC1 inhibition in cancer cells protects from glutaminolysis-mediated apoptosis during nutrient limitation.* Nat Commun, 2017. **8**: p. 14124.
110. Banerjee, K., et al., *Mild mitochondrial metabolic deficits by alpha-ketoglutarate dehydrogenase inhibition cause prominent changes in intracellular autophagic signaling: Potential role in the pathobiology of Alzheimer's disease.* Neurochem Int, 2016. **96**: p. 32-45.
111. Huang, H.M., et al., *Inhibition of alpha-ketoglutarate dehydrogenase complex promotes cytochrome c release from mitochondria, caspase-3 activation, and necrotic cell death.* J Neurosci Res, 2003. **74**(2): p. 309-17.
112. Gibson, G.E., et al., *The alpha-ketoglutarate-dehydrogenase complex: a mediator between mitochondria and oxidative stress in neurodegeneration.* Mol Neurobiol, 2005. **31**(1-3): p. 43-63.
113. Settembre, C., et al., *A block of autophagy in lysosomal storage disorders.* Hum Mol Genet, 2008. **17**(1): p. 119-29.
114. Platt, F.M., B. Boland, and A.C. van der Spoel, *The cell biology of disease: lysosomal storage disorders: the cellular impact of lysosomal dysfunction.* J Cell Biol, 2012. **199**(5): p. 723-34.
115. Jouandin, P., et al., *Lysosomal cystine efflux opposes mTORC1 reactivation through the TCA cycle.* 2019: p. 606541.
116. Kaushik, S. and A.M. Cuervo, *Chaperone-mediated autophagy: a unique way to enter the lysosome world.* Trends Cell Biol, 2012. **22**(8): p. 407-17.
117. Napolitano, G., et al., *Impairment of chaperone-mediated autophagy leads to selective lysosomal degradation defects in the lysosomal storage disease cystinosis.* EMBO Mol Med, 2015. **7**(2): p. 158-74.
118. Kiffin, R., et al., *Activation of chaperone-mediated autophagy during oxidative stress.* Mol Biol Cell, 2004. **15**(11): p. 4829-40.
119. Zhang, J., et al., *Cystinosin, the small GTPase Rab11, and the Rab7 effector RILP regulate intracellular trafficking of the chaperone-mediated autophagy receptor LAMP2A.* The Journal of Biological Chemistry, 2017. **292**(25): p. 10328-10346.
120. Johnson, J.L., et al., *Upregulation of the Rab27a-dependent trafficking and secretory mechanisms improves lysosomal transport, alleviates endoplasmic reticulum stress, and reduces lysosome overload in cystinosis.* Mol Cell Biol, 2013. **33**(15): p. 2950-62.
121. Donath, M.Y., *Targeting inflammation in the treatment of type 2 diabetes.* Diabetes Obes Metab, 2013. **15 Suppl 3**: p. 193-6.
122. Jaffer, U., R.G. Wade, and T. Gourlay, *Cytokines in the systemic inflammatory response syndrome: a review.* HSR Proc Intensive Care Cardiovasc Anesth, 2010. **2**(3): p. 161-75.
123. Pecoits-Filho, R., et al., *Associations between circulating inflammatory markers and residual renal function in CRF patients.* Am J Kidney Dis, 2003. **41**(6): p. 1212-8.

124. Strowig, T., et al., *Inflammasomes in health and disease.* Nature, 2012. **481**(7381): p. 278-86.
125. Schroder, K. and J. Tschopp, *The inflammasomes.* Cell, 2010. **140**(6): p. 821-32.
126. Kelley, N., et al., *The NLRP3 Inflammasome: An Overview of Mechanisms of Activation and Regulation.* Int J Mol Sci, 2019. **20**(13).
127. Rathinam, V.A., S.K. Vanaja, and K.A. Fitzgerald, *Regulation of inflammasome signaling.* Nat Immunol, 2012. **13**(4): p. 333-42.
128. Elmonem, M.A., et al., *Clinical utility of chitotriosidase enzyme activity in nephropathic cystinosis.* Orphanet J Rare Dis, 2014. **9**: p. 155.
129. Lobry, T., et al., *Interaction between galectin-3 and cystinosin uncovers a pathogenic role of inflammation in kidney involvement of cystinosis.* Kidney Int, 2019. **96**(2): p. 350-362.
130. Nishiyama, J., et al., *Up-regulation of galectin-3 in acute renal failure of the rat.* Am J Pathol, 2000. **157**(3): p. 815-23.
131. Henderson, N.C., et al., *Galectin-3 expression and secretion links macrophages to the promotion of renal fibrosis.* Am J Pathol, 2008. **172**(2): p. 288-98.
132. Jia, J., et al., *Galectin-3 Coordinates a Cellular System for Lysosomal Repair and Removal.* Dev Cell, 2020. **52**(1): p. 69-87.e8.
133. Chauhan, S., et al., *TRIMs and Galectins Globally Cooperate and TRIM16 and Galectin-3 Co-direct Autophagy in Endomembrane Damage Homeostasis.* Dev Cell, 2016. **39**(1): p. 13-27.
134. Dohil, R., et al., *Esomeprazole therapy for gastric acid hypersecretion in children with cystinosis.* Pediatr Nephrol, 2005. **20**(12): p. 1786-93.
135. Armas, D., et al., *A Phase 1 Pharmacokinetic Study of Cysteamine Bitartrate Delayed-Release Capsules Following Oral Administration with Orange Juice, Water, or Omeprazole in Cystinosis.* Adv Ther, 2018. **35**(2): p. 199-209.
136. Medic, G., et al., *A systematic literature review of cysteamine bitartrate in the treatment of nephropathic cystinosis.* Curr Med Res Opin, 2017. **33**(11): p. 2065-2076.
137. Langman, C.B., et al., *Quality of life is improved and kidney function preserved in patients with nephropathic cystinosis treated for 2 years with delayed-release cysteamine bitartrate.* J Pediatr, 2014. **165**(3): p. 528-33.e1.
138. Langman, C.B., et al., *A randomized controlled crossover trial with delayed-release cysteamine bitartrate in nephropathic cystinosis: effectiveness on white blood cell cystine levels and comparison of safety.* Clin J Am Soc Nephrol, 2012. **7**(7): p. 1112-20.
139. Dohil, R. and B.L. Cabrera, *Treatment of cystinosis with delayed-release cysteamine: 6-year follow-up.* Pediatr Nephrol, 2013. **28**(3): p. 507-10.
140. Ramazani, Y., et al., *Evaluation of carbohydrate-cysteamine thiazolidines as pro-drugs for the treatment of cystinosis.* Carbohydr Res, 2017. **439**: p. 9-15.
141. Frost, L., et al., *Synthesis of diacylated γ-glutamyl-cysteamine prodrugs, and in vitro evaluation of their cytotoxicity and intracellular delivery of cysteamine.* Eur J Med Chem, 2016. **109**: p. 206-15.
142. Omran, Z., et al., *Synthesis and in vitro evaluation of novel pro-drugs for the treatment of nephropathic cystinosis.* Bioorg Med Chem, 2011. **19**(11): p. 3492-6.
143. Omran, Z., et al., *PEGylated derivatives of cystamine as enhanced treatments for nephropathic cystinosis.* Bioorg Med Chem Lett, 2011. **21**(1): p. 45-7.

144. Omran, Z., et al., *Folate pro-drug of cystamine as an enhanced treatment for nephropathic cystinosis.* Bioorg Med Chem Lett, 2011. **21**(8): p. 2502-4.
145. Kaiser-Kupfer, M.I., et al., *Long-term ocular manifestations in nephropathic cystinosis.* Arch Ophthalmol, 1986. **104**(5): p. 706-11.
146. Rocca, C.J., et al., *Treatment of Inherited Eye Defects by Systemic Hematopoietic Stem Cell Transplantation.* Invest Ophthalmol Vis Sci, 2015. **56**(12): p. 7214-23.
147. Reda, A., et al., *Effect of Storage Conditions on Stability of Ophthalmological Compounded Cysteamine Eye Drops.* JIMD Rep, 2018. **42**: p. 47-51.
148. Lyseng-Williamson, K.A., *Cystadrops® (cysteamine hydrochloride 0.55% viscous eye-drops solution) in treating corneal cystine crystal deposits in patients with cystinosis: a profile of its use.* Drugs & Therapy Perspectives, 2017. **33**(5): p. 195-201.
149. Liang, H., et al., *A New Viscous Cysteamine Eye Drops Treatment for Ophthalmic Cystinosis: An Open-Label Randomized Comparative Phase III Pivotal Study.* Invest Ophthalmol Vis Sci, 2017. **58**(4): p. 2275-2283.
150. Luaces-Rodriguez, A., et al., *Cysteamine polysaccharide hydrogels: Study of extended ocular delivery and biopermanence time by PET imaging.* Int J Pharm, 2017. **528**(1-2): p. 714-722.
151. Marcano, D.C., et al., *Synergistic Cysteamine Delivery Nanowafer as an Efficacious Treatment Modality for Corneal Cystinosis.* Molecular Pharmaceutics, 2016. **13**(10): p. 3468-3477.
152. De Leo, E., et al., *Cell-based phenotypic drug-screening identifies luteolin as candidate therapeutic for nephropathic cystinosis.* J. Am. Soc. Nephrol., 2020. **in press**.
153. Pache de Faria Guimaraes, L., et al., *N-acetyl-cysteine is associated to renal function improvement in patients with nephropathic cystinosis.* Pediatr Nephrol, 2014. **29**(6): p. 1097-102.
154. Gottwald, E.M., et al., *The targeted anti-oxidant MitoQ causes mitochondrial swelling and depolarization in kidney tissue.* Physiol Rep, 2018. **6**(7): p. e13667.
155. Nagel-Wolfrum, K., et al., *Targeting Nonsense Mutations in Diseases with Translational Read-Through-Inducing Drugs (TRIDs).* BioDrugs, 2016. **30**(2): p. 49-74.
156. Midgley, J., *A breakthrough in readthrough? Could geneticin lead the way to effective treatment for cystinosis nonsense mutations?* Pediatric Nephrology, 2019.
157. Kurosaki, T. and L.E. Maquat, *Nonsense-mediated mRNA decay in humans at a glance.* J Cell Sci, 2016. **129**(3): p. 461-7.
158. Campofelice, A., et al., *Strategies against Nonsense: Oxadiazoles as Translational Readthrough-Inducing Drugs (TRIDs).* Int J Mol Sci, 2019. **20**(13).
159. Ryan, N.J., *Ataluren: first global approval.* Drugs, 2014. **74**(14): p. 1709-1714.
160. Brasell, E.J., et al., *The novel aminoglycoside, ELX-02, permits CTNSW138X translational read-through and restores lysosomal cystine efflux in cystinosis.* PLoS One, 2019. **14**(12): p. e0223954.
161. Syres, K., et al., *Successful treatment of the murine model of cystinosis using bone marrow cell transplantation.* Blood, 2009. **114**(12): p. 2542-52.
162. Cherqui, S., *Is genetic rescue of cystinosis an achievable treatment goal?* Nephrology, dialysis, transplantation : official publication of the European Dialysis and Transplant Association - European Renal Association, 2014. **29**(3): p. 522-528.
163. Baer, P.C. and H. Geiger, *Mesenchymal stem cell interactions with growth factors on kidney repair.* Curr Opin Nephrol Hypertens, 2010. **19**(1): p. 1-6.

164. Kunter, U., et al., *Transplanted mesenchymal stem cells accelerate glomerular healing in experimental glomerulonephritis.* J Am Soc Nephrol, 2006. **17**(8): p. 2202-12.
165. Togel, F., et al., *Autologous and allogeneic marrow stromal cells are safe and effective for the treatment of acute kidney injury.* Stem Cells Dev, 2009. **18**(3): p. 475-85.
166. Asanuma, H., D.R. Meldrum, and K.K. Meldrum, *Therapeutic applications of mesenchymal stem cells to repair kidney injury.* J Urol, 2010. **184**(1): p. 26-33.
167. Yeagy, B.A., et al., *Kidney preservation by bone marrow cell transplantation in hereditary nephropathy.* Kidney Int, 2011. **79**(11): p. 1198-206.
168. Iglesias, D.M., et al., *Stem cell microvesicles transfer cystinosin to human cystinotic cells and reduce cystine accumulation in vitro.* PLoS One, 2012. **7**(8): p. e42840.
169. Harrison, F., et al., *Hematopoietic stem cell gene therapy for the multisystemic lysosomal storage disorder cystinosis.* Mol Ther, 2013. **21**(2): p. 433-44.
170. Naphade, S., et al., *Brief reports: Lysosomal cross-correction by hematopoietic stem cell-derived macrophages via tunneling nanotubes.* Stem Cells, 2015. **33**(1): p. 301-9.
171. Gabriel, S.S., et al., *Bone marrow transplantation improves proximal tubule dysfunction in a mouse model of Dent disease.* Kidney Int, 2017. **91**(4): p. 842-855.
172. Gaide Chevronnay, H.P., et al., *Hematopoietic Stem Cells Transplantation Can Normalize Thyroid Function in a Cystinosis Mouse Model.* Endocrinology, 2016. **157**(4): p. 1363-71.
173. Hippert, C., et al., *Gene transfer may be preventive but not curative for a lysosomal transport disorder.* Mol Ther, 2008. **16**(8): p. 1372-81.
174. Elmonem, M.A., et al., *Allogeneic HSCT transfers wild-type cystinosin to nonhematological epithelial cells in cystinosis: First human report.* Am J Transplant, 2018. **18**(11): p. 2823-2828.
175. Dohil, R., et al., *The Effect of Food on Cysteamine Bitartrate Absorption in Healthy Participants.* Clin Pharmacol Drug Dev, 2012. **1**(4): p. 170-4.
176. U.S. National Institute of Health. *ClinicalTrials.gov.* 2020, April 2; Available from: https://www.clinicaltrials.gov/.
177. Omasits, U., et al., *Protter: interactive protein feature visualization and integration with experimental proteomic data.* Bioinformatics, 2014. **30**(6): p. 884-6.

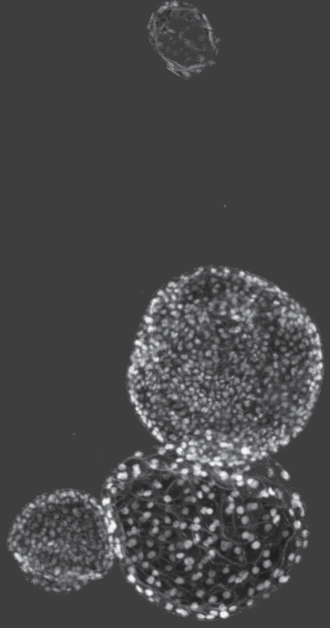

Quantification of cystine in human renal proximal tubule cells using liquid chromatography-tandem mass spectrometry

3

Amer Jamalpoor[1], Rolf W. Sparidans[2], Carla Pou Casellas[1], Johannes J.M. Rood[2], Mansi Joshi[1], Rosalinde Masereeuw[1], Manoe J. Janssen[1]

[1]Division of Pharmacology, Utrecht Institute for Pharmaceutical Sciences, Faculty of Science, Utrecht University, 3584 CG Utrecht, The Netherlands. [2]Utrecht University, Faculty of Science, Department of Pharmaceutical Sciences, Division of Pharmacoepidemiology & Clinical Pharmacology, Universiteitsweg 99, 3584 CG, Utrecht, The Netherlands.

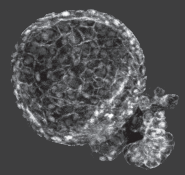

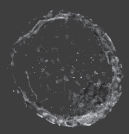

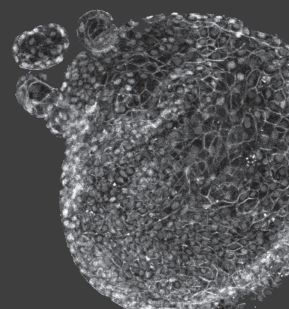

Biomedical Chromatography. 2018 Aug;32(8)
doi: 10.1002/bmc.4238

ABSTRACT

Nephropathic cystinosis is characterized by abnormal intralysosomal accumulation of cystine throughout the body causing irreversible damage to various organs, particularly the kidneys. Cysteamine, the currently available treatment, can reduce lysosomal cystine and postpone disease progression. However, cysteamine poses serious side effects and does not address all symptoms of cystinosis. To screen for new treatment options, a rapid and reliable high-performance liquid chromatography-tandem mass spectrometry (HPLC-MS/MS) method was developed to quantify cystine in conditionally immortalized human proximal tubular epithelial cells (ciPTEC). The ciPTEC were treated with N-ethylmaleimide, lysed and deproteinized with 15% (w/v) sulfosalicylic acid. Subsequently, cystine was measured using deuterium-labeled cystine-D4, as an internal standard. The assay developed demonstrated linearity to at least 20 µmol/L with a good precision. Accuracies were between 97.3-102.9% for both cell extracts and whole cell samples. Cystine was sufficiently stable under all relevant analytical conditions. The assay was successfully applied to determine cystine levels in both healthy and cystinotic ciPTEC. Control cells showed clearly distinguishable cystine levels compared to cystinotic cells treated with or without cysteamine. The method developed provides a fast and reliable quantification of cystine, and is applicable to screen for potential drugs that could reverse cystinotic symptoms in human kidney cells.

Keywords:
Cystinosis, cystine, ciPTEC, HPLC-MS/MS

INTRODUCTION

Nephropathic cystinosis (MIM219800) is a rare, but severe genetic disorder characterized by intralysosomal accumulation of cystine in different cell types. It is caused by pathogenic mutations in *CTNS*, a gene that encodes for the lysosomal cystine/proton symporter cystinosin. Mutations in *CTNS* lead to the lysosomal accumulation of cystine throughout the body and causes irreversible damage to various organs, particularly the kidneys [1]. Cysteamine, the only treatment available to date, can reduce lysosomal accumulation of cystine and postpone the disease progression [2]. In lysosomes, cysteamine reacts in a disulfide exchange reaction with cystine, leading to the formation of cysteine and cysteine-cysteamine molecules which can be transported out of lysosomes by the cysteine transporter and the PQLC2 transporter, respectively [3, 4]. However, cysteamine poses serious side effects and does not correct all symptoms associated with cystinosis.

To screen for new drugs to treat nephropathic cystinosis, a quantitative bioanalytical assay for cystine is a pre-requisite. Measurement of cystine concentrations in leukocytes of patients is a clinical routine for diagnosis of cystinosis and monitoring cysteamine treatment [5, 6]. For drug screening and development, however, measuring the cystine content in cultured renal proximal tubule cells can be of high value. In nephropathic cystinosis, kidneys are initially affected with generalized proximal tubular dysfunction, so called renal Fanconi syndrome [7]. In addition, it has been reported that cystinosin expression is predominantly high in renal proximal tubules when compared to other segments of the nephron, signifying that cystinosin is crucial for proximal tubular cell function [8]. Hence, measurement of cystine in renal proximal tubule cells can bring a new versatile tool to screen for potential drugs to reverse the cystinotic symptoms. Here, we used conditionally immortalized proximal tubular epithelial cells (ciPTEC) derived from urine samples of both healthy controls and cystinotic patients. Cystinotic ciPTEC are a well characterized human renal model of cystinosis, and have been demonstrated to have increased intracellular cystine levels when compared to healthy ciPTEC [9].

Critical steps must be considered in order to have reliable intracellular cystine measurements. Cystine is a biologically active aminothiol formed from the oxidation of two cysteine molecules via a disulfide bond formation. Since cysteine content of the cytosol greatly exceeds the cystine concentration in lysosomes [5], oxidation of cysteine to cystine would lead to an undesirable increase in cystine concentrations. Moreover, disulfide exchange reactions of cystine with other sulfhydryl groups can lead to the loss of cystine in the cells. To avoid these artifactual oxidation-reduction reactions and in order to have an adequate measurement of cystine in the cells, derivatization with N-ethylmaleimide (NEM) is required immediately during sample preparation [5, 10]. NEM, an alkylating agent, forms stable bonds with sulfhydryl containing molecules, enabling them to be permanently blocked and prevent disulfide bond formation.

Several methods have been developed to detect the levels of aminothiols in different biological samples [11-14]. Among which, high-performance liquid chromatography

(HPLC) with fluorescence detection is the most widely used [15]. Graaf-Hess et al. have applied such method for measuring cystine in leukocytes and fibroblasts of cystinotic patients [5]. On the other hand, Escobar et al. have recently reported a rapid and reliable bioanalytical assay for detection of cystine and other related thiols in whole blood using ultra-performance liquid chromatography coupled to tandem mass spectrometry (UPLC-MS/MS) [10]. Unfortunately, these methods are hampered in use because of their high limit of detection and poor cystine recovery.
Here, we describe a fast and reliable method to measure cystine in both healthy and cystinotic ciPTEC using HPLC-MS/MS (Fig. 1). Furthermore, the method is applicable in screening potential drugs that could reverse cystinotic symptoms *in vitro* using human kidney cells.

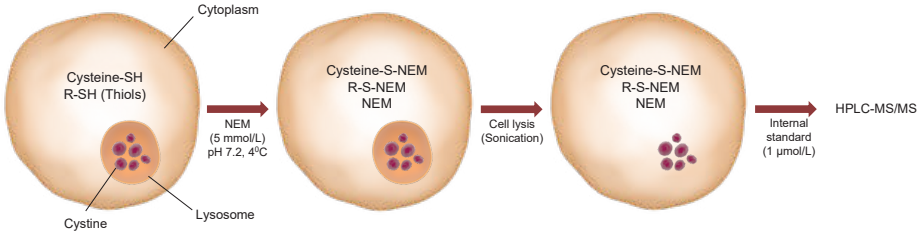

FIGURE 1. Schematic presentation of the method principle. N-ethylmaleimide (NEM)**,** an alkylating agent, forms stable bonds with cysteine and other thiols in cytosol, enabling them to be permanently blocked and prevent disulfide bond formation, while leaving cystine in lysosomes intact. This process is then followed by cell lysis and acid precipitation of proteins. This causes cystine to be present in the acid-soluble fraction, which can be quantified by HPLC-MS/MS.

MATERIALS AND METHODS

Reagents

Cystine, NEM, and sulfosalicylic acid were purchased from Sigma-Aldrich (Zwijndrecht, The Netherlands). Deuterated internal standard cystine-D4 was purchased from Cambridge Isotope Laboratories (Tewksbury, Massachusetts, USA). Acetonitrile (HPLC-S grade) was obtained from Biosolve (Valkenswaard, The Netherlands). Formic acid was purchased from Merck (Darmstadt, Germany). Ultrapure water was home-purified on a Milli-Q® Advantage A10 Water Purification Systems (Merck, The Netherlands).

Cell Sample preparation

The ciPTEC were cultured and matured as described before by Wilmer et al. [16] in ciPTEC complete medium (DMEM/F12; Gibco/Invitrogen, Breda, The Netherlands). In short, cells were seeded at a density of 55000 cells/cm^2 in tissue culture flasks (25 cm^2) and grown for 24 h at 33 °C, 5% (v/v) CO_2, for proliferation followed by 7 days of maturation at 37 °C. Next, the cells were harvested using accutase and centrifuged at 250 g for 5 min at 4 °C. The cell pellets were then quickly frozen in liquid nitrogen and stored at -80 °C until

quantification. Cell extracts were prepared by suspending the frozen pellets of ciPTEC in 100 µL of NEM solution (5 mmol/L NEM in 0.1 mol/L sodium phosphate buffer, pH 7.2) on ice. The cells were sonicated (Hielscher, UP50H; 1 cycle, 80% amplitude) on ice three times for 10 s with 20 s cooling intervals. Subsequently, 50 µL of 15% (w/v) sulfosalicylic acid was added to precipitate the proteins and the suspension was centrifuged at 20,000 g for 10 min at 4 °C. Protein concentration was determined by the method of the Pierce™ BCA protein assay kit according to the manufacturer's protocol (ThermoFischer, The Netherlands), and the cystine concentration was measured using HPLC-MS/MS.

Analytical sample pre-treatment

Sample supernatants were thawed on ice and diluted (1:10) in 0.1% (v/v) formic acid in ultrapure water. Subsequently, 5 µL of internal standard solution cystine-D4 (final concentration 1 µmol/L) was added to 95 µL of previously diluted supernatant. Finally, 100 µL of the clear supernatant were transferred into a glass injection vial and injected in the chromatographic system.

HPLC–MS/MS chromatographic system

The chromatographic system used consisted of a DUG14A degasser, two LC10-ADvp-µ pumps, a SIL-HTC auto-sampler and a CTO-10Avp oven (Shimadzu, Kyoto, Japan), coupled to a TSQ Quantum Discovery Max triple-quadrupole mass spectrometer with electrospray ionization (ThermoFischer Scientific, San Jose, CA, USA). The mass spectrometer was operating with positive ionization in the selected reaction monitoring (SRM) mode. Electrospray settings of the assay were a 3000 V spray voltage, a 323 °C capillary temperature and the skimmer voltage was set at -5 V. The SRM mode with 0.15 s dwell times was used with argon as the collision gas at 1.4 mTorr. The tube lens off set was 102 V for both cystine and the internal standard cystine-D4. Cystine was monitored at m/z 241.0 → 152.0 and 74.0 at -12 V and -28 V collision energies, and the internal standard cystine-D4 at m/z 245.0 → 154.0 at -12 V collision energy. The mass resolutions were set at 0.7 for both separating quadrupoles. Separation conditions were selected to achieve an appropriate chromatographic retention by injecting 1.0 µL on an Atlantis dC18 column (100×2.1 mm, dp = 3.0 µm, Waters, Milford, USA) with a ChromSep Guard Polaris 3 C18A pre-column (10×2.0 mm, dp = 3.0 µm, Agilent, Santa Clara, USA). The column temperature was maintained at 40 °C and the auto-sampler at 4 °C. Isocratic elution was performed at the rate of 0.5 mL/min with mobile phase A (0.1% (v/v) formic acid in ultrapure water), and B (acetonitrile). After injection, the percentage of solvent B was held at 0% (v/v) for 0.50 min, and was increased linearly to 100% (v/v) until 0.99 min. At 1.0 min the percentage of solvent B was decreased back to 0% (v/v) and finally, the column was equilibrated for 3.0 min until starting the next injection. The whole eluate was transferred to the electrospray probe at 0.3 min until 1.1 min using the MS diverter valve. Thermo Fisher Xcalibur software (version 2.0.7 SP1) was employed to acquire chromatography-mass spectrometric data and these data were further processed using Microsoft Excel (Office 2016, Version 15.11.2).

Method validation

The analytical parameters assayed during the validation procedure were linearity, lower limit of quantification (LLOQ), limit of detection (LOD), precision and accuracy as well as matrix effect and stability of cell samples and standards.

Calibration

Individual stock solutions of cystine and the internal standard cystine-D4 were prepared at a concentration of 20 µmol/L in 0.1% (v/v) formic acid in ultrapure water. The calibration samples were prepared daily in duplicate by serial dilution in 0.1% (v/v) formic acid in ultrapure water at concentrations ranging from 0.1 to 20 µmol/L of cystine. Least-squares weighted linear regression was employed to acquire the calibration curve, using the ratio of the peak areas of both cystine and the internal standard cystine-D4. The weighting factor was defined as the reversed square of the concentration ($1/x^2$). LOD and LLOQ were defined as the lowest concentrations required to generate a signal-to-noise (S/N) ratio of 3 and 10, respectively.

Accuracy and precision

The accuracy of the method was evaluated by means of the recovery test. To do this, cell extracts were spiked with three different concentration levels of cystine (i.e. low: 0.25, mid: 8.0, and high: 16.0 µmol/L), and were analyzed in three analytical runs on three separate days in triplicate. Non-spiked cell samples were also analyzed in each validation day in triplicate. In addition, to determine that the sample preparation (described above) does not result in cystine loss, recovery in whole cell samples was studied as well. For this purpose, cells were collected and spiked with the determined concentration of cystine (0.25, 8.0, and 16.0 µmol/L) before protein precipitation and the recovery was determined. The percentage recovery was calculated by subtracting the recovery value of the spiked cell samples from the non-spiked samples. To determine the precision of the method, spiked cell samples (the same samples used for accuracy determination) were analyzed within one validation batch (intra-day) and among validation batches (inter-day). The intra- and inter-day run precisions were subsequently calculated as the percentage coefficient of variations (CV).

Stability

Stability of cystine was investigated in spiked cell samples (cell extracts and whole cell samples) under both short-term (24 h at 4 °C), and long-term (three freeze-thaw cycles) storage conditions. For the long term stability test, spiked cell samples were frozen and thawed for three cycles (thawing at 20 °C and freezing again at -80 °C) within a period of minimum 1 month.

Matrix effect

The matrix effect was assessed at three different concentration levels (i.e. low, mid, and high) by processing each sample and correcting the relative peak area of the spiked cell

samples to that of the non-spiked samples. Thereafter, the areas were compared to the relative peak areas of cystine standard solutions.

Statistical Analysis

Statistical differences between groups were assessed using One-way Analysis of Variance (ANOVA) followed by Tukey's post-hoc multiple comparisons tests using GraphPad Prism software 6.01. A p value < 0.05 was considered to be statistically significant. Data is expressed as mean ± standard deviation (SD) of three independent experiments performed in triplicate.

RESULTS

HPLC–MS/MS method. To obtain maximal sensitivity, the electrospray ionization-MS/MS settings were optimized for cystine and the internal standard cystine-D4. The chromatographic method was adapted from Escobar et al [10] and optimized empirically based on MS response, peak shape, and retention time. Acetonitrile and 0.1% (v/v) formic acid in ultrapure water resulted in a good MS response with a narrow cystine peak. With a total run time of 3.0 min, both cystine and the internal standard cystine-D4 eluted at 0.63 min (± 0.003) without any peak interference in the 0.3 to 1.1 min time window. Representative chromatograms of extracted cells, with and without internal standard are shown in Fig. 2.

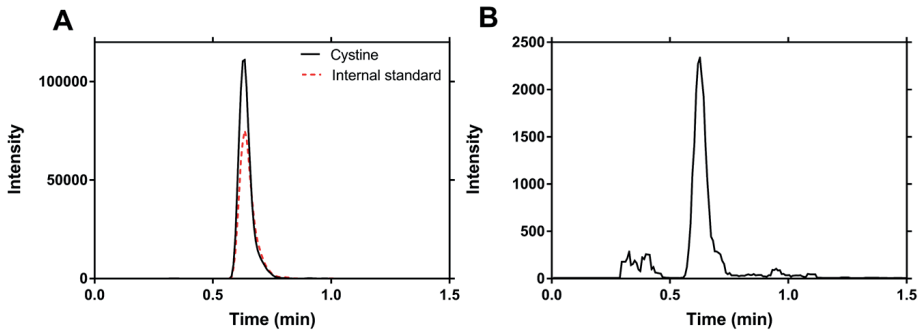

FIGURE 2. SRM chromatograms of cystine. (A) Representative chromatogram obtained from cystinotic ciPTEC (3.90 µmol/L) with internal standard cystine-D4 (1 µmol/L), showing the retention time of cystine at 0.63 min (± 0.003). (B) Representative chromatogram obtained from healthy control ciPTEC (0.21 µmol/L).

Analytical method validation

Calibration. The relative response of cystine showed a good linearity within the concentrations tested, ranging from 0.1 to 20 µmol/L. For 6 independent calibrations, the concentrations were back calculated from the ratio of the peak areas of both

TABLE 1. Cystine recovery (accuracy), precision and matrix effect measurements obtained after analysis of the spiked cell samples at three different concentrations.

	Recovery		Intra-day run precision	Inter-day run precision	Matrix effect
Cystine concentration (µmol/L)	Cell extracts ± SD (%)	Whole cells ± SD (%)	CV (%)	CV (%)	± SD (%)
0.25	99.9 ± 11.2	101.7 ± 15.4	13.16	13.24	100.8 ± 10.5
8.0	101.4 ± 13.0	102.9 ± 8.3	7.30	7.42	101.7 ± 4.7
16.0	97.3 ± 7.9	98.7 ± 13.6	4.71	4.69	99.4 ± 2.8

Recovery and matrix effect in ± SD and precision in CV of three independent experiments performed in triplicate

cystine and the internal standard cystine-D4. Deviations from the average of each level were not higher than 2.3% (data not shown), allowing linear regression analysis. The equation of the calibration curve revealed is y = 0.0034 (± 0.0008) + 0.0015 (± 0.00012) x with a coefficient of determination (R^2) value of 0.996 (± 0.002). Here, x is the cystine concentration (µmol/L) and y is the response of drug relative to the internal standard. The LOD and LLOQ of the assay were 0.05 and 0.1 µmol/L, respectively.

Accuracy and precision. Accuracy and precision of the method at three different concentrations are reported in Table 1. The method resulted in low intra- and inter-day run variations (<15%) with accuracies ranging from 97.3 to 102.9% for both cell extracts and whole cell samples.

Stability and Matrix effect. As shown in Table 2, cystine was sufficiently stable in spiked cell extracts and whole cell samples under both short-term (24 h at 4 °C) and long-term (after one, two, or three freeze-thaw cycles) storage conditions. The stability values ranged between 90.3 and 105.0%. No matrix effects could be observed at three different concentration levels (Table 1). The matrix factor ranged between 99.4 to 101.7%. Overall, the absence of matrix effect and high recovery and stability of the analyte contributed to a successful validation of the assay.

Cystine levels in healthy and cystinotic cells. After a successful validation procedure, the new assay was used to detect cystine levels in both healthy and cystinotic ciPTEC (Fig. 3). The results obtained by HPLC-MS/MS showed a significantly higher level of cystine in cystinotic ciPTEC (3.90 µmol/L; 2.22 ± 0.43 nmol/mg protein) when compared to that of healthy control cells (0.21 µmol/L; 0.057 ± 0.022 nmol/mg protein). This is in accordance with the pathophysiology of the disease, the hallmark being abnormal intracellular accumulation of cystine. Upon treatment with a known cystine depleting agent cysteamine (100 µmol/L) for 24 h, cystinotic cells showed a significant reduction in cystine levels (0.74 ± 0.051 nmol/mg protein). Such a concentration of cystine, however, was still significantly higher (13-fold) than found in healthy ciPTEC.

TABLE 2. Cystine stability obtained from the analysis of spiked cell extracts and whole cell samples at short-term (24 h at 4 °C) and long-term (1-3 freeze-thaw cycles; thawing at 20 °C and freezing again at -80 °C for a period of minimum 1 month) storage conditions.

Cell extracts				
Cystine concentration (µmol/L)	Short-term stability ± SD (%) 24 h at 4 °C	Long-term stability ± SD (%)		
		1 cycle	2 cycles	3 cycles
0.25	110.6 ± 14.8	99.2 ± 17.7	99.2 ± 24.7	93.1 ± 22.7
8.0	107.8 ± 9.5	103.3 ± 6	103.2 ± 10.8	99.0 ± 11.2
16.0	103.8 ± 5	102.2 ± 5	101.0 ± 11.2	97.4 ± 16.2
Whole cells				
Cystine Concentration (µmol/L)	Short-term stability ± SD (%) 24 h at 4 °C	Long-term stability ± SD (%)		
		1 cycle	2 cycles	3 cycles
0.25	108 ± 25.9	90.3 ± 22.6	105.0 ± 22.9	97.2 ± 12.4
8.0	105.3 ± 10.6	97.4 ± 27.3	93.6 ± 21.1	97.6 ± 14.5
16.0	110.0 ± 14.5	96.2 ± 23.1	103.0 ± 13.9	96.4 ± 5.7

Data is expressed as mean ± SD of three independent experiments performed in triplicate

The effect of N-ethylmaleimide. To demonstrate the added value of NEM, we measured the levels of cystine in cell samples treated either with or without NEM. The lack of NEM caused a significant increase in the amount of cystine in cystinotic ciPTEC (Fig. 4). This shows that in the absence of NEM, cysteine gets readily oxidized into cystine, leading to a cumulative amount of cystine and a false positive quantification of its intracellular levels. In contrast, the absence of NEM had no effect on the levels of cystine in healthy ciPTEC. This is likely due to the fact that healthy ciPTEC contain very low levels of cystine and cysteine.

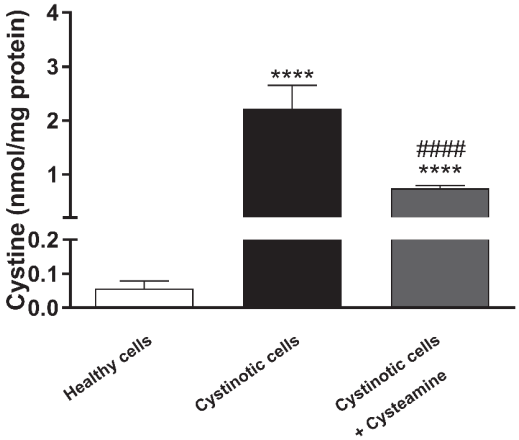

FIGURE 3. Cystinotic ciPTEC have increased intracellular cystine levels. Cystine levels (nmol/mg protein) measured in healthy cells, cystinotic cells (untreated), and cystinotic cells treated with 100 µmol/L cysteamine. HPLC-MS/MS analysis showed significantly elevated levels of cystine in cystinotic cells when compared to that of healthy cells (**** p<0.0001), while cysteamine was able to significantly reduce the levels of cystine in cystinotic ciPTEC (#### p<0.0001 compared to cystinotic cells). Data is expressed as mean ± SD of three independent experiments performed in triplicate.

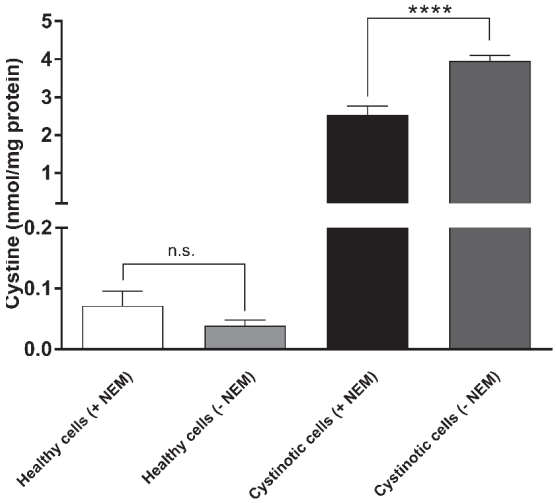

FIGURE 4. NEM is required to have reliable intracellular cystine measurements. Cystine levels (nmol/mg protein) measured in healthy and cystinotic ciPTEC in both presence and absence of NEM (5 mmol/L). The absence of NEM did not appear to have any significant effect on the measurement of cystine in healthy cells. In cystinotic cells, however, the absence of NEM caused a significant increase in the concentration of cystine (**** p<0.0001). Data is expressed as mean ± SD of three independent experiments performed in triplicate.

DISCUSSION

The past years, various methods have been developed to quantify cystine levels in different biological samples. HPLC with fluorescence detection assay described by Graaf-Hess et al. is currently used to quantify cystine levels in cystinotic fibroblasts, leukocytes, zebrafish and ciPTEC [7, 9, 17]. Nevertheless, the assay is hampered by its high limit of detection (0.3 µmol/L), low cystine recovery and tedious sample preparation procedure [5].

The method we describe in this study allows for fast sample processing with excellent analytical performance. The assay comprises two simple steps of sample preparation: i) treatment of cells with NEM followed by ii) acid precipitation and finally injection of the supernatant into the chromatographic system. In addition, LOD (0.05 µmol/L) and LLOQ (0.1 µmol/L) of the method are low enough to allow an accurate cystine measurement both in healthy (0.21 µmol/L) and cystinotic (3.90 µmol/L) cells.

The present chromatographic method was adapted from the UPLC-MS/MS assay described by Escobar et al. [10]. By comparing our HPLC-MS/MS method with the UPLC-MS/MS method, we have further optimized the method in terms of sensitivity (the volume of sample injected is, 1.0 µL versus 5.0 µL), and limit of detection for cystine (0.1 versus 0.34 µmol/L). Another important difference is that our method provided a better cystine recovery rate with low standard variations (97.3-102.9% versus 75-134%), contributing to a successful validation of the method.

One of the hallmarks of cystinosis is that patients accumulate lysosomal cystine due to a defective cystinosin transporter. Cysteamine, a cystine depleting agent, was able to significantly reduce cystine accumulation in cystinotic ciPTEC but not to the level of control cells. This is in agreement with clinical observations where cysteamine treatment does not offer a cure but only postpones disease progression. Hence, there is a clear need to screen for new treatment options for cystinosis and therefore our method could be used as a screening tool. Moreover, the assay can also be applied in clinical studies as a diagnostic and biochemical follow-up tool for cystinosis. Measurement of cystine concentrations in leukocytes of patients is a clinical routine for diagnosis of cystinosis and monitoring cysteamine treatment. The low detection limit of the method would enable us to accurately measure cystine concentrations in the leukocytes of healthy controls (0.04-0.13 nmol cystine/mg protein) and cystinotic patient (2.43 nmol cystine/mg protein) [5]. Of note, control and cystinotic ciPTEC had an accumulation of cystine similar to that of the leukocytes (fig. 3), indicating ciPTEC as a good representative of cystinosis model.

CONCLUSION

A fast and reliable method to measure cystine in both healthy and cystinotic ciPTEC was developed. The method was fully validated and can be applied to screen for potential drugs to reverse cystinotic symptoms *in vitro* in human kidney cells.

Acknowledgements
This work was financially supported by a grant from the Dutch Kidney Foundation (grant nr.150KG19).

REFERENCES

1. Town, M., et al., *A novel gene encoding an integral membrane protein is mutated in nephropathic cystinosis.* Nat Genet, 1998. **18**(4): p. 319-24.
2. Thoene, J.G., et al., *Cystinosis. Intracellular cystine depletion by aminothiols in vitro and in vivo.* J Clin Invest, 1976. **58**(1): p. 180-9.
3. Gahl, W.A., J.G. Thoene, and J.A. Schneider, *Cystinosis.* N Engl J Med, 2002. **347**(2): p. 111-21.
4. Besouw, M., et al., *Cysteamine: an old drug with new potential.* Drug Discov Today, 2013. **18**(15-16): p. 785-92.
5. de Graaf-Hess, A., F. Trijbels, and H. Blom, *New method for determining cystine in leukocytes and fibroblasts.* Clin Chem, 1999. **45**(12): p. 2224-8.
6. Garcia-Villoria, J., et al., *Improvement of the cystine measurement in granulocytes by liquid chromatograhy-tandem mass spectrometry.* Clin Biochem, 2013. **46**(3): p. 271-4.
7. Elmonem, M.A., et al., *Cystinosis (ctns) zebrafish mutant shows pronephric glomerular and tubular dysfunction.* Sci Rep, 2017. **7**: p. 42583.
8. Kalatzis, V., et al., *Molecular pathogenesis of cystinosis: effect of CTNS mutations on the transport activity and subcellular localization of cystinosin.* Hum Mol Genet, 2004. **13**(13): p. 1361-71.
9. Wilmer, M.J., et al., *Cysteamine restores glutathione redox status in cultured cystinotic proximal tubular epithelial cells.* Biochim Biophys Acta, 2011. **1812**(6): p. 643-51.
10. Escobar, J., et al., *Development of a reliable method based on ultra-performance liquid chromatography coupled to tandem mass spectrometry to measure thiol-associated oxidative stress in whole blood samples.* J Pharm Biomed Anal, 2016. **123**: p. 104-12.
11. Bayram, B., et al., *Rapid method for glutathione quantitation using high-performance liquid chromatography with coulometric electrochemical detection.* J Agric Food Chem, 2014. **62**(2): p. 402-8.
12. Hodakova, J., et al., *Sensitive determination of glutathione in biological samples by capillary electrophoresis with green (515 nm) laser-induced fluorescence detection.* J Chromatogr A, 2015. **1391**: p. 102-8.
13. Du, F., S. Cao, and Y.S. Fung, *A serial dual-electrode detector based on electrogenerated bromine for capillary electrophoresis.* Electrophoresis, 2014. **35**(24): p. 3556-63.
14. Donnelly, J.G. and C. Pronovost, *Evaluation of the Abbott IMx fluorescence polarization immunoassay and the bio-rad enzyme immunoassay for homocysteine: comparison with high-performance liquid chromatography.* Ann Clin Biochem, 2000. **37 (Pt 2)**: p. 194-8.
15. Steele, M.L., L. Ooi, and G. Munch, *Development of a high-performance liquid chromatography method for the simultaneous quantitation of glutathione and related thiols.* Anal Biochem, 2012. **429**(1): p. 45-52.
16. Wilmer, M.J., et al., *Novel conditionally immortalized human proximal tubule cell line expressing functional influx and efflux transporters.* Cell Tissue Res, 2010. **339**(2): p. 449-57.
17. Wilmer, M.J., et al., *Cystine dimethylester model of cystinosis: still reliable?* Pediatr Res, 2007. **62**(2): p. 151-5.

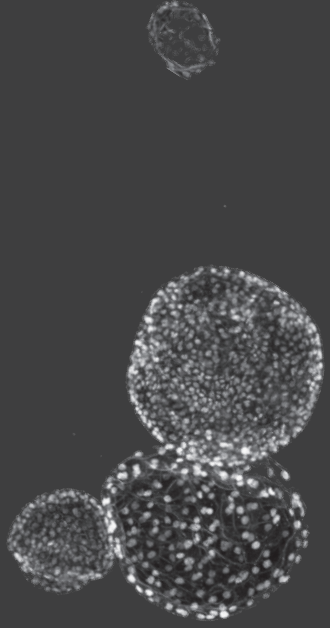

Cysteamine-bicalutamide combination therapy corrects proximal tubule phenotype in cystinosis

4

Amer Jamalpoor[1], Charlotte AGH van Gelder[2,3¥], Fjodor A Yousef Yengej[4,5¥], Esther A Zaal[2], Sante Princiero Berlingerio[6], Koenraad R Veys[6], Carla Pou Casellas[1], Koen Voskuil[1], Khaled Essa[1], Carola ME Ammerlaan[4,5], Laura Rita Rega[7], Reini van der Welle[8], Marc R Lilien[9], Maarten B Rookmaaker[5], Hans Clevers[4], Judith Klumperman[8], Elena Levtchenko[6], Celia R Berkers[2,10], Marianne C Verhaar[5], Maarten Altelaar[2,3], Rosalinde Masereeuw[1] and Manoe J Janssen[1]

¥ These authors contributed equally to this work

[1]Division of Pharmacology, Utrecht Institute for Pharmaceutical Sciences, Faculty of Science, Utrecht University, 3584 CG Utrecht, The Netherlands. [2]Biomolecular Mass Spectrometry and Proteomics, Bijvoet Center for Biomolecular Research and Utrecht Institute for Pharmaceutical Sciences, Utrecht University, Padualaan 8, 3584 CH Utrecht, The Netherlands. [3]Netherlands Proteomics Center, Padualaan 8, 3584 CH Utrecht, The Netherlands. [4]Hubrecht Institute-Royal Netherlands Academy of Arts and Sciences, Utrecht, the Netherlands. [5]Department of Nephrology and Hypertension, University Medical Centre Utrecht, Utrecht, the Netherlands. [6]Department of Pediatric Nephrology & Growth and Regeneration, University Hospitals Leuven & KU Leuven, Leuven, Belgium. [7]Renal Diseases Research Unit, Bambino Gesù Children's Hospital, IRCCS, Rome, Italy. [8]Section Cell Biology, Center for Molecular Medicine, University Medical Center Utrecht, Utrecht University, Utrecht, The Netherlands. [9]Department of Pediatric Nephrology, Wilhelmina Children's Hospital, University Medical Centre Utrecht, Utrecht, the Netherlands. [10]Department of Biochemistry and Cell Biology, Faculty of Veterinary Medicine, Utrecht University, Utrecht, The Netherlands.

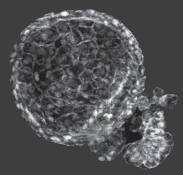

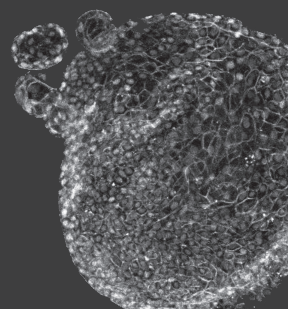

Under revision at EMBO Molecular Medicine
Published as preprint at bioRxiv 2020.02.10; doi: https://doi.org/10.1101/2020.02.10.941799

ABSTRACT

Nephropathic cystinosis is a severe monogenic kidney disorder caused by mutations in *CTNS*, encoding the lysosomal transporter cystinosin, resulting in lysosomal cystine accumulation. The sole treatment, cysteamine, slows down the disease progression, but does not correct the established renal proximal tubulopathy. Here, we developed a new therapeutic strategy by applying omics to expand our knowledge on the complexity of the disease and prioritize drug targets in cystinosis. We identified alpha-ketoglutarate as an important metabolite linking cystinosin loss, lysosomal autophagy defect and renal proximal tubular impairment in cystinosis. This insight combined with a drug screen revealed a bicalutamide-cysteamine combination treatment as a novel dual target pharmacological approach for the phenotypical correction of cystinotic renal proximal tubule cells, patient-derived kidney tubuloids and cystinotic zebrafish.

Keywords:
Alpha-ketoglutarate, cystinosis, cysteamine-bicalutamide combination therapy, renal Fanconi syndrome

INTRODUCTION

Nephropathic cystinosis (MIM219800) is a lysosomal storage disease (LSD) caused by mutations in *CTNS*, a gene that codes for the lysosomal cystine/proton symporter cystinosin [1]. The loss of cystinosin leads to the lysosomal accumulation of cystine throughout the body and causes irreversible damage to various organs, particularly the kidneys [2]. The first clinical signs develop during infancy (age of ~6 months) in the form of renal Fanconi syndrome and over time patients develop chronic kidney disease and finally renal failure in the first or second decade of life [3]. For the past decades, great efforts have been directed towards reducing cellular cystine accumulation in cystinotic patients. The cystine-depleting drug cysteamine can efficiently lower the lysosomal cystine levels and postpone disease progression. However, it poses serious side effects and does not correct the established proximal tubulopathy associated with cystinosis [3, 4].
Recent discoveries in lysosomal gene expressions and their regulatory networks have provided new insights in the studies of LSDs, including cystinosis [5-7]. Several studies based on *in vitro* and *in vivo* models have demonstrated that the loss of cystinosin is indeed associated with disrupted lysosomal autophagy dynamics [8], accumulation of distorted mitochondria [9, 10], and increased reactive oxygen species (ROS) levels [11], leading to abnormal proliferation and dysfunction of proximal tubule cells. Regardless of the observed cellular defects associated with cystinosis, the mechanism linking cystinosin loss, lysosomal defects and epithelial dysfunction remains unknown, hampering the development of an enduring intervention to combat the disease.
In this work, we aimed to develop a novel pharmacological strategy to treat cystinosis by correcting its renal tubular phenotype. By combining CRISPR/Cas9 technology and a dual proteomics and metabolomics approach, we identified alpha-ketoglutarate (αKG), an important intermediate of the tricarboxylic acid (TCA) cycle, as part of a unifying mechanism linking cystinosin loss, lysosomal autophagy disruption and proximal tubule impairment in *CTNS* deficient renal proximal tubule cells. Using this knowledge, we identified the bicalutamide-cysteamine combination treatment as a novel strategy for the phenotypical correction of cystinotic proximal tubule cells. This approach was validated further in cystinotic patient-derived kidney tubuloids and in cystinotic zebrafish, demonstrating the therapeutic potential for this combination therapy to treat patients with cystinosis.

MATERIALS AND METHOD

Reagent and antibodies

All chemicals and reagents were obtained from Sigma-Aldrich (Zwijndrecht, The Netherlands) unless specified otherwise. Primary antibodies used were mouse anti-LAMP1 (Santa Cruz Biotechnology #sc-18821, dilution 1:200), rabbit anti-mTOR (Cell Signaling Technology #2983, dilution 1:400), rabbit anti-LC3 (Novus Biologicals #NB600-

1384SS, dilution 1:1000), mouse anti- SQSMT1 (p62) (BD Biosciences #610832, dilution 1:1000), rabbit anti-β-actin (13E5) (Cell signaling technology #4970, dilution 1:4000), Rabbit anti-PAX8 (Proteintech, dilution 1:200), mouse anti-p63 (Abcam, dilution 1:200), and Phalloidin-AF488 (Life Technology, dilution 1:100). Polyclonal goat anti-rabbit (#P0448, dilution 1:5000) and polyclonal goat anti-mouse (#P0447, dilution 1:5000) secondary antibodies were obtained from Dako products (CA, USA). Alexa-488 goat anti-mouse (dilution 1:500), Alexa-647 goat anti-rabbit (dilution 1:200), donkey anti-rabbit-AF647 (dilution 1:300), and donkey anti-mouse-AF568 (dilution 1:200) secondary antibodies were from Life Technologies Europe BV (The Netherlands).

Generation of *CTNS*$^{-/-}$ isogenic cell line of ciPTEC using CRISPR

Guide RNAs (gRNAs) targeting exon 4 of the *CTNS* gene were designed using the online gRNA designing tool available at chopchop.cbu.uib.no. In order to maximize specificity, guide sequences with high scores for on-target efficiency and no predicted off-targets having at least 3 base pair mismatches in the genome were selected. Optimal gRNA (5'-GTCGTAAAGCTGGAGAACGG-3') was cloned into the pSPCas9(BB)-2A-GFP plasmid (Addgene #48138) as described previously by Ran et al. [12], and introduced into healthy ciPTEC using PolyPlus JetPrime. 72 hrs post-transfection, GFP-positive singlet cells were sorted using FACS Aria-II flow cytometer and expanded in 96-wells plate. The gRNA cut site was amplified with PCR using the primers flanking the cut region (F.CTNS_ex4 5'-GGCCTGTTTTCCTCCATCTCTG-3'; R.CTNS_ex4 5'-AAGTGCCAACCAGCAGCTC-3'). Knockouts were confirmed by Sanger sequencing followed by intracellular cystine accumulation.

CiPTEC culture

The ciPTEC were cultured as previously described by Wilmer et al. 2010 [13]. The culture medium was Dulbecco's modified Eagle medium DMEM/F-12 (GIBCO) supplemented with fetal calf serum 10% (v/v), insulin 5 µg/ml, transferrin 5 µg/ml, selenium 5 µg/ml, hydrocortisone 35 ng/ml, epidermal growth factor 10 ng/ml and tri-iodothyronine 40 pg/ml. In short, cells were seeded at a density of 55,000 cells/cm^2 and grown at 33°C for 24 hrs to enable them to proliferate and subsequently cultured at 37°C for 7 days to mature into fully differentiated epithelial cells. As a reference we also included a non-isogenic patient derived *CTNS*$^{-/-}$ ciPTEC line, which will be referred to as *CTNS*^{Patient}.

Tubuloid culture

Tubuloids were established from the urine of two pediatric cystinosis patients and healthy kidney tissue from two donors as previously described [14]. Urine was collected, cooled to 4°C, rinsed with phosphate buffered saline (PBS) and with advanced Dulbecco's modified Eagle's medium (ADMEM)-F12 (Gibco) supplemented with 1% HEPES, 1% glutamax, 1% penicillin/streptomycin, 0.1 mg/mL primocin (Invivogen) and 10 µM Y-27632 (Abmole). The pellets were resuspended in basement membrane extract (BME, SanBio/Trevigen) and plated. After BME droplets had solidified, ADMEM-F12 supplemented with 1% HEPES,

1% glutamax, 1% penicillin/streptomycin, 0,1 mg/mL primocin, 1,6% B27 (Gibco), 1% Rpsondin-3 conditioned medium (U-Protein Express), 50 ng/mL EGF (Peprotech), 100 ng/mL FGF10 (Peprotech), 1 mM N-acetylcysteine, 5 µM A83-01 (Tocris Bioscience) and 10 µM Y-27632 was added as expansion medium. In order to establish tubuloids from kidney tissue, the tissue was digested with 1 mg/mL collagenase for 45 min. Tissue fragments were resuspended in BME and plated. After BME droplets had solidified, expansion medium was added. For specific experiments, tubuloids were differentiated using ADMEM-F12 with 1% HEPES, 1% glutamax and 1% penicillin/streptomycin (differentiation medium).

Cell treatment

Standard starvation medium was Hank's balanced salt solution (HBSS; GIBCO). When indicated, the cell-permeable form of αKG, dimethyl α-ketoglutarate (DMKG) was added to a final concentration of 2 mM for 4 or 24 hrs. Cysteamine (100 µM), bicalutamide (35 µM), or the combination of cysteamine and bicalutamide (100 µM and 35 µM, respectively) were used as a treatment for 96 hrs (5 days).

Zebrafish maintenance and breeding

The animal care and experimental procedures were carried out in accordance with the ethical committee guidelines for laboratory animal experimentation at KU Leuven. Zebrafish (Danio rerio) were AB strain wild-type and *ctns*$^{-/-}$ mutant. Cystinotic and wild-type larvae were raised at 28.5 °C in egg water (Instant Ocean Sea Salts, 60µg/ml). At 48 hrs post fertilization, larvae were treated with cysteamine 1000 µM, bicalutamide 10 µM, or their combination. Drugs were administered at 48 hrs post fertilization in all experiments dissolved in the swimming water. The medium was refreshed every day and dead embryos were sorted out.

Intracellular cystine quantification by HPLC-MS/MS

Cystine levels were quantified using HPLC-MS/MS; a rapid and sensitive assay that has been developed and validated in house [15]. In brief, ciPTEC, tubuloids, and zebrafish larvae pellets were suspended in N-Ethylmaleimide (NEM) solution containing 5 mM NEM in 0.1 mM sodium phosphate buffer (pH 7.4). The cell suspension was precipitated and protein was extracted with sulfosalicylic acid 15% (w/v) and centrifuged at 20,000 g for 10 min at 4°C. Protein concentration was determined by the method of the Pierce™ BCA protein assay kit according to the manufacturer's protocol (Thermo Fischer, The Netherlands), and the cystine concentration was measured using HPLC-MS/MS. Data are expressed as the cystine values (nmol) corrected for total protein content (mg).

Quantitative real-time PCR

The mRNAs were extracted from cells using the Qiagen RNeasy mini kit according to the manufacturer's instructions. Total mRNA (600 ng) was reverse transcribed using iScript Reverse Transcriptase Supermix (Bio-Rad). Quantitative real-time PCR was

performed using iQ Universal SYBR Green Supermix (Bio-Rad) with the specific sense and anti-sense primers for *TFEB* (forward: 5'-GCAGTCCTACCTGGAGAATC-3'; reverse: 5'-GTGGGCAGCAAACTTGTTCC-3'). The ribosomal protein S13 (*RPS-13*) (forward: 5'-GCTCTCCTTTCGTTGCCTGA-3'; reverse: 5'- ACTTCAACCAAGTGGGGACG-3') was used as the reference gene for normalization and relative expression level were calculated as fold change using the $2^{-\Delta\Delta}Ct$ method.

Tubuloids were grown in expansion medium for a few days and then differentiated for 7 days. Tubuloids were lysed and RNA was isolated using the RNEasy Mini Kit (Qiagen) according to the manufacturer's protocol. Quantitative real-time qPCR was performed using the iQ SYBR Green Supermix (Bio-Rad). A 384-wells plate was used with a reaction volume of 12.5 µL and duplicates for each reaction. For the read-out, the CFX384 Touch Real-Time PCR Detection System (Bio-Rad) was used. Expression levels of the following genes were measured: *RPS-13* (housekeeping gene), *ANPEP*, *ABCC3*, *HNF1A*, *HNF4A*, *SLC12A1*, *SLC12A3*, *CALB1*, *AQP2* and *AQP3*. Primer sequences are provided in Table EV2. Expression was normalised to the expression of *RPS-13* within the same sample (ΔCt).

Immunofluorescence and confocal microscopy

To investigate mTORC1/LAMP1 co-localization, control and cystinotic ciPTEC lines were cultured on coverslips with the respective treatments. Thereafter, cells were fixed with 4% paraformaldehyde in PBS for 10 min, permeabilised with 0.1% Triton-X solution for 10 min, and blocked with 1% bovine serum albumin (BSA) diluted in PBS for 30 min. Subsequently, cells were stained with the primary antibodies diluted in blocking buffer overnight at 4°C. After 3 washes with PBS, the cells were incubated for 2 hrs at room temperature with the corresponding secondary antibodies. Nuclei were stained with Hoechst 33342 (1 µM) and cells were imaged with a Deltavision confocal microscope (Cell Microscopy Core, Department of Cell Biology, University Medical Centre Utrecht).

To assess TFEB intracellular distribution, cells were seeded in special optic 96-wells plate until to reach 50% confluence. Cells were then transfected with the TFEB-GFP plasmid (a kind gift from Dr. Annelies Michiels (Viral Vector Core, Leuven, Belgium)) using PolyPlus JetPrime reagent according to the manufacturer's instructions. After 48 hrs from transient transfection, cells were stained with Hoechst 33342 (1 µM) for 10 min and imaged using a Cell Voyager 7000 (CV7000) confocal microscope (Yokogawa Electric corporation, Tokyo, Japan). TFEB nuclear translocation data are expressed as number of cells with nucleus-TFEB positive over the total number of TFEB-transfected cells.

For tubuloid experiments, tubuloids were differentiated for 7 days. Tubuloids were fixed for 45 min with 4% formaldehyde in PBS and then permeabilised and blocked with 0.5% Triton-X100 plus 0,5% BSA in PBS for 30 min. Subsequently, tubuloids were stained with the primary antibodies diluted in 0.5% BSA plus 0.1% Tween20 in PBS overnight at 4°C. Tubuloids were rinsed twice with 0.5% BSA plus 0.1% Tween20 in PBS and then stained for 2 hrs at room temperature with the corresponding secondary antibodies and DAPI (1:1000) in 0.5% BSA plus 0.1% Tween20 in PBS. Tubuloids were washed twice

with 0.5% BSA + 0.1% Tween20 in PBS, mounted and imaged using a Leica SP8 confocal microscope.

Immunoblots

The ciPTEC were seeded in 6-well plates in triplicate with the respective treatments. Subsequently, cells were washed twice with PBS and lysed with RIPA buffer containing protease inhibitor cocktail (Roche). Protein quantification was performed using the method of the Pierce™ BCA protein assay kit according to the manufacturer's protocol. After the electrophoresis, the proteins were transferred to a nitrocellulose membrane (midi kit, Bio-Rad) with Trans-Blot Turbo Transfer System (Bio-Rad). Finally, membranes were imaged using the ChemiDoc™ XRS+ (Bio-Rad) and analysed using image J software.

Endocytosis assay

The endocytic uptake was monitored in ciPTEC following incubation for 1.5 hrs at 37°C with 50 µg/ml of either BSA-AlexaFluor-647 (A34785, Thermo Fisher Scientific) or DQ Red BSA (D12051, Invitrogen). The cells were then fixed and stained with Hoechst 33342 (1 µM) for 10 min and imaged using a CV7000 confocal microscope (Yokogawa Electric corporation, Tokyo, Japan). Data were quantified with Columbus™ Image Data Storage and analysis software (PerkinElmer, Groningen, The Netherlands). Data are expressed as the number of BSA/DQ-BSA spots per cell.

UHPLC/MS system and analysis of metabolomics data

Sample preparation

CiPTEC cells were washed with ice cold PBS and metabolites were extracted in 1 mL lysis buffer containing methanol/acetonitrile/dH_2O (2:2:1). Samples were centrifuged at 16.000g for 15 minutes at 4 °C and supernatants were collected for LC-MS analysis.

Mass spectrometry and data analysis

LC-MS analysis was performed on an Exactive mass spectrometer (Thermo Scientific) coupled to a Dionex Ultimate 3000 autosampler and pump (Thermo Scientific). The MS operated in polarity-switching mode with spray voltages of 4.5 kV and -3.5 kV. Metabolites were separated using a Sequant ZIC-pHILIC column (2.1 x 150 mm, 5 µm, guard column 2.1 x 20 mm, 5 µm; Merck) with elution buffers acetonitrile (A) and eluent B (20 mM (NH4)2CO3, 0.1% NH4OH in ULC/MS grade water (Biosolve)). Gradient ran from 20% eluent B to 60% eluent B in 20 min, followed by a wash step at 80% and equilibration at 20%, with a flow rate of 150 µl/min. Analysis was performed using LCquan software (Thermo Scientific). Metabolites were identified and quantified on the basis of exact mass within 5 ppm and further validated by concordance with retention times of standards. Peak intensities were normalised based on total peak intensities and data were analysed using MetaboAnalyst [16].

UHPLC/MS-MS system and analysis of proteomics data

Sample preparation

CiPTEC pellets were lysed in boiling guanidinium lysis buffer containing 6 M guanidinium HCl (GuHCl), 5 mM tris(2-carboxyethyl)phosphine (TCEP), 10 mM chloroacetamide, 100 mM Tris-HCl pH 8.5, supplemented with protease inhibitor (cOmplete mini EDTA-free, Roche). Pellets were boiled for 10 min at 99 °C, sonicated for 12 rounds of 5 seconds (Bioruptor Plus, Diagenode), and spun down at 20,000 x g for 15 min. Protein concentration was determined using Pierce™ BCA protein assay kit. Equal amounts of protein per condition were digested with Lys-C (1:100, Wako) for 4 hrs at 37 °C, diluted to a final concentration of 2 M GuHCl, followed by trypsin digestion (1:100, Sigma Aldrich) overnight at 37 °C. Tryptic peptides were acidified to a final concentration of 1% formic acid (FA) (Merck), cleaned up using SepPak cartridges (Waters), and dried *in vacuo*.

Mass spectrometry and data analysis

Peptide samples were analysed with an UHPLC 1290 system (Agilent technologies) coupled to an Orbitrap Q Exactive HF X mass spectrometer (Thermo Scientific). Peptides were trapped (Dr Maisch Reprosil C18, 3 µm, 2 cm x 100 µm) and then separated on an analytical column (Agilent Poroshell EC-C18, 2.7 µm, 50 cm x 75 µm). Trapping was performed for 5 min in solvent A (0.1% FA) and eluted with following gradient: 4 - 8% solvent B (0.1% FA in 80% acetonitrile) in 4 min, 8 - 24% in 158 min, 24 - 35% in 35 min, 35 - 60% in 17 min, 60 - 100% in 4 min and finally 100 % for 1 min. Flow was passively split to 300 nl/min. The mass spectrometer was operated in data-dependent mode. At a resolution of 35.000 *m/z* at 400 *m/z*, MS full scan spectra were acquired from *m/z* 375–1600 after accumulation to a target value of $3e^6$. Up to 15 most intense precursor ions were selected for fragmentation. HCD fragmentation was performed at normalised collision energy of 27% after the accumulation to a target value of $1e^5$. MS/MS was acquired at a resolution of 30,000. Dynamic exclusion was enabled with an exclusion duration of 32s. RAW data files were processed with MaxQuant (v1.6.0.16 (Cox, Mann 2008)) and MS2 spectra were searched with the Andromeda search engine against the Swissprot protein database of Homo Sapiens (20,259 entries, downloaded 31/01/2018) spiked with common contaminants. Cysteine carbamidomethylation was set as a fixed modification and methionine oxidation and protein N-term acetylation were set as variable modifications. Trypsin was specified as enzyme and up to two miss cleavages were allowed. Filtering was done at 1% false discovery rate (FDR) at the protein and peptide level. Label-free quantification (LFQ) was performed, and “match between runs” was enabled. The data was further processed using Perseus 1.6.0.7 [17].

Alpha-ketoglutarate measurement by LC-MS/MS

Alpha-ketoglutarate **(**2-KG; Fluka 75893) calibration standards of respectively 0.8, 1.6, 4.0, 8.0, and 20 µM, and an internal standard solution of 2.2 µM 3,3,4,4-D4 2kg (kind gift Prof. Dr. H. Blom VU Amsterdam) were prepared in dH2O. 50 µl plasma sample or calibration standard together with 50 µl internal standard solution and 50 µl dH2O

were pipetted onto a Microcon ultrafilter (30 kDa, Millipore) The resulting ultrafiltrate (15min 14000g 15°C) was acidified with 20 µl 4% formic acid (Merck) in dH2O. 3 µl of the acidified ultra-filtrate was injected onto a peek-lined InertSustain AQ-c18 (2.1*100mm dp 3µ) column using a I-Class Acquity (Waters) The column was run at 40°C in gradient mode using 0.5% acetic acid in H2O and Acetonitrile (initial conditions 100% 0.5% acetic acid in H2O at 250 µl/min). The column flow was directed to a Xevo TQSµ (Waters) fitted with an electrospray ionization probe operating in the negative mode at unit resolution. The capillary voltage was set at 0.6 kV. The temperature settings for the source and ionblock were respectively 550℃ and 150℃. As a drying gas nitrogen was used at a flow rate of 800 L/h. The conegas flow was set at 50 L/h. The collision cell was operated with argon as the collision gas at a pressure of 0.35 Pa. An area response was generated by recording the MRM transitions of the neutral loss CO2 for both 2kg an d4-2kg. The d4-2kg was used to normalize the area response. Quantification was performed using a linear regression curve constructed from the normalised area response from the prepared calibration standards.

Cell viability assays

To estimate the percentage of cell death, cells were seeded in a 96-well plate and after respective treatments, the percentage cell death was assessed using Presto Blue Cell Viability Reagent according to manufacturer's instructions.

For tubuloid experiments, the drug safety screening was performed using a protocol derived from Driehuis *et al.* [18]. In short, BME was dissolved by incubation in 1 mg/mL dispase II for 30 min at 37 °C. Tubuloids were digested into tiny fragments using Accutase. These fragments were plated in BME, grown for 1 day in expansion medium and then switched to differentiation medium for 2 days. Next, BME was dissolved using dispase II as described above, after which tubuloids were sieved using a 70 µm cell strainer (BD Falcon) and counted. 500 tubuloids in 40 µL differentiation medium with 5% BME were plated in a 384-wells plate using the Multidrop dispenser (Thermofisher) and treated with increasing concentrations of bicalutamide that were always combined with 100 µM cysteamine. Staurosporine (10 µM) was used as positive control. DMSO volume was 1% in all conditions. Drugs were added using the D300E digital dispenser (Tecan). After 5 days, tubuloids were lysed with 40 µL Cell-Titer Glo (Promega). Luminescence was measured using the Spark® multimode microplate reader (Tecan) to determine ATP levels as an indicator of the amount of tubuloids that had survived the treatment. Tubuloid viability was normalised to the viability (ATP levels) upon treatment with cysteamine alone (=100%).

Apoptosis assay

The ciPTEC were plated in an optic 96-well imaging plates and treated with DMKG in presence or absence of bicalutamide, cysteamine or their combination. Subsequently, the Cell Event Caspase-3/7 Green Detection Reagent (8 µM) was added and incubated for 30 min before imaging. Caspase-active cells were identified as described in manufacturer's

instruction. Each well was imaged using the CV7000 confocal microscope and analysed with Columbus™ Image Data Storage and analysis software (PerkinElmer, Groningen, The Netherlands).

ROS detection assay

The ciPTEC were seeded in 96-well plates and ROS levels were assessed using general oxidative stress indicator (CM-H2DCFDA; Invitrogen) according to the manufacturer's protocol. Briefly, the cells were treated with the CM-H2DCFDA reagent (10 µM) and incubated in the dark. Following 20 min incubation at 37°C, cells were rinsed once with HBSS and incubated with the different treatment conditions as previously stated. Fluorescence was measured using a fluorescent microplate reader (Fluoroskan Ascent, Thermo Fisher Scientific, Vantaa, Finland) at excitation wavelength of 492 nm and emission wavelength of 518 nm. Data are expressed as the fluorescence values normalised to the protein concentration.

Statistical analysis

Statistical analysis was performed using GraphPad Prism 7.0 (GraphPad Software, Inc., USA). Data are presented as mean ± standard error of the mean (SEM) of minimally three independent experiments performed in triplicate. Significance was evaluated using One-way Analysis of Variance (ANOVA), or where appropriate, unpaired two-tailed Student's t-test was applied. P-values < 0.05 were considered to be significant.

Data Availability

The mass spectrometry proteomics data have been deposited to the ProteomeXchange Consortium via the PRoteomics IDEntifications database (PRIDE) (https://www.ebi.ac.uk/pride/archive/) partner repository with the dataset identifier PXD020046.

RESULTS

CRISPR-generated *CTNS*$^{-/-}$ ciPTEC display increased cystine accumulation and impaired lysosomal autophagy dynamics. As cell lines obtained at different times and from different individuals often have variable phenotypes independent of the genetic defect that is being studied, we created isogenic cell lines by specifically knocking out *CTNS* in a well-established human proximal tubule line [19-21]. A guide RNA (gRNA) targeting exon 4 of the *CTNS* gene was used to introduce mutations by CRISPR/Cas9 in conditionally immortalised proximal tubule epithelial cells (ciPTEC). After cell sorting and subsequent clonal cell expansion, three clones with biallelic mutations (lines 3, 7, and 35) were initially selected and all displayed a similar phenotype (Supplementary figure S1), therefore, line 3 (hereafter referred to as *CTNS*$^{-/-}$) was used for subsequent experiments. This model enables direct evaluation of the effect of *CTNS* loss on proximal tubule epithelial cells independent of chronic exposure to other disease related changes in the body.

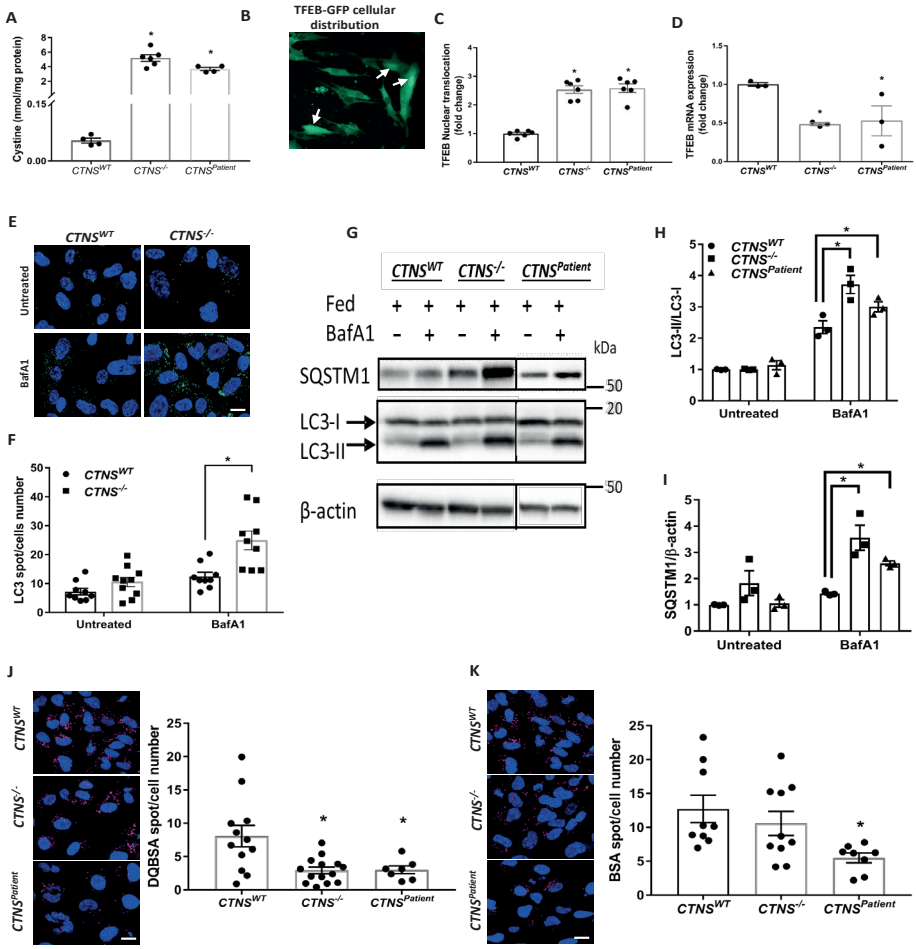

FIGURE 1. CRISPR-generated *CTNS*$^{-/-}$ ciPTEC demonstrate cystinosis phenotype. (A) Quantification of cystine levels (nmol/mg protein) in control (*CTNS*^{WT}), CRISPR-generated cystinotic cells (*CTNS*$^{-/-}$), and patient-derived cystinotic cells (*CTNS*^{Patient}). **(B)** Representative confocal micrographs of transcription factor EB (TFEB) cellular distribution. White arrows indicate TFEB nuclear location. Scale bars is 20 µm. **(C)** Quantification of TFEB-GFP nuclear translocation in *CTNS*^{WT}, *CTNS*$^{-/-}$, and *CTNS*^{Patient}, respectively. Data is demonstrated as the ratio between number of the cells with nucleus-TFEB positive over the total number of TFEB-transfected cells. The ratios were then presented as a fold change compared to control cells. **(D)** *TFEB* mRNA expression in *CTNS*$^{-/-}$ and *CTNS*^{Patient} cells compared to control cells. **(E**, **F)** representative confocal micrographs and quantification of LC3-II accumulation in *CTNS*^{WT} and *CTNS*$^{-/-}$ cells in presence and absence of 25 nM bafilomycin (BafA1) for 4 hrs, respectively. Scale bars are 20 µm. **(G, H**, **I)** Western blotting and densitometric analyses for LC3-II/LC3-I ratio and SQSTM1 protein levels in *CTNS*^{WT}, *CTNS*$^{-/-}$, and *CTNS*^{Patient} cells cultured in the presence or in the absence of 25 nM BafA1 for 4 h, respectively. **(J, K)** Representative confocal micrographs and quantification of DQ-BSA and BSA in *CTNS*^{WT}, *CTNS*$^{-/-}$, and *CTNS*^{Patient} cells, respectively. Scale bars are 20 µm. Data are expressed as mean ± SEM. P-values < 0.05 were considered to be significant.

As a reference, we also included a non-isogenic patient-derived cystinotic ciPTEC line bearing the homozygous 57-kb *CTNS* deletion [22, 23], referred to as $CTNS^{Patient}$ (this cell line was obtained at a different time from a different individual). In accordance with the pathophysiology of the disease, $CTNS^{-/-}$ cells displayed significantly increased levels of cystine compared to control $CTNS^{WT}$ cells (5.19 ± 0.30 vs. 0.05 ± 0.02 nmol/mg protein), comparable to $CTNS^{Patient}$ cells (Fig 1A). Next, we evaluated the effect of *CTNS* loss on mammalian target of rapamycin complex 1 (mTORC1) [8-10]. Under normal conditions, mTORC1 is bound to the lysosomes and is responsible for regulating a wide range of cellular processes, including autophagy [24, 25]. In the presence of nutrients (standard medium, fed condition), mTOR located to the lysosomal membranes of $CTNS^{WT}$ cells (Supplementary figure S2). Upon starvation (-AA), mTOR was released from the lysosomes and re-localised upon reintroduction of nutrients. In contrast, in $CTNS^{-/-}$ and $CTNS^{Patient}$ cells, mTOR was already released from lysosomes in the fed condition (Supplementary figure S2), indicating the dissociation of the mTOR complex in cystinosis. We further evaluated mTOR activity in the cells by tracking the subcellular localization of transcription factor EB (TFEB). If mTOR is deactivated, unphosphorylated TFEB can translocate to the nucleus (Fig 1B), where it regulates gene transcription and activates autophagy. A ~2.5-fold increase in TFEB nuclear translocation was observed after transfection with TFEB-GFP in $CTNS^{-/-}$ and $CTNS^{Patient}$ cells compared to $CTNS^{WT}$ cells (Fig 1C). As TFEB will downregulate its own expression after activation [26], we found that the endogenous *TFEB* mRNA expression was also reduced in $CTNS^{-/-}$ and $CTNS^{Patient}$ cells (2-fold) compared to control cells (Fig 1D). During autophagy LC3-II is recruited to autophagosomes and p62/SQSTM1 is degraded after the fusion of autophagosomes with the lysosomes [27]. Blocking the lysosomal fusion with bafilomycin showed a significant increase in both LC3-II and p62/SQSTM1 levels in $CTNS^{-/-}$ and $CTNS^{Patient}$ cells compared to $CTNS^{WT}$ cells (Fig 1E-I), indicating an increase in autophagy activation. Next, we evaluated the ability of these cells to process BODIPY dye-conjugated bovine serum albumin (DQ BSA), a dye that is endocytosed and becomes fluorescent after degradation inside the lysosomes. A delayed lysosomal cargo degradation (~2.5-fold) of $CTNS^{-/-}$ and $CTNS^{Patient}$ cells compared to control cells was observed (Fig 1J). $CTNS^{Patient}$ cells, but not $CTNS^{-/-}$ cells, demonstrated a decreased BSA uptake compared to control cells (Fig 1K), indicating the defect is related to degradation rather than protein uptake in $CTNS^{-/-}$ cells.

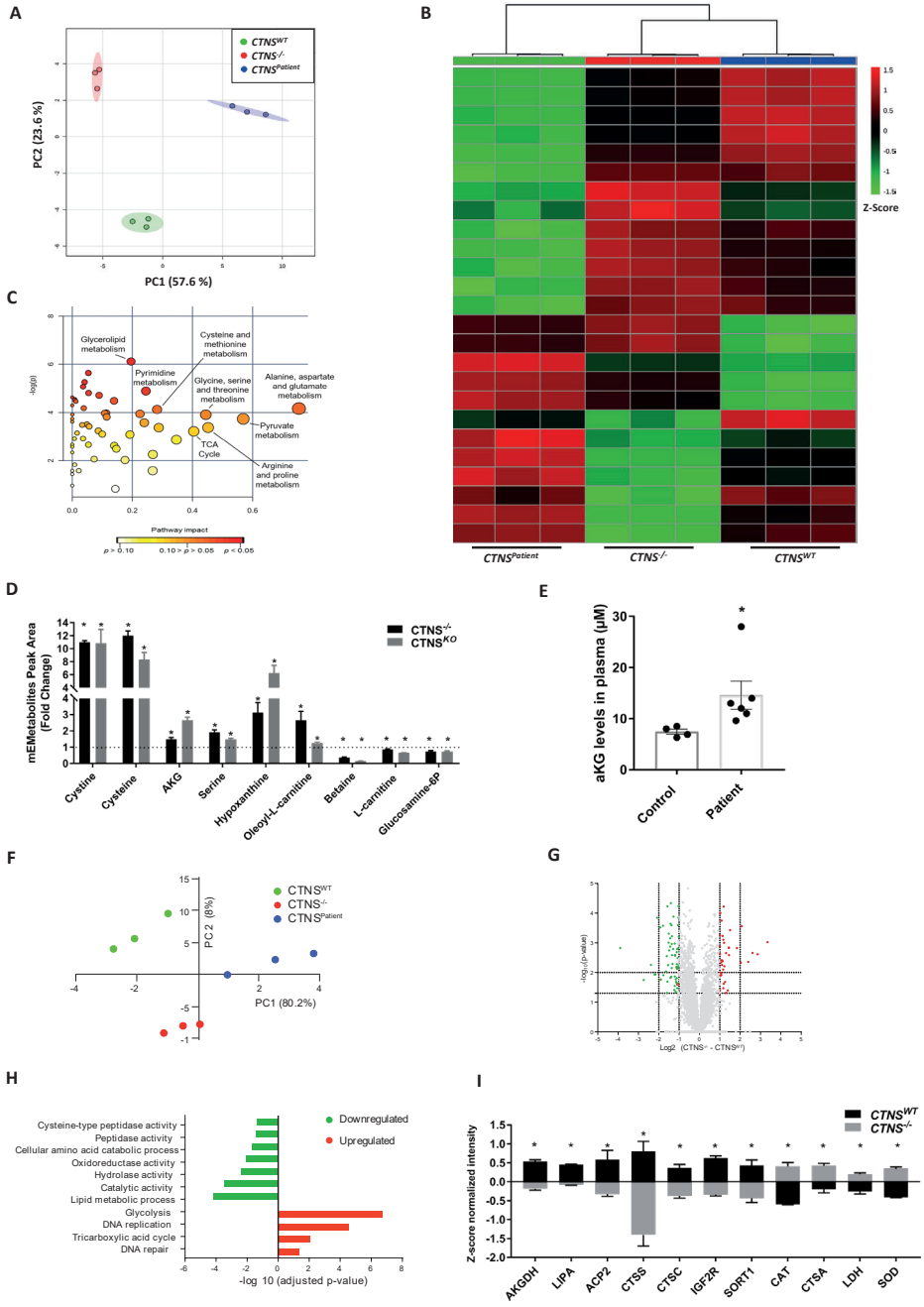

FIGURE 2. Metabolomic and proteomic profiling reveal αKG accumulation in cystinosis. (A) Principal component analysis (PCA) of control (*CTNS*^{WT}), CRISPR-generated cystinotic (*CTNS*$^{-/-}$), and patient-derived cystinotic (*CTNS*^{Patient}) cells based on the metabolites measured. Each dot represents one sample, and the dots of the same colour are biological replicates. **(B)** Heatmap

analysis of top 25 metabolites distinctively expressed in control and *CTNS*$^{-/-}$ cells. Metabolites significantly decreased ($P < 0.05$) were displayed in green, while metabolites significantly increased ($P < 0.05$) were displayed in red. **(C)** Global test pathway enrichment analysis of the intracellular metabolic interactions distinctively affected in *CTNS*$^{-/-}$ cells compared to healthy control cells. Larger circles further from the y-axis and orange-red colour show higher impact of pathway. **(D)** List of metabolites that were shared and significantly altered in both the *CTNS*$^{-/-}$ and *CTNS*^{Patient} cells compared to control cells. **(E)** Plasma levels of αKG (μM) in healthy individuals (n=4) and cystinotic patients (n=6). All cystinotic patients were on cysteamine treatment at the time of blood sampling. For this experiment, non-parametric Mann-Whitney t-test was used to demonstrate the significance. **(F)** Principal component analysis (PCA) of the measured proteins in *CTNS*^{WT}, *CTNS*$^{-/-}$, and *CTNS*^{Patient}. **(G)** Volcano plot illustrates differentially abundant proteins. The $-\log_{10}$ (Benjamini–Hochberg corrected P-value) is plotted against the $\log_2$ (fold change: *CTNS*^{WT}/*CTNS*$^{-/-}$). **(H)** Gene ontology (GO) analysis illustrates classes of proteins differing between *CTNS*^{WT} and *CTNS*$^{-/-}$ cells. **(I)** List of proteins that were significantly upregulated and downregulated in *CTNS*$^{-/-}$ cells compared to control cells. AKGDH; Alpha-ketoglutarate dehydrogenase, LIPA; Lysosomal acid lipase, ACP2; Lysosomal acid phosphatase, CTSS; Cathepsin S, CTSC; Dipeptidyl peptidase, IGF2R; Cation-independent mannose-6-phosphate receptor, SORT1; Sortilin, CAT; Catalase, CTSA; Lysosomal protective protein, and SOD; Superoxide dismutase. Data are expressed as mean ± SEM. P-values < 0.05 were considered to be significant.

Metabolomic and proteomic profiling reveal alpha-ketoglutarate accumulation in cystinosis. To gain in-depth knowledge of the affected cellular pathways and proximal tubule impairments in cystinosis, we performed targeted metabolomic profiling of 100 key metabolites and untargeted proteomics in the three cell lines (Fig 2). Principal component analysis (PCA) of the metabolites and over 4500 identified proteins (Fig 2A, F) showed that *CTNS*^{Patient} cells account for most of the variability in the data, indicating that the different genetic background of the *CTNS*^{Patient} cells affect the data more than the *CTNS* loss itself. This was further visualised by unsupervised hierarchical clustering in which the isogenic *CTNS*$^{-/-}$ cells clustered with *CTNS*^{WT} rather than *CTNS*^{Patient} cells (Fig 2B). To explore which pathways are directly linked to *CTNS* loss, we focused on the metabolites and proteins that were significantly altered in *CTNS*$^{-/-}$ cells compared to the *CTNS*^{WT}. Pathway enrichment analysis of the metabolites distinctively affected in *CTNS*$^{-/-}$ cells revealed several affected pathways, including cystine/cysteine metabolism, the TCA cycle, glycerolipid metabolism, and amino acid metabolism (Fig 2C). Proteomic profiling, on the other hand, revealed a total of 337 proteins that were up- or downregulated in *CTNS*$^{-/-}$ cells compared to control cells (Fig 2G). The differentially abundant proteins were then subjected to gene ontology (GO) classification via the Panther Classification System database [28] to highlight their molecular role in the cell (Fig 2H). The analysis showed an overall reduction in proteins involved in lipid metabolism and the breakdown of micromolecular cellular structures (peptidases, amino acid catabolism, reductases and hydrolases), and an increase in the glycolysis, TCA cycle, DNA replication and DNA repair, in line with the metabolomic data. Consistent with the reduced cargo degradation in cystinotic cells, we found an overall reduction in lysosomal catalytic-proteins expression including, lysosomal acid lipase (LIPA), lysosomal acid phosphatase (ACP2), and cysteine

proteases cathepsin (CTSS) (Fig 2I). Moreover, cation-independent mannose 6-phosphate receptor (IGF2R) was found downregulated in *CTNS*$^{-/-}$ cells (Fig 2I). IGF2R is responsible for the delivery of many newly synthesised lysosomal enzymes from Golgi to the lysosome, and its downregulation results in decreased lysosomal activity and production of ROS [29, 30].

When cross-checking the affected metabolites of both *CTNS*$^{-/-}$ and *CTNS*^{Patient} cells, we identified a set of key metabolites that were significantly changed as a result of *CTNS* loss: cystine, cysteine, αKG, serine, hypoxanthine, and oleoyl-L-carnitine levels were increased, whereas the levels of betaine, L-carnitine, and glucosamine-6-phosphate were decreased in both *CTNS*$^{-/-}$ and *CTNS*^{Patient} compared to control cells (Fig 2D). αKG was of particular interest as αKG is known to play a central role in the TCA cycle, maintaining the redox balance, regulating mTOR and autophagy. Moreover, αKG is a well-known antioxidant and its cellular levels can be increased in response to oxidative stress, contributing to the prevention and/or treatment of several disorders induced by such stress [31-33]. This is done through downregulation of the mitochondrial enzyme alpha-ketoglutarate dehydrogenase (AKGDH), reported to be severely diminished in human pathologies where oxidative stress is thought to play a vital role [33]. Indeed, we found a decreased expression of AKGDH in *CTNS*$^{-/-}$ cells (Fig 2I). We also observed a significantly increased level of αKG in plasma of cystinotic patients compared to healthy controls (Fig 2E, and supplementary Table 1), signifying that loss of *CTNS* also leads to an increase in aKG levels in patients. This prompted us to evaluate further the effect of increased levels of αKG in cystinosis pathology.

Alpha-ketoglutarate regulates the phenotypic alterations in cystinosis. The link between cystinosin loss-of-function and increased oxidative stress has been long-established [11, 22, 34, 35]. In line with this, both *CTNS*$^{-/-}$ and *CTNS*^{Patient} cells presented increased ROS levels (~1.5-fold) compared to control cells (Fig 3A). Starvation triggered ROS production further in all three cell lines (Fig 3B-D). Supplementing starved cells with dimethyl αKG (DMKG), a cell permeable form of αKG, for 4 hrs led to a reduction in ROS levels in *CTNS*^{WT} cells (2.1-fold), a modest reduction in *CTNS*$^{-/-}$ cells (1.2-fold), but increased ROS levels in *CTNS*^{Patient} cells (Fig 3B-D), showing limited anti-oxidative effect of αKG in *CTNS* deficient cells. Of note, exposure to DMKG for 4 hrs was not toxic in any of the three cell lines (Supplementary figure S3A), however, adding DMKG during the 24 hrs starvation had little to no effect in control cells, but led to massive cell death and apoptosis activation in cystinotic cells (Fig 3E-G, and supplementary figure S3B and C). We, therefore, hypothesised that the increased level of αKG could be key to perturbing autophagy and promoting cell death in cystinotic proximal tubule cells [36-38]. DMKG exposure indeed resulted in an increased level of LC3-II/LC3-I ratio in *CTNS*$^{-/-}$ and *CTNS*^{Patient} but not in control cells, confirming that DMKG induces autophagy in cystinotic cells (Fig 3H, I). In light of our data, we identified αKG as an important metabolite linking cystinosin loss, increased oxidative stress, autophagy disruption, and proximal tubule dysfunction in cystinosis (Fig 3J).

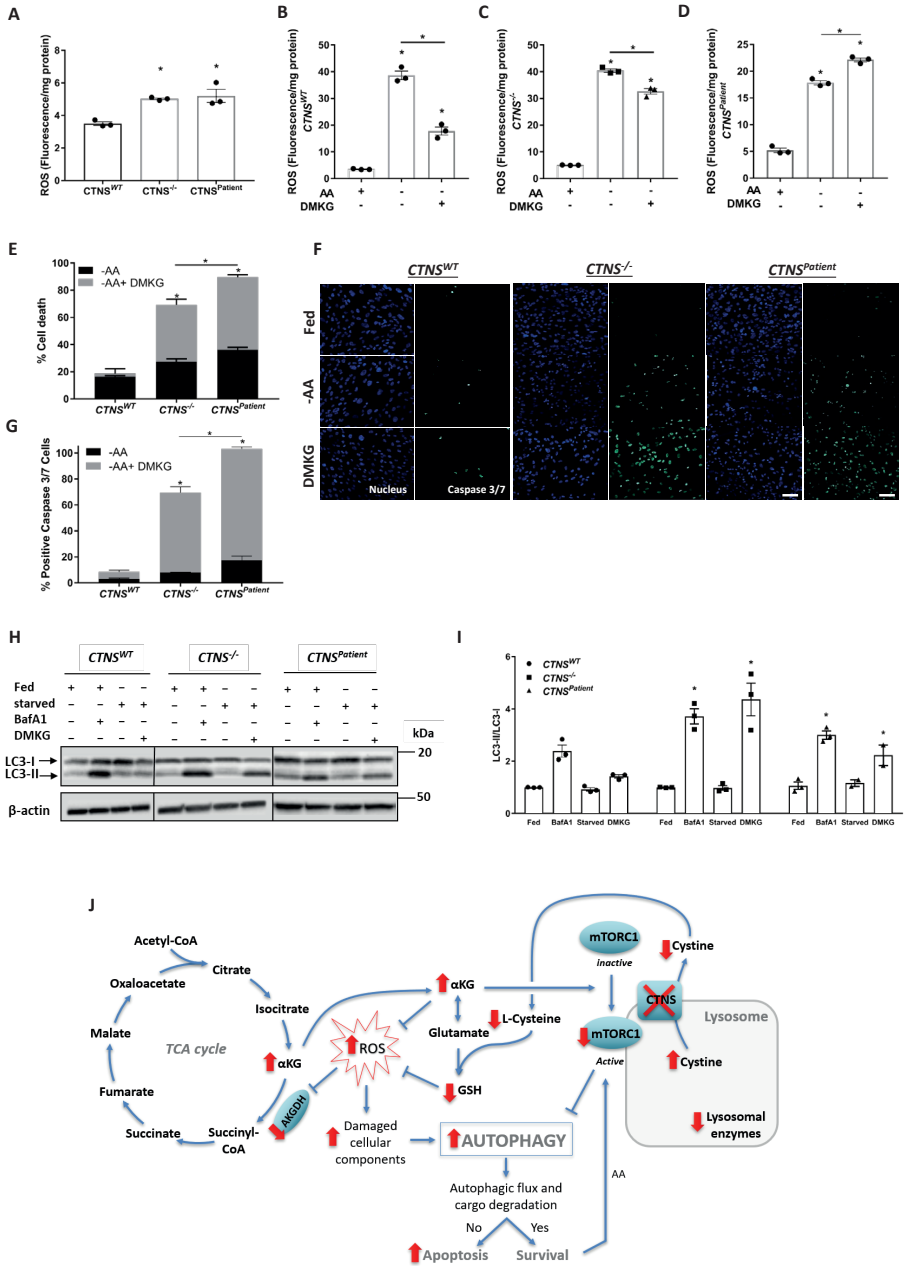

FIGURE 3. αKG is a key metabolite responsible for impaired autophagy and proximal tubule dysfunction in cystinotic proximal tubule cells. (A) Relative reactive oxygen species (ROS/mg protein) production in control (*CTNS*^{WT}), CRISPR-generated cystinotic cells (*CTNS*$^{-/-}$), and patient-derived cystinotic (*CTNS*^{Patient}) cells. **(B**, **C**, **D)** ROS production (ROS/mg protein) in *CTNS*^{WT}, *CTNS*$^{-/-}$, and *CTNS*^{Patient} cells upon starvation for 4 hrs in the presence and absence of DMKG (4 hrs), respectively. **E**, Viability test in starved (-AA) *CTNS*^{WT}, *CTNS*$^{-/-}$, and *CTNS*^{Patient} cells in the presence or absence

of DMKG (2 mM) for 24 hrs. Results are shown relative to the fed condition. **(F, G)** Representative confocal micrographs (scale bars are 20 µm) and immunofluorescence analysis of caspase 3/7 activation in DMKG (2 mM)-treated *CTNS*^{WT}, *CTNS*$^{-/-}$, and *CTNS*^{Patient} cells for 24 hrs. **(H**, **I)** Western blotting and densitometric analyses for LC3-II/LC3-I ratio in *CTNS*^{WT}, *CTNS*$^{-/-}$, and *CTNS*^{Patient} cells cultured in the presence or in the absence of BafA1 (25 nM) and DMKG (2 mM) for 4 hrs, respectively. **(J)** Working model summarizing the results obtained in this work. The red arrow indicates the up or down regulation of the process in cystinotic cells. TCA cycle; tricarboxylic acid cycle, αKG; alpha-ketoglutarate, AKGDH; alpha-ketoglutarate dehydrogenase, ROS; Relative reactive oxygen species, GSH; glutathione, mTORC1; mammalian target of rapamycin complex 1, AA; Amino acid. Data are expressed as mean ± SEM. P-values < 0.05 were considered to be significant.

Bicalutamide and cysteamine combination treatment phenotypically corrects *CTNS*$^{-/-}$ proximal tubule cells. Cysteamine is used to efficiently reduce cystine accumulation in patients with cystinosis, but it cannot correct the established proximal tubulopathy associated with the disease. We hypothesised that this may be linked to the inability of this drug to lower αKG and target other metabolic pathways associated with *CTNS* loss. We, therefore, screened different candidate drugs based on their ability to reduce cystine and αKG levels and to restore the metabolic profile using metabolomics. The concentrations of the drugs tested were within a non-cytotoxic range (Supplementary figure S3D-J). Cysteamine, as expected, boosted GSH and lowered cystine and cysteine levels. However, it had no significant impact on the other metabolites or on the proteome profiles (Fig 4A-E, and supplementary figure S4A). Among the candidate drugs tested, bicalutamide, an anti-androgenic agent, did not restore the high cystine and cysteine levels but could improve the overall metabolic phenotype, including αKG, serine, betaine, and oleoyl-L-carnitine (Fig 4A). In line with its metabolic effects, treatment with bicalutamide alone also resulted in the upregulation of several metabolic enzymes involved in cysteine conversion, lysosomal degradation, and the TCA cycle, including AKGDH (Fig 4C-E, and supplementary figure S4B). Furthermore, the cysteamine-bicalutamide combination treatment showed an additive effect and unsupervised clustering shows that the cells receiving the combination therapy are more similar to the *CTNS*^{WT} cells than the other conditions (Fig 4B). The combination treatment also led to the upregulation of more than 50 proteins, revealing an enrichment of proteins involved in the TCA cycle and in the metabolism of macromolecules such as lipids and vitamins that were shown to be downregulated in *CTNS*$^{-/-}$ cells (Fig 4C-E, and supplementary figure S4C).

As bicalutamide reduced the elevated level of αKG in cystinotic cells, we hypothesised that it could also resolve αKG-mediated downstream effects. Indeed, bicalutamide (but not cysteamine) reduced the DMKG-mediated cell death and increase in LC3-II/LC3-I ratio in *CTNS*$^{-/-}$ cells (Fig 5A and B). Although cysteamine alone showed no effect on autophagy, combined with bicalutamide it additively reduced the DMKG-mediated increase in LC3-II/I in *CTNS*$^{-/-}$ cells compared to bicalutamide alone (Fig 5B). Notably, cysteamine, bicalutamide, and their combination had no effect on the basal autophagy activity (Supplementary figure S4D).

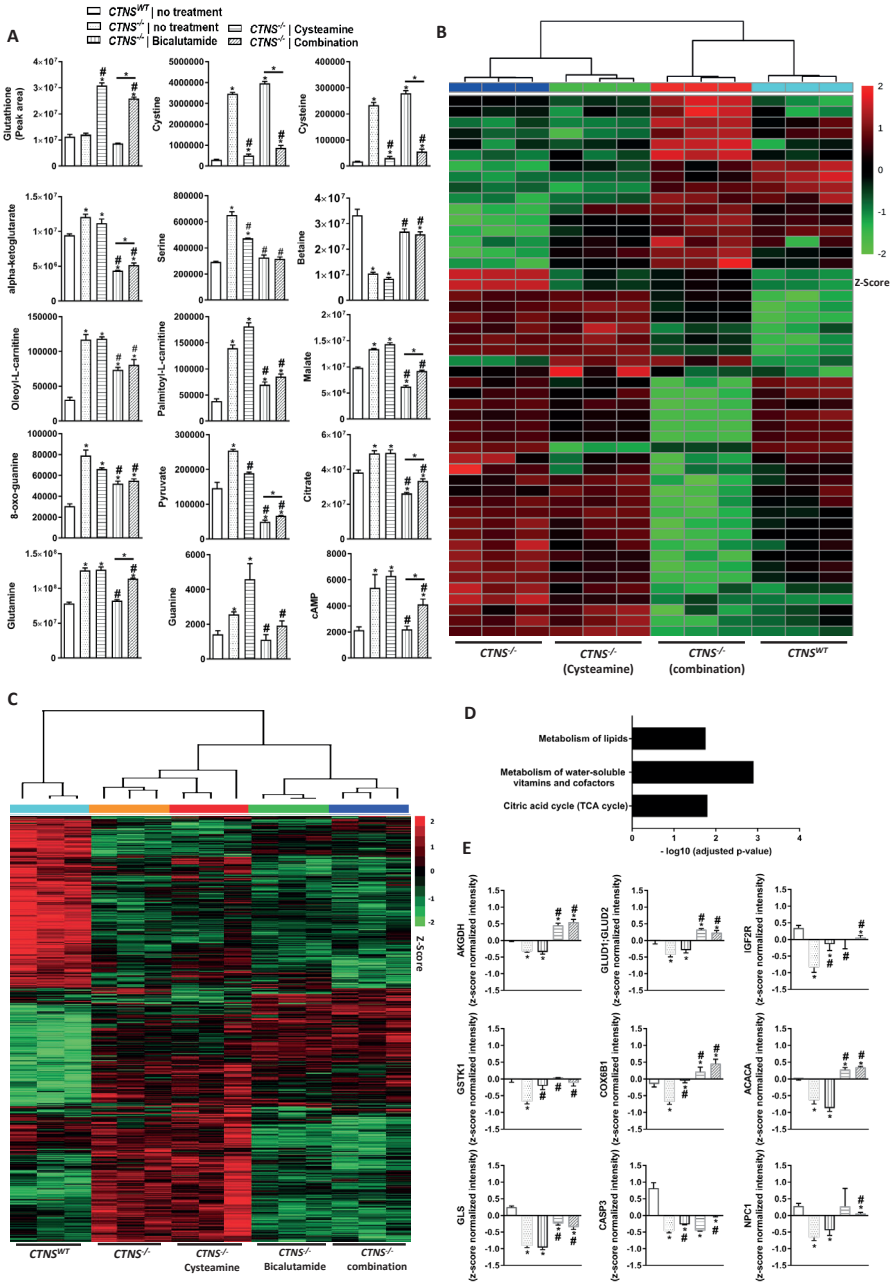

FIGURE 4. Bicalutamide-cysteamine combination treatment corrects the metabolome and proteome profile of cystinotic proximal tubule cells. (A) Metabolomic analysis of CRISPR-generated cystinotic cells (*CTNS*$^{-/-}$) treated with cysteamine (100 µM), bicalutamide (35 µM), and a combination of cysteamine and bicalutamide (100 µM and 35 µM, respectively). **(B)** Heatmap analysis of the measured metabolites in *CTNS*$^{-/-}$ cells upon treatment with cysteamine or cysteamine-bi-

calutamide combination treatment. Metabolites significantly decreased were displayed in green, while metabolites significantly increased were displayed in red. **(C, D)** Heatmap and REACTOME analysis of the altered proteins in *CTNS*$^{-/-}$ cells upon treatment with cysteamine, bicalutamide, and cysteamine-bicalutamide combination treatment. Proteins significantly decreased were displayed in green, while metabolites significantly increased were displayed in red. **(E)**, Proteomic analysis of *CTNS*$^{-/-}$ cells treated with cysteamine, bicalutamide, and a combination of cysteamine and bicalutamide, respectively. AKGDH; Alpha-ketoglutarate dehydrogenase, GLUD1; GLUD2; Mitochondrial glutamate dehydrogenase 1/2, IGF2R; Cation-independent mannose-6-phosphate receptor, GSTK1; Glutathione S-transferase kappa 1, COX6B1; Cytochrome c oxidase subunit 6B1, ACACA; Acetyl-CoA carboxylase 1-Biotin carboxylase, GLS; Glutaminase kidney isoform, mitochondrial, CASP3; Caspase-3, NPC1; Niemann-Pick C1 protein. Data are expressed as mean ± SEM. * Significantly different from *CTNS*^{WT} cells ($p < 0.05$). # significantly different from *CTNS*$^{-/-}$ cells ($p < 0.05$).

We next tested whether bicalutamide alone or in combination with cysteamine could recover the antioxidant effect of αKG in cystinotic cells. Similar to cysteamine, bicalutamide was able to retrieve the effect of DMKG in *CTNS*$^{-/-}$ cells (2.1-fold; Fig 5C). Further reduction in ROS levels was observed when bicalutamide and cysteamine were given together. Of note, bicalutamide alone had no effect on GSH levels (Fig 4A) but could significantly lower the ROS levels in presence of DMKG in cystinotic cells (Fig 5C), suggesting that bicalutamide, through a yet unknown mechanism, restores the antioxidant property of αKG in *CTNS*$^{-/-}$ cells.

Recently, bicalutamide has been patented for the treatment of several LSDs, promoting mTOR-associated autophagy and TFEB-mediated cellular exocytosis [39][32][32], and therefore allowing the relief and/or treatment of the symptoms of many LSDs. Indeed, bicalutamide was able to induce TFEB nucleus translocation in both control and *CTNS*$^{-/-}$ cells and downregulate *TFEB* mRNA expression in control cells (Supplementary figure S4E, and F). In agreement with the increased TFEB activity, bicalutamide also restored endocytic cargo processing in cystinotic cells (Fig 5D, and E), allowing us to test whether the increased degradation of lysosomal cargo results in decreased cystine accumulation. We used a more sensitive and quantitative LC-MS/MS method to measure cystine levels in cystinotic cells upon treatment with cysteamine, bicalutamide, or their combination. In line with metabolomics data, *CTNS*$^{-/-}$ cells treated with bicalutamide alone did not exhibit any reduction in cystine levels. Cysteamine alone resulted in a reduction of cystine in *CTNS*$^{-/-}$ cells (0.37 ± 0.08 nmol/mg protein; Fig 5F), but this was still higher (7.5-fold) than that found in control cells (0.05 ± 0.02 nmol/mg protein). Interestingly, combination treatment of bicalutamide and cysteamine resulted in a 2.8-fold decrease in cystine when compared to cysteamine alone (0.13 ± 0.003 *vs* 0.37 ± 0.08 nmol/mg protein; Fig 5F), bringing lysosomal cystine close to control. This effect was also found in *CTNS*^{Patient} cells (Fig 5G).

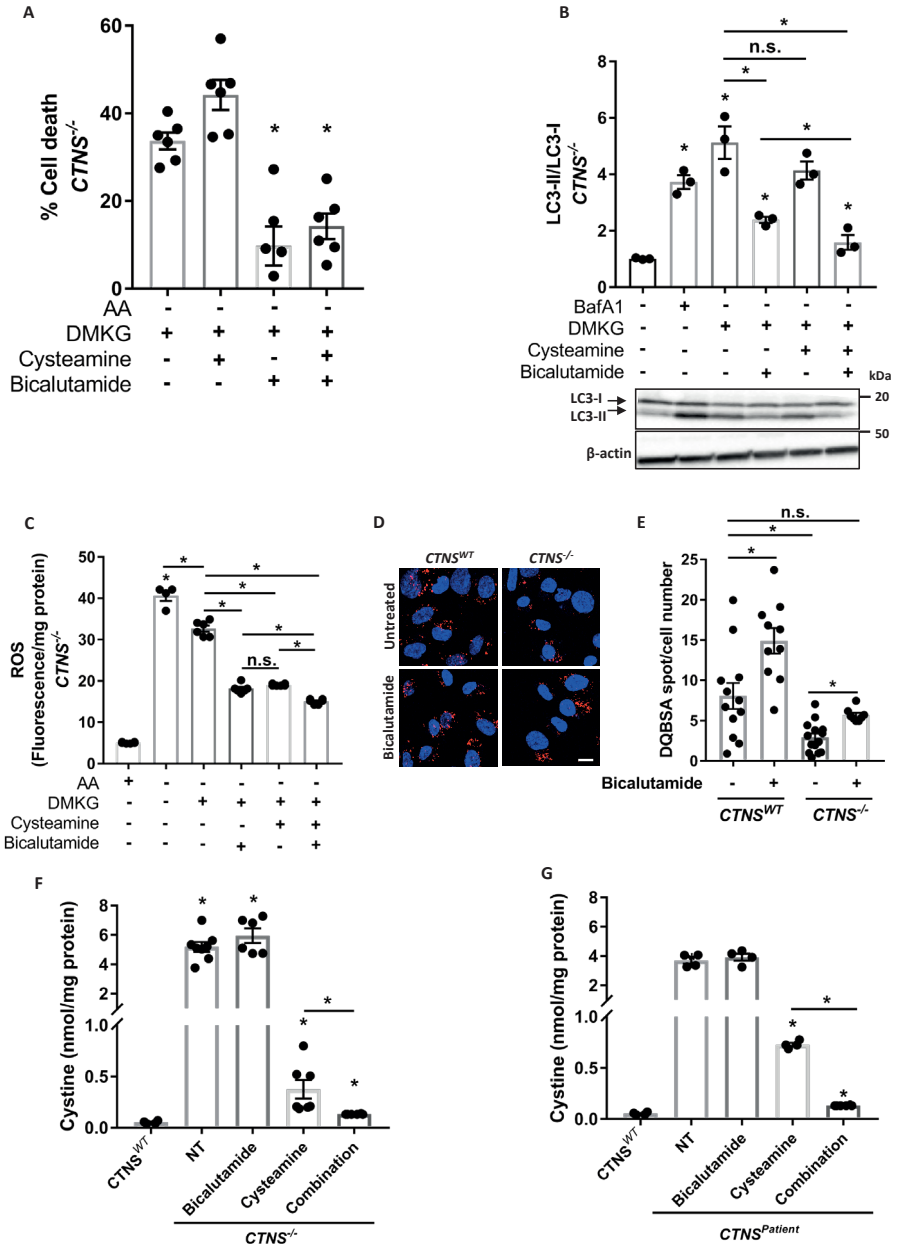

FIGURE 5. Cysteamine-bicalutamide combination treatment efficiently lowers lysosomal cystine, abolishes αKG-mediated autophagy distortion and cell death in cystinotic proximal tubule cells. (A) Cell viability test of DMKG (2 mM)-treated CRISPR-generated cystinotic cells (*CTNS*$^{-/-}$) upon pre-treatment with cysteamine (100 μM), bicalutamide (35 μM), and a combination of cysteamine and bicalutamide (100 μM and 35 μM, respectively). Results are shown relative to the starved condition. **(B)** Western blotting and densitometric analyses for LC3-II/LC3-I ratio in DMKG (2 mM)-treated *CTNS*^{WT} and *CTNS*$^{-/-}$ cells upon pre-treatment with cysteamine, bicalutamide,

and a combination of cysteamine and bicalutamide. **(C)** Relative reactive oxygen species (ROS/mg protein) production in DMKG-treated *CTNS*^{WT} and *CTNS*$^{-/-}$ cells upon pre-treatment with cysteamine, bicalutamide, and a combination of cysteamine and bicalutamide. **(D, E)** Representative confocal micrographs and quantification of DQ-BSA in *CTNS*^{WT}, and *CTNS*$^{-/-}$ cells upon treatment with bicalutamide. Scale bars are 20 µm. **(F, G)** Quantification of cystine levels (nmol/mg protein) by HPLC-MS/MS in *CTNS*$^{-/-}$, *CTNS*^{Patient} in the absence of the drug (NT) or upon treatment with cysteamine, bicalutamide, and a combination of cysteamine and bicalutamide. Data are expressed as mean ± SEM. P-values < 0.05 were considered to be significant.

Bicalutamide and cysteamine combination treatment efficiently lowers cystine and αKG levels in patient-derived cystinotic kidney tubuloids. Next, we evaluated the safety and efficacy of cysteamine-bicalutamide combination treatment in patient-derived tubuloids. Tubuloids are an advanced *in vitro* model that was successfully used before to model genetic, infectious and malignant kidney disease and to screen for therapeutic efficacy [14]. We established kidney tubuloids from urine samples of two pediatric cystinotic patients (*CTNS*$^{Patient-1}$ and *CTNS*$^{Patient-2}$) and compared their characteristics to tubuloids derived from healthy kidney tissue of two donors (*CTNS*$^{WT-1}$ *and CTNS*$^{WT-2}$). Urine-derived tubuloids were positive for paired-box gene 8 (PAX8) and negative for tumor protein p63 (Fig. 6A), confirming that these structures indeed consisted of kidney epithelium (PAX8+/p63-) and not urothelium (PAX8-/p63+) [40, 41]. Moreover, both patient and control tubuloids robustly expressed markers of the of proximal tubule, loop of Henle, distal tubule and collecting duct (Supplementary figure S5A) [14]. Both *CTNS*^{Patient} tubuloids displayed the cystinotic phenotype with increased increased cystine accumulation (~7-fold) compared to the controls (Fig 6B). In line with the previous findings in ciPTEC, treatment of *CTNS*^{Patient} tubuloids with a non-nephrotoxic dose of both cysteamine and bicalutamide (Supplementary figure S5B-D) resulted in a more potent reduction in cystine levels (~2-fold) than with cysteamine treatment alone (Fig 6C, and D). Furthermore, we performed targeted metabolomic profiling and identified that bicalutamide (but not cysteamine), either alone or in combination with cysteamine, reduced the αKG levels in *CTNS*$^{Patient-2}$ tubuloids (Fig 6E).

Bicalutamide and cysteamine combination treatment efficiently lowers cystine levels and improves survival of cystinotic zebrafish. Finally, we assessed the combination therapy in cystinotic zebrafish, a well-characterised *in vivo* model of cystinosis [42, 43]. Cystinotic zebrafish displayed significantly increased levels of cystine, dysmorphic features, delayed hatching, and reduced survival compared to controls (Fig 6F-K, and supplementary figure S5E-G). As expected, cysteamine was able to reduce cystine levels (1.5-fold; Fig 6H) and a trend towards an additive effect of bicalutamide was observed (1.8-fold reduction for the combination), though this was not significant. However, bicalutamide either alone or in combination with cysteamine significantly improved the survival and reduced the percentage of dysmorphism in the cystinotic zebrafish without having an effect on their hatching rate, when compared to cysteamine monotherapy (Fig 6I-K). This indicates that the combination treatment does not induce toxicity and is beneficial in cystinotic zebrafish compared to cysteamine treatment alone.

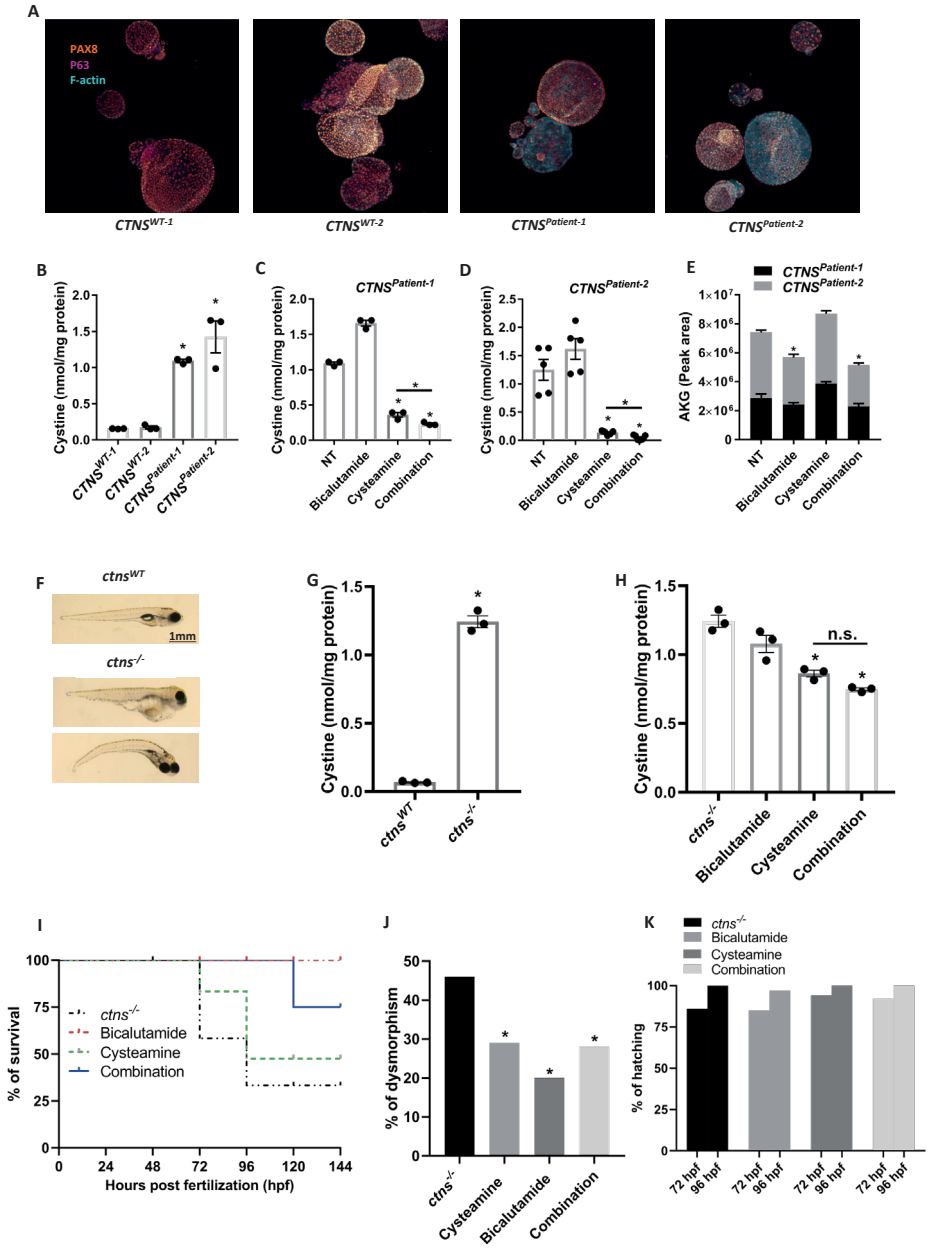

FIGURE 6. Cysteamine-bicalutamide combination treatment is effective in patient-derived cystinotic tubuloids and cystinotic zebrafish. (A) Immunohistochemistry of patient-derived cystinotic tubuloids (*CNTS*$^{Patient-1}$ and *CTNS*$^{Patient-2}$) and healthy kidney tissue-derived control tubuloids (*CNTS*$^{WT-1}$ and *CTNS*$^{WT-2}$) for PAX8, p63 and F-actin. **(B)** Quantification of cystine levels (nmol/mg protein) by HPLC-MS/MS in control and cystinotic tubuloids. **(C, D)** Quantification of cystine levels (nmol/mg protein) by HPLC-MS/MS in two different patient-derived cystinotic tubuloids in the

absence of the drug (NT) or upon treatment with cysteamine (100 μM), bicalutamide (35 μM) or cysteamine (100 μM)-bicalutamide (35 μM) combination treatment. **(E)** αKG levels measured in patient-derived cystinotic tubuloids (*CNTS*$^{Patient-1}$ and *CTNS*$^{Patient-2}$) in the absence of the drug (NT) or upon treatment with cysteamine, bicalutamide or cysteamine-bicalutamide combination treatment using metabolomics. **(F)** Representative images of control and cystinotic zebrafish. **(G)** Quantification of cystine levels (nmol/mg protein) by HPLC-MS/MS in control and cystinotic zebrafish. **(H)** Quantification of cystine levels (nmol/mg protein) by HPLC-MS/MS in cystinotic zebrafish after treatment with cysteamine (1000 μM), bicalutamide (10 μM), and a combination of cysteamine and bicalutamide (1000 μM and 10 μM, respectively). **(I)** Survival rates in *ctns*$^{-/-}$ zebrafish upon treatment with cysteamine, bicalutamide, and a combination of cysteamine and bicalutamide. **(J)** Deformity rates in *ctns*$^{-/-}$ zebrafish after treatment with cysteamine, bicalutamide, and a combination of cysteamine and bicalutamide. **(K)** Hatching rates in surviving *ctns*$^{-/-}$ zebrafish evaluated at 72 and 96 hrs post fertilization (hpf) with cysteamine, bicalutamide, and a combination of cysteamine and bicalutamide. The total numbers of embryos evaluated for survival, hatching, deformity rates, and cystine levels were 40 embryos per group. Data are expressed as mean ± SEM. P-values < 0.05 were considered to be significant.

DISCUSSION

In this work, we identified a new therapeutic target in nephropathic cystinosis by evaluating the persistent cellular link between cystinosin loss-of-function and proximal tubule cell dysfunction. Using an omics-based strategy, we identified αKG as an important metabolite linking autophagy disruption, increased oxidative stress, and proximal tubule dysfunction in cystinotic renal proximal tubule cells. These data also indicate that a bicalutamide-cysteamine combination treatment could provide a novel pharmacological approach for the phenotypical correction of cystinosis.

Consistent with previous reports, we found that *CTNS* deficient cells show high levels of cystine accumulation, reduced mTOR activation, delayed protein degradation and an increase in baseline ROS levels [10, 11, 22, 34, 35, 44-47]. This was confirmed further by metabolic and proteomic analyses, where we found a reduction in lysosomal catabolic proteins and an upregulation of enzymatic antioxidizing agents like catalase and superoxide dismutase in cystinotic cells, demonstrating delayed lysosomal cargo degradation and increased oxidative stress, respectively. In addition, we found that aKG levels are increased in *CTNS* deficient cells and in cystinotic patients, a metabolite known for its antioxidant properties and potential for the treatment of disorders induced by oxidative stress [31-33, 48]. During starvation, both control and *CTNS* deficient cells showed a strong increase in ROS (after 4 hrs), and the *CTNS* deficient cells seem to handle this well with only a slight reduction in cell viability compared to control cells after 24 hrs. Addition of DMKG (to increase intracellular aKG levels) during starvation led to a strong reduction in ROS in *CTNS*^{WT} cells but had a minor effect in *CTNS*$^{-/-}$ cells and even an opposite effect in *CTNS*^{Patient} cells. Even though DMKG had a minor effect on ROS levels in *CTNS*$^{-/-}$ cells during short term exposure, it still led to massive cell death after 24 hrs in *CTNS* deficient cell lines. We also found that addition of DMKG led to a strong increase

in LC3-II/LC3-I levels in *CTNS* deficient cells, suggesting that autophagy plays a role in the DMKG -induced cell death.

Many studies have investigated the role of αKG in response to ROS, mTOR and autophagy regulation, but the outcomes vary greatly depending on the context and the cell type studied. Overall, αKG is regarded as a health promoting metabolite, reducing liver fibrosis [49], delaying age-related disease and increasing life span in *in vivo* models such as *Caenorhabditis elegans* and mice [38, 50], and as a potential anti-cancer agent [36, 51]. However, long term accumulation of aKG can be rather harmful. Villar *et al.* showed that addition of DMKG in cancer cells for 24 hrs inhibits autophagy and induces glutaminolysis-mediated apoptosis during starvation [36]. In contrast, we here demonstrate that the addition of DMKG to cystinotic proximal tubule cells activates autophagy and mediates apoptosis.

In healthy cells, autophagy will lead to degradation of (dysfunctional) cellular components and this process will release nutrients and amino acids that will re-activate mTOR. It is also known that cystinosin directly interacts with Vacuolar H^+-ATPase-Ragulator-Rag Complex on the lysosomal membrane, and is responsible for recruiting and activating mTORC1 [52]. This was observed in our cystinotic cells, where both in fed and starved conditions mTOR remained dissociated from the lysosomal membrane, indicating that mTORC1 requires cystinosin to become active or to sense the nutritional state of the cell. It is, therefore, possible that in the *CTNS* deficient cells, due to the inactivated mTOR, reduced amino acid flux, and delayed cargo degradation, αKG activates autophagy and induces apoptosis, especially in starved condition.

Autophagy blockade is one of the key features in LSDs, including cystinosis [8, 46]. Recent studies showing that overexpression of TFEB activity stimulates lysosomal excretion and rescues the delayed endocytic cargo processing, allowing the relief and/or treatment of the symptoms of many LSDs [47]. This in line with the study of Rega *et al*., where stimulation of endogenous TFEB activity by genistein was shown to lower cystine levels and rescue the delayed endocytic cargo processing in cystinotic proximal tubule cells [26]. Furthermore, inhibition of mTOR signalling by everolimus was shown to activate autophagy, rescue the number of large lysosomes, and in combination with cysteamine, reverse the cystine/cysteine loading defect in patient-specific and CRISPR-edited cystinotic induced pluripotent stem cells and kidney organoids [53].

Bicalutamide has recently been patented for the treatment of several LSDs, promoting mTOR-associated autophagy and cellular exocytosis [39]. Here we find that in *CTNS*$^{-/-}$ cells, bicalutamide was able to increase endogenous TFEB activity, restore endocytic cargo processing and, in combination with cysteamine, normalize lysosomal cystine levels in both patient-derived and CRISPR-edited cystinotic proximal tubule cells. Furthermore, cysteamine-bicalutamide combination treatment, but not cysteamine alone, reversed the proteomic and metabolic phenotype and resulted in reduction of αKG levels, and upregulation of AKGDH and IGF2R proteins, resolving the αKG-mediated downstream effects in cystinotic proximal tubular cells.

So far, several murine models for cystinosis have been developed that recapitulate some of the clinical features seen in patients with cystinosis, including high blood cystine levels [54-57]. However**,** the renal phenotype is often mild, has a late onset or lacks signs of a proximal tubulopathy, or renal failure [58]. Furthermore, unlike the human situation where treatment with cysteamine does not improve the renal phenotype and only improves some parts of the cystinotic phenotype [59], it can completely resolve any renal symptoms in mice. This means that the unmet medical need that is currently present in humans is not observed in $Ctns^{-/-}$ mice, making this model unsuitable for studying any drug combination therapy aimed at improving the renal phenotype. Hence, to extend our knowledge on the beneficial effect of the combination treatment and bring the therapy one step closer to clinical application, we evaluated the safety and efficacy in patient-derived tubuloids, an advanced *in vitro* model, and *in vivo* in cystinotic zebrafish. Tubuloids offer several advantages over conventional mammalian cell lines. (1) They are human-derived three dimensional (3D) renal tubule epithelial cultures, offering physiological heterogeneity and recapitulating the *in vivo* situation. (2) Tubuloids are grown in 3D, allowing neighbouring cells to interact in a more physiological way than in conventional 2D culture models. (3) Tubuloids are not genetically modified or reprogrammed and can accurately mimic patients genotype and phenotype, allowing to develop personalised medicines [14]. Zebrafish can be valuable both for screening drug toxicity and as genetic disease models [60]. The $ctns^{-/-}$ zebrafish presents a robust and versatile model of cystinosis with early phenotypic characteristics of the disease that can be used for the *in vivo* screening of novel therapeutic agents [42, 43]. The fact that the improved cystine lowering-efficacy of the combination treatment could be reproduced in tubuloids from two different patients and in cystinotic zebrafish, underlines the robustness of these findings and increases the likelihood that this treatment can be successfully extrapolated to cystinosis patients.

Bicalutamide, a non-steroidal anti-androgenic agent, is also one of the most widely prescribed drugs for treating prostate cancer [61]. The use of any androgen deprivation therapy is generally associated with the risk of acute kidney injury (AKI) [62, 63], and up to 36% of patients who have taken bicalutamide for 1 to 6 months may experience AKI [63]. However, this association is mainly driven by a combination of gonadotropin- or luteinizing-releasing hormone agonists with bicalutamide [62]. Bicalutamide-cysteamine combination treatment at an effective concentration was not only found to be safe in our models, but also improved the survival and reduced the percentage of dysmorphism in the cystinotic zebrafish, confirming the safety profile of bicalutamide both in *in vitro* and *in vivo*. Anti-androgenic therapy is also known to reduce testosterone levels [62, 64], complicating the beneficial effect of bicalutamide in cystinotic male patients with delayed maturation [65-67]. Interestingly, bicalutamide is a racemate and its anti-androgenic activity is attributed solely to the (R)-enantiomer [68, 69], while the (S)-enantiomer with little, if any, anti-androgenic activity mediates autophagy effects [39]. Therefore, it would be of great scientific benefit to investigate further the effect of the (S)-bicalutamide and/or develop any structural analogues to treat cystinosis.

Taken together, we identified a new therapeutic target by evaluating the persistent cellular abnormalities using an omics-based strategy. We identified αKG as an important metabolite linking cystinosin loss, lysosomal autophagy defect, and proximal tubule cell impairment in cystinosis. Bicalutamide, but not cysteamine, was able to normalize αKG levels and resolve αKG-mediated downstream effects in cystinotic cells. Bicalutamide in combination with cysteamine demonstrated additively reduced cystine levels both *in vitro* and *in vivo*, suggesting this combination therapy holds great potential to treat patients with cystinosis.

Preclinical studies in a suitable animal model should determine if this combination therapy is able to improve or prevent the development of renal Fanconi syndrome and renal failure. Translation to the clinic should be further facilitated by the fact that bicalutamide is already an approved drug with a known safety profile. Although, a separate study should be performed to determine the right dose for cystinotic patients.

Acknowledgements

This work was financially supported by a grant from the Dutch Kidney Foundation (grant nr.150KG19) and the E-Rare 2-Joint Call 2014, Novel Therapies for Cystinosis grant from Zon-MW (grant nr. 113301402).

REFERENCES

1. Town, M., et al., *A novel gene encoding an integral membrane protein is mutated in nephropathic cystinosis.* Nat Genet, 1998. **18**(4): p. 319-24.
2. Cherqui, S. and P.J. Courtoy, *The renal Fanconi syndrome in cystinosis: pathogenic insights and therapeutic perspectives.* Nat Rev Nephrol, 2017. **13**(2): p. 115-131.
3. Gahl, W.A., J.G. Thoene, and J.A. Schneider, *Cystinosis.* N Engl J Med, 2002. **347**(2): p. 111-21.
4. Brodin-Sartorius, A., et al., *Cysteamine therapy delays the progression of nephropathic cystinosis in late adolescents and adults.* Kidney Int, 2012. **81**(2): p. 179-89.
5. Canonico, B., et al., *Defective Autophagy, Mitochondrial Clearance and Lipophagy in Niemann-Pick Type B Lymphocytes.* PLoS One, 2016. **11**(10): p. e0165780.
6. Gabande-Rodriguez, E., et al., *High sphingomyelin levels induce lysosomal damage and autophagy dysfunction in Niemann Pick disease type A.* Cell Death Differ, 2014. **21**(6): p. 864-75.
7. Lieberman, A.P., et al., *Autophagy in lysosomal storage disorders.* Autophagy, 2012. **8**(5): p. 719-30.
8. Sansanwal, P. and M.M. Sarwal, *p62/SQSTM1 prominently accumulates in renal proximal tubules in nephropathic cystinosis.* Pediatr Nephrol, 2012. **27**(11): p. 2137-2144.
9. Sansanwal, P., et al., *Mitochondrial autophagy promotes cellular injury in nephropathic cystinosis.* J Am Soc Nephrol, 2010. **21**(2): p. 272-83.
10. Festa, B.P., et al., *Impaired autophagy bridges lysosomal storage disease and epithelial dysfunction in the kidney.* Nat Commun, 2018. **9**(1): p. 161.
11. Levtchenko, E., et al., *Altered status of glutathione and its metabolites in cystinotic cells.* Nephrol Dial Transplant, 2005. **20**(9): p. 1828-32.
12. Ran, F.A., et al., *Genome engineering using the CRISPR-Cas9 system.* Nat Protoc, 2013. **8**(11): p. 2281-2308.
13. Wilmer, M.J., et al., *Novel conditionally immortalized human proximal tubule cell line expressing functional influx and efflux transporters.* Cell Tissue Res, 2010. **339**(2): p. 449-57.
14. Schutgens, F., et al., *Tubuloids derived from human adult kidney and urine for personalized disease modeling.* Nat Biotechnol, 2019. **37**(3): p. 303-313.
15. Jamalpoor, A., et al., *Quantification of cystine in human renal proximal tubule cells using liquid chromatography-tandem mass spectrometry.* Biomed Chromatogr, 2018: p. e4238.
16. Chong, J., M. Yamamoto, and J. Xia, *MetaboAnalystR 2.0: From Raw Spectra to Biological Insights.* Metabolites, 2019. **9**(3).
17. Tyanova, S., et al., *The Perseus computational platform for comprehensive analysis of (prote)omics data.* Nat Methods, 2016. **13**(9): p. 731-40.
18. Driehuis, E., et al., *Oral Mucosal Organoids as a Potential Platform for Personalized Cancer Therapy.* Cancer Discov, 2019. **9**(7): p. 852-871.
19. Caetano-Pinto, P., et al., *Fluorescence-Based Transport Assays Revisited in a Human Renal Proximal Tubule Cell Line.* Mol Pharm, 2016. **13**(3): p. 933-44.
20. Gorvin, C.M., et al., *Receptor-mediated endocytosis and endosomal acidification is impaired in proximal tubule epithelial cells of Dent disease patients.* Proc Natl Acad Sci U S A, 2013. **110**(17): p. 7014-9.

21. Jansen, J., et al., *A morphological and functional comparison of proximal tubule cell lines established from human urine and kidney tissue.* Exp Cell Res, 2014. **323**(1): p. 87-99.
22. Wilmer, M.J., et al., *Cysteamine restores glutathione redox status in cultured cystinotic proximal tubular epithelial cells.* Biochim Biophys Acta, 2011. **1812**(6): p. 643-51.
23. Peeters, K., et al., *Role of p-glycoprotein expression and function in cystinotic renal proximal tubular cells.* Pharmaceutics, 2011. **3**(4): p. 782-92.
24. Laplante, M. and D.M. Sabatini, *Regulation of mTORC1 and its impact on gene expression at a glance.* J Cell Sci, 2013. **126**(Pt 8): p. 1713-9.
25. Martina, J.A. and R. Puertollano, *RRAG GTPases link nutrient availability to gene expression, autophagy and lysosomal biogenesis.* Autophagy, 2013. **9**(6): p. 928-30.
26. Rega, L.R., et al., *Activation of the transcription factor EB rescues lysosomal abnormalities in cystinotic kidney cells.* Kidney Int, 2016. **89**(4): p. 862-73.
27. Tanida, I., T. Ueno, and E. Kominami, *LC3 and Autophagy.* Methods Mol Biol, 2008. **445**: p. 77-88.
28. Thomas, P.D., et al., *PANTHER: a browsable database of gene products organized by biological function, using curated protein family and subfamily classification.* Nucleic Acids Res, 2003. **31**(1): p. 334-41.
29. Probst, O.C., et al., *The 46-kDa mannose 6-phosphate receptor does not depend on endosomal acidification for delivery of hydrolases to lysosomes.* J Cell Sci, 2006. **119**(Pt 23): p. 4935-43.
30. Takeda, T., et al., *Upregulation of IGF2R evades lysosomal dysfunction-induced apoptosis of cervical cancer cells via transport of cathepsins.* Cell Death Dis, 2019. **10**(12): p. 876.
31. Mailloux, R.J., et al., *Alpha-ketoglutarate dehydrogenase and glutamate dehydrogenase work in tandem to modulate the antioxidant alpha-ketoglutarate during oxidative stress in Pseudomonas fluorescens.* J Bacteriol, 2009. **191**(12): p. 3804-10.
32. Satpute, R.M., J. Hariharakrishnan, and R. Bhattacharya, *Effect of alpha-ketoglutarate and N-acetyl cysteine on cyanide-induced oxidative stress mediated cell death in PC12 cells.* Toxicol Ind Health, 2010. **26**(5): p. 297-308.
33. Starkov, A.A., *An update on the role of mitochondrial alpha-ketoglutarate dehydrogenase in oxidative stress.* Mol Cell Neurosci, 2013. **55**: p. 13-6.
34. Chol, M., et al., *Glutathione precursors replenish decreased glutathione pool in cystinotic cell lines.* Biochem Biophys Res Commun, 2004. **324**(1): p. 231-5.
35. Rizzo, C., et al., *Pyroglutamic aciduria and nephropathic cystinosis.* J Inherit Metab Dis, 1999. **22**(3): p. 224-6.
36. Villar, V.H., et al., *mTORC1 inhibition in cancer cells protects from glutaminolysis-mediated apoptosis during nutrient limitation.* Nat Commun, 2017. **8**: p. 14124.
37. Duran, R.V., et al., *Glutaminolysis activates Rag-mTORC1 signaling.* Mol Cell, 2012. **47**(3): p. 349-58.
38. Chin, R.M., et al., *The metabolite alpha-ketoglutarate extends lifespan by inhibiting ATP synthase and TOR.* Nature, 2014. **510**(7505): p. 397-401.
39. *Bicalutamide Analogs Or (S)-Bicalutamide As Exocytosis Activating Compounds For Use In The Treatment Of A Lysosomal Storage Disorder Or Glycogenosis. https://patents.google.com/patent/US20160317489.*

40. Albadine, R., et al., *PAX8 (+)/p63 (-) immunostaining pattern in renal collecting duct carcinoma (CDC): a useful immunoprofile in the differential diagnosis of CDC versus urothelial carcinoma of upper urinary tract.* Am J Surg Pathol, 2010. **34**(7): p. 965-9.
41. Saito, K., et al., *Spatial and isoform specific p63 expression in the male human urogenital tract.* J Urol, 2006. **176**(5): p. 2268-73.
42. Elmonem, M.A., et al., *Genetic Renal Diseases: The Emerging Role of Zebrafish Models.* Cells, 2018. **7**(9).
43. Elmonem, M.A., et al., *Cystinosis (ctns) zebrafish mutant shows pronephric glomerular and tubular dysfunction.* Sci Rep, 2017. **7**: p. 42583.
44. Raggi, C., et al., *Dedifferentiation and aberrations of the endolysosomal compartment characterize the early stage of nephropathic cystinosis.* Hum Mol Genet, 2014. **23**(9): p. 2266-78.
45. Ivanova, E.A., et al., *Endo-lysosomal dysfunction in human proximal tubular epithelial cells deficient for lysosomal cystine transporter cystinosin.* PLoS One, 2015. **10**(3): p. e0120998.
46. Settembre, C., et al., *A block of autophagy in lysosomal storage disorders.* Hum Mol Genet, 2008. **17**(1): p. 119-29.
47. Platt, F.M., B. Boland, and A.C. van der Spoel, *The cell biology of disease: lysosomal storage disorders: the cellular impact of lysosomal dysfunction.* J Cell Biol, 2012. **199**(5): p. 723-34.
48. Liu, S., L. He, and K. Yao, *The Antioxidative Function of Alpha-Ketoglutarate and Its Applications.* Biomed Res Int, 2018. **2018**: p. 3408467.
49. Zhao, J., et al., *Dimethyl alpha-ketoglutarate reduces CCl4-induced liver fibrosis through inhibition of autophagy in hepatic stellate cells.* Biochem Biophys Res Commun, 2016. **481**(1-2): p. 90-96.
50. Su, Y., et al., *Alpha-ketoglutarate extends Drosophila lifespan by inhibiting mTOR and activating AMPK.* Aging (Albany NY), 2019. **11**(12): p. 4183-4197.
51. Rzeski, W., et al., *Alpha-ketoglutarate (AKG) inhibits proliferation of colon adenocarcinoma cells in normoxic conditions.* Scand J Gastroenterol, 2012. **47**(5): p. 565-71.
52. Andrzejewska, Z., et al., *Cystinosin is a Component of the Vacuolar H+-ATPase-Ragulator-Rag Complex Controlling Mammalian Target of Rapamycin Complex 1 Signaling.* J Am Soc Nephrol, 2016. **27**(6): p. 1678-88.
53. Hollywood, J.A., et al., *Use of human iPSCs and kidney organoids to develop a cysteamine/mTOR inhibition combination therapy to treat cystinosis.* bioRxiv, 2019: p. 595264.
54. Gaide Chevronnay, H.P., et al., *Time course of pathogenic and adaptation mechanisms in cystinotic mouse kidneys.* J Am Soc Nephrol, 2014. **25**(6): p. 1256-69.
55. Gaide Chevronnay, H.P., et al., *A mouse model suggests two mechanisms for thyroid alterations in infantile cystinosis: decreased thyroglobulin synthesis due to endoplasmic reticulum stress/unfolded protein response and impaired lysosomal processing.* Endocrinology, 2015. **156**(6): p. 2349-64.
56. Johnson, J.L., et al., *Upregulation of the Rab27a-dependent trafficking and secretory mechanisms improves lysosomal transport, alleviates endoplasmic reticulum stress, and reduces lysosome overload in cystinosis.* Mol Cell Biol, 2013. **33**(15): p. 2950-62.
57. Napolitano, G., et al., *Impairment of chaperone-mediated autophagy leads to selective lysosomal degradation defects in the lysosomal storage disease cystinosis.* EMBO Mol Med, 2015. **7**(2): p. 158-74.

58. Cherqui, S., et al., *Intralysosomal cystine accumulation in mice lacking cystinosin, the protein defective in cystinosis.* Mol Cell Biol, 2002. **22**(21): p. 7622-32.
59. Cherqui, S., *Cysteamine therapy: a treatment for cystinosis, not a cure.* Kidney Int, 2012. **81**(2): p. 127-9.
60. MacRae, C.A. and R.T. Peterson, *Zebrafish as tools for drug discovery.* Nat Rev Drug Discov, 2015. **14**(10): p. 721-31.
61. Osguthorpe, D.J. and A.T. Hagler, *Mechanism of androgen receptor antagonism by bicalutamide in the treatment of prostate cancer.* Biochemistry, 2011. **50**(19): p. 4105-13.
62. Lapi, F., et al., *Androgen deprivation therapy and risk of acute kidney injury in patients with prostate cancer.* Jama, 2013. **310**(3): p. 289-96.
63. Peng, C.C., et al., *Renal Damaging Effect Elicited by Bicalutamide Therapy Uncovered Multiple Action Mechanisms As Evidenced by the Cell Model.* Sci Rep, 2019. **9**(1): p. 3392.
64. Braga-Basaria, M., et al., *Lipoprotein profile in men with prostate cancer undergoing androgen deprivation therapy.* Int J Impot Res, 2006. **18**(5): p. 494-8.
65. Fivush, B., J.A. Flick, and W.A. Gahl, *Pancreatic exocrine insufficiency in a patient with nephropathic cystinosis.* J Pediatr, 1988. **112**(1): p. 49-51.
66. Winkler, L., et al., *Growth and pubertal development in nephropathic cystinosis.* Eur J Pediatr, 1993. **152**(3): p. 244-9.
67. Chik, C.L., et al., *Pituitary-testicular function in nephropathic cystinosis.* Ann Intern Med, 1993. **119**(7 Pt 1): p. 568-75.
68. Tucker, H. and G.J. Chesterson, *Resolution of the nonsteroidal antiandrogen 4'-cyano-3-[(4-fluorophenyl)sulfonyl]-2-hydroxy-2-methyl-3'- (trifluoromethyl)-propionanilide and the determination of the absolute configuration of the active enantiomer.* J Med Chem, 1988. **31**(4): p. 885-7.
69. Mukherjee, A., et al., *Enantioselective binding of Casodex to the androgen receptor.* Xenobiotica, 1996. **26**(2): p. 117-22.

SUPPLEMENTAL FILES

Supplementary TABLE 1. Plasma alpha-ketoglutarate levels in control and cystinotic patients.

Individuals	Age (Month)	Sex (m/f)	Mutations	Phenotype	αKG level (μM)
Control	37	M	Wild type	__	8.5
Control	29	F	Wild type	__	8.0
Control	38	M	Wild type	__	6.3
Control	32	M	Wild type	__	6.9
Cystinotic	34	F	Hom 57kb del	INF	28
Cystinotic	14	F	57kb del + c.del 198-218 (exon 5)	JUV	14
Cystinotic	17	M	Hom 57kb del	INF	9.6
Cystinotic	16	F	Hom 57kb del	INF	13
Cystinotic	42	F	57kb del + 922insG	INF	11
Cystinotic	6	M	57kb del + intronic IVS10-7G>A (intron 10)	INF	12

m, male; f, female; JUV, Juvenile; INF, Infantile

Supplementary TABLE 2. Sequences of the primers used for tubuloids study.

Gene name	*Forward primer 5' → 3'*	*Reverse primer 5' → 3'*
ANPEP	TGAGCTGTTTGACGCCATCT	GCCCTGCTTGAATACGTCCT
ABCC3	CACCAACTCAGTCAAACGTGC	GCAAGACCATGAAAGCGACTC
HNF1A	CCAGTAAGGTCCACGGTGTG	TTGGTGGAGGGGTGTAGACA
HNF4A	CACGGGCAAACACTACGGT	TTGACCTTCGAGTGCTGATCC
SLC12A1	AACTTTGGGCCACGCTTCAC	CCACACAGGCCCCTACACAA
SLC12A3	CTCCACCAATGGCAAGGTCAA	GGATGTCGTTAATGGGGTCCA
CALB1	TGATCAGGACGGCAATGGAT	AGCTTCCCTCCATCCGACAA
AQP2	CTCCATGAGATCACGCCAGC	TCATCGGTGGAGGCGAAGAT
AQP3	CTGGATCAAGCTGCCCATCT	CATTGGGGCCCGAAACAAAA

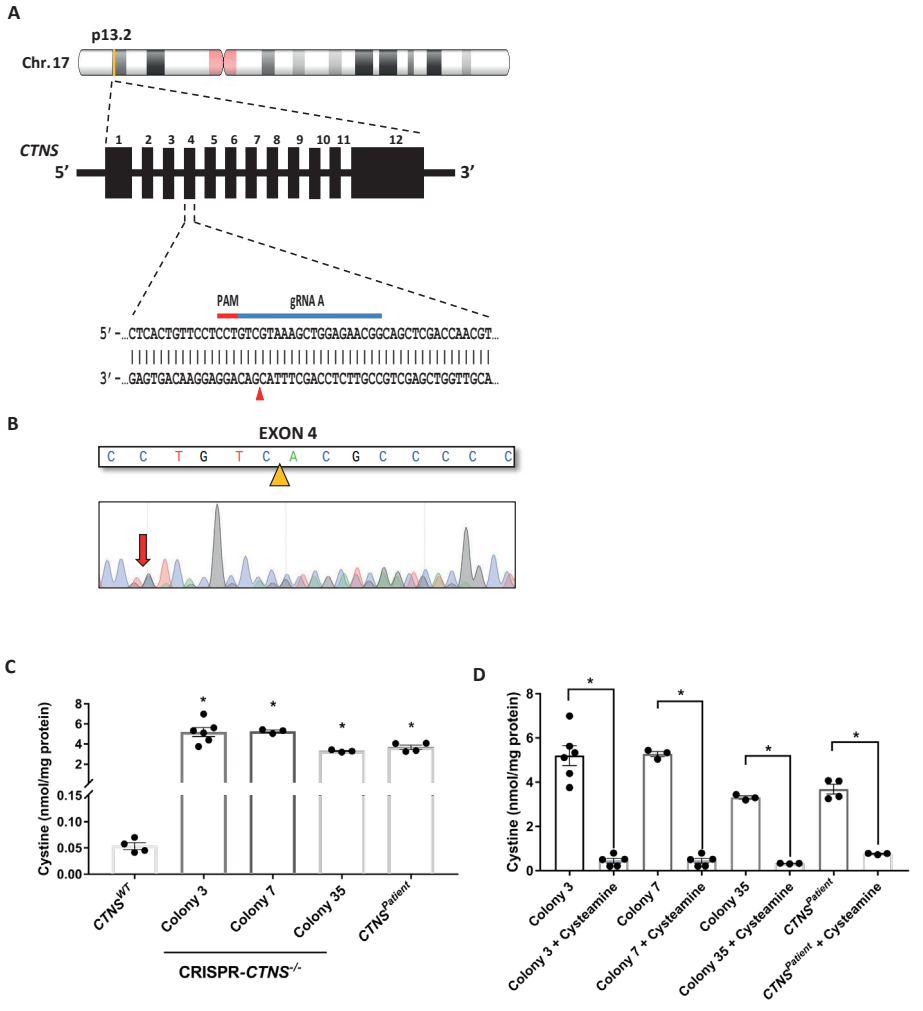

Supplementary FIGURE S1. Generation of *CTNS*$^{-/-}$ isogenic cell line of ciPTEC using CRISPR. (A) Schematic overview of the CRISPR-based strategy to knockout the *CTNS* gene in ciPTEC. **(B)** Sanger sequencing chromatogram shows resulting sequence in CRISPR-generated cystinotic cells (*CTNS*$^{-/-}$). **(C)** Quantification of cystine levels (nmol/mg protein) by HPLC-MS/MS in in control (*CTNS*^{WT}), CRISPR-generated cystinotic cells (*CTNS*$^{-/-}$; line 3, 7, and 35), and patient-derived cystinotic cells (*CTNS*^{Patient}). **(D)** Quantification of cystine levels (nmol/mg protein) by HPLC-MS/MS in *CTNS*$^{-/-}$ lines (3, 7, and 35), and *CTNS*^{Patient} cells upon treatment with cysteamine (100 µM). Data are expressed as mean ± SEM. P-values < 0.05 were considered to be significant.

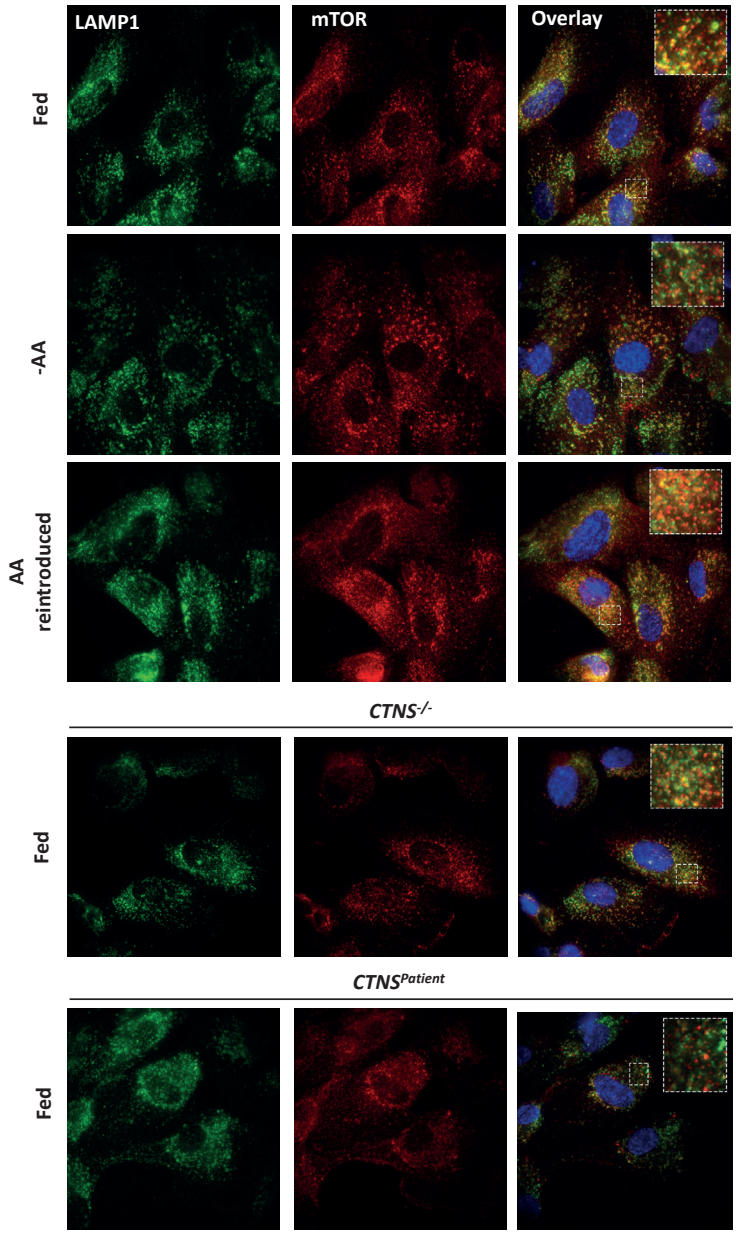

Supplementary FIGURE S2. Decreased retention of mTOR on the lysosomal membrane of cystinotic cells. Representative immunofluorescent staining of *CTNS*^{WT}, *CTNS*$^{-/-}$, and *CTNS*^{Patient} co-immunolabelled with lysosomal-associated membrane protein 1 (LAMP1; green) and mTOR (Red)**.** Merge images with zoomed areas are representative of the localization of mTOR with lysosomes in various experimental conditions. Scale bars are 10 µm**.** Unfortunately, technical hurdles did not allow us to quantify the co-localization between mTOR and LAMP-1 to show dissociation of the mTOR complex in cystinosis. In our cell lines, the size of lysosomes are so small and are generally clumped together hampering reliable quantification.

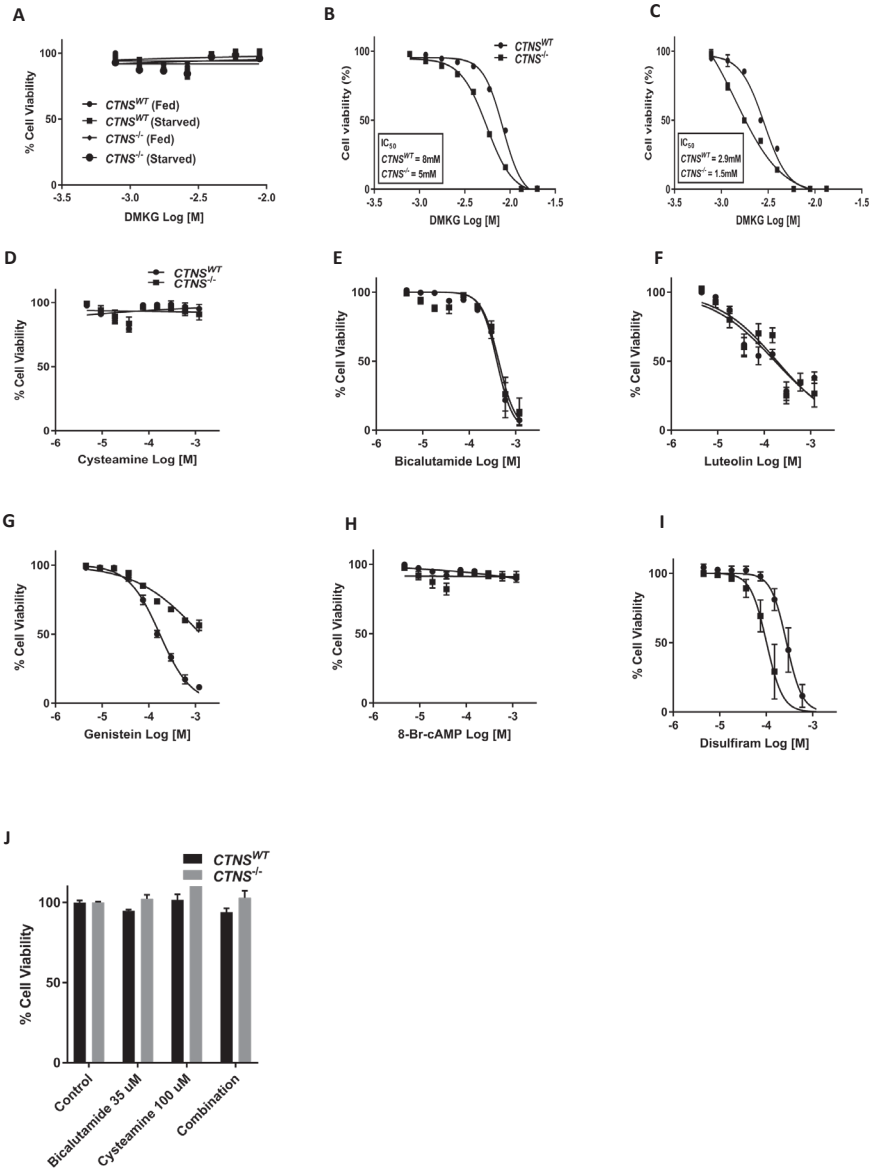

Supplementary FIGURE S3. Toxicity profile of dimethyl α-ketoglutarate (DMKG) and the drugs tested for the treatment of cystinosis. (A, B) Cell viability curves of the increasing concentration of dimethyl α-ketoglutarate (DMKG) in control (*CTNS*^{WT}) and CRISPR-generated cystinotic (*CTNS*$^{-/-}$) cells after 24 hrs of incubation in fed and starved condition, respectively. **(C)** Cell viability curves of DMKG in *CTNS*^{WT} and *CTNS*$^{-/-}$ cells after 4 hrs of incubation in fed and starved condition. **(D-J)**, Cell viability test in *CTNS*^{WT}, *CTNS*$^{-/-}$ cells treated with the increasing concentrations of cysteamine, bicalutamide, luteolin, genistein, 8-bromo-cAMP, disulfiram, and a combination of cysteamine and bicalutamide (100 µM and 35 µM, respectively), respectively. P-values < 0.05 were considered to be significant.

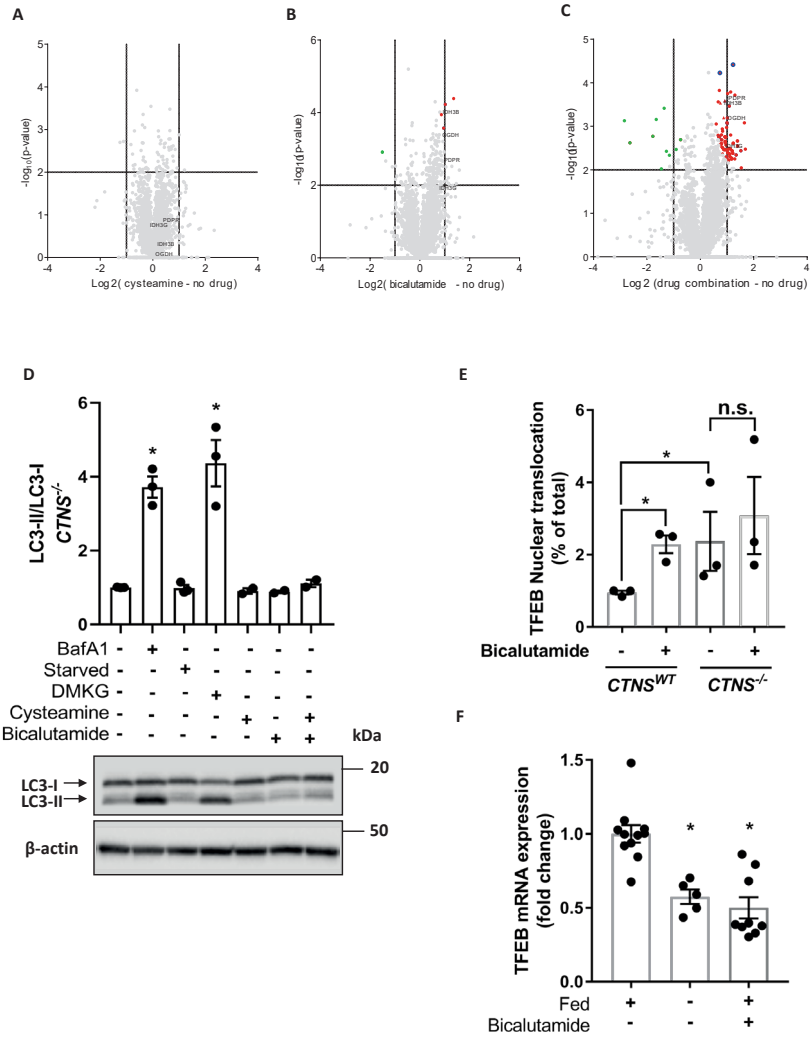

Supplementary FIGURE S4. Cysteamine-bicalutamide combination treatment shows a synergic effect in treatment of cystinotic ciPTEC. (A-C) Volcano plot illustrates significantly differentially abundant proteins. The -$\log_{10}$ (Benjamini–Hochberg corrected P-value) is plotted against the $\log_2$ (fold change: *CTNS*$^{-/-}$ no drug treatment/*CTNS*$^{-/-}$ cysteamine treatment), (fold change: *CTNS*$^{-/-}$ no drug treatment/*CTNS*$^{-/-}$ bicalutamide treatment), and (fold change: *CTNS*$^{-/-}$ no drug treatment/*CTNS*$^{-/-}$ combination treatment), respectively. The non-axial vertical lines denote ±1.5-fold change while the non-axial horizontal line denotes P = 0.05, which is our significance threshold (prior to logarithmic transformation). **(D)** Western blotting and densitometric analyses for LC3-II/LC3-I ratio in CRISPR generated *CTNS*$^{-/-}$ cells treated with cysteamine (100 µM), bicalutamide (35 µM), and a combination of cysteamine and bicalutamide (100 µM and 35 µM, respectively). β-Actin was used as a loading control. **(E)** Quantification of TFEB-GFP nuclear translocation in *CTNS*^{WT}, and *CTNS*$^{-/-}$ cells upon treatment with bicalutamide (35 µM). **(F)** *TFEB* mRNA expression of the *CTNS*^{WT} cells upon starvation and treatment with bicalutamide (35 µM). P-values < 0.05 were considered to be significant.

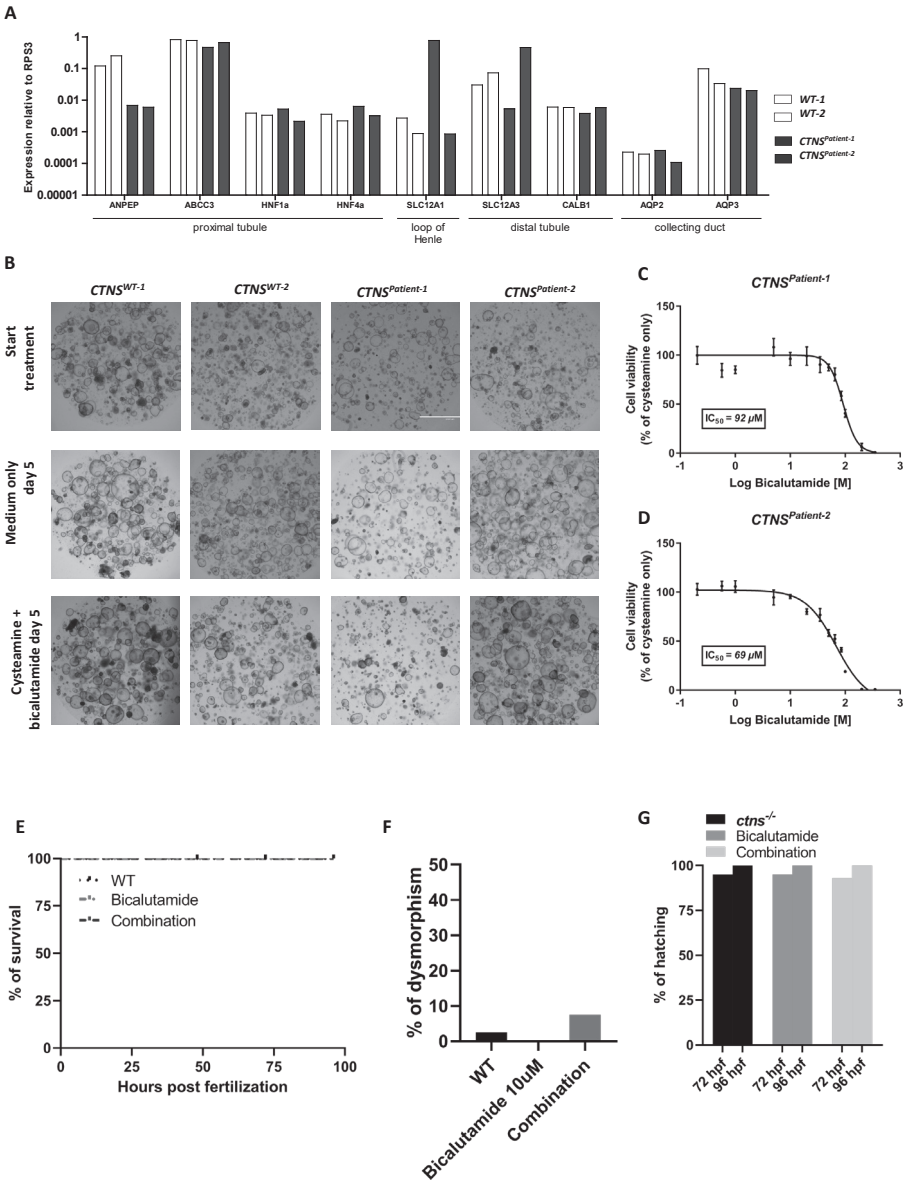

Supplementary FIGURE S5. Cysteamine-bicalutamide combination treatment is safe in patient-derived cystinotic kidney tubuloids and in wild type zebrafish. (A) Patient-derived cystinotic tubuloids (*CTNS*$^{Patient-1}$ and *CTNS*$^{Patient-2}$) and tubuloids established from healthy kidney tissue (*CTNS*$^{WT-1}$ and *CTNS*$^{WT-2}$) were differentiated for 7 days and analysed by quantitative real-time PCR for markers of various segments of the nephron. **(B)** Brightfield images of cystinotic tubuloids and healthy control tubuloids at the start of treatment and after 5 days of cysteamine (100 µM)-bicalutamide (35 µM) combination treatment or treatment with medium only (negative control). Scale bars are 2000 µm. **(C, D)** Bicalutamide safety screening in control and cystinotic tubuloids.

Tubuloid viability upon treatment with cysteamine (100 µM) in combination with increasing concentrations of bicalutamide was compared to treatment with cysteamine alone (= 100% viability). **(E)** Survival rates in wild type zebrafish upon treatment with bicalutamide (10 µM), and a combination of cysteamine and bicalutamide (1000 µM and 10 µM, respectively). **(F)** Deformity rates in wild type zebrafish upon treatment with bicalutamide (10 µM), and a combination of cysteamine and bicalutamide (1000 µM and 10 µM, respectively). **(G)** Hatching rates in surviving wild type zebrafish evaluated at 72 and 96 hrs post fertilization (hpf) with bicalutamide (10 µM), and a combination of cysteamine and bicalutamide (1000 µM and 10 µM, respectively). The total numbers of embryos evaluated for survival, hatching, and deformity rates were 40 embryos per group. Drugs were administered at 48 hpf in all experiments dissolved in the swimming water with the specified concentrations. Data are expressed the mean ± SEM. Where appropriate, unpaired two-tailed Student's t-test were used. P-values < 0.05 were considered to be significant.

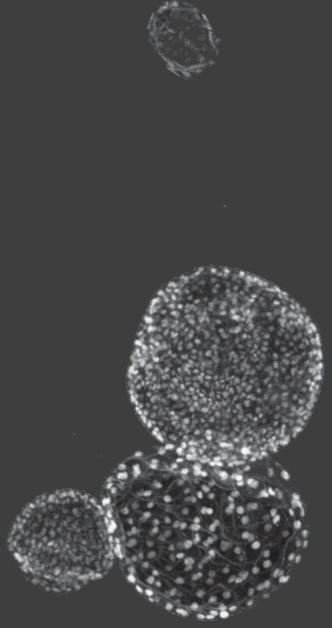

The lysosomal V-ATPase B1 subunit in proximal tubule is linked to nephropathic cystinosis

5

Amer Jamalpoor[1], Albertien M van Eerde[2], Marc R Lilien[3], Charlotte AGH van Gelder[4,5], Esther A Zaal[4], Floris A Valentijn[6], Roel Broekhuizen[6], Eva Zielhuis[1], Julia E Egido[1], Maarten Altelaar[4,5], Celia R Berkers[4,7], Rosalinde Masereeuw[1], and Manoe J Janssen[1]

[1]Division of Pharmacology, Utrecht Institute for Pharmaceutical Sciences, Faculty of Science, Utrecht University, 3584 CG Utrecht, The Netherlands. [2]Department of Genetics, University Medical Centre Utrecht, Utrecht, the Netherlands. [3]Department of Pediatric Nephrology, Wilhelmina Children's Hospital, University Medical Centre Utrecht, Utrecht, the Netherlands. [4]Biomolecular Mass Spectrometry and Proteomics, Bijvoet Center for Biomolecular Research and Utrecht Institute for Pharmaceutical Sciences, Utrecht University, Utrecht, The Netherlands. [5]Netherlands Proteomics Center, Utrecht, The Netherlands. [6]Department of Pathology, University Medical Centre Utrecht, Utrecht, the Netherlands. [7]Division of Cell Biology, Metabolism & Cancer, Department of Biomolecular Health Sciences, Faculty of Veterinary Medicine, Utrecht University, Utrecht, The Netherlands.

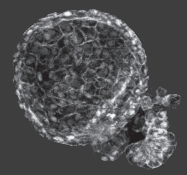

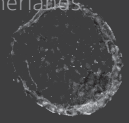

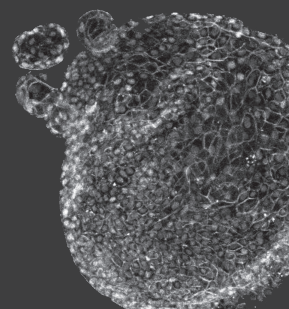

Manuscript submitted
Published as preprint at bioRxiv 2020.07.24; doi: https://doi.org/10.1101/2020.07.24.219808

ABSTRACT

Recently, a 23-month-old girl presented with increased granulocyte cystine levels, metabolic acidosis and symptoms of renal Fanconi syndrome. Cystinosis was suspected and treatment with electrolytes and cysteamine, a cystine depleting agent, was started that appeared effective. However, genetic testing did not detect any variants in *CTNS* (the gene affected in cystinosis) but instead revealed pathogenic variants in *ATP6V1B1*. This gene encodes the B1 subunit of the vacuolar H^+-ATPase (V-ATPase) that is linked to autosomal recessive distal renal tubular acidosis, a metabolic disorder with an inappropriately alkaline urine and deafness. Here, the unknown link between *ATP6V1B1* deficiency and proximal tubulopathy, as well as a possible link to cystinosis pathophysiology was investigated. We used CRISPR/Cas9 technology to selectively knockout *ATP6V1B1* or *CTNS* in human renal proximal tubule cells and compared their proteomic and metabolomic profiles with isogenic wild type proximal tubule cells. ATP6V1B1 was found to be expressed along the human distal but also the proximal segments of the nephron. Consistent with the clinical data, loss of ATP6V1B1 in renal proximal tubule cells resulted in increased cystine levels with autophagy activation. Further, omics profiling showed that both *ATP6V1B1*$^{-/-}$ and *CTNS*$^{-/-}$ cells are in metabolic acidosis with impaired autophagy and signs of proximal tubular epithelial dysfunction. We identified the lysosomal V-ATPase B1 subunit to play an important role in proximal tubule function, regulating cystine transport and autophagy in human renal proximal tubule cells through its interaction with cystinosin and mTOR-signaling.

Keywords:
Renal tubular acidosis, cystinosis, cystine accumulation, autophagy, renal Fanconi syndrome

INTRODUCTION

A 23-month-old girl presented with increased granulocyte cystine levels, metabolic acidosis and signs of renal Fanconi syndrome. The patient was diagnosed with nephropathic cystinosis and treatment with cysteamine, a cystine depleting agent, and electrolytes were started that improved the patient's clinical conditions.

Nephropathic cystinosis (MIM_219800) is an autosomal recessive lysosomal storage disease caused by pathogenic variants in the *CTNS* gene, which encodes the lysosomal H^+/cystine symporter, cystinosin [1]. The disease is characterized by the accumulation of cystine throughout the body, causing irreversible damage to various organs, particularly the kidneys [2]. Clinically, nephropathic cystinosis patients first develop renal Fanconi syndrome, a general renal proximal tubular dysfunction characterized by phosphaturia, glucosuria, impaired bicarbonate reabsorption and generalized aminoaciduria [2, 3]. With time, this progresses to other complications such as growth retardation, rickets, and chronic kidney disease. The main treatment option currently available is cysteamine, an aminothiol that reduces cystine by converting it into cysteine and cysteine-cysteamine mixed disulfide, both of which are able to exit the lysosomes [4]. Although this drug is found effective in depleting cystine, it is not efficient to revert the signs associated with renal Fanconi syndrome [5].

After starting treatment with cysteamine in this patient, the cystine levels dropped below the reference level, which is considered very unusual for any patient with nephropathic cystinosis. This prompted diagnostic renal gene panel sequencing and the analysis revealed pathogenic variants in the *ATP6V1B1* gene (NM_001692.3), while the *CTNS* gene was found to be intact. The *ATP6V1B1* gene codes for the kidney isoform of the B1 subunit of the V1 domain of the vacuolar H^+-ATPase (V-ATPase; ATP6V1B1), responsible for acidification of intracellular organelles and maintaining renal acid-base homeostasis. Variants in this gene lead to autosomal recessive distal renal tubular acidosis (dRTA) with sensorineural deafness [6, 7]. Diverse intracellular processes, such as protein sorting, receptor-mediated endocytosis, and synaptic vesicle proton gradient generation, depend on V-ATPase mediated organelle acidification, and the enzyme's relevance in kidney functioning is widely characterized in the distal tubule [8-10]. However, it has been reported previously that two siblings with distal renal tubular acidosis and *ATP6V1B1* gene variants displayed proximal tubular dysfunction, suggesting a role for this gene in the proximal tubule as well [11].

Both ATP6V1B1 and cystinosin can be found in the lysosomal membrane of kidney cells and may cooperate in several ways. As a subunit of the V-ATPase, ATP6V1B1 is thought to play a role in lysosome acidification, which in turn is important for the function of cystinosin that depends on this proton gradient for the export of protons and cystine from the lysosome into the cytosol [12, 13]. Besides this chemiosmotic coupling, both cystinosin and the V-ATPase complex closely interact with mammalian target of rapamycin complex 1 (mTORC1), regulating autophagy [12, 14, 15]. Intriguingly, different

variants of V-ATPases are also found to regulate transcription factor EB (TFEB), a master regulator of autophagy,[16] whose function is also dysregulated in cystinosis [17, 18].
In this study, we aimed to investigate the role of the B1 subunit of the lysosomal V-ATPase in proximal tubules and compare *ATP6V1B1* loss to *CTNS* loss, which is the most common cause of renal Fanconi syndrome in children and has been well studied in proximal tubule cells. We hypothesized that renal proximal tubular acidosis leads to cystinosis-like features. To this end, we confirmed the presence of ATP6V1B1 in human kidney tissue and developed CRISPR-generated *ATP6V1B1*-deficient proximal tubule cells, serving as a disease model, and compared their phenotype to well-characterized isogenic *CTNS*$^{-/-}$ cells [17]. Furthermore, we applied a dual-omics approach, combining proteomics and metabolomics, to bridge the gap between the *ATP6V1B1* gene defect and cystinosis by identifying the pathways commonly affected in cystinosis and acidosis proximal tubule cells.

MATERIALS AND METHOD

Reagents

All chemicals and reagents were obtained from Sigma-Aldrich (Zwijndrecht, The Netherlands) unless specified otherwise. Primary antibodies used were rabbit anti-ATP6V1B1 (Abcam #ab192612, dilution 1:500) and mouse anti-LC3 (Novus Biologicals #NB600-1384SS, dilution 1:1000). Secondary antibodies used were goat anti-rabbit BrightVision Horse Radish Peroxidase (Klinipath, Duiven, The Netherlands) and goat anti-mouse (#A32723, dilution 1:5000) obtained from Dako products (CA, USA).

Immunohistochemistry on human renal tissue sections

A tumor-free human kidney tissue section was derived from a patient undergoing nephrectomy for renal carcinoma at the University Medical Center Utrecht (UMCU). The patient sample was anonymized. Because leftover material from routine clinical procedures in the UMCU was used, informed patient consent and additional ethical approval were not required. The UMCU policy allows anonymous use of redundant tissue for research purposes as part of the standard treatment agreement with patients in the UMCU.[19] Renal tissue was fixed in a 4% buffered formalin solution for 24 hrs and subsequently embedded in paraffin blocks. Sections of 3 µm were cut and mounted on adhesive slides (Leica Xtra) and rehydrated through a series of xylene and alcohol washes after which slides were rinsed in distilled water. First, endogenous peroxidase was blocked using H_2O_2. This was followed by heat-based antigen retrieval in citrate buffer (pH 6) and primary antibody incubation (anti-ATP6V1B1, Abcam ab192612, 1:500) diluted in PBS/1%BSA. After incubation with goat anti-rabbit BrightVision Horse Radish Peroxidase linked secondary antibody (Klinipath, Duiven, The Netherlands), sections were stained using Nova Red substrate (Vector Laboratories, Burlingame, CA, USA) and

counterstained with Mayer's hematoxylin. Images were acquired using a Nikon Eclipse E800 microscope.

CiPTEC culture

The conditionally immortalized proximal tubular epithelial cells (ciPTEC) (MTA #A16-0147) were obtained from Cell4Pharma (Nijmegen, The Netherlands) and were cultured as described previously by Wilmer et al. 2010 [20]. In short, these cells were immortalized using the temperature sensitive SV40ts A58 and human telomerase gene (hTERT), which allows them to be expanded at 33°C and regain a mature phenotype after culturing at 37°C . The culture medium was Dulbecco's modified Eagle medium DMEM/F-12 (GIBCO) supplemented with fetal calf serum 10% (v/v), insulin 5 µg/ml, transferrin 5 µg/ml, selenium 5 µg/ml, hydrocortisone 35 ng/ml, epidermal growth factor 10 ng/ml and tri-iodothyronine 40 pg/ml. Cells were seeded at a density of 55,000 cells/cm^2 and grown at 33°C for 24 hrs to enable them to proliferate and subsequently cultured at 37°C for 7 days to mature into fully differentiated tubular epithelial cells.

Generation of *ATP6V1B1*$^{-/-}$ and *CTNS*$^{-/-}$ isogenic ciPTEC lines

We previously created an isogenic CRISPR-mediated cystinotic ciPTEC line [17] referred to as *CTNS*$^{-/-}$. Using the same parent ciPTEC line, we created the *ATP6V1B1*$^{-/-}$ cell line as outlined. Guide RNAs (gRNAs) targeting exon 4 of the *ATP6V1B1* gene were designed using the online gRNA designing tool available at chopchop.cbu.uib.no. To maximize specificity, guide sequences with high scores for on-target efficiency and no predicted off-targets having at least 3 base pair mismatches in the genome were selected. Optimal gRNA (5'-CCTACGAACTCCGGTGTCAG-3') was cloned into the pSPCas9(BB)-2A-GFP plasmid (Addgene #48138) as described previously by Ran et al.,[21] and introduced into ciPTEC using PolyPlus JetPrime. At 72 hrs post-transfection, GFP-positive singlet cells were sorted using FACS Aria-II flow cytometer and expanded in 96-wells plate. The gRNA cut site was amplified with PCR using the primers flanking the cut region (F. *ATP6V1B1*_ex4 5'-ACTCTGAAGGCAGGAAATGGTC-3; R .*ATP6V1B1*_ex4 5'-GAGGAAGGTGGGTTCAATAAC-3'). Finally, knockouts were confirmed by Sanger sequencing.

Intracellular cystine quantification by HPLC-MS/MS

Cystine levels were quantified using high-performance liquid chromatography-tandem mass spectrometry (HPLC-MS/MS) using a rapid and sensitive assay developed and validated in house [22]. In brief, cell pellets were suspended in N-Ethylmaleimide (NEM) solution containing 5 mM NEM in 0.1 mM sodium phosphate buffer (pH 7.4). The cell suspension was then precipitated, and protein was extracted with sulfosalicylic acid 15% (w/v) and centrifuged at 20,000 g for 10 min at 4°C. Protein concentration was determined by the method of the Pierce™ BCA protein assay kit according to the manufacturer's protocol (Thermo Fisher, The Netherlands), and the cystine concentration

was measured using HPLC-MS/MS. Data are expressed as the cystine values (nmol) corrected for protein content (mg).

Quantitative real-time PCR

The mRNAs were extracted from cells using the Qiagen RNeasy mini kit according to the manufacturer's instructions. Total mRNA (600 ng) was reverse transcribed using iScript Reverse Transcriptase Supermix (Bio-Rad). Quantitative real-time PCR was performed using iQ Universal SYBR Green Supermix (Bio-Rad) with the specific sense and anti-sense primers for *ATP6V1B1* (forward: 5'-TGGATATCAATGGCCAGCCC-3'; reverse: 5'-CTTCGCCATCGTCTTTGCAG-3'), *CTNS* (forward: 5'-AGCTCCCCGATGAAGTTGTG-3'; reverse: 5'-GTCAGGTTCAGAGCCACGAA-3'), and *TFEB* (forward: 5'-GCAGTCCTACCTGGAGAATC-3'; reverse: 5'- TGGGCAGCAAACTTGTTCC-3'). The ribosomal protein S13 (RPS-13) (forward: 5'-GCTCTCCTTTCGTTGCCTGA-3'; reverse: 5'-ACTTCAACCAAGTGGGGACG-3') was used as the reference gene for normalization and relative expression levels were calculated as fold change using the $2^{-\Delta\Delta}Ct$ method.

Immunofluorescence and confocal microscopy

To investigate LC3-II accumulation, cells were seeded in a special optic 96-well plate in presence of 25 nM bafilomycin (BafA1) for 4 hrs. Thereafter, cells were fixed with 4% paraformaldehyde in phosphate buffered saline (PBS) for 10 min, permeabilized with 0.1% Triton-X solution for 10 min, and blocked with 1% bovine serum albumin (BSA) diluted in PBS for 30 min. Subsequently, cells were stained with the primary antibody (mouse anti-LC3, dilution 1:1000) diluted in blocking buffer overnight at 4°C. After 3 washes with PBS, the cells were incubated for 2 hrs at room temperature with the secondary antibody (goat anti-mouse, dilution 1:5000). Nuclei were stained with Hoechst 33342 (1 µM) and cells were imaged using a Cell Voyager 7000 (CV7000) confocal microscope (Yokogawa Electric corporation, Tokyo, Japan).

To assess TFEB intracellular distribution, cells were seeded in a special optic 96-well plate until reaching 50% confluence. Cells were then transfected with the TFEB-GFP plasmid (a kind gift from Dr. Annelies Michiels (Viral Vector Core, Leuven, Belgium)) using PolyPlus JetPrime reagent according to the manufacturer's instructions. After 48 hrs from transient transfection, cells were stained with Hoechst 33342 (1 µM) for 10 min and imaged using a Cell Voyager 7000 (CV7000) confocal microscope (Yokogawa Electric corporation, Tokyo, Japan). TFEB nuclear translocation data are expressed as number of cells with nucleus-TFEB positive over the total number of TFEB-transfected cells.

Endocytosis assay

The endocytic uptake was monitored in ciPTEC following incubation for 1.5 hr at 37°C with 50 µg/ml of either BSA-AlexaFluor-647 (A34785, Thermo Fisher Scientific) or DQ Red BSA (D12051, Invitrogen). The cells were then fixed and stained with Hoechst 33342 (1 µM) for 10 min and imaged using a CV7000 confocal microscope (Yokogawa Electric corporation, Tokyo, Japan). Data were quantified with Columbus™ Image Data Storage

and analysis software (PerkinElmer, Groningen, The Netherlands). Data are expressed as the number of BSA/DQ Red BSA spots per cell.

Metabolomics and Proteomics

The omics analyses were performed using high performance liquid chromatography mass spectrometry (HPLC/MS) and the data were analyzed as described previously [17]. The mass spectrometry proteomics data have been deposited to the ProteomeXchange Consortium via the PRoteomics IDEntifications database (PRIDE) (https://www.ebi.ac.uk/pride/archive/) partner repository with the dataset identifier PXD020950.

Ethical Approval

For the clinical case presented here appropriate informed consent was obtained from the parents of the patient for the publication of the anonymized data. Immunohistochemistry was performed on leftover material from routine clinical procedures in the UMCU, for which informed patient consent and additional ethical approval were not required.

Statistical analysis

Statistical analysis was performed using GraphPad Prism 7.0 (GraphPad Software, Inc., USA). Data are presented as mean ± standard error of the mean (SEM) of at least three independent experiments performed in triplicate, unless stated otherwise. Significance was evaluated using One-way Analysis of Variance (ANOVA), or where appropriate unpaired two-tailed Student's t-test was applied. P-values < 0.05 were considered significant.

TABLE 1. Laboratory results of a 23-month-old girl with pathogenic ATP6V1B1 variants.

Parameters	Reference	Pre-treatment	After-treatment
Blood Parameters			
pH	7.35 - 7.45	7.28	7.36
Bicarbonate (mmol/L)	22 - 29	8.9	22.6
Sodium (mmol/L)	136 - 146	141	139
Potassium (mmol/L)	3.8 - 5.0	2.9	3.9
Chloride (mmol/L)	99 - 108	111	105
BUN (mmol/L)	3.0 - 7.5	5.8	6.6
Creatinine (µmol/L)	11 - 34	30	29
Ionized calcium (mmol/L)	1.15 - 1.32	0.96	1.32
Magnesium (mmol/L)	0.70 - 1.00		0.98
Inorganic phosphate (mmol/L)	1.25 - 2.10	0.74	1.74
Glucose (mmol/L)	3.6 - 5.6	4.8	4.4
Cystine (nmol/mg protein)	< 0.17	1.02	0.22
Urine Parameters*			
Creatinine (mmol/L)	NA	-	1.3
Sodium (mmol/L)	NA	-	49
Potassium (mmol/L)	NA	-	50
Calcium (mmol/L)	NA	-	< 1.00
Phosphate (mmol/L)	NA	-	11.7
TmP/GFR (mmol/L)	1.31 - 1.73	-	1.48
Glucose (mmol/L)	NA	-	< 1.00
Citrate (mmol/L)	0.6 - 4.8	-	0.2
Albumin (mg/L)	< 30	-	8
Albumin/creatinine ratio (mg/mmol)	< 2.5	-	5.9
β2 microglobulin (mg/L)	< 0,2	-	94
β2 MG/creatinine ratio (mg/mmol)	< 0.04	-	72.3
Urine Metabolites (mmol/mol creatinine)			
Free sialic acid	16 - 44	28	-
Total sialic acid	52 - 126	118	-
Bound sialic acid	33 - 83	90	-
Taurine	12 - 159	175	-
Asparaginic acid	3 - 10	30	-
Threonine	15 - 62	888	-

TABLE 1. Continued.

Parameters	Reference	Pre-treatment	After-treatment
Serine	45 - 124	1045	-
Asparagine	< 32	475	-
Glutamic acid	< 11	74	-
Glutamine	62 - 165	1895	-
Proline	< 13	< 24	-
Glycine	110 - 356	468	-
Alanine	41 - 130	157	-
Citrulline	< 7	298	-
Alpha-aminobutyric acid	< 8	49	-
Valine	7 - 21	312	-
Cysteine	5 - 13	166	-
Isoleucine	< 6	45	-
Leucine	3 - 17	124	-
Tyrosine	13 48	474	-
phenylalanine	10 - 31	180	-
Ornithine	< 8	171	-
Lysine	16 - 69	1034	-
Histidine	87 - 287	1025	-
Arginine	< 8	66	-

*, There were no results obtained on urine biochemistry prior to the treatment as it was not possible to collect urine; NA, Not applicable; TmP/GFR, Tubular maximal phosphate reabsorption related to glomerular filtration rate.

RESULTS

Patient with *ATP6V1B1* variant displays a cystinosis-like phenotype of increased cystine levels, metabolic acidosis and symptoms of renal Fanconi syndrome. A 23-month-old girl presented with symptoms of failure to thrive (height Z-score of -2.5 and weight Z-score of -2), and abnormal gait. The patient had impaired hearing from infancy. This was attributed to an enlarged vestibular aqueduct, demonstrated by CAT-scan at the age of four months.

Upon physical examination, she showed plump knee joints with varus deformity. Laboratory examination showed a normal anion-gap metabolic acidosis, hypokalemia, hypophosphatemia, generalized aminoaciduria and elevated cystine levels in granulocytes (Table 1). Renal ultrasound showed bilateral medullary hyper echogenicity and conventional X-ray examination of the knees showed epiphyseal fraying and cupping

deformity. Based on the clinical and laboratory findings, the diagnosis of renal rickets due to generalized proximal tubular dysfunction (renal Fanconi syndrome) as a result of nephropathic cystinosis was made. Supplementation with potassium citrate, sodium phosphate, alfacalcidol (active vitamin D) and cysteamine bitartrate (Cystagon^{Ò}) was started. This resulted in an improvement of the patient's clinical conditions. However, diagnostic sequencing and multiplex ligation-dependent probe amplification did not show variants in the *CTNS* gene. Pending further genetic analysis, treatment with cysteamine bitartrate was continued. Cysteamine bitartrate treatment completely normalized cystine levels in granulocytes (0.03 nmol/mg), which was considered very unusual for a patient with nephropathic cystinosis. Further, ophthalmologic examination did not show corneal deposition of cystine crystals. Cysteamine bitartrate treatment was therefore withheld, after which cystine levels in granulocytes increased slightly to levels below those reported in heterozygous carriers of *CTNS* variants (0.22 nmol/mg). Diagnostic renal gene panel (a panel of renal genes from whole exome sequencing data) analysis was performed, which reiterated the negative result in *CTNS* but demonstrated two heterozygous pathogenic variants in *ATP6V1B1* (NM_001692.3:c.[175-1G>C];[1155dup], p.[(?)];[(Ile386fs)]) [23]. By analyzing the parents, the variants were shown to be in trans.
With these findings, a definite diagnosis of distal renal tubular acidosis and deafness (OMIM #267300) was established. Sodium phosphate and alfacalcidol supplementation was stopped, while treatment with potassium citrate was continued. The treatment resolved hypophosphatemia, generalized aminoaciduria, rickets, and improved the height Z-score to -0.65. However, the patient still presented a mildly increased urinary excretion of b2-microglobulin (Table 1), suggesting a mild defect in proximal tubules. This prompted us to further investigate the possible link between *ATP6V1B1* gene deficiency and the occurrence of a generalized proximal renal tubular defect.

V-ATPase B1 subunit is expressed along the human distal and proximal segments of the nephron. To study the role of the V-ATPase B1 subunit in proximal tubules, we first assessed its expression in healthy human kidney tissue by immunohistochemistry. As shown in Figure 1A, ATP6V1B1 is expressed in both proximal and distal tubules although with different levels of intensity. High-intensity staining was observed mainly in distal tubules, whereas low-intensity staining was mostly located to proximal tubules. In contrast, no staining was observed in the glomeruli.

CRISPR-generated *ATP6V1B1*$^{-/-}$ ciPTEC display increased cystine accumulation and autophagy activation. To dissect the underlying cellular mechanisms of the lysosomal V-ATPase B1 subunit in proximal tubules, we introduced a pathogenic variant in the *ATP6V1B1* gene by CRISPR/Cas9 in proximal tubule cells. After cell sorting and subsequent clonal cell expansion, two clones with biallelic variants (*ATP6V1B1*$^{-/-1}$ and *ATP6V1B1*$^{-/-2}$) were selected for subsequent experiments. Both *ATP6V1B1*-deficient renal proximal tubule cells displayed a significant increase in cystine levels (~3-fold), indicating that cystinosin transport function is reduced in absence of the lysosomal V-ATPase B1

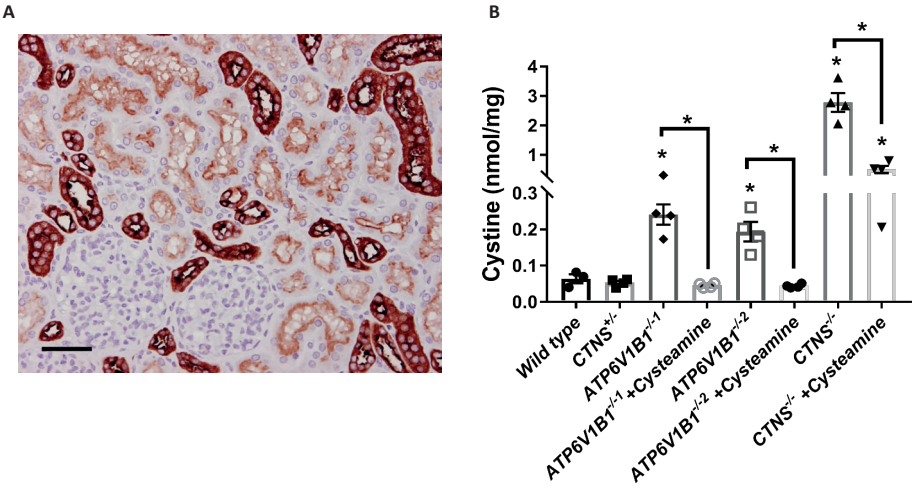

FIGURE 1. The V-ATPase B1 subunit is expressed in human proximal tubules and regulates cystinosin. (A) Immunostaining for the V-ATPase B1 subunit (ATP6V1B1) in human kidney tissue with the ATP6V1B1 antibody. Scale bar is 50 µm. **(B)** Quantification of cystine levels (nmol/mg protein) by HPLC-MS/MS in wild type (control), two clones of *ATP6V1B1*$^{-/-}$, *CTNS*$^{+/-}$, and *CTNS*$^{-/-}$ cells treated with or without cysteamine (100 µM). Data are expressed as the mean ± SEM of at least three independent experiments performed in triplicate. Statistical analysis was performed using one-way analysis of variance (ANOVA) followed by Dunnett's multiple comparisons test. Where appropriate, unpaired two-tailed Student's t-test were used. P-values < 0.05 were significant.

subunit (Figure 1B). Nevertheless, the cystine levels were not as high as those found in the isogenic *CTNS*$^{-/-}$ cells (45-fold increase compared to control) (Figure 1B). Consistent with the patient data, cysteamine treatment completely normalized cystine levels in *ATP6V1B1*$^{-/-}$ cells, but not in *CTNS*$^{-/-}$ cells (Figure 1B). Cystine levels in *CTNS*$^{-/-}$ cells treated with cysteamine was still higher (7.5-fold) than that found in control cells (Figure 1B).

When looking at the mRNA levels, we found a small (less than 2-fold) reduction in *CTNS* mRNA expression in the *ATP6V1B1* deficient cells (Supplementary figure S1A). It is not expected that this change in mRNA will directly affect the cystine transport function, especially as the same reduction in mRNA is seen in the proximal tubule cells bearing a heterozygous *CTNS* mutation (*CTNS*$^{+/-}$ cells), which does not result in cystine accumulation (Supplementary figure S1A, figure 1B). This indicates that the accumulation of cystine in *ATP6V1B1*$^{-/-}$ cells is not due to a lack in cystinosin protein levels, but rather caused by a reduced efficiency in the cystinosin activity. It is worth mentioning that *CTNS*$^{-/-}$ cells also show a decreased *ATP6V1B1* mRNA expression (1.5-fold) compared to control cells (supplementary figure S1B), suggesting there may be a regulatory link between the expression of these genes.

The lysosomal V-ATPase is a component of the mTOR complex and is involved in autophagy regulation [12]. Disruption of the mTORC1 complex and its dissociation from lysosomes is correlated with TFEB nuclear translocation and induction of autophagy, as also seen

in cystinosis [17]. In agreement with reduced mTOR activity, a ~3.0-fold increase in TFEB nuclear translocation was observed in both *ATP6V1B1* knockout lines compared to control cells, comparable to *CTNS*$^{-/-}$ cells (2.3-fold; Figure 2A, 2B). In agreement with TFEB known to downregulate its own expression after activation, we found that the endogenous *TFEB* mRNA expression was reduced in all three lines (~1.5-fold) when compared to control cells (Figure 2C). During autophagy, LC3-II (Microtubule-associated protein 1A/1B-light chain 3) is recruited to autophagosomes and its accumulation is correlated with abnormal induction of autophagy.[24] In accordance, we found significantly increased LC3-II levels in both the *CTNS* and *ATP6V1B1* knockout cells compared to control cells (Figure 2D). We also assessed the effect of the *ATP6V1B1* gene defect on endocytosis and lysosomal-cargo degradation in the knockout lines using BSA and DQ-BSA uptake, respectively. *ATP6V1B1* knockout lines maintained endocytosis and displayed increased endocytic cargo processing function (Figure 2E, 2F). *CTNS*$^{-/-}$ cells, similar to *ATP6V1B1*$^{-/-}$ cells, maintained endocytosis functionality but, in contrast displayed a reduced ability (~2.5-fold) to degrade endocytic cargo compared to control cells (Figure 2E, 2F).
Together, our data indicate that in proximal tubule cells, ATP6V1B1 plays a role in autophagy activation and lysosomal cystine transport, without having an effect on the lysosomal vesicular trafficking and degradation.

Metabolic and proteomic profiling link the lysosomal V-ATPase B1 subunit to nephropathic cystinosis. To further investigate the role of the B1 subunit of the lysosomal V-ATPase in proximal tubules and its contribution to cystinosis pathophysiology, we performed semi-targeted metabolomics and untargeted proteomics in *ATP6V1B1*$^{-/-}$, *CTNS*$^{-/-}$ and control cells (Figure 3, 4). Principal component analysis (PCA) of the 100 measured metabolites and over 3,474 identified proteins (Figure 3A, 4A) demonstrated that both *CTNS*$^{-/-}$ and *ATP6V1B1*$^{-/-}$ cells share quite similar metabolic and proteomic profiles and are different from the control cells. This was further visualized by unsupervised hierarchical clustering in which *ATP6V1B1*$^{-/-}$ cells clustered with *CTNS*$^{-/-}$ cells but not with control cells (Figure 3B). Moreover, pathway enrichment analysis of the metabolites revealed multiple similarly affected pathways in the two diseased cells, including the arginine and proline metabolism, the ß-alanine metabolism, and the alanine, aspartate and glutamate metabolism (Figure 3C, 3D), providing additional evidence that defects in both genes result in similar metabolic disruptions in proximal tubule cells.
To unravel the role of the lysosomal V-ATPase B1 subunit in proximal tubules, we first evaluated metabolite and protein expression differences between *ATP6V1B1*$^{-/-}$ and control cells (Figure 3E, 4B), and the differentially expressed metabolites and proteins were then compared with those in *CTNS*$^{-/-}$ cells. About 50% of the quantified metabolites (especially amino acids that are involved in acid regulation) [25, 26] were altered as a result of ATP6V1B1 loss in proximal tubule cells (Figure 3E). Cross-checking individual metabolites that were similarly affected in both *ATP6V1B1*$^{-/-}$ and *CTNS*$^{-/-}$ cells, revealed that *CTNS*$^{-/-}$ cells also present a fairly similar metabolite alteration as those found in *ATP6V1B1*$^{-/-}$ cells

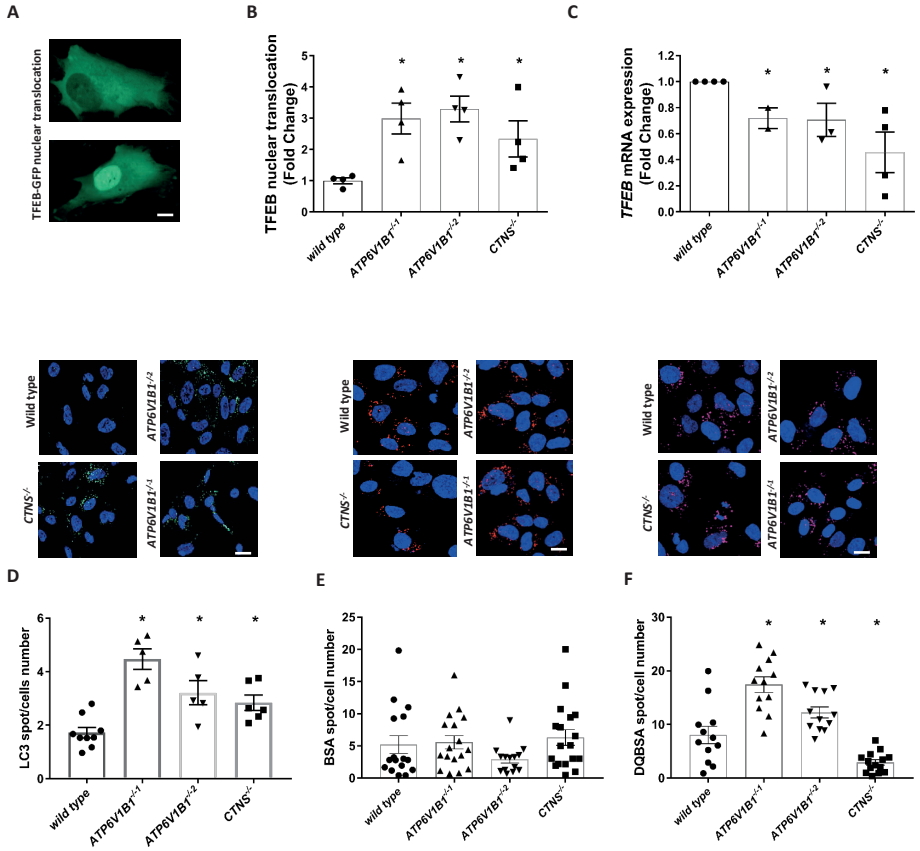

FIGURE 2. The V-ATPase B1 subunit regulates autophagy without having an effect on the lysosomal vesicular trafficking in proximal tubule cells. (A, B) Representative confocal micrographs and quantification of transcription factor EB (TFEB) nuclear translocation in wild type (control), two clones of *ATP6V1B1*$^{-/-}$, and *CTNS*$^{-/-}$ cells, respectively. Scale bars are 20 µm. **(C)** The levels of *TFEB* mRNA expression in control, two clones of *ATP6V1B1*$^{-/-}$, and *CTNS*$^{-/-}$ cells. **(D)** Representative confocal micrographs and quantification of LC3-II accumulation in control, two clones of *ATP6V1B1*$^{-/-}$, and *CTNS*$^{-/-}$ cells in presence of 25 nM bafilomycin (BafA1) for 4 hrs. Scale bars are 20 µm. **(E, F)** Representative confocal micrographs and quantification of BSA and DQ-BSA in control, two clones of *ATP6V1B1*$^{-/-}$, and *CTNS*$^{-/-}$ cells, respectively. Scale bars are 20 µm. Data are expressed as the mean ± SEM of at least three independent experiments performed in triplicate. Statistical analysis was performed using one-way analysis of variance (ANOVA) followed by Dunnett's multiple comparisons test. Where appropriate, unpaired two-tailed Student's t-test were used. P-values < 0.05 were significant.

(Figure 3F, 3G). Proteomic profiling, on the other hand, revealed a total of 562 proteins that were differentially expressed in *ATP6V1B1*$^{-/-}$ and *CTNS*$^{-/-}$ cells compared to controls (Figure 4C). Hierarchical clustering of these proteins resulted in five main protein clusters. Clusters A and E (in orange) represent proteins that were similarly affected in both

ATP6V1B1$^{-/-}$ and *CTNS*$^{-/-}$ cells compared to control cells, clusters B and D (in blue) show proteins affected differently in the *ATP6V1B1*$^{-/-}$ as compared to the *CTNS*$^{-/-}$ and control cells, and cluster C (in black) indicates proteins affected differently in the *CTNS*$^{-/-}$ as compared to *ATP6V1B1*$^{-/-}$ and control cells. The differentially abundant proteins were then subjected to gene ontology classification via the Panther Classification System database [27] to highlight their biological and molecular functions, and cellular component in the cells (Figure 4D). The analysis showed an overall reduction in proteins involved in catalytic activity, oxidoreductase activity, cell-cell adhesion, organelle organization, and focal adhesion in *ATP6V1B1*$^{-/-}$ and *CTNS*$^{-/-}$ cells compared to controls. Key proteins involved in lysosomal cargo degradation, namely lysosomal acid phosphatase (ACP2), Cathepsin B (CTSB), and mannose 6-phosphate receptors (M6PRs; IGFR2, receptors responsible for the delivery of newly synthesised lysosomal enzymes from Golgi to the lysosome), that were shown to be dysregulated in *CTNS*$^{-/-}$ cells,[17] were not affected in *ATP6V1B1*$^{-/-}$ cells (Figure 4E-Cluster-C). However, lysosome-associated membrane glycoprotein-1 (LAMP1), and Ragulator complex protein LAMTOR1 were found significantly downregulated in both *ATP6V1B1*$^{-/-}$ and *CTNS*$^{-/-}$ cells compared to controls (Figure 4E-Cluster-E). *ATP6V1B1*$^{-/-}$ cells also showed a decreased expression of several autophagy-regulatory proteins, Rab proteins (Figure 4E-Cluster-B, D), confirming that the loss of ATP6V1B1 in proximal tubule cells results in abnormal autophagy activation, but without influencing the lysosomal cargo degradation. *ATP6V1B1*$^{-/-}$ and *CTNS*$^{-/-}$ cells also presented decreased expression of tight junction protein, Zonula occludin-1 (TJP1; ZO-1) and gap junction alpha-1 protein (GJA1), and increased expression of lectin and β-galactoside-binding protein family 21, galectin-3 (LGALS3; Figure 4E-Cluster-A), markers of kidney disease progression. Altogether, our findings revealed a previously unrecognized role of the lysosomal V-ATPase B1 subunit in renal proximal tubular epithelial cells and signified its link to cystinosis pathophysiology.

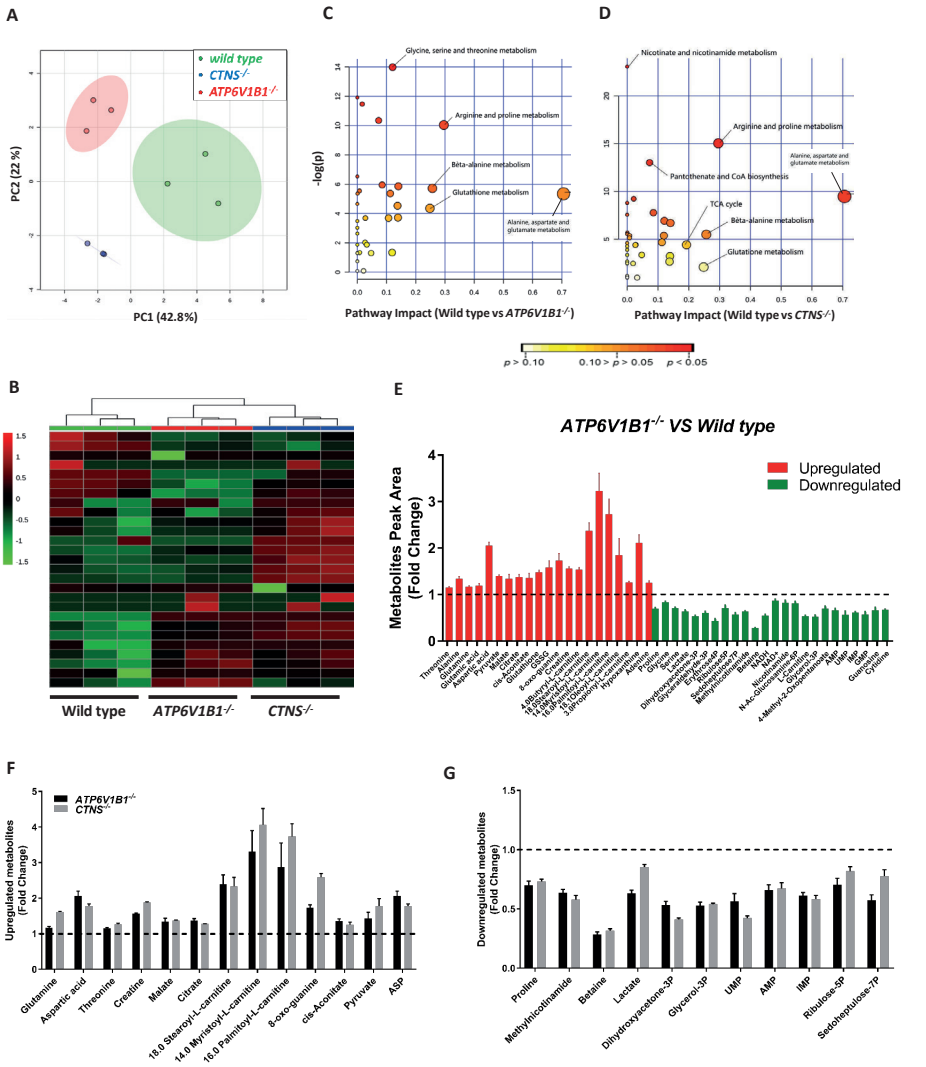

FIGURE 3. Defects in both *ATP6V1B1* and *CTNS* genes result in similar metabolic disruptions in proximal tubule cells. (A) Principal component analysis (PCA) of wild type (control), *ATP6V1B1*$^{-/-}$, and *CTNS*$^{-/-}$ cells based on the 100 metabolites measured. **(B)** Heatmap analysis of metabolites distinctively expressed in control, *ATP6V1B1*$^{-/-}$, and *CTNS*$^{-/-}$ cells. Color code: green lower than control ($p<0.05$), red higher than control ($p<0.05$). **(C, D)** Global test pathway enrichment analysis of the intracellular metabolic interactions distinctively affected in *ATP6V1B1*$^{-/-}$ and *CTNS*$^{-/-}$ cells compared to control cells, respectively. Larger circles further from the y-axis and orange-red color show higher impact of pathway affected in cells. **(E)** List of metabolites that were significantly altered in *ATP6V1B1*$^{-/-}$ compared to control cells. **(F, G)** List of metabolites that were shared and significantly upregulated and downregulated in both *ATP6V1B1*$^{-/-}$ and *CTNS*$^{-/-}$ cells compared to control cells, respectively. Data are expressed as the mean ± SEM of one experiment performed in triplicate. Statistical analysis was performed using one-way analysis of variance (ANOVA). Where appropriate, unpaired two-tailed Student's t-test were used. P-values < 0.05 were significant.

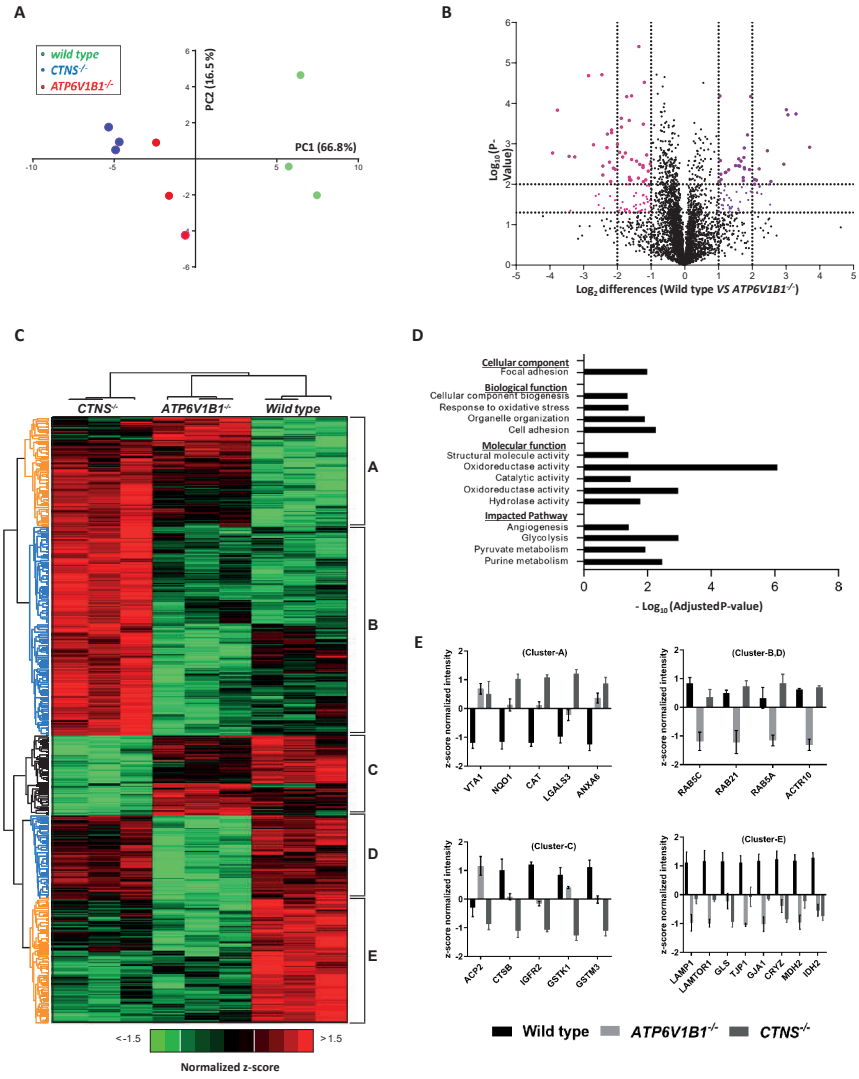

FIGURE 4. Proteomic profiling bridges the lysosomal V-ATPase B1 subunit to nephropathic cystinosis. (A) Principal component analysis (PCA) of the measured proteins in wild type (control), *ATP6V1B1*$^{-/-}$, and *CTNS*$^{-/-}$ cells. **(B)** Volcano plot illustrates significantly differentially abundant proteins. The -$\log_{10}$ (Benjamini–Hochberg corrected P-value) is plotted against the $\log_2$ (fold change: wild type/ *ATP6V1B1*$^{-/-}$). The non-axial vertical lines denote ±1.5-fold change while the non-axial horizontal line denotes P=0.05, which is our significance threshold (prior to logarithmic transformation). **(C)** Heatmap analysis of the proteins distinctively expressed in control, *ATP6V1B1*$^{-/-}$, and *CTNS*$^{-/-}$ cells. The row displays protein feature and the column represents the samples. The row Z-score of each feature is plotted in red-green colour scale. Proteins significantly decreased were displayed in green, while metabolites significantly increased were displayed in red. Hierarchical clustering of these proteins resulted in five main protein clusters. Clusters A and E (in orange) represent proteins that were similarly affected in both *ATP6V1B1*$^{-/-}$ and *CTNS*$^{-/-}$ cells compared to

control cells, clusters B and D (in blue) show proteins affected differently in the *ATP6V1B1*$^{-/-}$ as compared to the *CTNS*$^{-/-}$ and control cells, and cluster C (in black) indicates proteins affected differently in the *CTNS*$^{-/-}$ as compared to *ATP6V1B1*$^{-/-}$ and control cells. **(D)** Gene ontology analysis of the proteins in cluster-A, E and cluster-B, D of the Heatmap. **(E)** List of proteins that were significantly altered in *ATP6V1B1*$^{-/-}$, and *CTNS*$^{-/-}$ cells compared to control cells. VTA1; Vacuolar protein sorting-associated protein VTA1 homolog, NQO1; NAD(P)H dehydrogenase [quinone] 1, CAT; Catalase, LGALS3; Galectin-3, ANXA6; Annexin A6, RAB5C; Ras-related protein Rab-5C, RAB21; Ras-related protein Rab-21, RAB5A; Ras-related protein Rab-5A, ACTR10; Actin-related protein 10, ACP2; Lysosomal acid phosphatase, CTSB; Cathepsin B, IGF2R; Mannose-6-phosphate receptors, GSTK1; Glutathione S-transferase kappa-1, GSTM3; Glutathione S-transferase Mu-3, LAMP1; Lysosome-associated membrane glycoprotein 1, LAMTOR1; Ragulator complex protein LAMTOR1, GLS; Glutaminase kidney isoform, TJP1 (ZO-1); Tight junction protein-1, GJA1; Gap junction alpha-1 protein, CRYZ; Quinone oxidoreductase, MDH2; Malate dehydrogenase, IDH2; Isocitrate dehydrogenase. Data are expressed as the mean ± SEM of one experiment performed in triplicate. Statistical analysis was performed using one-way analysis of variance (ANOVA). Where appropriate, unpaired two-tailed Student's t-test were used. P-values < 0.05 were significant.

DISCUSSION

In this work, we revealed a previously unrecognized role of the lysosomal V-ATPase B1 subunit in renal proximal tubular epithelial cells and showed its loss could have similar effects on the cells as *CTNS* loss. In line with the clinical findings, the *ATP6V1B1* gene defect in proximal tubule cells hampered cystinosin regulation and resulted in cystine accumulation, which was completely normalized by cysteamine. The loss of ATP6V1B1 also entailed drastic cellular changes with a marked induction of autophagy and metabolic acidosis in proximal tubule cells, without influencing the lysosomal vesicular trafficking.

V-ATPases are large multisubunit complexes that utilize the energy derived from the hydrolysis of cytosolic ATP to transport protons across biological membranes and maintain the acidic pH of endocytic and secretory organelles [28, 29]. They are ubiquitously distributed on intracellular tubulo-vesicular membranes, and at the plasma membrane in specialized cell types. The B1 subunit of the V-ATPase has been found expressed only in intercalated cells of the kidney [8-10, 30], inner ear[7], ocular ciliary epithelium [31], male reproductive tract [32], and placenta [33]. The functional importance of the *ATP6V1B1* gene in kidney and auditory physiology is evidenced by the fact that mice and humans with variants in this gene develop the autosomal recessive dRTA with deafness [6, 7, 34]. However, the fact that our patient with *ATP6V1B1* variants also developed symptoms of cystinosis and renal Fanconi syndrome, demonstrated by increased granulocyte cystine levels, generalized aminoaciduria, and urinary excretion of b2-microglobulin, prompted us to investigate the possible link between *ATP6V1B1* gene deficiency and the occurrence of a generalized renal proximal tubular defect.

We demonstrated that ATP6V1B1 is expressed in proximal tubules in human kidney tissue, though to a lesser extent than in distal tubules. In addition, when we specifically

knocked out the *ATP6V1B1* gene in human renal proximal tubule cells, we found increased cystine levels with autophagy activation. Cystinosin is a H^+/cystine symporter that requires lysosomal H^+ influx mediated by the lysosomal V-ATPase to transport cystine to the cytoplasm [13]. The loss of ATP6V1B1 likely disrupted the chemiosmotic coupling between the lysosomal V-ATPase B1 subunit and cystinosin and resulted in intralysosomal accumulation of cystine in proximal tubule cells (Figure 5). Using an omics-based strategy, we provided evidence that defects in both genes may cause proximal renal tubular acidosis. The proximal tubule is the primary site for active solute reabsorption and secretion, and plays a central role in acid-base balance [35, 36]. During metabolic acidosis, the proximal tubule alters its metabolism and transport properties, leading to increased glutamine levels and renal ammoniagenesis to excrete more acid into urine [25, 37, 38]. In accordance, we observed an accumulation of glutamine in the both diseased cells. This could be due to either increased uptake or decreased catabolism of glutamine as a result of decreased expression of glutamines enzyme (GLS) in *ATP6V1B1* and *CTNS* deficient cells.

Furthermore, *ATP6V1B1*$^{-/-}$ and *CTNS*$^{-/-}$ proximal tubule cells showed decreased levels of lactate and increased levels of pyruvate and tricarboxylic acid (TCA) cycle intermediates, namely cis-aconitate, malate and citrate. This is in agreement with the findings of LaMonte *et al.*, where they demonstrated that metabolic acidosis induces aerobic glycolysis, redirecting glucose away from lactate production and towards the TCA cycle in human cancer cells [26]. Proteomic analysis, on the other hand, revealed that the loss of either ATP6V1B1 or cystinosin is accompanied with decreased expression of tight junction protein (ZO-1 and GJA1), indicating proximal tubular epithelial dysfunction and disrupted tight junction integrity [15, 39, 40]. *ATP6V1B1*$^{-/-}$ and *CTNS*$^{-/-}$ cells also presented increased expression of galectin-3, a protein demonstrated to be markedly upregulated in acute tubular injury [41] and in progressive renal fibrosis [42]. Lobry *et al*., demonstrated that cystinosin loss-of-function results in galectin-3 overexpression in cystinotic mice kidneys, inducing macrophage infiltration and kidney disease progression [43]. In light of our present data, together with the clinical findings, we indicate that the V-ATPase B1 subunit plays an important role in acid-base homeostasis and is involved in the occurrence of a generalized proximal renal tubular defect that could functionally overlap with the one seen in cystinosis.

Nephropathic cystinosis is the most common genetic cause of renal Fanconi syndrome in children. Variants in *CTNS* lead to lysosomal accumulation of cystine, reduced mTOR activation, delayed protein degradation and increased oxidative stress in proximal tubule cells [15, 17, 44-51]. It is known that cystinosin can directly interact with V-ATPase-Ragulator-Rag Complex at the lysosomal membrane, regulating mTOR-mediated autophagy [12]. On the other hand, V-ATPase was also identified as a potential amino acid sensing protein that can recruit and activate mTORC1 [52]. Here, we demonstrated that the defect or the decreased *ATPV1B1* gene expression is corelated with the increased TFEB nuclear translocation and subsequent autophagy activation (Figure 5). Hence, the fact that *CTNS*$^{-/-}$ cells have increased autophagy activation could be a direct result of

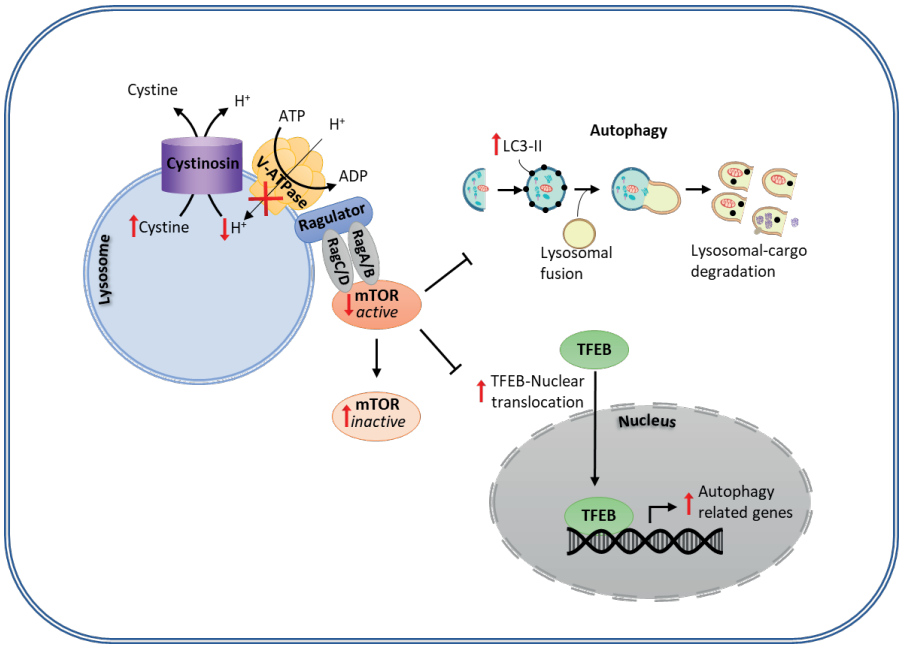

FIGURE 5. The lysosomal V-ATPase B1 subunit is the central interplay between cystinosin and mTOR-signaling, regulating cystine transport and autophagy in proximal tubule cells. ATP; adenosine triphosphate, ADP; adenosine diphosphate, GTP; Guanosine triphosphate, GDP; Guanosine diphosphate, mTOR; mammalian target of rapamycin complex, LC3-II; Microtubule-associated protein 1A/1B-light chain 3, TFEB; transcription factor EB.

the decreased activity of ATP6V1B1, disabling mTOR recruitment to the lysosomes and subsequent deactivation of mTOR signaling, in line with previous reports demonstrating reduced mTOR activity in *in vitro* and *in vivo* models of cystinosis [12, 15, 17, 53, 54]. This was further evidenced by Ragulator complex protein LAMTOR1 and LAMP1 being downregulated in both *ATP6V1B1*$^{-/-}$ and *CTNS*$^{-/-}$ cells. LAMTOR1 as a part of V-ATPase-Ragulator-Rag Complex is required for lysosomal recruitment of mTORC1 and consequent activation. Depletion in LAMTOR1 prevents mTOR shuttling to lysosomal surface, resulting in autophagy activation [55, 56].

Taken together, our study identified ATP6V1B1 as a central player in proximal tubule cells, regulating cystine transport and autophagy, and its absence can lead to proximal tubule dysfunction.

Acknowledgements

This work was financially supported by a grant from the Dutch Kidney Foundation (grant nr.150KG19 and KSTP12-010) and the stofwisselkracht (Druggable Targets In Lysosomal V-ATPase Dysfunction).

REFERENCES

1. Town, M., et al., *A novel gene encoding an integral membrane protein is mutated in nephropathic cystinosis.* Nat Genet, 1998. **18**(4): p. 319-24.
2. Cherqui, S. and P.J. Courtoy, *The renal Fanconi syndrome in cystinosis: pathogenic insights and therapeutic perspectives.* Nat Rev Nephrol, 2017. **13**(2): p. 115-131.
3. Foreman, J.W., *Fanconi Syndrome.* Pediatr Clin North Am, 2019. **66**(1): p. 159-167.
4. Kleta, R. and W.A. Gahl, *Pharmacological treatment of nephropathic cystinosis with cysteamine.* Expert Opin Pharmacother, 2004. **5**(11): p. 2255-62.
5. Wilmer, M.J., F. Emma, and E.N. Levtchenko, *The pathogenesis of cystinosis: mechanisms beyond cystine accumulation.* Am J Physiol Renal Physiol, 2010. **299**(5): p. F905-16.
6. Fry, A.C. and F.E. Karet, *Inherited renal acidoses.* Physiology (Bethesda), 2007. **22**: p. 202-11.
7. Karet, F.E., et al., *Mutations in the gene encoding B1 subunit of H+-ATPase cause renal tubular acidosis with sensorineural deafness.* Nat Genet, 1999. **21**(1): p. 84-90.
8. Frische, S., et al., *H(+)-ATPase B1 subunit localizes to thick ascending limb and distal convoluted tubule of rodent and human kidney.* Am J Physiol Renal Physiol, 2018. **315**(3): p. F429-f444.
9. Miller, R.L., et al., *The V-ATPase B1-subunit promoter drives expression of Cre recombinase in intercalated cells of the kidney.* Kidney Int, 2009. **75**(4): p. 435-9.
10. Miller, R.L., et al., *V-ATPase B1-subunit promoter drives expression of EGFP in intercalated cells of kidney, clear cells of epididymis and airway cells of lung in transgenic mice.* Am J Physiol Cell Physiol, 2005. **288**(5): p. C1134-44.
11. Tasic, V., et al., *Atypical presentation of distal renal tubular acidosis in two siblings.* Pediatr Nephrol, 2008. **23**(7): p. 1177-81.
12. Andrzejewska, Z., et al., *Cystinosin is a Component of the Vacuolar H+-ATPase-Ragulator-Rag Complex Controlling Mammalian Target of Rapamycin Complex 1 Signaling.* J Am Soc Nephrol, 2016. **27**(6): p. 1678-88.
13. Kalatzis, V., et al., *Cystinosin, the protein defective in cystinosis, is a H(+)-driven lysosomal cystine transporter.* Embo j, 2001. **20**(21): p. 5940-9.
14. Sansanwal, P. and M.M. Sarwal, *p62/SQSTM1 prominently accumulates in renal proximal tubules in nephropathic cystinosis.* Pediatr Nephrol, 2012. **27**(11): p. 2137-2144.
15. Festa, B.P., et al., *Impaired autophagy bridges lysosomal storage disease and epithelial dysfunction in the kidney.* Nat Commun, 2018. **9**(1): p. 161.
16. Sardiello, M., et al., *A gene network regulating lysosomal biogenesis and function.* Science, 2009. **325**(5939): p. 473-7.
17. Jamalpoor, A., et al., *Cysteamine-bicalutamide combination treatment restores alpha-ketoglutarate and corrects proximal tubule phenotype in cystinosis.* bioRxiv, 2020: p. 2020.02.10.941799.
18. Rega, L.R., et al., *Activation of the transcription factor EB rescues lysosomal abnormalities in cystinotic kidney cells.* Kidney Int, 2016. **89**(4): p. 862-73.
19. van Diest, P.J., *No consent should be needed for using leftover body material for scientific purposes. For.* Bmj, 2002. **325**(7365): p. 648-51.
20. Wilmer, M.J., et al., *Novel conditionally immortalized human proximal tubule cell line expressing functional influx and efflux transporters.* Cell Tissue Res, 2010. **339**(2): p. 449-57.
21. Ran, F.A., et al., *Genome engineering using the CRISPR-Cas9 system.* Nat Protoc, 2013. **8**(11): p. 2281-2308.

22. Jamalpoor, A., et al., *Quantification of cystine in human renal proximal tubule cells using liquid chromatography-tandem mass spectrometry.* Biomed Chromatogr, 2018: p. e4238.
23. Richards, S., et al., *Standards and guidelines for the interpretation of sequence variants: a joint consensus recommendation of the American College of Medical Genetics and Genomics and the Association for Molecular Pathology.* Genet Med, 2015. **17**(5): p. 405-24.
24. Yoshii, S.R. and N. Mizushima, *Monitoring and Measuring Autophagy.* Int J Mol Sci, 2017. **18**(9).
25. Tannen, R.L. and A. Sahai, *Biochemical pathways and modulators of renal ammoniagenesis.* Miner Electrolyte Metab, 1990. **16**(5): p. 249-58.
26. Lamonte, G., et al., *Acidosis induces reprogramming of cellular metabolism to mitigate oxidative stress.* Cancer Metab, 2013. **1**(1): p. 23.
27. Thomas, P.D., et al., *PANTHER: a browsable database of gene products organized by biological function, using curated protein family and subfamily classification.* Nucleic Acids Res, 2003. **31**(1): p. 334-41.
28. Forgac, M., *Vacuolar ATPases: rotary proton pumps in physiology and pathophysiology.* Nat Rev Mol Cell Biol, 2007. **8**(11): p. 917-29.
29. Marshansky, V. and M. Futai, *The V-type H+-ATPase in vesicular trafficking: targeting, regulation and function.* Curr Opin Cell Biol, 2008. **20**(4): p. 415-26.
30. Nelson, R.D., et al., *Selectively amplified expression of an isoform of the vacuolar H(+)-ATPase 56-kilodalton subunit in renal intercalated cells.* Proc Natl Acad Sci U S A, 1992. **89**(8): p. 3541-5.
31. Wax, M.B., et al., *Vacuolar H+-ATPase in ocular ciliary epithelium.* Proc Natl Acad Sci U S A, 1997. **94**(13): p. 6752-7.
32. Breton, S., et al., *Acidification of the male reproductive tract by a proton pumping (H+)-ATPase.* Nat Med, 1996. **2**(4): p. 470-2.
33. van Hille, B., et al., *Heterogeneity of vacuolar H(+)-ATPase: differential expression of two human subunit B isoforms.* Biochem J, 1994. **303 (Pt 1)**: p. 191-8.
34. Finberg, K.E., et al., *The B1-subunit of the H(+) ATPase is required for maximal urinary acidification.* Proc Natl Acad Sci U S A, 2005. **102**(38): p. 13616-21.
35. Curthoys, N.P. and O.W. Moe, *Proximal tubule function and response to acidosis.* Clin J Am Soc Nephrol, 2014. **9**(9): p. 1627-38.
36. Wang, K. and B. Kestenbaum, *Proximal Tubular Secretory Clearance: A Neglected Partner of Kidney Function.* Clin J Am Soc Nephrol, 2018. **13**(8): p. 1291-1296.
37. Taylor, L. and N.P. Curthoys, *Glutamine metabolism: Role in acid-base balance*.* Biochem Mol Biol Educ, 2004. **32**(5): p. 291-304.
38. Lotspeich, W.D., *Metabolic aspects of acid-base change.* Science, 1967. **155**(3766): p. 1066-75.
39. Raggi, C., et al., *Dedifferentiation and aberrations of the endolysosomal compartment characterize the early stage of nephropathic cystinosis.* Human Molecular Genetics, 2013. **23**(9): p. 2266-2278.
40. Lima, W.R., et al., *ZONAB Promotes Proliferation and Represses Differentiation of Proximal Tubule Epithelial Cells.* Journal of the American Society of Nephrology, 2010: p. ASN.2009070698.
41. Nishiyama, J., et al., *Up-regulation of galectin-3 in acute renal failure of the rat.* Am J Pathol, 2000. **157**(3): p. 815-23.
42. Henderson, N.C., et al., *Galectin-3 expression and secretion links macrophages to the promotion of renal fibrosis.* Am J Pathol, 2008. **172**(2): p. 288-98.

43. Lobry, T., et al., *Interaction between galectin-3 and cystinosin uncovers a pathogenic role of inflammation in kidney involvement of cystinosis.* Kidney Int, 2019. **96**(2): p. 350-362.
44. Wilmer, M.J., et al., *Cysteamine restores glutathione redox status in cultured cystinotic proximal tubular epithelial cells.* Biochim Biophys Acta, 2011. **1812**(6): p. 643-51.
45. Levtchenko, E., et al., *Altered status of glutathione and its metabolites in cystinotic cells.* Nephrol Dial Transplant, 2005. **20**(9): p. 1828-32.
46. Chol, M., et al., *Glutathione precursors replenish decreased glutathione pool in cystinotic cell lines.* Biochem Biophys Res Commun, 2004. **324**(1): p. 231-5.
47. Rizzo, C., et al., *Pyroglutamic aciduria and nephropathic cystinosis.* J Inherit Metab Dis, 1999. **22**(3): p. 224-6.
48. Raggi, C., et al., *Dedifferentiation and aberrations of the endolysosomal compartment characterize the early stage of nephropathic cystinosis*. Hum Mol Genet, 2014. **23**(9): p. 2266-78.
49. Ivanova, E.A., et al., *Endo-lysosomal dysfunction in human proximal tubular epithelial cells deficient for lysosomal cystine transporter cystinosin.* PLoS One, 2015. **10**(3): p. e0120998.
50. Settembre, C., et al., *A block of autophagy in lysosomal storage disorders*. Hum Mol Genet, 2008. **17**(1): p. 119-29.
51. Platt, F.M., B. Boland, and A.C. van der Spoel, *The cell biology of disease: lysosomal storage disorders: the cellular impact of lysosomal dysfunction.* J Cell Biol, 2012. **199**(5): p. 723-34.
52. Zoncu, R., et al., *mTORC1 senses lysosomal amino acids through an inside-out mechanism that requires the vacuolar H(+)-ATPase.* Science, 2011. **334**(6056): p. 678-83.
53. Hollywood, J.A., et al., *Use of Human Induced Pluripotent Stem Cells and Kidney Organoids To Develop a Cysteamine/mTOR Inhibition Combination Therapy for Cystinosis.* J Am Soc Nephrol, 2020.
54. Ivanova, E.A., et al., *Altered mTOR signalling in nephropathic cystinosis.* J Inherit Metab Dis, 2016. **39**(3): p. 457-464.
55. Sancak, Y., et al., *Ragulator-Rag complex targets mTORC1 to the lysosomal surface and is necessary for its activation by amino acids.* Cell, 2010. **141**(2): p. 290-303.
56. Bar-Peled, L., et al., *Ragulator is a GEF for the rag GTPases that signal amino acid levels to mTORC1.* Cell, 2012. **150**(6): p. 1196-208.

SUPPLEMENTAL FILES

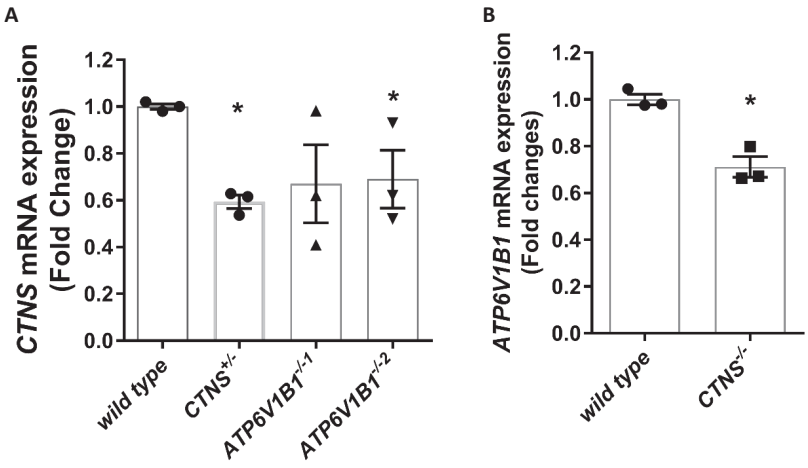

Supplementary FIGURE S1. The lysosomal V-ATPase B1 interacts with cystinosin. (A) *CTNS* mRNA expression in two clones of *ATP6V1B1*$^{-/-}$ and *CTNS*$^{+/-}$ cells was measured using real-time quantitative polymerase chain reaction, with ribosomal protein S13 (RPS-13) as a reference gene, normalized to wild type (control) cells. **(B)** The levels of *ATP6V1B1* mRNA expression in *CTNS*$^{-/-}$ and control cells. Data are expressed as the mean ± SEM of at least three independent experiments. Statistical analysis was performed using one-way analysis of variance (ANOVA) followed by Dunnett's multiple comparisons test. P-values < 0.05 were significant.

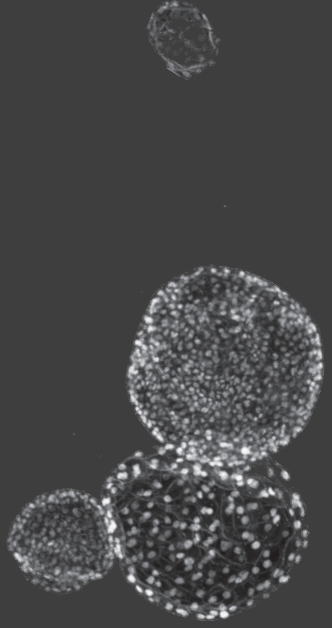

6

Gene repair in cystinosis

Amer Jamalpoor[1], Patrick T Harrison[2], Rosalinde Masereeuw[1] and Manoe J Janssen[1]

[1]Division of Pharmacology, Utrecht Institute for Pharmaceutical Sciences, Faculty of Science, Utrecht University, 3584 CG Utrecht, The Netherlands. [2]Department of Physiology, Biosciences Research Institute, University College Cork, College Road, Cork, Ireland.

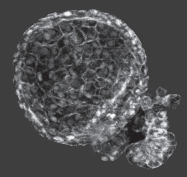

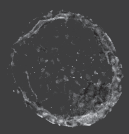

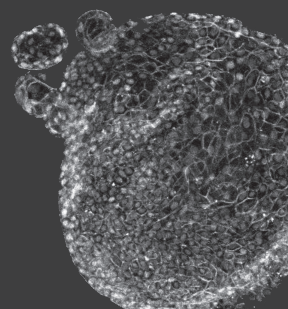

Ongoing work

ABSTRACT

Nephropathic cystinosis is a severe monogenetic kidney disorder caused by mutations in *CTNS*, encoding the lysosomal transporter cystinosin, resulting in lysosomal cystine accumulation. The first clinical signs develop during infancy (age of ~6 months) in the form of renal Fanconi syndrome, which often develops into kidney failure in the first decade of life. The sole treatment, cysteamine, slows down the disease progression, however, it poses serious side effects and offers no cure for the renal Fanconi syndrome. Here, we used CRISPR/Cas9-based strategy, termed homology-independent targeted insertion (HITI) as a new therapeutic strategy to repair and restore the *CTNS* gene function in cystinotic human kidney cells containing the large 57kb deletion. We identified target region and generated the region-specific guide RNAs in cystinotic cells. Next, a SuperExon donor DNA comprising the endogenous *CTNS* promotor and cDNA sequence of the missing exons was designed and constructed. As proof-of-concept, we successfully incorporated the donor DNA into the genome of HEK-293 cells using the HITI approach. In cystinotic proximal tubule cells, however, CRISPR-HITI did not result in a detectable incorporation of the donor DNA into the cells' genome. Future studies will be directed to optimize the protocol for CRISPR-HITI delivery and evaluate *CTNS* repair efficiency in cystinotic proximal tubular cells. We believe that this technique will not only serve as a proof-of-principle for future gene and/or cell-based therapies, but also might provide a long-lasting cure for patients with cystinosis.

Keywords:
Cystinosis, cystine accumulation, CRISPR-HITI, gene repair

INTRODUCTION

Recent advances in targeted gene editing using the CRISPR/Cas9 system have made it possible to repair a site-specific mutation without additional alterations to the genome [1-3]. The system uses guide RNAs (gRNAs) to guide Cas9 endonuclease to the target site, where it induces DNA double strand breaks (DSBs). These DSBs are mainly repaired by the non-homologous end joining (NHEJ) pathway, an error prone pathways causing micro-insertions or deletions. However, in the presence of a donor DNA template, the homologous recombination (HR) pathway is engaged to a lesser extent to precisely repair the damaged DNA site. Although this system is flexible and fast for generating small mutations in organisms and cells, its use has been unsuitable for the insertion of large DNA fragments. Recently, a unique CRISPR/Cas9-based strategy, termed homology-independent targeted insertion (HITI), was developed that is ideally suited for the precise insertion of large DNA fragments in dividing and non-dividing cells, both *in vitro* and *in vivo* [4, 5].

Nephropathic cystinosis (MIM219800) is a lysosomal storage disease caused by mutations in *CTNS*, a gene that codes for the lysosomal cystine/proton symporter cystinosin [6]. The loss of cystinosin leads to the lysosomal accumulation of cystine throughout the body and causes irreversible damage to various organs, particularly the kidneys [7]. For the past decades, great efforts have been directed towards reducing cellular cystine accumulation in cystinotic patients. The cystine-depleting drug cysteamine can efficiently lower the lysosomal cystine levels and postpone disease progression. However, it poses serious side effects and does not correct the established proximal tubulopathy associated with cystinosis [8, 9]. Here, we used CRISPR-HITI as a new therapeutic strategy to repair and restore the *CTNS* gene function in cystinotic human kidney cells containing the large 57kb deletion, the most prevalent mutation in cystinotic patients resulting in loss of exons 1-10 of the *CTNS* gene [10]. When successful, this could not only serve as a proof-of-principle for future gene and/or cell-based therapies, but also provides a long-lasting cure for patients with cystinosis.

MATERIALS AND METHOD

Reagents

All chemicals and reagents were obtained from Sigma-Aldrich (Zwijndrecht, The Netherlands) unless specified otherwise.

CiPTEC and HEK-293 cells culture

Conditionally immortalized proximal tubular epithelial cells (ciPTEC) were cultured as previously described by Wilmer et al. 2010 [11]. The culture medium was Dulbecco's modified Eagle medium DMEM/F-12 (GIBCO) supplemented with fetal calf serum 10% (v/v), insulin 5 µg/ml, transferrin 5 µg/ml, selenium 5 µg/ml, hydrocortisone 35 ng/ml,

epidermal growth factor 10 ng/ml and tri-iodothyronine 40 pg/ml. In short, cells were seeded at a density of 55,000 cells/cm^2 and grown at 33°C for 24 hrs to enable them to proliferate and subsequently cultured at 37°C for 7 days to mature into fully differentiated epithelial cells. Human embryonic kidney 293 (HEK-293) cells were cultured in Dulbecco's modified Eagle medium with low glucose (GIBCO) supplemented with fetal calf serum 10% (v/v). Cells were seeded at a density of 55,000 cells/cm^2 and grown at 37℃ in a humidified atmosphere containing 5% (v/v) CO_2. Mycoplasma contamination was checked every 2 months and was found to be negative in the cell lines used.

Guide RNAs design and optimisation

Three different guide (g) RNAs (Target plasmid) targeting upstream of the exon 11 were designed and cloned into the pSPCas9(BB)-2A-GFP plasmid (Addgene #48138) as described previously by Ran et al. [2] (Supplementary table 1). In order to maximize specificity, guide sequences with high scores for on-target efficiency and no predicted off-targets having at least 3 base pair mismatches in the genome were selected.

Gene repair construct for CRISPR-HITI

The gene repair construct consists of the endogenous *CTNS* promotor, *CTNS* exons 1-10 (ENST00000046640.7) and part of the intron following exon 10 containing the splice donor site. This *CTNS* sequence is flanked by gRNA sequences that will allow excision of the *CTNS* SuperExon upon release in the cell (see full sequence of the repair construct in Supplementary table 1). The repair construct was cloned into a pUC57 plasmid (Donor plasmid; GenScript, USA) for amplification and transfection. To improve the correct integration of the SuperExon into the genome, the construct contained the same gRNAs/protospacer adjacent motif (PAM) sequences that were used for the target plasmids, but in opposite orientations. In this way, the correct integration would destroy the gRNA/PAM sequence whereas the inverted integration would result in restoration of the gRNA/PAM sequence and excision of the SuperExon from the genome. Finally, to facilitate PCR-based genomic analysis upon successful donor DNA integration, the repair construct contained a primer sequence.

Cell transfection

Cells were seeded in a special optic 96-well plate (Corning) for 24 hrs until reaching 50% confluency. Cells were then transfected with the gRNAs or in combination with the repair construct using PolyPlus JetPrime reagent according to the manufacturer's instructions, and transfection efficiency were evaluated after 72 hrs. Transfection efficiency were assessed by visualizing green fluorescent protein (GFP)-positive cells using a Cell Voyager 7000 (CV7000) confocal microscope (Yokogawa Electric corporation, Tokyo, Japan), or by fluorescence-activated cell sorting (FACS) analysis. For FACS, the cells were first forced through a 70 µm cell strainer to dissociate cell clumps and GFP-positive cells were then sorted using a FACS Aria II (Core Flow cytometry Facility, University Medical Center Utrecht, The Netherland).

Evaluate gene repair efficiency

The gRNA cut site was amplified with PCR (~700 bp) using the primers flanking the cut region (Forward 5'-AGGAAACAGGACGGAAAGCCA-3'; R.reverse 5'-AGCTTCCCAGCTTCAACATGC-3'). The PCR product were then analysed both by Sanger sequencing (Macrogen Europe B.V, The Netherlands) and gel electrophoresis (Bio-rad ChemiDoc XRS$^+$ system).

RESULTS

Identification of the target region and generation of the region-specific guide RNAs in cystinotic ciPTEC. To repair the *CTNS* mutation in cystinotic ciPTEC bearing a 57-kb deletion mutation (the most common mutation in cystinotic patients), we first identified and analyzed the target region upstream of exon 11 using PCR-based Sanger sequencing (Figure 1, Supplementary Table 1). Next, gRNAs were designed to target the identified region (Figure 1).

Guide RNAs demonstrate cutting efficiency in cystinotic ciPTEC. Cells were transfected with gRNA plasmids either alone or in combination using Polyplus JetPrime reagent according to the manufacturer's instructions. At 72 hrs post-transfection, cells were visualized using the Cell Voyager 7000 confocal microscope (Figure 2A). After visualization, GFP-positive were sorted by FACS, and the transfection efficiency measured was ~25% (Figure 2B). However, the combination of gRNAs (gRNAs 1+3 and 2+3 that are located ~200 bp apart) still resulted in a successful DNA excision with the desired size in the target region (Figure 3).

Incorporation of SuperExon donor DNA into the genome. After optimizing the gRNA in ciPTEC we attempted the co-transfection of the gRNAs with the repair construct in ciPTEC, but did not detect successful incorporation of the SuperExon donor DNA into the genome. This is likely due to the low transfection efficiency observed in ciPTEC, making them less amenable to gene editing [12]. To overcome this problem we next tested our strategy in HEK-293 cells. The target region in HEK-293 cells was identical to that previously identified in ciPTEC (Figure 4A, Supplementary Table 1). We therefore used the same gRNAs that were designed for ciPTEC. Compared to ciPTEC, HEK-293 cells indeed had a higher gRNA-transfection efficiency as was demonstrated by the higher number of GFP-positive cells (~60-70%; Figure 4B, C). Next, we co-transfected the gRNAs with the repair construct using different ratios of gRNA: repair construct (1:0.5, 1:1, and 2:1). At 72 hrs post-transfection, DNA was extracted and analyzed by PCR-base Sanger sequencing and gel electrophoresis. A successful insertion of donor DNA was achieved when combined with gRNA-3 only (gRNA to repair construct ratio: 1:0.5)(Figure 4D).

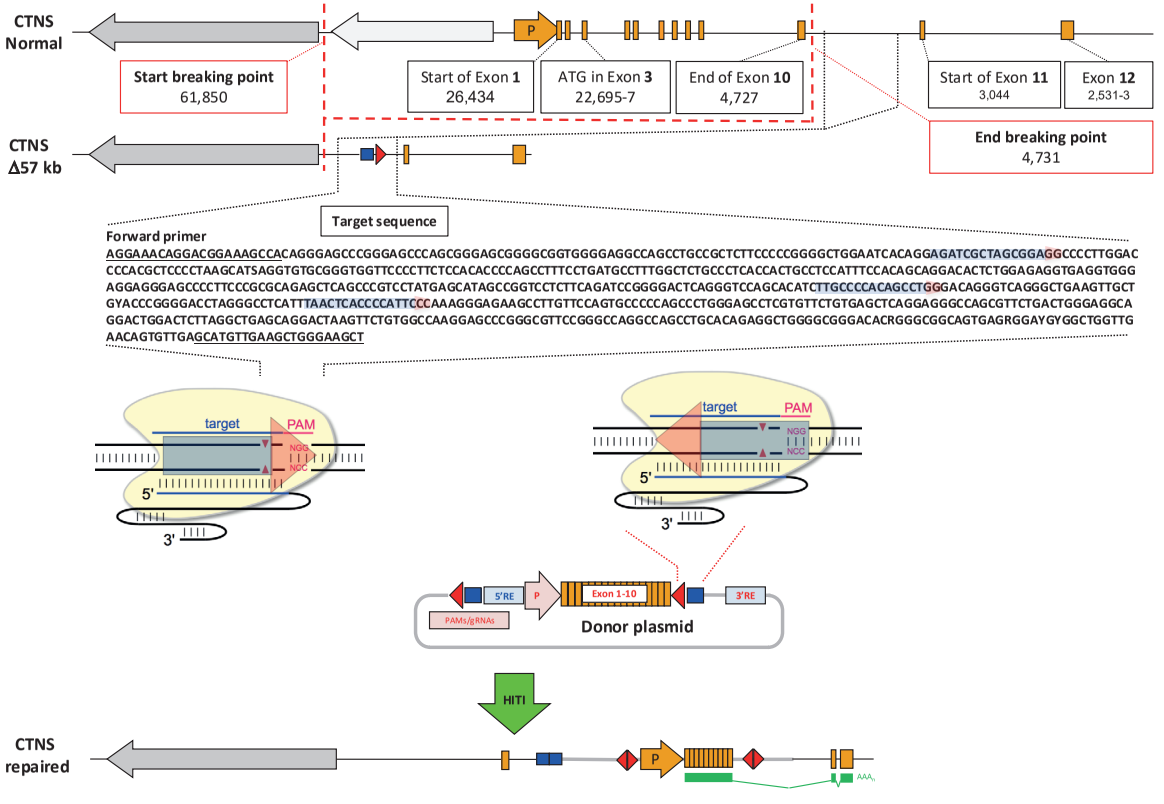

1. The first 9 exons, and a part of the 10th exon of the CTNS gene is deleted in 57kb deletion mutation.

2. The sequence of the target region downstream the exon 10 identified by PCR-based Sanger sequencing.

3. Donor plasmids consists of the endogenous *CTNS* promotor and cDNA sequence of exons 1-10, flanked by target-specific guide RNAs but in opposite direction.

4. Successful integration of donor DNA Restores all functions of the CTNS gene in the transduced cell

FIGURE 1. Gene repair using CRISPR-HITI technique as a new treatment option for cystinosis. Schematic representation of how CRISPR-HITI technique works.

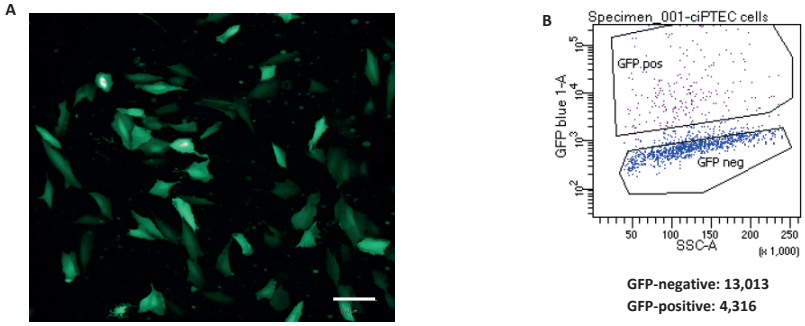

FIGURE 2. Transfection efficiency of the target gRNAs in cystinotic ciPTEC. (A) Representative confocal micrographs of cystinotic ciPTEC transfected with gRNAs. GFP-positive cells were visualized using the Cell Voyager 7000 confocal microscope. Scale bar is 20 µm. **(B)** The transfection efficiency measured by fluorescence-activated cell sorting (FACS).

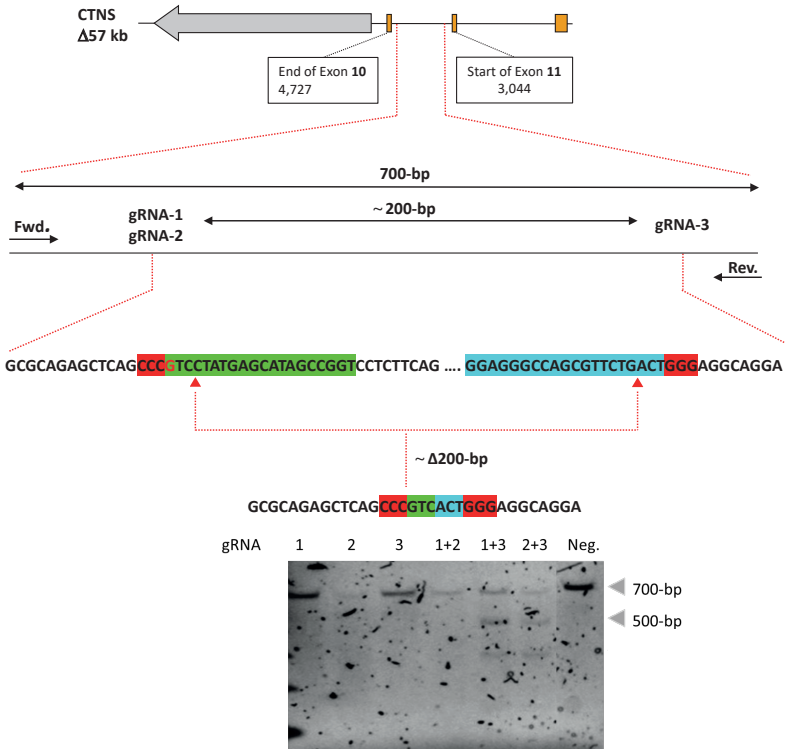

FIGURE 3. Cutting efficiency of the target gRNAs in cystinotic ciPTEC. Paired gRNAs are designed to excise a locus in the identified target region. Target sequences and PAMs (red) are shown in respective colors, and sites of cleavage by Cas9 are indicated by red triangles. A predicted junction is shown below. Individual clones isolated from cell populations transfected with gRNA 1, 2, 3, or their combinations are assayed by PCR (using the forward and revers primers), reflecting a deletion of ~200 bp.

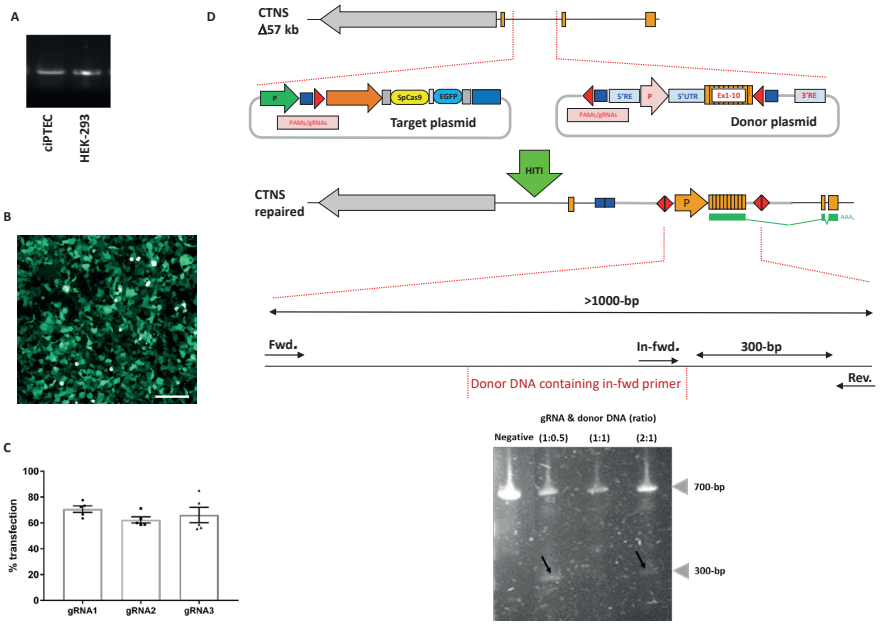

FIGURE 4. CRISPR-HITI approach in HEK-293 cells. (A) Representative PCR product bands demonstrating that target region in HEK-293 cells is identical to that of previously identified in ciPTEC. **(B, C)** Representative confocal micrograph of HEK-293 cells transfected with gRNAs and the percentage transfection efficiency of gRNAs. GFP-positive cells were visualized using the Cell Voyager 7000 confocal microscope. Scale bars is 20 µm. **(D)** CRISPR-HITI approach in HEK-293 cells. The repair construct contained an in-forward primer to facilitate genomic analysis. Once donor DNA is incorporated into the genome, PCR will result in a primer product size of 300-bp otherwise, a 700-bp product. Of note the forward and in-forward primers are identical. Co-transfection of the gRNA-3 with the repair construct resulted in a successful incorporation of the SuperExon donor DNA into the genome of HEK-293-cells.

DISCUSSION

In this work, we used CRISPR-HITI technology as a new treatment option for nephropathic cystinosis. We identified the target region in cystinotic ciPTEC, where exons 1-10 of the *CTNS* gene are deleted [10]. Next, a SuperExon donor DNA, comprising *CTNS* exons 1-10 fused as a cDNA was constructed and co-transfected with the region-specific guide RNAs. In cystinotic ciPTEC, co-transfection of the gRNAs with the repair construct did not result in a successful incorporation of the donor DNA into the cells's genome. We believe this is due to the low transfection efficiency observed in ciPTEC (max 25%). As proof-of-concept, we optimized our protocol in HEK-293 cells, the gold standard cell model to study gene therapy. HEK-293 cells indeed had a higher transfection efficiency (60-70%) and co-transfection of the gRNAs with the repair construct resulted in a successful insertion of donor DNA into the genome of HEK-cells.

The non-homologous end joining is the major DNA repair pathway that ligates DNA ends directly and is active throughout the cell cycle in a large variety of adult cells [13]. In 2016, Suzuki *et al*. devised a fundamentally improved NHEJ-based transgene integration, CRISPR-HITI and showed that the targeted knock-in is 10 times higher than that of the homology-directed repair method [5]. Moreover, the targeted genes were free of indels, demonstrating the error-free tendency of this technique. Accordingly, Auer *et al*., reported the successful use of CRISPR-HITI in integrating a 5.7kb gene repair construct into the genome of zebrafish at a very high rate [14]. The study reported CRISPR-HITI as an easy, feasible, and simple method for gene editing.

There are still, however, challenges to translate HITI technology into a clinical application. One major hurdle is the repair efficiency. Although the current HITI technology can insert DNA at a specific target site, the knock-in efficiency can be very low. As demonstrated in our study, transfection efficiency is the rate limiting step for HITI to work. Hence, to improve repair efficiency, mechanistic studies to increase transfection efficiency and to identify the major regulators of HITI activity are prerequisite.

Adenovirus-based delivery is one of the most popular delivery methods in the field of gene therapy. Adenoviruses have the advantage of being a non-integrating virus, with high transduction efficiency and facilitating gene repair in the target genome [15, 16]. Adenoviral vectors can transduce quiescent and dividing cells, including mouse kidney, liver and Hematopoietic stem cells from both mouse and human [17-19]. Hence, viral delivery of CRSPR-HITI could result in a better transfection efficiency, improving gene repair in cystinotic ciPTEC. However, a great care should be taken as viral vectors can trigger an immunogenic response and provide additional risks for treatment. Polymer-based transfection reagent is a yet another gene delivery system that forms a stable complex with oligonucleotides (DNA or RNA). There is no limit to the size of the plasmids used and due to its cationic charge it will interact with anionic proteoglycans at the cell surface and enter cells by endocytosis [20-22]. The polymer is thought to promote endosome osmotic swelling and rupture, which provides an escape mechanism for oligonucleotides to the cytoplasm, resulting in effective oligonucleotide delivery with low toxicity. Apart from improving delivery methods, the use of Cas9 mRNA or ribonucleoprotein (RNP) complexes as an alternative to Cas9 expression plasmids, can result in increased gene repair efficiency. RNP complexes are shown to have increased nuclease resistance, increasing the editing efficiency [23]. In general, RNP delivery of the CRISPR found to be the preferred delivery method to target primary cell lines [24]. Hence, future studies will be directed towards the use of viral or polymer-based delivery methods to improve HITI approach in cystinotic ciPTEC. Moreover, Cas9 mRNA or RNP complexes as an alternative to Cas9 expression plasmids will be used. In this way we will be able to compare the approaches and determine which one can result in a better repair efficiency.

Acknowledgements

This work was financially supported by a grant from the Dutch Kidney Foundation (grant nr.150KG19) and the Cystinosis Ireland Seedcorn.

REFERENCES

1. Hsu, P.D., E.S. Lander, and F. Zhang, *Development and applications of CRISPR-Cas9 for genome engineering.* Cell, 2014. **157**(6): p. 1262-1278.
2. Ran, F.A., et al., *Genome engineering using the CRISPR-Cas9 system.* Nat Protoc, 2013. **8**(11): p. 2281-2308.
3. Luo, J.J., et al., *CRISPR/Cas9-based genome engineering of zebrafish using a seamless integration strategy.* Faseb j, 2018. **32**(9): p. 5132-5142.
4. Suzuki, K. and J.C. Izpisua Belmonte, *In vivo genome editing via the HITI method as a tool for gene therapy.* J Hum Genet, 2018. **63**(2): p. 157-164.
5. Suzuki, K., et al., *In vivo genome editing via CRISPR/Cas9 mediated homology-independent targeted integration.* Nature, 2016. **540**(7631): p. 144-149.
6. Town, M., et al., *A novel gene encoding an integral membrane protein is mutated in nephropathic cystinosis.* Nat Genet, 1998. **18**(4): p. 319-24.
7. Cherqui, S. and P.J. Courtoy, *The renal Fanconi syndrome in cystinosis: pathogenic insights and therapeutic perspectives.* Nat Rev Nephrol, 2017. **13**(2): p. 115-131.
8. Brodin-Sartorius, A., et al., *Cysteamine therapy delays the progression of nephropathic cystinosis in late adolescents and adults.* Kidney Int, 2012. **81**(2): p. 179-89.
9. Gahl, W.A., J.G. Thoene, and J.A. Schneider, *Cystinosis.* N Engl J Med, 2002. **347**(2): p. 111-21.
10. Gahl, W.A., J.Z. Balog, and R. Kleta, *Nephropathic cystinosis in adults: natural history and effects of oral cysteamine therapy.* Ann Intern Med, 2007. **147**(4): p. 242-50.
11. Wilmer, M.J., et al., *Novel conditionally immortalized human proximal tubule cell line expressing functional influx and efflux transporters.* Cell Tissue Res, 2010. **339**(2): p. 449-57.
12. Veach, R.A. and M.H. Wilson, *CRISPR/Cas9 engineering of a KIM-1 reporter human proximal tubule cell line.* PLoS One, 2018. **13**(9): p. e0204487.
13. Lieber, M.R., *The mechanism of double-strand DNA break repair by the nonhomologous DNA end-joining pathway.* Annu Rev Biochem, 2010. **79**: p. 181-211.
14. Auer, T.O., et al., *Highly efficient CRISPR/Cas9-mediated knock-in in zebrafish by homology-independent DNA repair.* Genome Res, 2014. **24**(1): p. 142-53.
15. Holkers, M., et al., *Adenoviral vector DNA for accurate genome editing with engineered nucleases.* Nat Methods, 2014. **11**(10): p. 1051-7.
16. Giacca, M. and S. Zacchigna, *Virus-mediated gene delivery for human gene therapy.* J Control Release, 2012. **161**(2): p. 377-88.
17. Yang, B., et al., *Partial correction of the urinary concentrating defect in aquaporin-1 null mice by adenovirus-mediated gene delivery.* Hum Gene Ther, 2000. **11**(4): p. 567-75.
18. Saydaminova, K., et al., *Efficient genome editing in hematopoietic stem cells with helper-dependent Ad5/35 vectors expressing site-specific endonucleases under microRNA regulation.* Mol Ther Methods Clin Dev, 2015. **1**: p. 14057.
19. Li, C. and A. Lieber, *Adenovirus vectors in hematopoietic stem cell genome editing.* FEBS Lett, 2019. **593**(24): p. 3623-3648.
20. Nakamura, S., et al., *Improvement of hydrodynamics-based gene transfer of nonviral DNA targeted to murine hepatocytes.* Biomed Res Int, 2013. **2013**: p. 928790.
21. Duffy, M.R., et al., *Manipulation of adenovirus interactions with host factors for gene therapy applications.* Nanomedicine (Lond), 2012. **7**(2): p. 271-88.

22. Yamano, S., et al., *Long-term efficient gene delivery using polyethylenimine with modified Tat peptide.* Biomaterials, 2014. **35**(5): p. 1705-15.
23. Hendel, A., et al., *Chemically modified guide RNAs enhance CRISPR-Cas genome editing in human primary cells.* Nat Biotechnol, 2015. **33**(9): p. 985-989.
24. Farboud, B., et al., *Enhanced Genome Editing with Cas9 Ribonucleoprotein in Diverse Cells and Organisms.* J Vis Exp, 2018(135).

SUPPLEMENTAL FILES

Supplementary TABLE 1. Sequence of the repair construct and gRNAs for CRISPR-HITI approach

	Sequence (5' → 3')	Description
Target sequence in both ciPTEC and HEK-293 cells	CAGCGGGAGCGGGGCGGTGGGGAGGCCAG CCTGCCGCTCTTCCCCCGGGGCTGGAATCA CAGGAGATCGCTAGCGGAGGCCCCTTGGACC CCACGCTCCCCTAAGCATCAGGTGTGCGGGTG GTTCCCCTTCTCCACACCCCAGCCTTTCCTGAT GCCTTTGGCTCTGCCCTCACCACTGCCTCCAT TTCCACAGCAGGACACTCTGGAGAGGTGAGGT GGGAGGAGGGAGCCCCTTCCCGCGCAGAGCTC AG**C**CCGTCCTATGAGCATAGCCGGT**C**CTCTTCAG ATCCGGGGACTCAGGGTCCAGCACATCTTGCCC CACAGCCTGGGACAGGGTCAGGGCTGAAGT TGCTGCACCCGGGGACCTAGGGCCTCATTTA ACTCACCCCATTCCCAAAGGGAGAAGCCTTG TTCCAGTGCCCCCAGCCCTGGGAGCCTCGTGT TCTGTGAGCTCAGGAGGGCCAGCGTTCTGA CTGGGAGGCAGGACTGGACTCTTAGGCTGA GCAGGACTAAGTTCTGTGGCCAAGGAGCCCGG GCGTTCCGGGCCAGGCCAGCCTGCACAGAGG CTGGGGCGGGACACGGGGCGGCAGTGAGGGG ATGTGGCTGGTTGAACAGTGTTGAGCATGTTG AAGCTGGGA	Obtained from sanger sequencing
Repair construct	GATCGCCTCCGCTAGCGATCTCCTGTGAGATC GGACCGGCTATGCTCATAGGACGGGGTCACC CAGTCAGAACGCTGGCCCTCCCATGccggctat aggcggagaggcggcggaaggcgggacctaaaggggg ccccgccccacgggctctgatttccgcccaatggagggcg gtctgagcttcgctcacgaaaggagccgggaggcgctgg cggctccaagagtctctgtgtccctggcagcggacctcatc ttccctcacgccggagccccgatctctgcgccccggcccga cccagctgcgctctgtccgtctaagacgc gcggaaactacaactcccagagctcatctcgccgagatcc ggccccacgagtcaggtggcggaggtcaggtgacagcgg acccgcctctcccaaagtctagccgggcaggggaacgcg gtgcattcctgaccggcacctggcgaggctcatgcgtcccg tgagggcggttcctcgagcctgggggcgctcagattgcttt ggagacgctgagagaacctttgcgagagcgccggttgacg tgcggagtgcggggctccgggggactgagcagcacgaga ccccatcctccccctccgggttttcacactgggcgaagggag gactcctgagctctgcctcttccagtaac attgaggattactgtgttttgtgagagctcgctaggcgccct aagcaacagagttctgagaaatcgagaaacATGATAA GGAATTGGCTGACTATTTTTATCCTTTTTCCCC	Cloned into the pUC57 plasmid Yellow = Spacer modification to alter repeat sequences and palindromic sites. Blue = The sequence matching the gRNA. Red = PAM sequence. Green (lower case) = The promotor region. Green (upper case) = The SuperExon region Black = UTR associated with the promotor plus a splice factor region.

Supplementary TABLE 1. Continued.

	Sequence (5' → 3')	Description
	TGAAGCTCGTAGAGAAATGTGAGTCAAGCGT CAGCCTCACTGTTCCTCCTGTCGTAAAGCTG GAGAACGGCAGCTCGACCAACGTCAGCCTC ACCCTGCGGCCACCATTAAATGCAACCCTGG TGATCACTTTTGAAATCACATTTCGTTCCAAA AATATTACTATCCTTGAGCTCCCCGATGAAGT TGTGGTGCCTCCTGGAGTGACAAACTCCTC TTTTCAAGTGACATCTCAAAATGTTGGACAAC TTACTGTTTATCTACATGGAAATCACTCCAATC AGACCGGCCCGAGGATACGCTTTCTTGTGATC CGCAGCAGCGCCATTAGCATCATAAACCAGGT GATTGGCTGGATCTACTTTGTGGCCTGGTCCA TCTCCTTCTACCCTCAGGTGATCATGAATTGG AGGCGGAAAAGTGTCATTGGTCTGAGCTTC GACTTCGTGGCTCTGAACCTGACGGGCTTCG TGGCCTACAGTGTATTCAACATCGGCCTCCTC TGGGTGCCCTACATCAAGGAGCAGTTTCTCCT CAAATACCCCAACGGAGTGAACCCCGTGAAC AGCAACGACGTCTTCTTCAGCCTGCACGCGGT TGTCCTCACGCTGATCATCATCGTGCAGTGCTG CCTGTATGAGCGCGGTGGCCAGCGCGTGTCCT GGCCTGCCATCGGCTTCCTGGTGCTCGCGTGGC TCTTCGCATTTGTCACCATGATCGTGGCTGCAGT GGGAGTGACCACGTGGCTGCAGTTTCTCTTCTG CTTCTCCTACATCAAGCTCGCAGTCACGCTGGTCA AGTATTTTCCACAGGCCTACATGAACTTTTACTAC AAAAGCACTGAGGGCTGGAGCATTGGCAACGTGC TCCTGGACTTCACCGGGGGCAGCTTCAGCCTCC TGCAGATGTTCCTCCAGTCCTACAACAACGgtacc tccagggccctgttcacatggccggtggcaggagaggtgaga gctacatggcccaggccctgctccggtggggcagctcctgcc ggcgtgaggaaacaggacggaaagccacagggagcccggg agcccagcgggagcggggcggtggggaggccagcctgcc gctcttcccccggggctggaaCCTCCGCTAGCGATCT CCTGTGAGATCGGACCGGCTATGCTCATAGGA CGGGGTCACCCAGTCAGAACGCTGGCCCTCC CATG	Green = primer sequence.
gRNA 1	GTCCTATGAGCATAGCCGGT	Cloned into the pSPCas9(BB)-2A-GFP plasmid expressing Cas9 protein.
gRNA 2	TCCTATGAGCATAGCCGGTC	
gRNA 3	GGAGGGCCAGCGTTCTGACT	

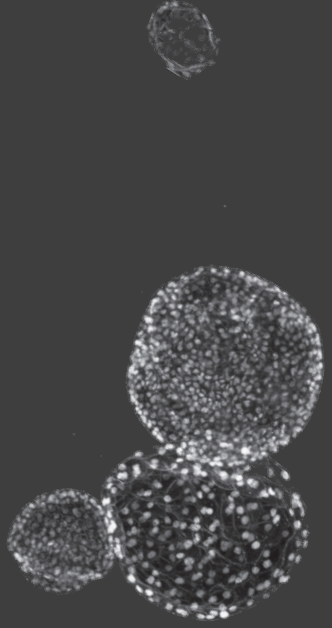

7

General discussion

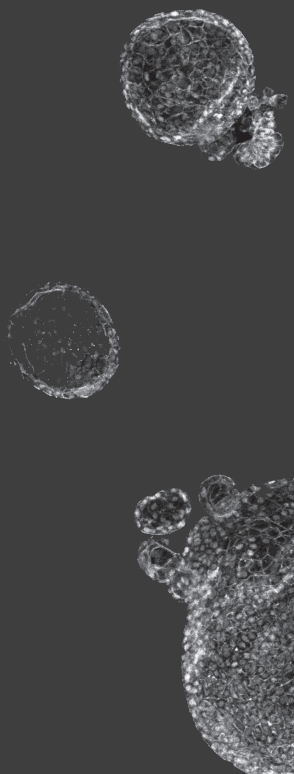

Over the last decades, the clinical outcomes of patients with infantile nephropathic cystinosis have changed from an early fatal disorder to a moderately manageable disease with most patients surviving into adulthood. This is mainly due to the wide availability of the cystine depleting agent, cysteamine and renal replacement therapy [1]. Cysteamine can efficiently lower the lysosomal cystine levels and postpone the disease progression. However, it poses serious side effects and does not correct the established proximal tubulopathy associated with nephropathic cystinosis [2, 3]. This could be explained by the complex pathophysiological processes involved in the development of the disease that may or may not be directly related to the cystine overload. Several studies based on *in vitro* and *in vivo* models have demonstrated that cystinosin loss-of-function is indeed associated with disrupted lysosomal autophagy dynamics [4], accumulation of distorted mitochondria [5, 6], and increased reactive oxygen species (ROS) levels [7], leading to abnormal proliferation and dysfunction of proximal tubule cells. This underscores the urgent need for the development of an enduring intervention to combat the disease. In the current thesis, a new CRISPR-mediated conditionally immortalized cystinotic human renal proximal tubule cells (ciPTEC) and primary adult stem cell-derived cystinotic tubuloids were developed and validated, which simulate the human proximal phenotype in many aspects and allow the discovery of novel pathophysiological mechanisms and therapeutic agents for the disease.

Development of new isogenic cystinotic *in vitro* models

Successful murine models for cystinosis have been developed and found valuable in unveiling the pathogenesis of cystinosis [8-11]. However, animal experiments are usually expensive, laborious and time-consuming, and more importantly, they do not fully represent the human situation. The currently available cystinotic rodent models often have mild, late onset renal phenotype and generally lack the signs of proximal tubulopathy [12]. Furthermore, unlike the human situation where treatment with cysteamine does not correct the renal phenotype and only improves some parts of the cystinotic phenotype [13], data from our collaborators at the Renal Diseases Research Unit at Bambino Gesù Children's Hospital (Rome) showed that cysteamine can completely resolve the renal symptoms in cystinotic mice. As a substitute for cystinotic mouse models, Elmonem *et al*. and Festa *el al*. utilized anti-sense morpholino or transcription activator-like effector nucleases technologies to develop two cystinotic zebrafish models, respectively [6, 14]. Both cystinotic zebrafish models demonstrated that cystinotic larvae have a cystinosis phenotype similar to the early disease manifestations in the human disease, and are valuable for high throughput screening of new treatments [6, 14, 15]. In spite of the many advantages of zebrafish in unravelling novel pathophysiological mechanisms, the model still has limitations that need to be taken into account. General limitations of zebrafish models include the retention of many duplicated genes that may code for similar proteins with similar functions [16]. Moreover, although cystine accumulation and impaired lysosome-autophagy pathways were observed in the cystinotic zebrafish model developed by Festa *el al*., the developing cystinotic zebrafish larvae displayed

normal morphology with no developmental defects or proximal tubular dysfunction [6]. It is also difficult to translate a therapeutic approach from zebrafish to mammals, due to different hemodynamics, physiology and the lack of some organs in zebrafish (such as lungs and mammary glands) [17, 18].

The pioneering studies that extended our understanding of the pathogenesis of cystinosis is largely based on *in vitro* cell models. Cystinotic patient-derived ciPTEC, have proven to recapitulate multiple features of cystinosis [19-22]. CiPTEC are a well-established human proximal tubule cell lines, characterized by expression of all relevant drug transporters, and protein reabsorption machinery vital for proximal tubular function [23-25]. However, the different genetic backgrounds of cystinotic ciPTEC limits their comparison to control ciPTEC. Thus, to unravel the circuitry behind cystinosis pathogenesis and screen for new therapeutic strategies, availability of cystinotic cells and their healthy isogenic controls is a pre-requisite. Recent advances in targeted gene editing using the CRISPR/Cas9 system has enabled a rapid and precise genetic manipulation without alterations to the genome [26, 27]. The technique is notably easy and effective in completely knocking out one or multiple genes and creating new animal and cell models [28-31]. In chapter 4, we have utilized CRISPR/Cas9 technology and created isogenic cystinotic ciPTEC [32]. The model exhibited robust cystinotic phenotypes of increased cystine accumulation as measured by a sensitive LC-MS/MS method developed in chapter 3, reduced mTOR activation, delayed protein degradation and an increase in baseline ROS levels. Moreover, proteomic and metabolomic profiling revealed that CRISPR-generated ciPTEC are a reliable isogenic cystinosis model of healthy control cells, allowing the correct evaluation of *CTNS* loss in our cell model [32].

Kidney organoids are yet another advanced *in vitro* model that offer physiological heterogeneity and recapitulate the *in vivo* situation. They are three dimensional (3D) renal tubule epithelial cultures, allowing neighbouring cells to interact in a more physiological way than in conventional 2D culture models. Hollywood *et al*. was first to generate and characterize human induced pluripotent stem cell and kidney organoid models of cystinosis [33]. The model demonstrated a cystinosis phenotype of large lysosomes with activated autophagy (due to cystine load), which were resolved by treatment with the combination of an mTOR pathway inhibitor, everolimus and cysteamine [33]. We, on the other hand, developed primary adult stem cell-derived cystinotic tubuloids from urine samples of pediatric cystinotic patients [32]. The advantages of this model are that they are not genetically modified or reprogrammed, can accurately mimic patients genotype and phenotype, and recapitulate renewal and repair in the adult kidney tubule allowing to develop personalized medicine strategies [34, 35].

Multifaceted effect of cystinosin loss in cystinosis

Over the past years, several studies have demonstrated that the loss of cystinosin is correlated with disrupted lysosomal-autophagy dynamics, increased oxidative stress, and delayed protein degradation, greatly extending our understanding of cystinosis pathology beyond lysosomal cystine accumulation [6, 7, 22, 36-41].

Autophagy is a highly conserved biological mechanism by which long-lived or dysfunctional organelles are degraded via the lysosomal pathway, thereby maintaining cellular homeostasis [42]. The nutrient sensor mammalian target of rapamycin complex 1 (mTORC1) is the fundamental coordinator of autophagy [43]. In the presence of amino acids, mTORC1 is bound to lysosomes and is active, triggering protein synthesis and inhibiting autophagy. Under amino acid starvation, however, mTORC1 is inactivated which activates autophagy to supply nutrients and comply with cellular energy demands [44]. It has been reported that defective cystinosin induces abnormal autophagy activation [22, 44-49]. Indeed, Ivanova *et al.* observed that cystinosin loss-of-function in human proximal tubule cells was associated with decreased retention of mTOR on the lysosomal membrane, and therefore defective mTOR signaling [47]. Accordingly, a decreased mTOR activity was also observed in proximal tubule cells derived from cystinotic mice [46]. mTOR also physically interacts with transcription factor EB (TFEB), a protein regulating lysosomal biogenesis and autophagy related gene expression [20, 50]. Lysosomal-dissipated mTOR is unable to phosphorylate TFEB, resulting in increased TFEB nuclear translocation and therefore induction of autophagic gene expression [51]. In line with the defective mTOR activity and aberrant autophagy activation, Rega *et al*. demonstrated increased TFEB nuclear translocation in cystinotic ciPTEC [20]. Similarly, we showed an increased autophagy activation, presented by decreased retention of mTOR on the lysosomal membrane, increased TFEB nuclear translocation and increased LC3-II accumulation in CRISPR-generated and patient-derived cystinotic ciPTEC. Using omics technologies, we have also identified that the elevated levels of alpha-ketoglutarate (αKG) found in cystinotic ciPTEC and in plasma of cystinotic patients could be the link bridging cystinosin loss to autophagy activation. Overall, αKG, a tricarboxylic acid cycle (TCA) metabolite, is regarded as a key regulator of apoptosis and autophagy processes [32, 48, 49, 52, 53]. αKG was shown as a health promoting metabolite, attenuating liver fibrosis [54], increasing life span and delaying age-related disease in *Caenorhabditis elegans* or mice [55, 56]. Villar *et al.* also showed that αKG inhibits autophagy and induces glutaminolysis-mediated apoptosis during starvation in cancer cells [53]. Moreover, αKG is a well-known antioxidant and its cellular levels can be elevated in response to oxidative stress, contributing to the prevention or treatment of several disorders induced by such stresses [57-59]. Intracellular levels of αKG are upregulated through downregulation of the mitochondrial enzyme alpha-ketoglutarate dehydrogenase (AKGDH), reported to be severely diminished in disorders where oxidative stress plays a major role [59]. Studies on neurons have shown that oxidative stress-induced decreased activity of AKGDH may cause prominent alterations in intracellular autophagic/apoptotic signaling [60-62]. Indeed, we found a decreased expression of AKGDH in cystinotic cells, further confirming the established link between cystinosin loss-of-function and increased oxidative stress and autophagy activation in cystinosis [7, 36-38].

While several reports show an abnormal induction of autophagy in cystinosis, the accumulation of the autophagy substrate SQSTM1 and the decreased lysosomal cargo processing postulate the lack of autophagy completion in cystinosis. This is in

agreement with the reports demonstrating an impairment of autophagy flux in many lysosomal storage diseases (LSDs), including cystinosis [33, 40, 41]. Festa *et al*. provided evidence that *CTNS* loss affects lysosomal function by inhibiting the maturation of the lysosomal enzymes in *in vitro and in vivo* models of cystinosis [6]. Consistent with the reduced cargo degradation in cystinotic cells, we also found an overall reduction in lysosomal catalytic-proteins expression including, lysosomal acid lipase, lysosomal acid phosphatase, and cysteine proteases cathepsin. Moreover, cation-independent mannose 6-phosphate receptor (IGF2R) was found downregulated in cystinotic ciPTEC. IGF2R is responsible for the delivery of many newly synthesised lysosomal enzymes from Golgi to the lysosome, and its downregulation results in decreased lysosomal activity [63, 64]. mTOR inhibition has been found to resolve the impaired autophagic flux observed in cystinotic cells. Utilizing recently developed human induced pluripotent stem cell and kidney organoid models of cystinosis, Hollywood *et al.* showed that an mTOR inhibitor (everolimus) reduces the large lysosomes and activated autophagy, and in combination with cysteamine normalizes the cystine load [33].

Recently, studies have also shown that apart from lysosomal malfunctions, LSDs pathology is associated with mitochondrial abnormalities, signifying the mitochondria-lysosomes crosstalk in these diseases. The role of mitochondria in cystinosis pathology has also gained much attention. Sansanwal *et al.* described fewer mitochondria and abnormal mitochondrial morphology in cystinotic fibroblast and proximal tubular cells [5]. Accordingly, Bellomo *et al.* found a significant decrease in complex I and IV activity with lower cAMP levels in cystinotic ciPTEC [65]. Proteins involved in mitochondrial fusion and fission were found to be dysregulated resulting in decreased mitochondrial cristae number and an increase of cristae lumen and cristae junction width in cystinotic ciPTEC [66]. Using omics technologies, we also demonstrated an overall decrease in expression of mitochondrial enzymes and increased levels of αKG in cystinotic ciPTEC. Similar to cystinosis, the effects of lysosomal malfunction on mitochondrial clearance, function and biogenesis has also been demonstrated in other LSDs (Table 1). So far, several mitochondrial targeted antioxidants have been developed as a new avenue for potential treatment of cystinosis. Mitoquinone, a mitochondrial targeted antioxidant, was shown to delay the initiation of swan neck lesions in cystinotic mice [67]. Mito_TEMPO, yet another mitochondrial targeted antioxidant, restored mitochondrial integrity and transport function in cystinotic proximal tubular cells and mice [6]. Therefore, unravelling the role of mitochondria in the progression of LSDs can further result in the development of potential new therapies.

TABLE 1. List of lysosomal storage diseases having mitochondrial abnormalities.

LSDs	Inheritance pattern	Mutation type	Lysosomal Phenotype	Mitochondrial Phenotype	Ref
Niemann-Pick Disease	Autosomal recessive	NPA & NPB: *SMPD1* NPC: *NPC1, NPC2*	lipid accumulation in the lysosomes of various tissues	Downregulation of mitochondrial genes, impaired mitophagy, mitochondrial fragmentation	[109-111]
Gaucher Disease	Autosomal recessive	*GBA1*	lysosomal aggregation of glucosylceramide	Mitochondrial enlargement, decreased mitochondrial membrane potential	[112, 113]
Fabry Disease	X-linked, neither recessive nor dominant	*GLA*	Lysosomal accumulation of globotriaosylceramide	Decreased mitochondrial membrane potential, malfunctional respiratory chain enzymes, abnormal mitochondrial morphology	[114, 115]
GM1-gangliosidosis	Autosomal recessive	*GLB1*	Elevated intralysosomal GM1-ganglioside levels	Decreased mitochondrial membrane potential, mitochondrial deformities, increased permeabilization of the mitochondrial membrane, malfunctioning cytochrome c oxidase	[116-118]
Mucopolysaccharidoses	Autosomal recessive	MPS I: *IDUA*	Lysosomal accumulation of glycosaminoglycans	Fewer mitochondria, fewer cristae, mitochondrial enlargement,	[119, 120]
	X-linked recessive	MPS II: *IDS*			
	Autosomal recessive	MPS VII: *GUSB*			

TABLE 1. Continued.

LSDs	Inheritance pattern	Mutation type	Lysosomal Phenotype	Mitochondrial Phenotype	Ref
Mucolipidoses I-III	Autosomal recessive	ML I: *NEU1* ML II α/β: *GNPTAB* ML III α/β: *GNPTAB* ML III γ: *GNPTG*	Cellular buildup of carbohydrates and lipids	Abnormal mitochondrial morphology, increased mitochondrial fragmentation,	[121, 122]
Mucolipodosis IV	Autosomal recessive	*MCOLN1*	Accumulation of mucopolysaccharides, phospholipids and sphingolipids	Mitochondrial fragmentation, aggregation of degraded mitochondria in autophagosomes/autolysosomes, fewer cristae, lower mitochondrial membrane potential	[123, 124]

Link between cystinosin and lysosomal ATP6V1B1

Lysosomal vacuolar H^+-ATPase (V-ATPase) are large multisubunit complexes that utilize the energy derived from the hydrolysis of cytosolic ATP to transport protons across biological membranes and maintain the acidic pH of endocytic and secretory organelles [68, 69]. They are ubiquitously distributed on intracellular tubulo-vesicular membranes, and at the plasma membrane in specialized cell types. The ATP6V1B1 is the B1 subunit of the lysosomal V-ATPase and its loss-of-function leads to autosomal recessive distal renal tubular acidosis (dRTA) with sensorineural deafness [70, 71]. As described in chapter 5, a 23-month-old girl with mutations in *ATP6V1B1* presented with metabolic acidosis as well as features of cystinosis-like phenotype including increased granulocyte cystine levels and renal Fanconi syndrome. This finding postulated a possible link between *ATP6V1B1* gene deficiency and proximal tubulopathy in cystinosis.

Cystinosin is a H^+/cystine symporter that depends on lysosomal H^+ influx mediated by the lysosomal V-ATPase to transport cystine to the cytoplasm [72]. Besides this chemiosmotic coupling, both cystinosin and the V-ATPase-Ragulator-Rag Complex closely interact with mTORC1, regulating autophagy [4, 6, 73]. Multiple variants of V-ATPases, on the other hand, have also found to regulate TFEB [50], whose function is also impaired in cystinosis [20]. We revealed that ATP6V1B1 is indeed expressed in human renal proximal tubular epithelial cells and its loss could have similar effects on the cells as *CTNS* loss. In line with the clinical findings, the *ATP6V1B1* gene defect in proximal tubule cells

disrupted the chemiosmotic coupling between the lysosomal V-ATPase B1 subunit and cystinosin and resulted in a cystinosis like phenotype of increased lysosomal cystine accumulation and autophagy activation. We also provided evidence that the increased autophagy activation in cystinotic cells could be a direct result of the decreased activity of ATP6V1B1, disabling mTOR recruitment to the lysosomes and subsequent deactivation of mTOR signaling. This was further supported by downregulation of Ragulator complex protein LAMTOR1 and LAMP1 in both *ATP6V1B1* and *CTNS* deficient cells. LAMTOR1 as a part of V-ATPase-Ragulator-Rag Complex is required for recruitment of mTORC1 on the lysosomal membrane and its consequent activation. Depletion in LAMTOR1 prevents mTOR shuttling to the lysosomal surface, resulting in autophagy activation [74, 75].

Pharmacological treatments for nephropathic cystinosis

Currently, cysteamine is the one and only treatment available for the patients with cystinosis [76]. In lysosomes, cysteamine reacts with cystine, leading to the formation of cysteine and cysteine-cysteamine molecules which are exported out of lysosomes via their respective carriers [76, 77]. Cysteamine efficiently lowers lysosomal cystine and improves the clinical outcomes, however, it does not reverse established renal Fanconi syndrome, suggesting multiple roles for cystinosin, beyond the export of cystine. Downregulation of mTOR, decreased TFEB activity, and abnormal autophagy induction, together with impaired energy metabolism and increased oxidative stress, have been reported in cystinosis presenting new avenues for potential treatments [78]. Recently, several small molecules and biologics correcting non-transport functions of cystinosin have emerged and have shown to be effective either alone or in combination with cysteamine in *in vitro* and *in vivo* models of cystinosis as summarized in chapter 2.
Studies have demonstrated that increasing TFEB activity can be beneficial in stimulating lysosomal excretion and rescuing the delayed endocytic cargo processing in many LSDs [41]. Indeed, Rega *et al*. have shown that the stimulation of endogenous TFEB activity by genistein lowers cystine accumulation and rescues the delayed lysosomal cargo processing in cystinotic proximal tubule cells [20]. Furthermore, inhibition of mTOR signalling by everolimus was shown to activate autophagy, resolve large lysosomes, and in combination with cysteamine, reverse the cystine load in induced pluripotent stem cells and kidney organoids [79]. Accordingly, we have shown that bicalutamide, a non-steroidal anti-androgenic agent, increases endogenous TFEB activity and restores endocytic cargo processing, and in combination with cysteamine, reverses the proteome and metabolic phenotype and efficiently normalizes cystine levels in cystinotic proximal tubule cells. The combination therapy was also found to be beneficial in both patient-derived kidney tubuloids and cystinotic zebrafish, proposing the therapeutic potential of this combination therapy in treating patients with cystinosis [32]. Of note, great care must be taken on interpreting the beneficial effect of these emerging therapies. The multiple effects of these treatment on different molecular pathways can provoke safety issue during long-term exposure in patients. For instance, in the case of genistein, the prolonged activation of TFEB may further exacerbate the inhibition of mTOR signaling

already existing in cystinotic cells [46]. Similarly, bicalutamide as an anti-androgenic agent is also known to reduce testosterone levels [80, 81], which could complicate the beneficial effect of bicalutamide in cystinotic male patients with delayed maturation [82-84]. Interestingly, bicalutamide is a racemate and its hormonal effect is attributed solely to the (R)-enantiomer, while the (S)-enantiomer mediating autophagy effects [85, 86]. Therefore, it would be of great scientific benefit to further assess the effect of (S)-bicalutamide and/or develop any structural analogues for testing in *in vitro* and *in vivo* models of cystinosis.

Translational Read-Through-Inducing Drugs (TRIDs) have also emerged recently as a new therapeutic approach for cystinosis. TRIDS are able to insert aminoacyl-transfer RNAs and inhibit translation termination at the premature stop codon, thereby restoring the full-length mRNA and protein [87]. Indeed, Brasell *et al.* showed that geneticin, an aminoglycoside-based TRID, restores the production of functional cystinosin, and lowers cystine accumulation in patient fibroblasts with the nonsense mutation [88]. However, the treatment is limited only to cystinotic patients with nonsense mutations.

Gene therapy in cystinosis

Cystinosis is a monogenic disorder and a functional *CTNS* gene transfer could have the potential to reverse the cystinotic phenotype. Hematopoietic stem and progenitor cells have the ability to engraft in the damaged tissues and transfer the functional gene to the neighboring cells, allowing the treatment of multisystemic non-hematological disorders [89]. Syres *et al.* was first to observe a large quantity of wild-type bone marrow cells (BMCs) in multiple organs of cystinotic mice, resulting in lowering organ-specific cystine levels in BMC-treated cystinotic mice. Renal dysfunction and corneal cystine deposition were also corrected. Similarly, transplantation of cystinotic mice with wild-type hematopoietic stem cell (HSCs) resulted in similar beneficial effects [90]. Gaide Chevronnay *et al.*, also highlighted the potential multisystemic benefits of HSCs transplantation in cystinotic mice, normalizing thyroid function [91]. Given the promising preclinical outcomes of HSCs transplantation in cystinosis, Elmonem *et al.* recently transplanted and validated allogeneic HSCs in a 16-year-old infantile nephropathic cystinotic patient who was intolerant to cysteamine therapy [92]. The treatment resulted in successful transfer of wild-type cystinosin RNA and protein to epithelial tissues of multiple organs and reduced tissue cystine-crystal and signs of clinical improvement of renal and ocular cystinosis. However, the patient developed early signs of tacrolimus-mediated toxicity, systemic infection with multiple drug resistant pseudomonas, and severe graft-versus-host-disease which ultimately led to the death of this patient. Hence, despite the potential of HSCs transplantation for treatment of cystinotic patients, the associated risks and mortality of allogenic HSCT must be considered carefully and weighed against the benefits.

Viral vector-mediated gene therapy is yet one of the most promising treatment options for many inherited diseases. In fact, clinical trials using such technology have demonstrated remarkable therapeutic benefits in many diseases [93]. Hippert *et al.* evaluated a direct *in vivo* gene therapy strategy using an adenoviral-based vector to transduce liver cells

in cystinotic mice [94]. The advantage of this approach is that various organs and tissues can be directly targeted and, if successful, their function can be restored. However, the major limitations of this method are limited control over transgene expression levels, their copy numbers and risk of adverse events (*e.g*. insertional mutagenesis or activation of (proto)-oncogenes) [93]. Moreover, the duration of the therapeutic benefit is also unpredictable, especially when non-integrating viral-vectors are used. For instance, the first results of a clinical trial for Leber's congenital amaurosis, a loss of vision disease, showed that subretinal delivery of transgenes using non-integrating adeno-associated virus vector was safe and showed therapeutic efficacy in restoring human visual function [95, 96]. However, follow-up studies from the same and other groups demonstrated that the initial gains in retinal sensitivity declined over time, resulting in loss of meaningful improvements in visual function [97, 98]. These data show that, although non-integrating vector-based gene therapy is safe and beneficial during the initial stage of treatment, the therapeutic effects may not be permanent. Furthermore, such strategy cannot be used to treat gain-of-function genetic variants.

Recent advances in the targeted genome-editing via engineered nucleases have revolutionized methods for generating novel genetic resources that hold potentials for clinical applications. The homology-directed repair (HDR) represents the most promising way of overcoming limitations of current gene replacement therapies. This technique can be exploited to realize site-specific transgene integration and to replace both loss-of-function and gain-of-function alleles with wild-type sequences [99-101]. However, the use of HDR-based approaches is limited by their low efficiency in inserting large DNA fragments in most cell types. Moreover, HDR only occurs during the S/G2 phases of the cell cycle, making it unsuitable for use in non-dividing cells that are prevalent in post-natal tissues [102, 103]. The non-homologous end joining (NHEJ) is yet another major DNA repair pathway that ligates DNA ends directly and is active throughout the cell cycle in a large variety of adult cells [104]. In addition, in most higher organisms, NHEJ activity far exceeds HDR activity in inserting large DNA fragments [104]. These advantages signify that harnessing the NHEJ-based knock-in may represent a viable way of overcoming technical hurdles associated with HDR-based gene therapy. In 2016, Suzuki *et al.* created a fundamentally improved NHEJ-based transgene integration (CRISPR-HITI) system and showed that the targeted knock-in is 10 times higher than that of the HDR-based method [105]. Moreover, the targeted genes were free of indels, demonstrating the error-free tendency of this technique. Accordingly, Auer *et al*., reported the successful use of CRISPR-HITI in integrating a 5.7kb gene repair construct into the genome of zebrafish at a very high rate [106]. The study reported CRISPR-HITI as an easy, feasible, simple, and highly efficient method for gene editing. In chapter 6, CRISPR-HITI was applied to restore *CTNS* function in cystinotic ciPTEC. The most common mutation in cystinotic patients is a large genomic deletion (57kb) resulting in loss of exons 1-10 of the *CTNS* gene [107]. To restore *CTNS* function, we constructed a DNA insert containing the endogenous *CTNS* promotor and cDNA sequence of exons 1-10, flanked by target-specific guide RNAs. The gRNAs were designed to target upstream exon 11, after the breaking point. In cystinotic

ciPTEC, co-transfection of Cas 9 and the gRNAs with the repair construct did not result in a detectable incorporation of the donor DNA into the cells' genome. This could be mainly due to low transfection efficiency in ciPTEC (max. 25%). As proof-of-concept, we tested our strategy in HEK-293 cells, the gold standard cell model to study gene therapy. HEK-293 cells indeed had a higher transfection efficiency (60-70%) and co-transfection of the gRNAs with the repair construct resulted in a successful insertion of donor DNA into the genome of HEK-cells. Optimizing the transfection efficiency could improve the repair efficiency and, therefore, restore *CTNS* function in cystinotic ciPTEC. To improve repair efficiency, mechanistic studies to increase transfection efficiency and to identify the major regulators of HITI activity are a prerequisite. We believe that this technique will not only serve as a proof-of-principle for future gene and/or cell-based therapies, but also might provide a long-lasting cure for patients with cystinosis.

Future perspectives

Nephropathic cystinosis is the prototype disease for lysosomal transporter defects and is the leading cause of inherited renal Fanconi syndrome in young children. Although early initiation and adequate adherence to cysteamine therapy is associated with increased life expectancy, cystinotic patients still suffer from the complications of the disease at a later stage of life including renal failure and the complications associated with renal replacement therapies like transplantation or dialysis.

Until recently, many small molecules and biologics correcting non-transport functions of cystinosin are introduced and have shown to be effective either alone or in combination with cysteamine *in vitro*. To evaluate the therapeutic potential of these therapies and bring them one step closer to the clinic, pre-clinical testing in a rodent model of cystinosis is required. The CRISPR/Cas9-mediated genome editing shows incredible promise as a tool for studying gene function and to create new *in vitro* and *in vivo* disease models. Recently, a new CRISPR-mediated cystinotic rat model was developed and validated at Department of Molecular Medicine and Pathology, University of Auckland, New Zealand (J.A. Hollywood, personal communication), which offers the promise of faithfully recapitulating the human disease and facilitating the safety and efficacy testing of new combination treatment regimens.

Effective treatment, however, will require early detection and intervention. This is a challenge everywhere and is only expected to fundamentally change once detection of cystinosis can be included in the new born screening programs. In addition, a well-organized metabolomics search for identifying the perfect biomarker(s) in the blood or urine of cystinotic patients should be undertaken. Elmonem *et al*. have recently identified the increased plasma chitotriosidase activity (an enzyme activated during inflammation), as a promising candidates for the evaluation of disease severity and response to treatment [108]. Further, identifying and assessing other biochemical markers, including αKG could also be beneficial in the disease monitoring. The fact that αKG level is increased in plasma of cystinotic patients, makes it a very promising biomarker for monitoring cystinosis and

other diseases that are associated with proximal tubulopathy. However, this requires further validation process in future.

In conclusion, cystinosis is a rare LSD with limited therapeutic options that do not meet the demand of ameliorating patients' life quality. In this thesis, detailed insights into multi-facets of nephropathic cystinosis were provided, including new concepts in disease pathophysiology and novel *in vitro* models that will be used for further unravelling the pathogenesis and for validating new therapeutic strategies. The use of the model together with a drug screen revealed a bicalutamide-cysteamine combination treatment as a novel dual target pharmacological approach, which holds a great potential to treat patients with cystinosis. These findings provide an important platform upon which we can build and efficiently translate the results into preclinical studies and hopefully provide a better management protocols for cystinotic patients in near future.

REFERENCES

1. Nesterova, G. and W.A. Gahl, *Cystinosis: the evolution of a treatable disease.* Pediatr Nephrol, 2013. **28**(1): p. 51-9.
2. Brodin-Sartorius, A., et al., *Cysteamine therapy delays the progression of nephropathic cystinosis in late adolescents and adults.* Kidney Int, 2012. **81**(2): p. 179-89.
3. Gahl, W.A., J.G. Thoene, and J.A. Schneider, *Cystinosis.* N Engl J Med, 2002. **347**(2): p. 111-21.
4. Sansanwal, P. and M.M. Sarwal, *p62/SQSTM1 prominently accumulates in renal proximal tubules in nephropathic cystinosis.* Pediatr Nephrol, 2012. **27**(11): p. 2137-2144.
5. Sansanwal, P., et al., *Mitochondrial autophagy promotes cellular injury in nephropathic cystinosis.* J Am Soc Nephrol, 2010. **21**(2): p. 272-83.
6. Festa, B.P., et al., *Impaired autophagy bridges lysosomal storage disease and epithelial dysfunction in the kidney.* Nat Commun, 2018. **9**(1): p. 161.
7. Levtchenko, E., et al., *Altered status of glutathione and its metabolites in cystinotic cells.* Nephrol Dial Transplant, 2005. **20**(9): p. 1828-32.
8. Gaide Chevronnay, H.P., et al., *Time course of pathogenic and adaptation mechanisms in cystinotic mouse kidneys.* J Am Soc Nephrol, 2014. **25**(6): p. 1256-69.
9. Gaide Chevronnay, H.P., et al., *A mouse model suggests two mechanisms for thyroid alterations in infantile cystinosis: decreased thyroglobulin synthesis due to endoplasmic reticulum stress/unfolded protein response and impaired lysosomal processing.* Endocrinology, 2015. **156**(6): p. 2349-64.
10. Johnson, J.L., et al., *Upregulation of the Rab27a-dependent trafficking and secretory mechanisms improves lysosomal transport, alleviates endoplasmic reticulum stress, and reduces lysosome overload in cystinosis.* Mol Cell Biol, 2013. **33**(15): p. 2950-62.
11. Napolitano, G., et al., *Impairment of chaperone-mediated autophagy leads to selective lysosomal degradation defects in the lysosomal storage disease cystinosis.* EMBO Mol Med, 2015. **7**(2): p. 158-74.
12. Cherqui, S., et al., *Intralysosomal cystine accumulation in mice lacking cystinosin, the protein defective in cystinosis.* Mol Cell Biol, 2002. **22**(21): p. 7622-32.
13. Cherqui, S., *Cysteamine therapy: a treatment for cystinosis, not a cure.* Kidney Int, 2012. **81**(2): p. 127-9.
14. Elmonem, M.A., et al., *Cystinosis (ctns) zebrafish mutant shows pronephric glomerular and tubular dysfunction.* Sci Rep, 2017. **7**: p. 42583.
15. Outtandy, P., et al., *Zebrafish as a model for kidney function and disease.* Pediatric Nephrology, 2018.
16. Howe, K., et al., *The zebrafish reference genome sequence and its relationship to the human genome.* Nature, 2013. **496**(7446): p. 498-503.
17. Vliegenthart, A.D., et al., *Zebrafish as model organisms for studying drug-induced liver injury.* Br J Clin Pharmacol, 2014. **78**(6): p. 1217-27.
18. Santoriello, C. and L.I. Zon, *Hooked! Modeling human disease in zebrafish.* J Clin Invest, 2012. **122**(7): p. 2337-43.
19. Wilmer, M.J., F. Emma, and E.N. Levtchenko, *The pathogenesis of cystinosis: mechanisms beyond cystine accumulation.* Am J Physiol Renal Physiol, 2010. **299**(5): p. F905-16.

20. Rega, L.R., et al., *Activation of the transcription factor EB rescues lysosomal abnormalities in cystinotic kidney cells.* Kidney Int, 2016. **89**(4): p. 862-73.
21. Bellomo, F., et al., *Impact of atypical mitochondrial cyclic-AMP level in nephropathic cystinosis.* Cell Mol Life Sci, 2018.
22. Ivanova, E.A., et al., *Endo-lysosomal dysfunction in human proximal tubular epithelial cells deficient for lysosomal cystine transporter cystinosin.* PLoS One, 2015. **10**(3): p. e0120998.
23. Caetano-Pinto, P., et al., *Fluorescence-Based Transport Assays Revisited in a Human Renal Proximal Tubule Cell Line.* Mol Pharm, 2016. **13**(3): p. 933-44.
24. Gorvin, C.M., et al., *Receptor-mediated endocytosis and endosomal acidification is impaired in proximal tubule epithelial cells of Dent disease patients.* Proc Natl Acad Sci U S A, 2013. **110**(17): p. 7014-9.
25. Jansen, J., et al., *A morphological and functional comparison of proximal tubule cell lines established from human urine and kidney tissue.* Exp Cell Res, 2014. **323**(1): p. 87-99.
26. Ran, F.A., et al., *Genome engineering using the CRISPR-Cas9 system.* Nat Protoc, 2013. **8**(11): p. 2281-2308.
27. Hsu, P.D., E.S. Lander, and F. Zhang, *Development and applications of CRISPR-Cas9 for genome engineering.* Cell, 2014. **157**(6): p. 1262-78.
28. Schokrpur, S., et al., *CRISPR-Mediated VHL Knockout Generates an Improved Model for Metastatic Renal Cell Carcinoma.* Sci Rep, 2016. **6**: p. 29032.
29. Ran, F.A., et al., *In vivo genome editing using Staphylococcus aureus Cas9.* Nature, 2015. **520**(7546): p. 186-91.
30. Wang, H., et al., *One-step generation of mice carrying mutations in multiple genes by CRISPR/Cas-mediated genome engineering.* Cell, 2013. **153**(4): p. 910-8.
31. Xue, W., et al., *CRISPR-mediated direct mutation of cancer genes in the mouse liver.* Nature, 2014. **514**(7522): p. 380-4.
32. Jamalpoor, A., et al., *Cysteamine-bicalutamide combination treatment restores alpha-ketoglutarate and corrects proximal tubule phenotype in cystinosis.* bioRxiv, 2020: p. 2020.02.10.941799.
33. Hollywood, J.A., et al., *Use of Human Induced Pluripotent Stem Cells and Kidney Organoids To Develop a Cysteamine/mTOR Inhibition Combination Therapy for Cystinosis.* J Am Soc Nephrol, 2020.
34. Schutgens, F., et al., *Tubuloids derived from human adult kidney and urine for personalized disease modeling.* Nat Biotechnol, 2019. **37**(3): p. 303-313.
35. Yousef Yengej, F.A., et al., *Kidney Organoids and Tubuloids.* Cells, 2020. **9**(6).
36. Wilmer, M.J., et al., *Cysteamine restores glutathione redox status in cultured cystinotic proximal tubular epithelial cells.* Biochim Biophys Acta, 2011. **1812**(6): p. 643-51.
37. Chol, M., et al., *Glutathione precursors replenish decreased glutathione pool in cystinotic cell lines.* Biochem Biophys Res Commun, 2004. **324**(1): p. 231-5.
38. Rizzo, C., et al., *Pyroglutamic aciduria and nephropathic cystinosis.* J Inherit Metab Dis, 1999. **22**(3): p. 224-6.
39. Raggi, C., et al., *Dedifferentiation and aberrations of the endolysosomal compartment characterize the early stage of nephropathic cystinosis.* Hum Mol Genet, 2014. **23**(9): p. 2266-78.
40. Settembre, C., et al., *A block of autophagy in lysosomal storage disorders.* Hum Mol Genet, 2008. **17**(1): p. 119-29.
41. Platt, F.M., B. Boland, and A.C. van der Spoel, *The cell biology of disease: lysosomal storage disorders: the cellular impact of lysosomal dysfunction.* J Cell Biol, 2012. **199**(5): p. 723-34.
42. Rabinowitz, J.D. and E. White, *Autophagy and metabolism.* Science, 2010. **330**(6009): p. 1344-8.

43. Jung, C.H., et al., *mTOR regulation of autophagy.* FEBS letters, 2010. **584**(7): p. 1287-1295.
44. Bar-Peled, L., et al., *An expanded Ragulator is a GEF for the Rag GTPases that signal amino acid levels to mTORC1.* Cell, 2012. **150**(6): p. 1196-1208.
45. Raggi, C., et al., *Dedifferentiation and aberrations of the endolysosomal compartment characterize the early stage of nephropathic cystinosis.* Human Molecular Genetics, 2013. **23**(9): p. 2266-2278.
46. Andrzejewska, Z., et al., *Cystinosin is a Component of the Vacuolar H(+)-ATPase-Ragulator-Rag Complex Controlling Mammalian Target of Rapamycin Complex 1 Signaling.* Journal of the American Society of Nephrology : JASN, 2016. **27**(6): p. 1678-1688.
47. Ivanova, E.A., et al., *Altered mTOR signalling in nephropathic cystinosis.* J Inherit Metab Dis, 2016. **39**(3): p. 457-464.
48. Tennant, D.A. and E. Gottlieb, *HIF prolyl hydroxylase-3 mediates alpha-ketoglutarate-induced apoptosis and tumor suppression.* Journal of Molecular Medicine, 2010. **88**(8): p. 839-849.
49. Tang, Z., et al., *Atg2A/B deficiency switches cytoprotective autophagy to non-canonical caspase-8 activation and apoptosis.* Cell Death Differ, 2017. **24**(12): p. 2127-2138.
50. Sardiello, M., et al., *A gene network regulating lysosomal biogenesis and function.* Science, 2009. **325**(5939): p. 473-7.
51. Yao, Z. and D.J. Klionsky, *The symphony of autophagy and calcium signaling.* Autophagy, 2015. **11**(7): p. 973-974.
52. Marino, G., et al., *Dimethyl alpha-ketoglutarate inhibits maladaptive autophagy in pressure overload-induced cardiomyopathy.* Autophagy, 2014. **10**(5): p. 930-2.
53. Villar, V.H., et al., *mTORC1 inhibition in cancer cells protects from glutaminolysis-mediated apoptosis during nutrient limitation.* Nat Commun, 2017. **8**: p. 14124.
54. Zhao, J., et al., *Dimethyl alpha-ketoglutarate reduces CCl4-induced liver fibrosis through inhibition of autophagy in hepatic stellate cells.* Biochem Biophys Res Commun, 2016. **481**(1-2): p. 90-96.
55. Su, Y., et al., *Alpha-ketoglutarate extends Drosophila lifespan by inhibiting mTOR and activating AMPK.* Aging (Albany NY), 2019. **11**(12): p. 4183-4197.
56. Chin, R.M., et al., *The metabolite alpha-ketoglutarate extends lifespan by inhibiting ATP synthase and TOR.* Nature, 2014. **510**(7505): p. 397-401.
57. Mailloux, R.J., et al., *Alpha-ketoglutarate dehydrogenase and glutamate dehydrogenase work in tandem to modulate the antioxidant alpha-ketoglutarate during oxidative stress in Pseudomonas fluorescens.* J Bacteriol, 2009. **191**(12): p. 3804-10.
58. Satpute, R.M., J. Hariharakrishnan, and R. Bhattacharya, *Effect of alpha-ketoglutarate and N-acetyl cysteine on cyanide-induced oxidative stress mediated cell death in PC12 cells.* Toxicol Ind Health, 2010. **26**(5): p. 297-308.
59. Starkov, A.A., *An update on the role of mitochondrial alpha-ketoglutarate dehydrogenase in oxidative stress.* Mol Cell Neurosci, 2013. **55**: p. 13-6.
60. Banerjee, K., et al., *Mild mitochondrial metabolic deficits by alpha-ketoglutarate dehydrogenase inhibition cause prominent changes in intracellular autophagic signaling: Potential role in the pathobiology of Alzheimer's disease.* Neurochem Int, 2016. **96**: p. 32-45.
61. Huang, H.M., et al., *Inhibition of alpha-ketoglutarate dehydrogenase complex promotes cytochrome c release from mitochondria, caspase-3 activation, and necrotic cell death.* J Neurosci Res, 2003. **74**(2): p. 309-17.

62. Gibson, G.E., et al., *The alpha-ketoglutarate-dehydrogenase complex: a mediator between mitochondria and oxidative stress in neurodegeneration.* Mol Neurobiol, 2005. **31**(1-3): p. 43-63.
63. Probst, O.C., et al., *The 46-kDa mannose 6-phosphate receptor does not depend on endosomal acidification for delivery of hydrolases to lysosomes.* J Cell Sci, 2006. **119**(Pt 23): p. 4935-43.
64. Takeda, T., et al., *Upregulation of IGF2R evades lysosomal dysfunction-induced apoptosis of cervical cancer cells via transport of cathepsins.* Cell Death Dis, 2019. **10**(12): p. 876.
65. Bellomo, F., et al., *Impact of atypical mitochondrial cyclic-AMP level in nephropathic cystinosis.* Cell Mol Life Sci, 2018. **75**(18): p. 3411-3422.
66. De Rasmo, D., et al., *Mitochondrial Dynamics of Proximal Tubular Epithelial Cells in Nephropathic Cystinosis.* Int J Mol Sci, 2019. **21**(1).
67. Galarreta, C.I., et al., *The swan-neck lesion: proximal tubular adaptation to oxidative stress in nephropathic cystinosis.* Am J Physiol Renal Physiol, 2015. **308**(10): p. F1155-66.
68. Forgac, M., *Vacuolar ATPases: rotary proton pumps in physiology and pathophysiology.* Nat Rev Mol Cell Biol, 2007. **8**(11): p. 917-29.
69. Marshansky, V. and M. Futai, *The V-type H+-ATPase in vesicular trafficking: targeting, regulation and function.* Curr Opin Cell Biol, 2008. **20**(4): p. 415-26.
70. Fry, A.C. and F.E. Karet, *Inherited renal acidoses.* Physiology (Bethesda), 2007. **22**: p. 202-11.
71. Karet, F.E., et al., *Mutations in the gene encoding B1 subunit of H+-ATPase cause renal tubular acidosis with sensorineural deafness.* Nat Genet, 1999. **21**(1): p. 84-90.
72. Kalatzis, V., et al., *Cystinosin, the protein defective in cystinosis, is a H(+)-driven lysosomal cystine transporter.* Embo j, 2001. **20**(21): p. 5940-9.
73. Andrzejewska, Z., et al., *Cystinosin is a Component of the Vacuolar H+-ATPase-Ragulator-Rag Complex Controlling Mammalian Target of Rapamycin Complex 1 Signaling.* J Am Soc Nephrol, 2016. **27**(6): p. 1678-88.
74. Sancak, Y., et al., *Ragulator-Rag complex targets mTORC1 to the lysosomal surface and is necessary for its activation by amino acids.* Cell, 2010. **141**(2): p. 290-303.
75. Bar-Peled, L., et al., *Ragulator is a GEF for the rag GTPases that signal amino acid levels to mTORC1.* Cell, 2012. **150**(6): p. 1196-208.
76. Ariceta, G., V. Giordano, and F. Santos, *Effects of long-term cysteamine treatment in patients with cystinosis.* Pediatr Nephrol, 2017.
77. Jezegou, A., et al., *Heptahelical protein PQLC2 is a lysosomal cationic amino acid exporter underlying the action of cysteamine in cystinosis therapy.* Proc Natl Acad Sci U S A, 2012. **109**(50): p. E3434-43.
78. Cherqui, S. and P.J. Courtoy, *The renal Fanconi syndrome in cystinosis: pathogenic insights and therapeutic perspectives*. Nature reviews. Nephrology, 2017. **13**(2): p. 115-131.
79. Hollywood, J.A., et al., *Use of human iPSCs and kidney organoids to develop a cysteamine/mTOR inhibition combination therapy to treat cystinosis.* bioRxiv, 2019: p. 595264.
80. Braga-Basaria, M., et al., *Lipoprotein profile in men with prostate cancer undergoing androgen deprivation therapy.* Int J Impot Res, 2006. **18**(5): p. 494-8.
81. Lapi, F., et al., *Androgen deprivation therapy and risk of acute kidney injury in patients with prostate cancer.* Jama, 2013. **310**(3): p. 289-96.
82. Fivush, B., J.A. Flick, and W.A. Gahl, *Pancreatic exocrine insufficiency in a patient with nephropathic cystinosis.* J Pediatr, 1988. **112**(1): p. 49-51.

83. Winkler, L., et al., *Growth and pubertal development in nephropathic cystinosis.* Eur J Pediatr, 1993. **152**(3): p. 244-9.
84. Chik, C.L., et al., *Pituitary-testicular function in nephropathic cystinosis.* Ann Intern Med, 1993. **119**(7 Pt 1): p. 568-75.
85. Tucker, H. and G.J. Chesterson, *Resolution of the nonsteroidal antiandrogen 4'-cyano-3-[(4-fluorophenyl)sulfonyl]-2-hydroxy-2-methyl-3'- (trifluoromethyl)-propionanilide and the determination of the absolute configuration of the active enantiomer.* J Med Chem, 1988. **31**(4): p. 885-7.
86. Mukherjee, A., et al., *Enantioselective binding of Casodex to the androgen receptor.* Xenobiotica, 1996. **26**(2): p. 117-22.
87. Nagel-Wolfrum, K., et al., *Targeting Nonsense Mutations in Diseases with Translational Read-Through-Inducing Drugs (TRIDs).* BioDrugs, 2016. **30**(2): p. 49-74.
88. Brasell, E.J., et al., *The aminoglycoside geneticin permits translational readthrough of the CTNS W138X nonsense mutation in fibroblasts from patients with nephropathic cystinosis.* Pediatr Nephrol, 2018.
89. Rocca, C.J. and S. Cherqui, *Potential use of stem cells as a therapy for cystinosis.* Pediatr Nephrol, 2018.
90. Syres, K., et al., *Successful treatment of the murine model of cystinosis using bone marrow cell transplantation.* Blood, 2009. **114**(12): p. 2542-2552.
91. Gaide Chevronnay, H.P., et al., *Hematopoietic Stem Cells Transplantation Can Normalize Thyroid Function in a Cystinosis Mouse Model.* Endocrinology, 2016. **157**(4): p. 1363-71.
92. Elmonem, M.A., et al., *Allogeneic HSCT transfers wild-type cystinosin to nonhematological epithelial cells in cystinosis: First human report*. Am J Transplant, 2018. **18**(11): p. 2823-2828.
93. Naldini, L., *Gene therapy returns to centre stage.* Nature, 2015. **526**(7573): p. 351-60.
94. Hippert, C., et al., *Gene transfer may be preventive but not curative for a lysosomal transport disorder.* Mol Ther, 2008. **16**(8): p. 1372-81.
95. Maguire, A.M., et al., *Safety and efficacy of gene transfer for Leber's congenital amaurosis.* N Engl J Med, 2008. **358**(21): p. 2240-8.
96. Bainbridge, J.W., et al., *Effect of gene therapy on visual function in Leber's congenital amaurosis.* N Engl J Med, 2008. **358**(21): p. 2231-9.
97. Jacobson, S.G., et al., *Improvement and decline in vision with gene therapy in childhood blindness.* N Engl J Med, 2015. **372**(20): p. 1920-6.
98. Bainbridge, J.W., et al., *Long-term effect of gene therapy on Leber's congenital amaurosis.* N Engl J Med, 2015. **372**(20): p. 1887-97.
99. Li, H., et al., *In vivo genome editing restores haemostasis in a mouse model of haemophilia.* Nature, 2011. **475**(7355): p. 217-21.
100. Genovese, P., et al., *Targeted genome editing in human repopulating haematopoietic stem cells.* Nature, 2014. **510**(7504): p. 235-240.
101. Lombardo, A., et al., *Site-specific integration and tailoring of cassette design for sustainable gene transfer.* Nat Methods, 2011. **8**(10): p. 861-9.
102. Iyama, T. and D.M. Wilson, 3rd, *DNA repair mechanisms in dividing and non-dividing cells.* DNA Repair (Amst), 2013. **12**(8): p. 620-36.
103. Orthwein, A., et al., *A mechanism for the suppression of homologous recombination in G1 cells.* Nature, 2015. **528**(7582): p. 422-6.
104. Lieber, M.R., *The mechanism of double-strand DNA break repair by the nonhomologous DNA end-joining pathway.* Annu Rev Biochem, 2010. **79**: p. 181-211.

105. Suzuki, K., et al., *In vivo genome editing via CRISPR/Cas9 mediated homology-independent targeted integration.* Nature, 2016. **540**(7631): p. 144-149.
106. Auer, T.O., et al., *Highly efficient CRISPR/Cas9-mediated knock-in in zebrafish by homology-independent DNA repair.* Genome Res, 2014. **24**(1): p. 142-53.
107. Gahl, W.A., J.Z. Balog, and R. Kleta, *Nephropathic cystinosis in adults: natural history and effects of oral cysteamine therapy.* Ann Intern Med, 2007. **147**(4): p. 242-50.
108. Elmonem, M.A., et al., *Clinical utility of chitotriosidase enzyme activity in nephropathic cystinosis.* Orphanet J Rare Dis, 2014. **9**: p. 155.
109. Torres, S., et al., *Lysosomal and mitochondrial liaisons in Niemann-Pick disease.* Frontiers in Physiology, 2017. **8**.
110. Visentin, S., et al., *The stimulation of adenosine A2A receptors ameliorates the pathological phenotype of fibroblasts from Niemann-Pick type C patients.* Journal of Neuroscience, 2013. **33**: p. 15388-15393.
111. De Nuccio, C., et al., *Adenosine A2A receptor stimulation restores cell functions and differentiation in Niemann-Pick type C-like oligodendrocytes.* Scientific Reports, 2019. **9**: p. 1-10.
112. De La Mata, M., et al., *Pharmacological chaperones and coenzyme Q10 treatment improves mutant β-glucocerebrosidase activity and mitochondrial function in neuronopathic forms of gaucher disease.* Scientific Reports, 2015. **5**.
113. De La Mata, M., et al., *Coenzyme Q10 partially restores pathological alterations in a macrophage model of Gaucher disease.* Orphanet Journal of Rare Diseases, 2017. **12**: p. 1-15.
114. Lee, K., et al., *A biochemical and pharmacological comparison of enzyme replacement therapies for the glycolipid storage disorder Fabry disease.* Glycobiology, 2003. **13**: p. 305-313.
115. Zhu, X., et al., *Systemic mRNA Therapy for the Treatment of Fabry Disease: Preclinical Studies in Wild-Type Mice, Fabry Mouse Model, and Wild-Type Non-human Primates.* American Journal of Human Genetics, 2019. **104**: p. 625-637.
116. Takamura, A., et al., *Enhanced autophagy and mitochondrial aberrations in murine GM1-gangliosidosis.* Biochemical and Biophysical Research Communications, 2008. **367**: p. 616-622.
117. Kajihara, R., et al., *Novel Drug Candidates Improve Ganglioside Accumulation and Neural Dysfunction in GM1 Gangliosidosis Models with Autophagy Activation.* Stem Cell Reports, 2020. **14**: p. 909-923.
118. Condori, J., et al., *Enzyme replacement for GM1-gangliosidosis: Uptake, lysosomal activation, and cellular disease correction using a novel β-galactosidase: RTB lectin fusion.* Molecular Genetics and Metabolism, 2016. **117**: p. 199-209.
119. Bayó-Puxan, N., et al., *Lysosomal and network alterations in human mucopolysaccharidosis type VII iPSC-derived neurons.* Scientific Reports, 2018. **8**.
120. Maeda, M., et al., *Autophagy in the central nervous system and effects of chloroquine in mucopolysaccharidosis type II mice.* International Journal of Molecular Sciences, 2019. **20**.
121. Otomo, T., et al., *Inhibition of autophagosome formation restores mitochondrial function in mucolipidosis II and III skin fibroblasts.* Molecular Genetics and Metabolism, 2009. **98**: p. 393-399.
122. Otomo, T., et al., *Lysosomal Storage Causes Cellular Dysfunction in Mucolipidosis II Skin Fibroblasts.* Journal of Biological Chemistry, 2011. **286**: p. 35283-35290.
123. Coblentz, J., C. St. Croix, and K. Kiselyov, *Loss of TRPML1 promotes production of reactive oxygen species: Is oxidative damage a factor in mucolipidosis type IV?* Biochemical Journal, 2014. **457**: p. 361-368.

124. Weinstock, L.D., et al., *Fingolimod phosphate inhibits astrocyte inflammatory activity in mucolipidosis IV.* Human Molecular Genetics, 2018. **27**: p. 2725-2738.

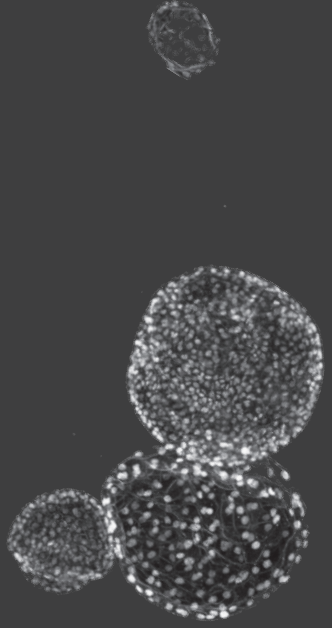

8

Summary
Nederlandse Samenvatting

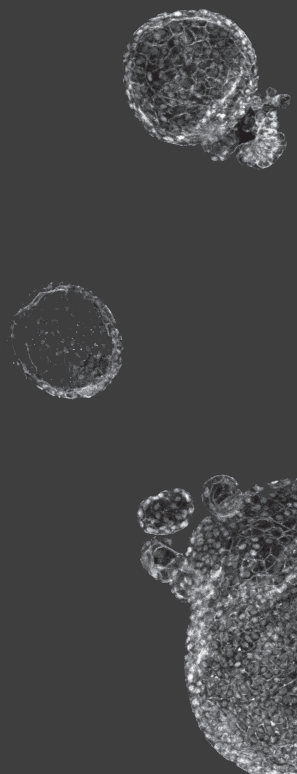

Investigating the pathophysiology and potential therapeutic approaches for nephropathic cystinosis

Nephropathic cystinosis is an autosomal recessive monogenic kidney disorder characterized by lysosomal accumulation of cystine throughout the body, causing organ damage, particularly the kidneys. This is due to pathogenic mutations in the *CTNS* gene, which encodes for the lysosomal cystine transporter cystinosin, transporting cystine from the lysosome into the cytoplasm. Patients with nephropathic cystinosis usually develop symptoms of renal Fanconi syndrome, and if not treated, progress to end stage renal disease within the first 12 years of life. The mainstay for cystinosis treatment is life-long therapy with cysteamine, a cystine depleting agent. Although cysteamine efficiently lowers lysosomal cystine levels and improves some clinical outcomes, it does not reverse the established renal Fanconi syndrome and cannot prevent the loss in renal function. This suggests involvement of complex pathophysiological processes in disease progression that may not be directly related to cystine overload. Therefore, this thesis aimed to investigate the disease pathophysiology and to find new potential therapeutic interventions that could replace or compliment cysteamine therapy for patients with cystinosis.

Chapter 2 gives a literature overview of the molecular mechanisms underlying nephropathic cystinosis as well as emerging therapies that are able to correct the transport and non-transport functions of cystinosin either alone or in combination with cysteamine. We report a multifaceted impact of cystinosin loss-of-function in cystinosis pathology, involving increased oxidative stress, apoptosis, and impaired autophagy and energy metabolism that may or may not be necessarily related to lysosomal cystine accumulation. This information expanded our knowledge on the disease pathology and might facilitate the development of new treatment options for cystinosis.

In chapter 3 we developed a fast, relatively easy and reliable method to quantify intracellular cystine levels in both healthy and cystinotic proximal tubule cells, using liquid chromatography-tandem mass spectrometry. In this method, we used N-ethylmaleimide, an alkylating agent to permanently block cysteine-cystine conversion in cytosol, enabling us to reliably measure intracellular cystine levels. Compared to other methods, our assay is more sensitive, has a lower limit of detection and requires less sample preparation procedure for cystine quantification. The method appeared applicable in screening potential cystine lowering drugs in human proximal tubule cells, human kidney organoids, and zebrafish as shown in this thesis, and can potentially be applied in clinical studies as a diagnostic and biochemical follow-up tool.

To expand our knowledge on the complexity of the disease and prioritize drug targets in cystinosis, in **Chapter 4** we created human cystinotic proximal tubule cells, which were used along with primary adult stem cell-derived cystinotic tubuloids to model cystinosis and evaluate drug therapy. Using metabolomic and proteomics, we found that CRISPR-generated isogenic cystinotic proximal tubule cells are suitable as cystinosis model, allowing us to correctly assess the effect of cystinosin loss. This model exhibits robust cystinotic phenotypes of increased cystine accumulation, reduced mTOR

activation, delayed protein degradation and an increase in baseline ROS levels, further confirming the multifaceted impact of cystinosin loss-of-function. Performing a detailed metabolomic profiling, we also revealed increased levels of alpha-ketoglutarate (aKG) in cystinotic proximal tubule cells, inducing abnormal autophagy and apoptosis activation, and proximal tubule dysfunction. The increased aKG was also evidenced in plasma of cystinotic patients, further signifying the important role of aKG in the cystinosis pathology. This insight combined with a drug screen, revealed a bicalutamide-cysteamine combination therapy as a novel dual target pharmacological approach for the phenotypical correction of cystinotic renal proximal tubule cells. Bicalutamide (but not cysteamine) resolved αKG-mediated downstream effects and restored endocytic cargo processing, and in combination with cysteamine, efficiently normalized cystine levels in cystinotic proximal tubule cells. The combination therapy was also found beneficial in both patient-derived kidney tubuloids and cystinotic zebrafish, paving the way of this combination therapy for future testing in patients with cystinosis.

In **chapter 5** we demonstrated a novel interaction between the B1 subunit of the vacuolar H^+-ATPase (*ATP6V1B1*) and cystinosin in human proximal tubule cells. Mutations in *ATP6V1B1* generally lead to distal renal tubular acidosis and hearing loss of variable degree. Through the presentation of a 23-month-old girl with a *ATP6V1B1* mutation demonstrating cystinosis-like phenotype of increased granulocyte cystine levels and symptoms of renal Fanconi syndrome, it was suggested that a link between *ATP6V1B1* gene deficiency and proximal tubulopathy in cystinosis might exist. We developed and characterized CRISPR-generated ATP6V1B1-deficient proximal tubular cells and performed a full metabolomic and proteomic analysis to compare their phenotype to the isogenic *CTNS*$^{-/-}$ cells (obtained in chapter 4). We demonstrated that ATP6V1B1 is expressed in proximal tubules of human kidney tissue, though to a lesser extent than in distal tubules. In line with the clinical data, the loss of ATP6V1B1 disrupted the chemiosmotic coupling between the lysosomal V-ATPase B1 subunit and cystinosin and resulted in intralysosomal accumulation of cystine and autophagy activation in proximal tubule cells. Our study identified ATP6V1B1 as a central player in proximal tubule cells, regulating lysosomal cystine transport and autophagy, and its absence can lead to proximal tubule dysfunction.

In **chapter 6** we aimed to repair and restore the *CTNS* gene function in cystinotic cells using gene editing. Restoring the *CTNS* gene function in kidney cells could provide a long-lasting cure for patients with cystinosis and prevent kidney function decline in the future. To target the large genomic deletion (57kb), we used a unique CRISPR/Cas9-based strategy, termed homology-independent targeted insertion (HITI). Using this approach, the endogenous promotor and missing *CTNS* exons can be inserted at the correct location in the genome. As proof-of-concept, we tested our strategy in HEK-293 cells, the gold standard cell model to initially study gene therapy, which resulted in a successful insertion of donor DNA into the genome of HEK-cells. Future studies will be directed to optimize the protocol for CRISPR-HITI delivery and evaluate the *CTNS* repair efficiency in cystinotic proximal tubular cells.

Finally, **chapter 7** gives an in-depth discussion of the results obtained in this thesis, and provides an overview of the current knowledge on and perspectives for cystinosis pathology. The development of new isogenic cystinotic *in vitro* models presented in this thesis, offer a valuable insight in discovering new druggable targets and potential therapeutic options, and encourage preclinical testing of dual targeted therapies in cystinosis for future clinical trials.

Onderzoek naar de pathofysiologie van nefropathische cystinose en ontwikkeling van een nieuwe farmacologische behandeling van de ziekte

Nefropathische cystinose is een autosomaal-recessieve monogenetische nieraandoening die wordt gekenmerkt door ophoping van het aminozuur-dimeer cystine in de lysosomen van alle lichaamscellen, wat leidt tot orgaanschade waar vooral de nieren gevoelig voor zijn. Deze aandoening wordt veroorzaakt door pathogene mutaties in het *CTNS*-gen. Dit gen codeert voor het lysosomale transporteiwit cystinosine die het cystine vanuit de lysosomen naar het cytoplasma vervoert. Patiënten met nefropathische cystinose ontwikkelen meestal binnen 6 maanden na geboorte al symptomen van het renaal Fanconisyndroom en nierfalen voor hun 12^{e} levensjaar. De basis voor de behandeling van cystinose is een levenslange therapie met cysteamine om de ophoping van cystine tegen te gaan. Hoewel cysteamine de lysosomale cystine-concentraties efficiënt verlaagt en een aantal klinische parameters verbetert, heeft deze behandeling geen effect op de ontwikkeling van het renaal Fanconisyndroom en kan het geneesmiddel ook het verlies in nierfunctie niet voorkomen. Dit suggereert dat andere pathologische processen betrokken zijn bij het ziektebeeld die mogelijk geen direct verband houden met de cystine-stapeling. Het doel van dit onderzoek was om de processen die een rol spelen bij de ontwikkeling van nierfalen op cellulair en moleculair niveau in kaart te brengen en nieuwe therapeutische aangrijpingspunten te identificeren waarop interventies getest kunnen worden die de behandeling van cystinosepatiënten kan verbeteren.

Hoofdstuk 2 geeft een literatuuroverzicht van de moleculaire mechanismen die ten grondslag liggen aan de ontwikkeling van nefropathische cystinose en een opsomming van nieuwe, opkomende therapieën die in staat zouden kunnen zijn om de functies van cystinosine te corrigeren, alleen of in combinatie met cysteamine. De impact van het verlies van cystinosinefunctie op de cel, waaronder een verhoogde oxidatieve stress, een disfunctionerende apoptose en verminderde autofagie en energiemetabolisme, is hier in detail beschreven. Deze processen blijken niet allemaal direct gekoppeld te zijn aan de lysosomale cystine-stapeling en het hoofdstuk biedt ons meer inzicht in de complexe pathologie van cystinose en de mogelijkheden van nieuwe behandelopties.

In hoofdstuk 3 hebben we een snelle, relatief eenvoudige en betrouwbare methode ontwikkeld om met behulp van vloeistofchromatografie-massaspectrometrie (LC-MS) het cystine-gehalte in zowel gezonde als cystinose-niertubuluscellen te kunnen kwantificeren. Bij deze methode wordt het N-ethylmaleimide, een alkyleringsmiddel om de cysteïne-cystine-omzetting te blokkeren, gebruikt wat de betrouwbaarheid van de meting bevorderde. In vergelijking met andere methoden is de hier ontwikkelde test gevoeliger, heeft een lagere detectielimiet en vereist minder monstervoorbereiding. Zoals aangetoond in dit proefschrift is de methode ook geschikt voor het screenen van nieuwe, potentiële cystine-verlagende geneesmiddelen op menselijke niertubuluscellen, menselijke nierorganoïden en in zebravissen, en kan het mogelijk als een diagnostische en biochemische analysemethode worden toegepast in klinische studies.

Om onze kennis over de complexiteit van de ziekte verder uit te breiden en potentiële nieuwe geneesmiddelen voor de behandeling van cystinose te kunnen ontwikkelen,

hebben we in **Hoofdstuk 4** menselijke cystinose-niertubuluscellen gemaakt met behulp van CRISPR/Cas9-technologie. Deze cellen hebben we samen met zogenaamde cystinose tubuloïds gebruikt om verschillende geneesmiddeltherapieën te kunnen testen. Met behulp van een uitgebreide metabolieten- en eiwittenanalyse ontdekten we dat de CRISPR/Cas9-gegenereerde cystinose-niertubuluscellen het verlies van cystinosine, met eigenschappen van verhoogde cystine-stapeling, verminderde mTOR-activiteit, vertraagde eiwitafbraak en een toename in oxidatieve stress, vertoonden. Een gedetailleerde analyse van de cellulaire metabolieten liet zien dat het alfa-ketoglutaraat (aKG) in cystinose-niertubuluscellen een sleutelrol speelt bij het ziektebeeld. Dit metaboliet draagt bij aan een abnormale autofagie, een activatie van apoptose en proximale niertubulusdisfunctie. In bloedcellen van cystinosepatiënten werden ook verhoogde aKG concentraties aangetroffen, wat de sleutelrol van aKG in de cystinose-pathologie verder bevestigt. Dit inzicht, gecombineerd met een uitgebreide test met potentiële geneesmiddelen, leidde uiteindelijk tot een combinatietherapie van het antiandrogene bicalutamide met cysteamine als een nieuwe farmacologische manier om nefropathische cystinose te behandelen. Bicalutamide was in staat om de αKG-gemedieerde effecten op te heffen en het defect in de eiwitafbraak te herstellen, hetgeen cysteamine niet kan. Maar bicalutamide had weer geen effect op de verhoogde cystine-concentraties in de cystinose-niertubuluscellen. De combinatietherapie bleek ook een gunstig effect te hebben op de niertubuloïds afkomstig van cystinosepatiënten en op cystinose-zebravissen. Deze resultaten maken de weg vrij om in de toekomst de combinatietherapie te gaan onderzoeken bij patiënten met nefropathische cystinose.

In **hoofdstuk 5** hebben we een nieuwe interactie aangetoond tussen de B1-subeenheid van de vacuolaire H^+-ATPase (*ATP6V1B1*) en het cystinosine in humane niertubuluscellen. Mutaties in *ATP6V1B1* leiden tot distale renaal tubulaire-acidose met verschillende gradaties van gehoorverlies. Bij een meisje van 23 maanden oud werd na onderzoek een *ATP6V1B1*-mutatie gevonden terwijl het meisje cystinose symptomen vertoonde, waaronder verhoogde cystine-concentraties in bloedcellen en het renaal Fanconisyndroom. Deze bevinding deed vermoeden dat er een verband zou kunnen bestaan tussen een *ATP6V1B1* gen-deficiëntie en nierbuisfalen bij cystinose. Onderzoek op menselijk nierweefsel toonde het ATP6V1B1-eiwit in de proximale nierbuisjes aan, hoewel het minder sterk aanwezig was dan in distale nierbuisjes. Om de functie van het eiwit verder te onderzoeken hebben we met behulp van CRISPR/Cas9-technologie ATP6V1B1-deficiënte menselijke niertubuluscellen ontwikkeld. Vervolgens is met deze cellen een volledige metabolieten- en eiwittenanalyse uitgevoerd om de celeigenschappen te kunnen vergelijken met die van de cystinosecellen (verkregen in hoofdstuk 4). In overeenstemming met de klinische gegevens verstoorde het verlies van ATP6V1B1 de chemiosmotische koppeling tussen de lysosomale V-ATPase B1-subeenheid en het cystinosine. Dit resulteerde in een ophoping van cystine in de lysosomen en een activatie van autofagie in de cellen. Hiermee hadden we het bewijs gevonden dat afwezigheid van ATP6V1B1 kan leiden tot proximale niertubulusdisfunctie.

In **hoofdstuk 6** hebben we ons gericht op de reparatie van het CTNS-gen en het daarmee gepaard gaande functionele herstel van cystinosecellen. Dit zou een duurzame genezing kunnen bieden aan patiënten met cystinose en de achteruitgang van hun nierfunctie in de toekomst kunnen voorkomen. Bij de meeste Westerse cystinosepatiënten ontbreekt een groot stuk van het gen, een zgn. genomische deletie van 57kb, en om dit te kunnen herstellen hebben we een unieke CRISPR/Cas9-gebaseerde strategie gebruikt, namelijk *homology-independent targeted insertion* (HITI). Met deze aanpak kunnen de oorspronkelijke promotor en de ontbrekende *CTNS*-exonen op de juiste locatie in het genoom worden ingebouwd waardoor het gen in zijn geheel hersteld kan worden. Als proof-of-concept hebben we onze strategie getest in HEK-293-cellen, de gouden standaard voor het optimaliseren van nieuwe gen-reparatie strategieën. Dit resulteerde in een succesvolle inbouw van het donor-DNA in het genoom van de HEK-293-cellen. Vervolgstudies zullen gericht zijn op het optimaliseren van de afgifte van CRISPR-HITI en het *CTNS*-genherstel in cystinose-niertubuluscellen.
Ten slotte bevat **hoofdstuk 7** een diepgaande bespreking van de resultaten die in dit proefschrift zijn verkregen, en geeft het een overzicht van de huidige kennis van en perspectieven voor cystinosepathologie. De nieuwe *in vitro* modellen die in dit proefschrift worden gepresenteerd hebben waardevolle inzichten in deze pathologie gegeven, wat weer heeft geleid tot aanknopingspunten voor nieuwe medicamenten en potentiële therapeutische opties. De hiermee ontdekte combinatietherapie biedt een goede mogelijkheid voor toekomstig klinisch onderzoek bij cystinosepatiënten en hoop op vermindering van nierfunctieverlies bij nefropathische cystinose.

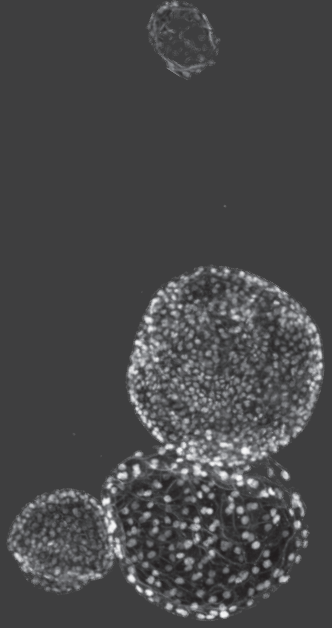

9

Curriculum Vitae
List of publications
Acknowledgements

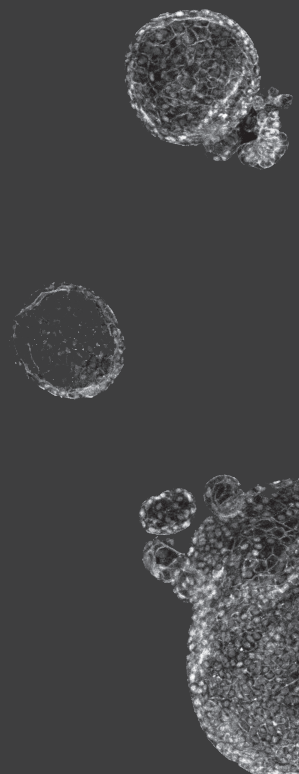

CURRICULUM VITAE

Amer Jamalpoor is Iranian but was born (15th January 1988) and raised in Dubai, United Arab Emirates. After graduating from high school in 2006, he moved to Bangalore, India where he studied Pharmacy at the Rajiv Gandhi University of Health Sciences. After obtaining his Pharmacy degree in December 2011, he travelled to Tehran, Iran and worked as a retail Pharmacist. To accomplish his burning desire for a scientific career, in September 2014 he started the master program Biomedical Sciences (specialization Human Toxicology) at Radboud University, The Netherlands. His excellent academic record, insatiable and persistent drive for excellence was recognized with 2 prestigious scholarship awards (Radboud Scholarship Program and Radboud University Medical Center Study fund). He carried out his graduation projects at Pharmacology and Toxicology, Radboud Institute for Molecular Life Sciences in Nijmegen, and at Netherland Cancer Institute, Amsterdam, the Netherlands. He developed a strong understanding of pharmacokinetic concepts by using existing humanized cells and animal models, which allowed evaluating the potential for clinically relevant drug-drug interactions and drug toxicity. After his graduation in September 2016, he started his Ph.D. research at Utrecht Institute for Pharmaceutical Sciences, Utrecht University, The Netherlands, under the supervision of Prof. dr. Roos Masereeuw and Dr. Manoe Janssen. His research project was focused on investigating the pathophysiology and potential therapeutic interventions for nephropathic cystinosis. Here, he was also selected to join the NWO-funded Future Medicines Fellows, a group of ambitious students involved in outreach activities, such as developing summer school and organizing seminar series at Utrecht University. He completed his doctoral research project in September 2020, for which the most important results are reported in this dissertation. Amer now continued his career as a lead scientist developmental toxicology at Toxys.

LIST OF PUBLICATIONS

Caetano-Pinto, Pedro; **Jamalpoor, Amer**; Ham, Janneke; Goumenou, Anastasia; Mommersteeg, Monique; Pijnenburg, Dirk; Ruijtenbeek, Rob; Sánchez-Romero, Natalia; van Zelst, Bertrand; Heil, Sandra, Jansen, Jitske; Wilmer, Martijn J; van Herpen, Carla M L & Masereeuw, Rosalinde. Cetuximab prevents methotrexate-induced cytotoxicity in vitro through epidermal growth factor dependent regulation of renal drug transporters. *Molecular Pharmaceutics* (**2017**) 14(6):2147-2157.

Jamalpoor, Amer; Sparidans, Rolf W; Casellas, Carla Pou; Rood, Johannes J M; Joshi, Mansi; Masereeuw, Rosalinde & Janssen, Manoe J. Quantification of cystine in human renal proximal tubule cells using liquid chromatography-tandem mass spectrometry. *Biomedical Chromatography* (**2018**) 32(8):e4238.

van Hoppe, Stéphanie; **Jamalpoor, Amer**; Rood, Johannes J M; Wagenaar, Els; Sparidans, Rolf W; Beijnen, Jos H & Schinkel, Alfred H. Brain accumulation of osimertinib and its active metabolite AZ5104 is restricted by ABCB1 (P-glycoprotein) and ABCG2 (breast cancer resistance protein). *Pharmacological Research* (**2019**) 146:104297.

Abyar, Selda; Khandar, Ali Akbar; Salehi, Roya; Abolfazl Hosseini-Yazdi, Seyed; Alizadeh, Effat; Mahkam Mehrdad; **Jamalpoor, Amer**; White, Jonathan M; Shojaei, Motahhareh; Aizpurua-Olaizola, O; Masereeuw, Rosalinde & Janssen, Manoe J. In vitro nephrotoxicity and anticancer potency of newly synthesized cadmium complexes. *Scientific Reports* (**2019**) 9(1):14686.

Rood, Johannes J M; **Jamalpoor, Amer**; van Hoppe, Stephanie; van Haren, Matthijs J; Wasmann, Roeland E; Janssen, Manoe J; Schinkel, Alfred H & Masereeuw, Rosalinde; Beijnen, Jos H & Sparidans, Rolf W. Extrahepatic metabolism of ibrutinib. *Investigational New Drugs* (**2020**).

Jamalpoor, Amer; van Gelder, Charlotte AGH.; Yousef Yengej, Fjodor A.; Zaal Esther A.; Berlingerio, Sante Princiero; Veys, Koenraad R; Pou Casellas, Carla; Voskuil, Koen; Essa, Khaled; Ammerlaan, Carola ME.; Rega, Laura Rita; van der Welle, Reini; Lilien, Marc R.; Rookmaaker, Maarten B.; Clevers , Hans; Klumperman, Judith; Levtchenko, Elena N.; Berkers, Celia R.; Verhaar, Marianne C.; Altelaar, Maarten; Masereeuw, Rosalinde & Janssen, Manoe J. Cysteamine-bicalutamide combination therapy corrects proximal tubule phenotype in cystinosis. *Under Revision at EMBO Molecular Medicine*

Jamalpoor, Amer; Othman, Amr; Levtchenko, Elena N.; Masereeuw, Rosalinde, Manoe Janssen J. Molecular mechanisms underlying nephropathic cystinosis. *Submitted.*

Jamalpoor, Amer; van Eerde, Albertien M.; Lilien, Marc R.; van Gelder, Charlotte AGH.; Zaal Esther A.; Valentijn, Floris A.; Broekhuizen, Roel; Zielhuis, Eva; Egido, Julia E.; Altelaar, Maarten; Berkers, Celia R.; Masereeuw, Rosalinde & Janssen, Manoe J. The lysosomal V-ATPase B1 subunit in proximal tubule is linked to nephropathic cystinosis. *Submitted*

Jamalpoor, Amer; Harrison, Patrick T.; Masereeuw, Rosalinde & Janssen, Manoe J. Gene repair in cystinosis. *In preparation*

Jamalpoor, Amer; Magalhães, Pedro; Masereeuw, Rosalinde & Mischak, Harald. Renal proximal tubule cells selectively handle urinary collagen peptides. *In preparation*

Jamalpoor, Amer; Mustafa, Ola; Masereeuw, Rosalinde & Janssen, Manoe J. Insulin-dependent regulation of drug transporters in human renal proximal tubule cells. *In preparation*

ACKNOWLEDGMENT

Dear **Roos**, first and foremost, I would like to express my deepest and sincere gratitude to you. You have changed my life personally and scientifically. You allowed me to embark in my scientific journey and provided me an endless array of opportunities that deepened my professional and personal development. Very few people I have met, show the ability to sincerely empower people and allowing their talents, professional abilities and personality to flourish. Thank you for being a caring and considerate supervisor. Thank you for everything!

Dear co-promotor, dear **Manoe**, I would also like to thank you for sharing your expertise, your dedicated and strategic advice, and critical appraisals of our experimental data and manuscript preparations. Thank you for helping me to improve my skills and the way of thinking. Thank you for all your guidance and support during the past 4 years. I really appreciate everything you have done. Thank you!

Furthermore, my sincere gratitude goes to the **members of the committee**, Prof. Dr. Nine Knoers, Prof. Dr. Jan Danser, Dr. Roel Goldschmeding, Prof. Dr. Ineke Braakman and Prof. Dr. Enrico Mastrobattista for accepting to be part of the thesis committee and for reading critically the manuscript.

Dear **Katja** and **Carla**, I am very proud and happy of having two of my best friends next to me in my PhD defense as my paranymphs. Katja, it has been great having you around since the very beginning and even now standing right next to me in this very special moment. I will never forget the times we spent hearing out each other's problems both in life and in science. Without you, many things would have been very difficult. Thank you. Carla, you have been one of my best students and now I am very happy that you will be right next to me in my promotion session as my friend. We have great memories together and many more to come. Thanks for your unusual, outside the box way of thinking and critical touch with the right amount of perfectionism in all tasks you undertook. Good luck with your Ph.D.

I cannot stress enough my gratitude to my colleagues and friends who have helped me during my PhD at the Pharmacology division. I would like to start by thanking **Pedro** (my master internship supervisor), who left the lab shortly after I started, allowing me to take over his working space. Pedro you provided me the opportunity to shine and demonstrate myself as a talented researcher. **Milos**, my dearest colleague, many thanks for your help and support, and for all the scientific and non-scientific discussions. You are a very talented scientist with immerse patience and remarkable working capability. I will not forget the funny times that we had in the train, trying to embarrass you in public with fake, tuberculosis-like sudden cough attacks. **Anne Metje,** many thanks for all your assistance and help in the lab. You were the one that always reminded us of the

good practice in the lab. A special thank you goes to **Jitske**, **Silvia**, **Rafael, Hossein** and **Haysam** for helpful discussions and for being the most energizing colleagues with so many great ideas. You guys are awesome. Dear **João**, **Rawan**, **Elena**, **Yi**, **Zhenguo**, **Sabbir**, **Marta**, **Laura** and **Alasdair** thank you for all the nice moments we shared as a team in the morning meetings, and I am really looking forward to your future contributions to the Pharmacology group. Great path a head of you all. **Paul** and **Paula**, many thanks for keeping our spirits high. Working without you felt like a bike without wheels. Thanks for always being extremely honest and transparent and I wish you both a lot of success.

I also want to thank all current and former UIPS colleagues: Dear **Johan**, **Aletta**, **Paul H**, **Betty**, **Frank**, **Astrid**, **Liesbeth**, **Linette**, **Daphne**, **Erik**, **Gert**, **Lucianne**, **Mechiel**, **Joris V**, **Ferdi**, **Rolf**, **Mara**, **Damiën**, **Marlotte**, **Atanaska**, **Suzanne**, **Veronica**, **Suzan**, **Melanie**, **Gert-Jan**, **Kirsten**, **Michele B**, **Susan**, **Jing**, **Yulong**, **Yang**, **Aurora**, **Sandra**, **Charlotte**, **Saskia**, **Xiaoli**, **Yuanpeng**, **Lei**, **Naika**, **Mengshan**, **Puqiao**, **Lili**, **Mirelle**, **Marit**, **Alejandro**, **Reshmi**, **Mitch**, **Mojtaba**, **Bart**, **Pieter**, **Thea**, **Ingrid**, **Monika**, all former students and others whom, unintentionally, I have forgotten to mention. Thanks for welcoming and embracing me as a member of the Pharmacology division.

Dear **Lidija**, **Karin**, **Brenda**, **Gemma**, and **Koen** please accept my deep appreciation for all your help, administration supports, and for being so friendly to me.

I would like to also express my sincere respect to my Iranian friends and colleagues. Dear **Adel**, **Hamed**, **Soheil**, **Pouya**, **Negisa**, **Selda, Ali** and **Mahsa** thank you very much for your warm support and help during my PhD. I do not forget the time we spent specially during our lunch meetings. I truly enjoyed the moment being with you guys. I wish all of you the best of luck.

Dear Future Medicine Fellows: **Charlotte**, **Saar**, **Donna**, **Katja**, **Carl**, **Tom, Gerlof**, **Lourens**, and **Rick**. It was a pleasure working with you, organizing future medicine seminars and summer schools. Thank you all.

Now a word of appreciation to my students. I sincerely hope that you learned and enjoyed working with me. **Koen**, **Mansi**, **Anastasia**, **Ola**, **Julia**, **Khaled**, **Carla**, **Eva**, **Joris**, **Besher**, **Georgia**, and **Amr**, thanks a million for being part my journey in the cystinosis project. I really learned a lot from you all. Because of you, I could develop myself towards becoming a good supervisor. Your dedication, motivation and enthusiasm greatly contributed to the success of the research of this thesis. I am very glad that we never had a supervisor-student relationship, and we all remained friends even after you completed your studies. Very proud of you and good luck in every stage of your life.

I would also like to thank my collaborators in different projects. Many thanks to **Elena** Levtchenko and her group members in Leuven, **Sante**, **Koenraad, Mohamed**, **Ahmed**,

Dries and **Rik.** Thanks to **Patrick, Maarten**, **Charlotte**, **Celia**, **Esther**, **Judith**, **Reini**, **Marc**, **Albertien**, **Maarten**, **Marianne**, **Fjodor**, **Floris** and **Roel** for contributing to this project with helpful insights and suggestions. I am very grateful for your support over these 4 years and it was a real pleasure being able to share with you all my progresses, no matter how small or big they were. Also, I want to express my immense gratitude to all members of **cystinosis Ireland** for their support, organizing wonderful cystinosis seminars and inviting me to present my work in Ireland each year.

Dear **Aaron**, I was so lucky to be your classmate during our master education in Nijmegen. We always had each other's back, and this makes me so proud. I wish you and your family all the best and I hope I can visit you sometime in Canada.

Dear **Rakib** and **Farzana**, you are the angels that Niloufar and me found in Nijmegen. Rakib, you really helped me a lot during my studies and I always considered you as my big brother. You guys are awesome. Thank you for everything.

Thomas and **Elly**, you guys are awesome! All the lovely times (Shabe yalda, BBQ, etc) we had together will always be the core of my wonderful memories from Odjk, Utrecht.

برای پدر و مادر عزیزم که مرا به این دنیا اوردند و اولین قدمهایم را در حالیکه دستان پر مهرشان را میفشردم برداشتم. تاکید و تشویق شما ریشهای علاقه ی من به تحصیل شد. عاشقانه دوستتان دارم.

برای پدر و مادر همسرم، برای شما که سهم بزرگی در مهاجرت و اغاز زندگی علمی من در هلند داشتید. این مسیر بدون همراهی شما ممکن نبود. سپاسگذارم.

برای ۴ برادرم و خانوادهایشان، شما ۴ نفر که از کودکی تا به امروز همواره شریک شادی، غم، شکستها و موفقیتهایم بودید و هستید. برای همسران و فرزندانتان که خوانواده ما را بزرگتر و گرمتر کردند. برای حمده، فاطمه، ابتسام، مریم و فرح کوچک و دوست داشتنی که لذت عمو شدن را به من بخشیدید. به امید دیدار.

برای محسن و آذین عزیز، خوشحالم که نزدیک ما هستید. راحتان باز و زندگیتان روشن.

برای عمو علی، خاله عارفه، سونیا و سارا عزیز، زمستان ها، تابستان ها، عید ها و روزهای دوری از خانواده با حضور شما شیرین گذشت. حضورتان همواره مایه شادمانی بوده و هست. پایدار باشید.

برای فاروق، رفیق کودکی و زنگهای تفریـــح مدرسه تا دانشگاه در هندوستان. با هم بزرگ شدیم و سفر کردیم و این رفاقت را تا به امروز به اینجا رساندیم. شاه داماد، برای تو و همسرت لیلا ارزو خوشبختی میکنم.

برای مهسا، هم دانشگاهی دیروز و رفیق تا به امروز. تمام این سالها از راه دور همیشه حاضر بودی. امیدوارم در گذر سالها همیشه همینطور خوش قلب بمانی.

برای علیرضا و آرش، خاطرات شیرین دانشکده داروسازی در هندوستان بدون شما ممکن نبود. شما رفیق شبهای امتحان در بنگلور و پایه گپهای شبانه در هلند و خیال پردازیهای اینده هستید. زندگی پربار و موفقیت های روز افزون را برایتان ارزومندم.

Finally, I would like to dedicate this work to my miracle of life: my wife, Niloufar. This defense is a once-in-a-lifetime adventure, and it would have not been possible without you. I cannot forget your endless and unconditional efforts, support and love you provided me since we met each other. You always believed in me and I am honored to have you here today to witness my promotion. Love you forever!

هرگز دل من ز علم محروم نشد

کم ماند ز اسرار که معلوم نشد

هفتاد و دو سال فکر کردم شب و روز

معلومم شد که هیچ معلوم نشد

(خیام)